

Research Infrastructure Quality Assurance

GAW Report No. 268

Ozonesonde Measurement Principles and Best Operational Practices

ASOPOS 2.0

(Assessment of Standard Operating Procedures for Ozonesondes)

August 2021

WEATHER CLIMATE WATER



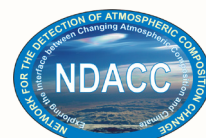
WORLD
METEOROLOGICAL
ORGANIZATION



GLOBAL
ATMOSPHERE
WATCH



JÜLICH
Forschungszentrum



GAW Report No. 268

Ozonesonde Measurement Principles and Best Operational Practices

ASOPOS 2.0

(Assessment of Standard Operating Procedures for Ozonesondes)

Prepared by Herman G.J. Smit and Anne M. Thompson
And the ASOPOS 2.0 Panel

October 2021



WORLD
METEOROLOGICAL
ORGANIZATION

© World Meteorological Organization, NASA and FZ-Jülich, 2021

The right of publication in print, electronic and any other form and in any language is reserved by WMO, NASA and FZ-Jülich. Short extracts from WMO publications may be reproduced without authorization, provided that the complete source is clearly indicated. Editorial correspondence and requests to publish, reproduce or translate this publication in part or in whole should be addressed to:

Chair, Publications Board
World Meteorological Organization (WMO)
7 bis, avenue de la Paix
P.O. Box 2300
CH-1211 Geneva 2, Switzerland

Tel.: +41 (0) 22 730 84 03
Fax: +41 (0) 22 730 81 17
Email: publications@wmo.int

NOTE

The designations employed in WMO publications and the presentation of material in this publication do not imply the expression of any opinion whatsoever on the part of WMO concerning the legal status of any country, territory, city or area, or of its authorities, or concerning the delimitation of its frontiers or boundaries.

The mention of specific companies or products does not imply that they are endorsed or recommended by WMO in preference to others of a similar nature which are not mentioned or advertised.

The findings, interpretations and conclusions expressed in WMO publications with named authors are those of the authors alone and do not necessarily reflect those of WMO or its Members.

This publication has been issued without formal editing.

ABSTRACT

The ozonesonde is a small balloon-borne instrument that is attached to a standard radiosonde to measure ozone profiles from the surface to 35 km with ~ 100 m vertical resolution. The electrochemical concentration cell (ECC) ozonesonde has been used at over 100 stations worldwide starting 50 years ago. Ozonesonde data are a mainstay of satellite calibration and of climatologies used in satellite algorithms and ozone trends analysis. Each ozonesonde instrument is unique so it must be carefully prepared before launch; this introduces some uncertainty into a station time series. Tests in simulation chambers or in the field show a relative bias of $\sim 5\%$ between sondes from the two manufacturers when charged with the same chemical sensing solution. Likewise, a 3%–10% bias results when sondes of the same type are charged with different sensing solutions. These biases must be accounted for in the preparation steps and post-flight data processing corrections, all of which contribute to random and systematic errors in ozonesonde records. Since 2004, the WMO/GAW-sponsored ASOPOS (Assessment of Standard Operating Procedures [SOP] of OzoneSondes) team of experts has periodically evaluated ozone records and the results of field and laboratory experiments that intercompare ECC instruments.

This report updates the first ASOPOS Guidebook that was published in 2014: GAW Report No. 201 [*Smit and ASOPOS, 2014*]. The update is based on analyses of reprocessed sonde data since 2015, laboratory tests of ozonesonde components and the 2017 Jülich OzoneSonde Intercomparison Experiment (JOSIE; *Thompson et al., 2019*). The measurement principles of the ozonesonde instrument, the uncertainty chain of the parameters affecting the measurement and revised data processing protocols are described in detail. Expanded guidelines on data quality indicators and the rationale for enhanced metadata are given. There are new recommendations on sonde preparation steps, metadata collection as well as traceability to the world standard ozone photometer. The appendices cover detailed measurement protocols and uniform guidelines for software providers about metadata that need to be recorded by the sounding systems. With adoption of these SOP's, the global ozonesonde community has the potential to achieve the 5% uncertainty level in tropospheric and stratospheric ozone requested by the satellite and trends communities.

Main title: Ozonesonde Measurement Principles and Best Operational Practices

Subtitle: ASOPOS 2.0 (Assessment of Standard Operating Procedures for OzoneSondes)

Editors: Herman G.J. Smit & Anne M. Thompson

Contents

PREFACE (O. Tarasova, GAW).....	9
1. INTRODUCTION (A.M. Thompson, H.G.J. Smit, D.E. Kollonige)...	10
1.1. Role of Ozonesonde Data in the Global Ozone Observing System.....	10
1.2. Active Ozonesonde Stations.....	12
1.3. Ozonesonde Quality Assurance/ Quality Control Overview.....	12
1.3.1. WCCOS & JOSIE Laboratory Tests. BESOS and ASOPOS GAW Report 201 (2014).....	15
1.3.2. ASOPOS and JOSIE Activities since 2010.....	15
1.4. Scope of Present Report.....	18
2. OZONESONDE-ELECTROCHEMICAL CONCENTRATION CELL (ECC) (H.G.J. Smit).....	22
2.1. Introduction.....	22
2.2. Principle of Operation and Instrument Design.....	23
2.3. Aspects of Instrumentation and Different Sensing Solutions.....	27
2.4. Ozonesonde and Radiosonde Systems.....	29
2.4.1. Comparison of Ozonesondes in the WCCOS (JOSIE Campaigns).....	29
2.4.2. Radiosonde Evolution.....	30
2.4.3. Air Pressure, Geopotential Height and Geometric Height.....	31
3. OZONESONDE MEASUREMENT AND UNCERTAINTY (D.W. Tarasick, G.A. Morris, B.J. Johnson).....	34
3.1. Introduction.....	34
3.2. Performance of the Sondes.....	34
3.2.1. Introduction.....	34
3.2.2. Instrument Biases.....	34
3.2.3. Stratospheric Performance.....	35
3.2.4. Tropospheric Performance.....	36
3.2.5. Artefacts/Interferences Due to Local Pollution including SO ₂	37
3.3. Factors Influencing Sonde Performance.....	39
3.3.1. Instrumental Uncertainties.....	39
3.3.2. Pump Flowrate at Ground (Φ_{PO}).....	39
3.3.3. Pump Efficiency (η_P).....	41
3.3.4. Absorption Efficiency (η_A).....	43
3.3.5. Conversion Efficiency (η_C).....	43
3.3.6. Cell Current I_M and Background Current I_B	45
3.3.7. Motor Speed.....	48
3.3.8. Temperature of Gas Sampling Pump (T_P).....	48
3.3.9. Sensor Response Time.....	48

3.3.10.	Radiosonde Pressure Offsets	49
3.3.11.	Total Ozone Normalization Factor (N_T)	49
3.3.12.	Two Examples of Uncertainty Budgets	50
4.	ASSESSMENT OF STANDARD OPERATING PROCEDURES FOR OZONESONDES (Roeland Van Malderen, Peter von der Gathen & Richard Querel) ..	53
4.1.	Introduction	53
4.1.1.	Ozonesonde Operations and the Need for SOP.....	53
4.1.2.	Ozonesonde Testing as the Basis for Recommended SOP.....	53
4.1.3.	ASOPOS 2.0 Panel Summary SOP Recommendations.....	54
4.2.	Rationale for ASOPOS 2.0 Panel Recommendations on ECC Ozonesonde Preparation SOPS	55
4.2.1.	Introduction	55
4.2.2.	Annotated SOP for Preparing ECC Ozonesondes.....	56
4.2.3.	SOP for Re-Use of Recovered Sondes	60
4.2.4.	Issues to Avoid, Potential Pitfalls, and Troubleshooting.....	62
4.2.5.	Hardware to Prepare Ozonesondes	63
4.3.	Data Processing and Archiving.....	64
4.3.1.	Introduction	64
4.3.2.	Processing Ozonesonde Data-Corrections and Uncertainties.....	65
4.3.3.	Metadata.....	66
4.3.4.	Overview of Required Ozonesonde Data to be Archived	66
5.	DATA QUALITY INDICATORS (DQI) (H. Vömel and R. M. Stauffer).....	70
5.1.	Introduction	70
5.2.	Screening individual vertical ozonesonde profiles	70
5.2.1.	Total Ozone Normalization Factor (See Section 3.3.11)	71
5.2.2.	Pump Flow Rate (See also Section 3.3.2)	71
5.2.3.	Response Time (see also Section 3.3.9)	72
5.2.4.	Pump Temperature (See also Section 3.3.8).....	72
5.2.5.	Pump Motor Current.....	72
5.2.6.	Pump Motor Voltage	72
5.2.7.	Background Current (See also Section 3.3.6)	73
5.2.8.	Sensing Solution Type (SST) and ECC sonde Type (See Sections 1.3 and 2.3.2).....	73
5.2.9.	Removal of Artefacts and Interferences	74
5.2.10.	Metadata Record	74
5.2.11.	ECC Manufacturer Changes	75
5.3.	Homogenization of Temporal and Spatial Ozonesonde Records ...	75
5.4.	General DQI's for Ozonesondes	76

5.4.1.	Station Information and Sounding Practices	76
5.4.2.	Traceability	76
5.4.3.	Data Reprocessing.....	76
5.4.4.	Data Usage	77
REFERENCES		78
Acknowledgements		88
Annex A	Standard Operating Procedures for ECC Ozonesondes: A Practical Guide	90
Annex B	Meta Data (Extended Version)	117
Annex C	Practical Guidelines to Determine Ozone Partial Pressure by ECC Sonde, and Its Associated Uncertainty	131
Annex D	Practical Guidelines to Homogenize Historical Ozonesonde Records	143
Annex E	List of Acronyms	165
Annex F	ASOPOS 2.0 People Involved	168

PREFACE (Oksana Tarasova, GAW)

Since its inception in 1989, the Global Atmosphere Watch Programme of WMO through its community, has worked on the provision of reliable information on atmospheric composition changes and the drivers thereof. The earlier activities demonstrated that “collecting adequate information on the chemical composition of the atmosphere is valuable and possible only if all the relevant measurements are expressed in the same units and on the same scale and if data from different countries and from different sites are comparable”, ([WMO Global Atmosphere Watch \(GAW\), Implementation Plan: 2016–2023, GAW Report No. 228](#)). The quality of underlying data impacts the delivery of products and services of adequate quality for the intended use.

The WMO Global Atmosphere Watch (GAW) Implementation Plan: 2016-2023 ([GAW Report No. 228](#)) greatly emphasizes the quality of the data produced by its programme partners and contributors. Quality Assurance and Quality Control (QA/QC) activities apply to all elements of the GAW, starting from assignment of the network primary standards to capacity building and training of the personnel performing the measurements. Central Facilities constitute an essential institutional foundation for the implementation of GAW’s quality assurance activities. Operated by national institutions, these Facilities provide indispensable services to the community by keeping primary standards, organizing and conducting intercomparison and stations audits, preparing measurement guidelines, standard operating procedures and more.

In order to assess the performance of various ozonesondes and to guarantee consistency in ozonesonde data, the World Calibration Centre for Ozone Sondes (WCCOS) hosted by the Research Centre in Jülich was established in 1995. It played and continues to play an important role in the establishment and regular updating of the Standard Operating Procedures for ozonesondes and organization of the ozonesondes intercomparisons.

With the adoption of upgraded quality indicators and a recognition that evolving ozonesonde instruments require periodic evaluation in the WCCOS, the assessment of the measurement quality will be ongoing. WMO/GAW will continue to rely on the WCCOS and the dedicated scientists who evaluate the ozone profile record and who ensure that the best procedures for ozonesondes are documented for the community.

WMO/GAW appreciates the contributions made by the report authors who were led by Dr Herman G.J. Smit (Lead WCCOS, Forschungszentrum Jülich) and Prof. Dr Anne M. Thompson (NASA/Goddard Space Flight Centre). WMO/GAW acknowledges and appreciates valuable suggestions of the reviewers that greatly enhanced this report.

1. INTRODUCTION (Anne M. Thompson, Herman G.J. Smit, Debra E. Kollonige)

1.1. Role of Ozone Data in the Global Ozone Observing System

Although ozone is a minor constituent in the Earth's atmosphere, it plays a key role in the physics and chemistry of both the stratosphere and troposphere. In the stratosphere where 90% of ozone is located, it is an important absorber of both infrared- and ultraviolet radiation, with ozone acting as a UV-filter that protects the biosphere. In the upper troposphere ozone is a powerful greenhouse gas; it has been estimated that increasing tropospheric ozone has contributed ~20% as much as positive radiative forcing as CO₂ since 1750 [IPCC, 2013]. In the troposphere the relatively small amount of ozone is the starting point for photodissociation into the highly reactive O(¹D) radical that reacts with water vapor to form OH, the hydroxyl radical. The hydroxyl radical removes hundreds of trace gas molecules in the troposphere. It is sometimes referred to as the tropospheric cleanser or detergent because it shortens the lifetime of many harmful species. The global burden of OH is the major component of the Earth's "oxidizing capacity" [Thompson, 1992].

Ozone is an environmental concern when human activities perturb its natural balance. The stratosphere is vulnerable to trace amounts of free radicals that can destroy ozone catalytically. Chlorofluorocarbons (CFCs) and nitrogen oxides, NO_x (=NO+NO₂), the latter originating from the breakdown of nitrous oxide in fertilizers are presently the greatest sources of such radicals. In the troposphere the naturally low ozone concentrations are modified by many human activities that release NO_x, carbon monoxide (CO) and hydrocarbons, also referred to as volatile organic compounds (VOCs). The latter chemicals react in the presence of sunlight to produce ozone in amounts that can be tens of times greater than natural amounts. In that case, ozone is a major component of smog and detrimental to human health [Lippmann, 1989].

The following questions express the scientific motivations for continuous observations of in-situ ozone and for enhanced understanding of the chemical and physical processes determining the distribution of ozone. What is the effect of human activity on stratospheric and tropospheric ozone? How is the UV flux at the surface of the Earth changing in response to changes in the ozone column density? How is the Earth's radiation budget (climate forcing) responding to stratospheric and tropospheric ozone changes? Which chemical and physical factors are controlling ozone concentrations? How is the oxidizing power of the atmosphere changing with time? What is the influence of human activity? How is regional air quality degraded by industrial and other anthropogenic emissions in populated areas of the world?

WMO has long supported programs for ozone monitoring by sponsoring the Quadrennial Ozone Assessments [WMO/UNEP, 1991; 1995; 1999; 2003; 2007; 2011; 2015; 2019] on stratospheric ozone and by organizing activities to promote global monitoring of ozone with an emphasis on the sharing of data and promulgating the best techniques for ozone measurements. Since 1987 the WMO has formalized these activities under the Global Atmospheric Watch program (GAW: <https://public.wmo.int/en/programmes/global-atmosphere-watch-programme>). GAW helps coordinate observing networks and the associated infrastructure needed for supplying basic information to policy makers [Global Atmosphere Watch Guide, GAW Report No. 86, 1993]. Under the auspices of WMO/GAW, regional instrument calibrations and training for operators of the ground-based Dobson and Brewer total ozone instruments are conducted.

Ozone sounding records provide the longest record of the vertical ozone distribution and constitute a key component for monitoring changes in stratospheric ozone in accordance with the Montreal Protocol [WMO/UNEP, 2019]. Recently, Antarctic soundings indicated that the springtime ozone profile is recovering and the ozone hole healing [Kuttippurath and Nair, 2017]. However, on 6 October 2020 the most extensive Antarctic ozone hole in the past 15 years was recorded. Both size and extent of depletion set records in November and December 2020 (<https://ozonewatch.gsfc.nasa.gov>). Earlier in 2020, Arctic springtime ozonesonde profiles exhibited severe northern hemisphere stratospheric ozone depletion [Wohltmann et al., 2020]. These losses would have been far worse had concerted global action

not reduced emissions of Ozone Depleting Substances (ODSs) over the past 30 years. Some of the springtime losses may also stem from global climate change, i.e. cooling of the Arctic stratosphere [Hu *et al.*, 2018].

Over the last 20 years, ozonesondes have become increasingly important in understanding tropospheric ozone pollution. Soundings provide insight into long-range transport of ozone from anthropogenic and natural sources. They can identify stratosphere-troposphere air mass exchange processes [Tarasick *et al.*, 2019 a; Kuang *et al.*, 2012; Thompson *et al.*, 2007a], the downward transport of upper tropospheric air [Hayashi *et al.*, 2008] and the influence of air masses containing ozone precursors released by biomass burning (e.g. Morris *et al.*, 2006; Thompson *et al.*, 2001; 2003 a, b), as well as ozone production resulting from lightning (e.g. Kotsakis *et al.* [2017]; Cooper, *et al.* [2006; 2007]).

WMO/GAW has helped organize ozonesonde intercomparison tests for nearly 25 years (**Section 1.3**). GAW promotes the World Ozone and Ultraviolet Radiation Data Centre (<https://www.woudc.org>) where Brewer and Dobson data, as well as sonde profiles, are archived for open distribution, and coordinates the World Data Centre for Reactive Gases (WDCRG; <http://ebas.nilu.no>) for surface ozone data archiving. **Figure 1–1** displays the comprehensive framework for global ozone observations, including related networks, satellites, models and assessments. Since 2004 GAW has supported the Assessment of Standard Operating Procedures for OzoneSondes (ASOPOS), a group of ~20 ozonesonde experts that represent nearly all of the active sounding stations. Meetings of ASOPOS with reports on related laboratory tests have taken place approximately yearly as described in **Section 1.3**.

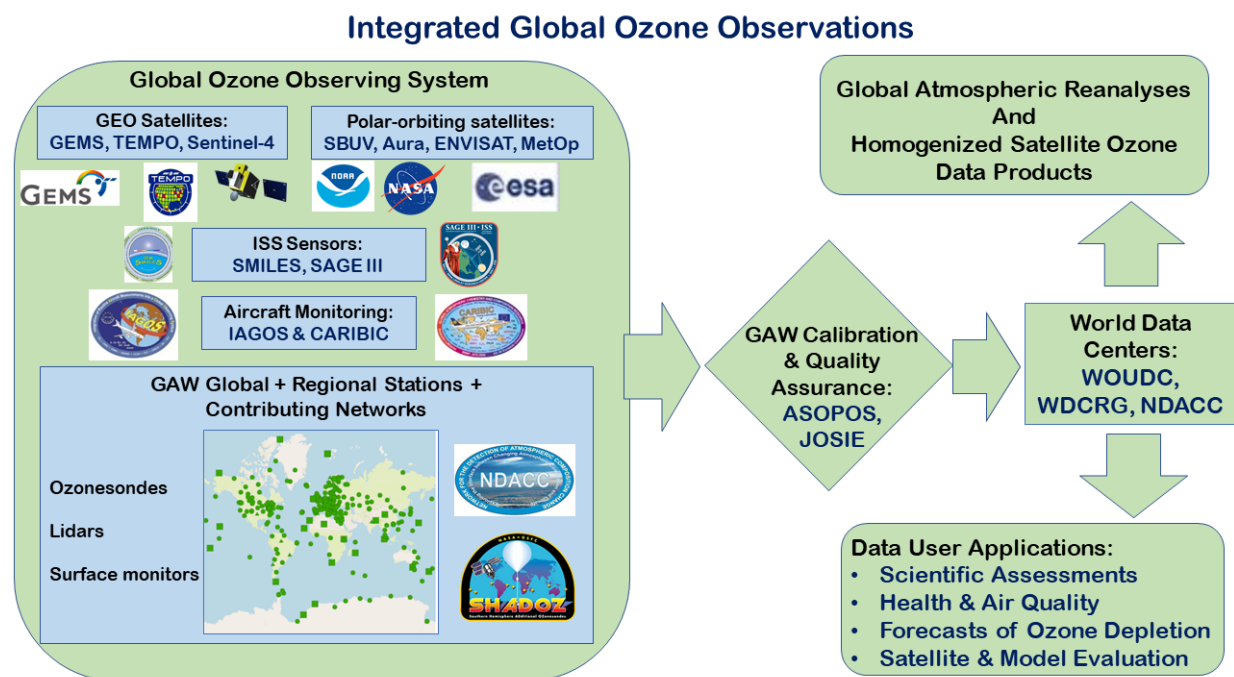


Figure 1–1. Diagram of integrated ozone observations showing connection among the global ozone observing system, GAW calibration and quality assurance activities, and the data products and applications. GEO signifies geostationary. GEMS is operational. TEMPO and Sentinel 4 are due to launch in 2022 or later

1.2. Active Ozonesonde Stations

Table 1–1 lists more than 50 currently active and 12 inactive ozonesonde stations that have sent data to WOUDC and/or the Network for the Detection of Atmospheric Composition Change (NDACC; <http://www.ndaccdemo.org>) since 2005 when the Aura satellite was launched by NASA with four ozone sensors onboard. Since that time, a series of operational ozone-measuring satellites, the GOME and IASI series (EUMETSAT), OMPS (joint NASA/NOAA) and the European TROPOMI research satellite have used ozone profile data for algorithms and validation. A total of 56 stations have provided ≥ 150 ozone profiles each between 2005 and 2019 (**Table 1–1**); they are illustrated in **Figure 1–2** with colours denoting the number of ozone profiles for each station.

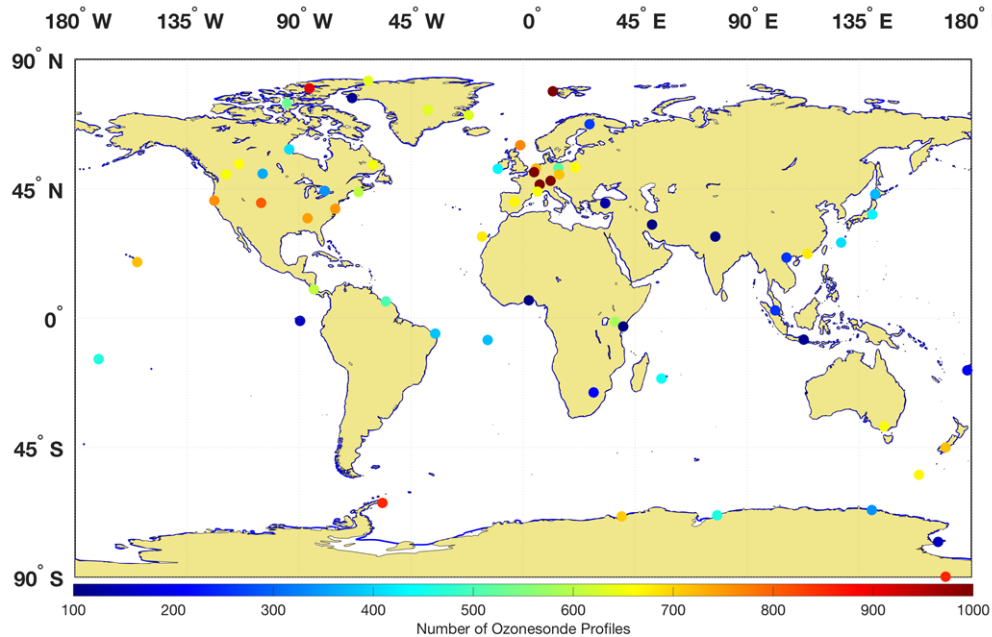


Figure 1–2: Global ozonesonde station locations with the number of ozonesonde profiles from 2005–2019 indicated as shown by the colour-scale

1.3. Ozonesonde Quality Assurance/Quality Control Overview

The ozonesonde is a small and lightweight instrument that measures atmospheric ozone profiles up to about 30–35 km [e.g. Komhyr, 1969; Smit, 2002; Johnson *et al.*, 2002; Thompson *et al.*, 2011]. Interfaced with a regular radiosonde for data transmission, the ozonesonde is flown on a rubber weather balloon (**Figure 1–4**) or in polar conditions with a plastic balloon. During operation the ozone partial pressure, pressure-temperature-humidity (PTU) and wind data are recorded telemetrically by a ground station during an ascent (and at many stations, descent as well) over ~ 2 hours. **Figure 1–5** shows a typical ozone profile, along with temperature, relative humidity and winds. The ozone measurement is based on a chemical reaction between O_3 molecules and differing concentrations of potassium iodide (KI) solutions in cells of inert material (**Chapter 2**). The chemical transformation generates an electric current proportional to the amount of ozone; hence, the name electrochemical concentration cell (ECC). Given the reaction time and typical balloon ascent rate, 5 ms^{-1} , the vertical resolution of the ozone reading is 100–150 m, much better than is possible with remote sensing instruments employed on most satellites.

Ozonesondes are virtually all-weather (i.e. unaffected by clouds and precipitation although launches in extreme weather tend to be avoided), in contrast to most spectroscopic techniques, and they are relatively inexpensive and easy to operate. This makes sondes practical for widespread usage and explains their ubiquity, popularity, and enduring legacy. Satellite algorithms are based on ozonesonde climatologies and operational satellites are validated by the sondes. As the sonde instrument has become more accurate and the number

of long-lasting satellites has increased (**Figure 1–3**), the demand for ozonesonde data has grown. Sonde profiles are being used to detect drift in limb-measuring ozone satellites [Hubert *et al.*, 2016]. Current sonde data are used by the Copernicus Atmospheric Monitoring Service ((<http://atmosphere.copernicus.eu>; CAMS) for Evaluation and Quality Assurance reports and near real time evaluation tools (<https://atmosphere.copernicus.eu/provision-ndacc-observations>).

Since the introduction of the ozonesonde instrument in the 1960s, there have been five designs, including those of European, US, Japanese, Indian and Chinese manufacture [GAW Report No. 201, 2014; Zhang *et al.*, 2014 a, b]. At the present time all but one of the global stations in **Figure 1–2** (Hohenpeissenberg, Germany) use the electrochemical concentration cell (ECC) type of sonde [Komhyr, 1969]. **Figure 1–4** shows ECC sondes in preparation and operation.

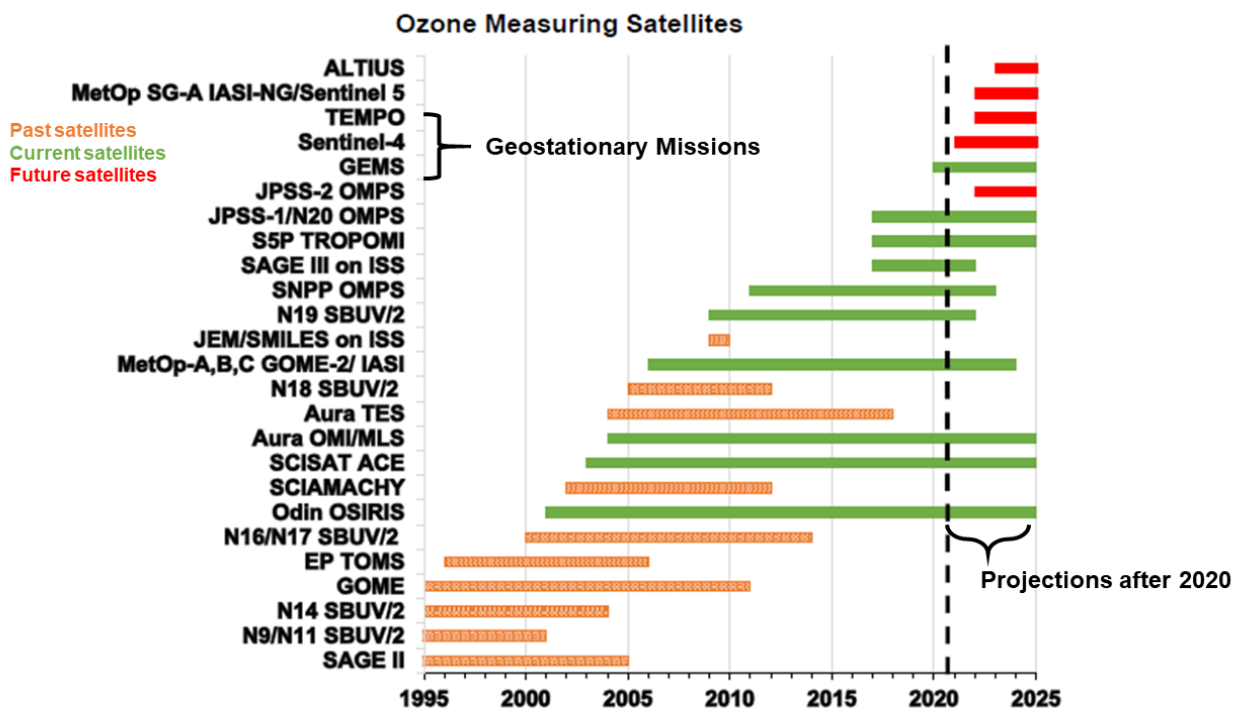


Figure 1–3: Timeline of major ozone-measuring satellites that use ozonesonde data for algorithm development, ground-truth and drift-detection

Each sonde is a unique instrument and needs to be prepared and tested prior to launch. Thus, a standard set of procedures and an accepted common reference are required to ensure the comparability of data taken with different instruments. Two essential aspects of quality assurance that have been developed over the past two decades are: (1) laboratory and field tests in which different types of ozone instruments and preparation procedures are intercompared, and checked against an independent ozone reference instrument in a chamber [Thompson *et al.*, 2019] that simulates ozone, pressure and temperature conditions of standard atmospheres (polar, midlatitude, tropical); and (2) requirements to record metadata for each instrument launched that allow traceability of archived profiles [Witte *et al.*, 2017]. The laboratory tests are described in **Section 1.3.1**. Metadata requirements are outlined in **Annex B**. Routine testing of freshly manufactured sondes should, in principle, detect changes in instruments and/or instrument materials and give more confidence in the reliability of trends that are based on sounding data. A third component of quality assurance is the ASOPOS process by which a group of ~20 ozonesonde data providers regularly test and evaluate sonde performance to recommend operating procedures for new and existing ozonesonde stations. ASOPOS activities, culminating in this volume, are described in **Sections 1.3.1 and 1.3.2** below.

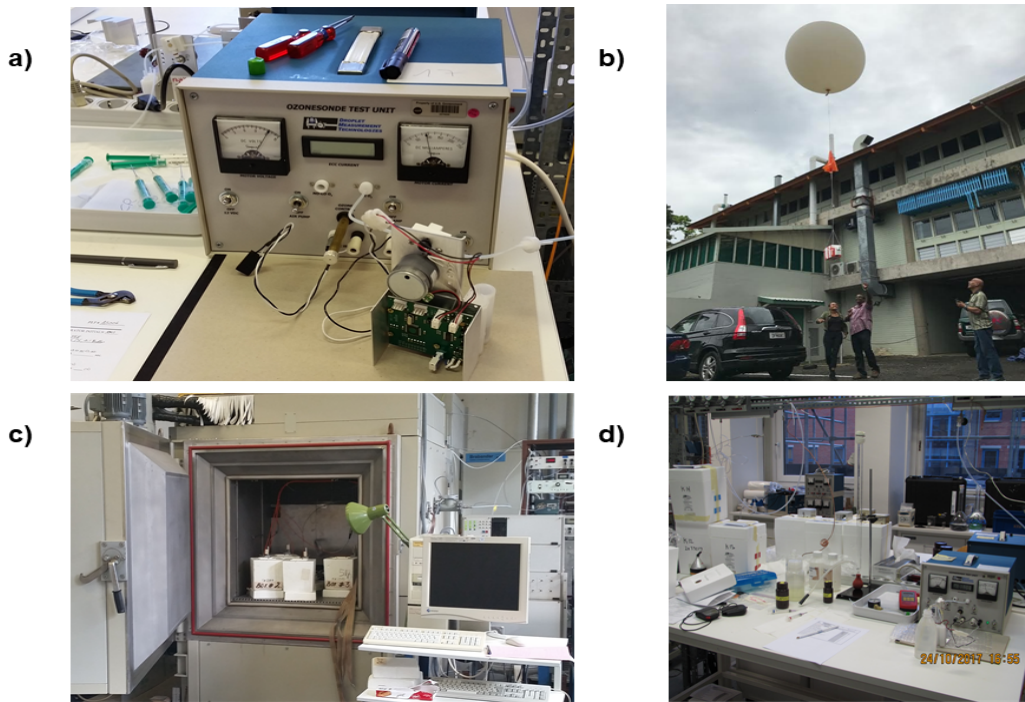


Figure 1–4: (a) ECC ozonesonde being prepared on Test Unit; (b) sonde launch at the Fiji SHADOZ station; (c) WCCOS environmental simulation chamber in Jülich, Germany; (d) JOSIE laboratory (2017) with ozonesonde preparation.

Credits: (a) (c) (d): A. M. Thompson (NASA); (b) B. J. Johnson (NOAA)

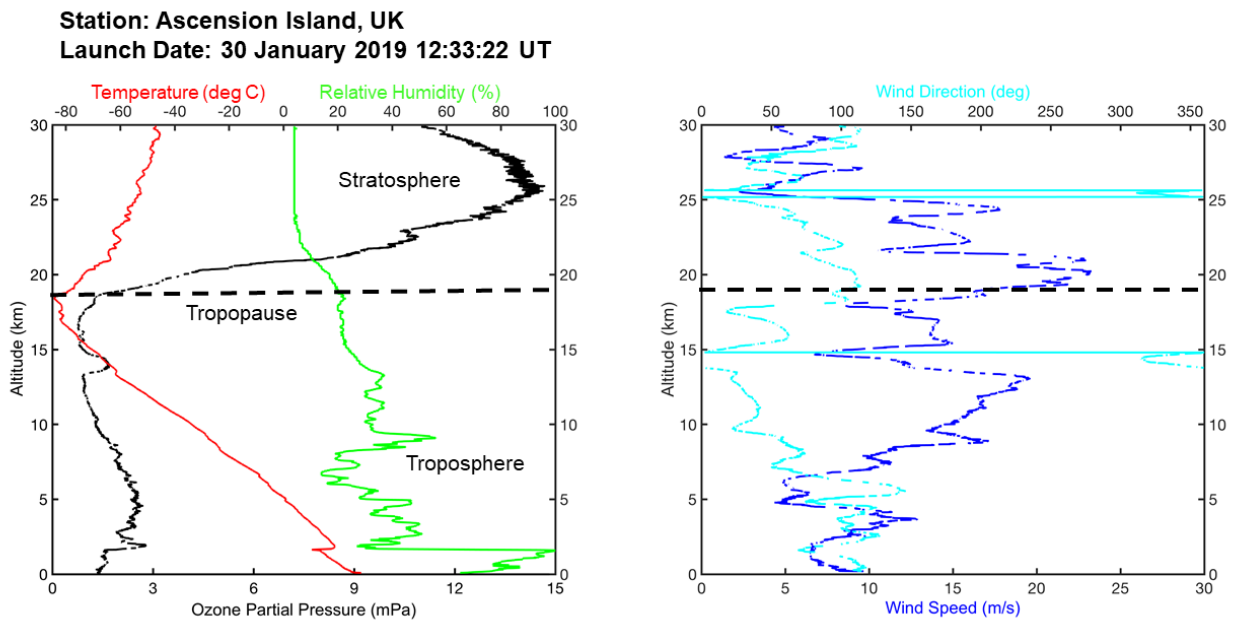


Figure 1–5: Left: Typical tropical ozonesonde profiles with ozone partial pressure (black), RH (%), green) and temperature (°C, red). Right: wind speed (m/s, blue) and direction (degrees, cyan)

1.3.1. WCCOS & JOSIE Laboratory Tests. BESOS and ASOPOS GAW Report No. 201 (2014)

The laboratory tests are conducted in a custom-built environmental simulation chamber at the WMO/GAW designated World Calibration Centre for OzoneSonde (WCCOS: <https://www.wccos-josie.org/wccos>) operated by the Research Centre Jülich. The WCCOS was established in 1995 as part of the quality assurance plan of GAW [GAW Report No. 104, 1995]. Details of the WCCOS are described in [Smit and Kley, 1998; Smit et al., 2000] and follow-on publications [Smit et al., 2004a; 2004b; 2007; Thompson et al., 2019]. The simulation facility controls pressure, temperature and ozone concentration, thereby simulating the flight conditions of ozone soundings up to an altitude of 35 km. A fast response dual-beam UV-absorption ozone photometer (OPM) [Profitt and McLaughlin, 1983] serves as the reference instrument for the test chamber (**Figure 1-4c**). A series of laboratory tests (**Table 1-2**), each one known as a Jülich OzoneSonde Intercomparison Experiment (JOSIE; <https://www.wccos-josie.org/josie>), has been carried out since 1996 as summarized in Smit and Kley, 1998 [GAW Report No. 130] and Smit and Straeter, 2004 a,b [GAW Reports No. 157, 158]. JOSIE results support the following aspects of quality assurance:

- The establishment and updating of standard operating procedures (SOP) for various sonde types
- Periodic performance checks on sondes from various manufacturers against a common reference
- Tests of time response and other aspects of solutions with varying composition
- Evaluation of sonde preparation practices from various sounding laboratories

The performance characteristics evaluated in JOSIE are used to determine the accuracy and precision of individual sondes. Also studied are the responses of various ozonesondes as a function of altitude, temperature and ambient ozone concentration over a range of simulated atmospheric conditions. The JOSIE campaigns address evolving issues, with a focus since 2000 on handling procedures and performance of the ECC sonde type [Smit et al., 2007; Thompson et al., 2007b; Thompson et al., 2019].

The JOSIEs have demonstrated that high precision and accuracy depend not only on sonde manufacturer, but also on the KI sensing solution composition and preparation procedures, with the latter affecting important parameters like initial response time and background current [Smit et al., 2007]. Specifically, the two ECC sonde versions most commonly used today, the Science Pump Corporation SPC-6A and the (originally labelled) Environmental Science Corporation (or EN-SCI) Model Z or 2Z, differ by 3%–5%, when the same cathode sensing solution is used. As a result, the report prepared by H. Smit and ASOPOS, *GAW Report 201* [2014], recommended unique sensing solutions for each ECC sonde type (See Chapter 2 for details). *GAW Report No. 201* [2014] was heavily based on the 1996 and 1998–2000 JOSIE results and a 2004 field campaign, the WMO/BESOS (Balloon Experiment on Standards for Ozonesondes) in Laramie, Wyoming, USA. BESOS deployed a large gondola with 18 ozonesondes prepared according to the preliminary SOP and flown with the same UV-photometer (OPM) as used in JOSIE-2000 at WCCOS in Jülich. Similar to JOSIE-2000 [Smit et al., 2007], BESOS primarily tested variations in sensing solutions [Deshler et al., 2008]. At the first ASOPOS meeting, held in Geneva in 2004, panellists unanimously agreed that because the sonde differences observed in JOSIE 1998–2000 were confirmed in BESOS, the JOSIE-simulation chamber experiments are representative of the actual atmosphere itself. The ASOPOS-2004 recommendations for SOP for ECC sondes were approved by the May 2007 meeting of the WMO/GAW Scientific Advisory Group for ozone (SAG-O₃) in Tenerife, Spain.

1.3.2. ASOPOS and JOSIE Activities since 2010

Several developments after the approval of the ASOPOS 2007 [GAW Report 201, 2014] recommendations have dominated the topic of ozonesonde Quality Assurance in the past decade. One is the use of “non-standard” sensing solution types by a number of ozonesonde measuring groups. Measurements using the new solution formulations need to be tested and

compared with the measurements from currently recommended sonde-solution pairings in a controlled experiment. Second, the growing popularity of sonde data for ozone profiles trends, validation of satellite instruments and evaluation of secondary satellite products have led to demand for higher accuracy and precision than the 10%–15% cited in early WMO/UNEP quadrennial ozone assessments [*WMO/UNEP*, 1991; 1995; 1999] and similar studies (ie. SI²N (supported by SPARC, IOC [International Ozone Commission], IGACO [Integrated Global Atmospheric Chemistry Observations, *IGACO*, 2008], NDACC), LOTUS [Long-term Ozone Trends and Uncertainties in the Stratosphere; <https://www.sparc-climate.org/activities/ozone-trends/>]). The LOTUS activity highlighted the large uncertainties in lower stratospheric trends, a region of the atmosphere in which sonde resolution is superior to that of the satellites used in trends analysis.

1.3.2.1. Homogenization of Data Records

Major contributors to uncertainties in ozone trends were identified as discontinuities and biases in the records for many ozonesonde stations decades with long data records. Thus, ASOPOS initiated an activity on “homogenizing” time series for a given site to compensate for instrument changes. Guidelines for homogenizing records, largely based on JOSIE-2000 and BESOS, were published in 2012 (<https://www.wccos-josie.org/o3s-dqa/>); an update can also be found in [Annex D](#) of this report.

Homogenization recommendations include specifications for how to treat variations in background current and pump properties (temperature and pump efficiency changes at low pressures). An important foundation for homogenization is the use of “transfer functions” based on altitude dependent ratios of the measurement of one solution-instrument combination with another [*Deshler et al.*, 2017].

About half the current regularly operating stations have homogenized their data [*Van Malderen et al.*, 2016; *Tarasick et al.*, 2016; *Thompson et al.*, 2017; *Sterling et al.*, 2018; *Witte et al.*, 2017; 2018]. However, evaluations of reprocessed data revealed persistent discontinuities and biases at several tropical stations that appear to have instrumental origins [*Thompson et al.*, 2017; *Sterling et al.*, 2018]. It was noted that in 2011 and again in 2015 that the manufacturer of one of the two types of ECC sensors – the ENSCI instrument – changed ([Chapter 2](#)). The current designation of the latter instrument, ENSCI (<https://en-sci.com>), is used in this report.

1.3.2.2. JOSIE-SHADOZ (2017)

The participants and procedures in the 2017 JOSIE were drawn from the Southern Hemisphere Additional Ozonesonde (SHADOZ) project as part of a training and capacity building effort [*Thompson et al.*, 2019]. The campaign (**Table 1–2**) was designed with two purposes in mind. The first goal was to re-visit the SOP of the GAW Report 201 [*Smit and ASOPOS Panel*, 2014] by re-evaluating the instrument-solution pairings of JOSIE-2000 and BESOS as well as certain preparation and handling procedures. Second, non-standard solutions were tested along with unused instruments of different ages, including some of those corresponding to the periods before and after the ENSCI manufacturer change. In addition, a series of tests with alternate preparation steps and non-standard solutions was performed. The preliminary results showed excellent agreement with the WCCOS reference UV-photometer. The mean total ozone from the SHADOZ protocols (conforming to the SOP-2014 recommended instrument-solution pairings for 7 of 8 participants) and the tests with the “alternate” solutions and handling techniques were all within 3% of the reference. Biases in the instrument type that were noted in the 1998–2000 JOSIEs and BESOS [*Smit et al.*, 2007; *Thompson et al.*, 2007b; *Deshler et al.*, 2008] were confirmed. Although measurements with the alternate solution type showed an improvement in the upper tropospheric portion of the profiles, with smaller errors in the sensitive near-tropopause region, they were on average 5%–6% lower in the stratospheric portion of the profile than with the SHADOZ protocols (**Figure 1–6**).

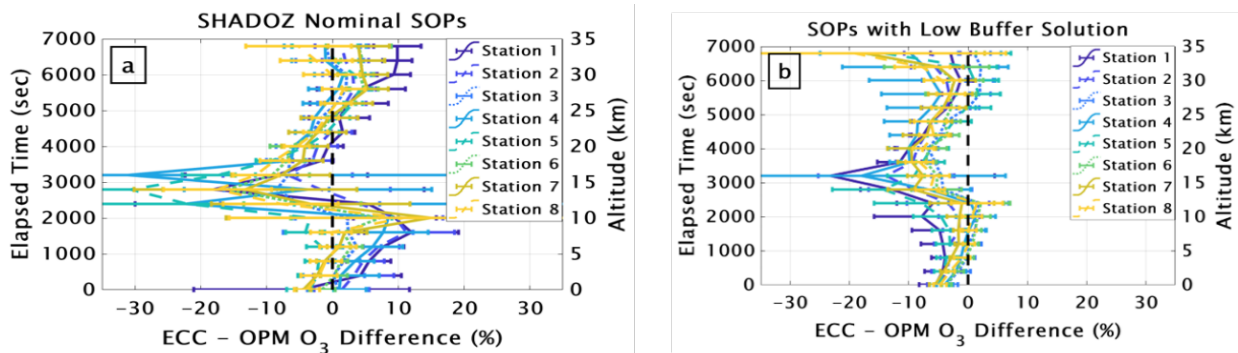


Figure 1–6: Summary of JOSIE-SHADOZ profiles, each based on 40 total simulations [Thompson *et al.*, 2019]. The ozonesondes were new and collected from a variety of laboratories. (a) SHADOZ operators used their individual station preparation steps and sensing solutions; (b) all operators used the same low-buffer solution and preparation procedures

1.3.2.3. Uncertainties, Reprocessing, New ECC Instrument Issues

Stimulated partly by interactions between GCOS Reference Upper Air Network (GRUAN; <https://www.gruan.org>) and the SHADOZ project (https://www.gruan.org/gruan/editor/documents/meetings/icm-10/pres/pres_0723_Smit_JOSIE-2017_SHADOZ.pdf) and partly by the sonde data user communities, ASOPOS has recently given much attention to analyses of uncertainties (Tarasick *et al.*, 2021; Chapter 3 below). To date, only the reprocessed SHADOZ [Witte *et al.*, 2018] and Wallops [Witte *et al.*, 2019] data have been archived with a total uncertainty for each ozone reading. Ozonesonde stations are continuing to reprocess their data, especially in Europe where to date two stations have documented new datasets [Van Malderen *et al.*, 2016].

Sonde profile reprocessing has produced datasets that are more consistent and have lower and better quantified uncertainties than before. For example, within the SHADOZ network, agreement between the total column ozone (TCO) sonde data and TCO from satellite overpasses and co-located ground-based instruments improved from a typical offset of 6%–8% in the Total Ozone Mapping Spectrometer (TOMS)-era evaluation [Thompson *et al.*, 2003a,b] to an average 2% for the reprocessed data covering three generations of BUUV-type sensors from 1998–2016 [Thompson *et al.*, 2017]. In principle, this implies that we have more confidence in trends based on the reprocessed data. On the other hand, with better overall precision, the reprocessed data have unmasked an unexpected sudden post-2014 drop-off in TCO at a number of SHADOZ and Canadian stations. Further, when the data from currently active non-polar stations are examined carefully, Stauffer *et al.* [2020] found that ozone at about a third of the global stations displays post-2014 TCO drop-offs, ranging from 3% to 6%. Since the publication of Stauffer *et al.* [2020], 23 additional stations have been analysed for 60 datasets total. Only one of the 23, Idabel, OK, USA (**Table 1–1**), currently inactive, showed a small (3%) TCO drop. The magnitude of the TCO low bias at most affected stations has become smaller in the last 1–2 years. The reason(s) for the drop-off remain uncertain but appear to be related to instrument manufacture and sensing solution type. Several groups are investigating the issue further, examining detailed metadata from existing stations, conducting laboratory tests, and designing special field tests.

1.4. Scope of Present Report

This report serves as an update of GAW Report No. 201 (*Smit and ASOPOS panel, 2014*; hereafter referred to as [GAW Report No. 201, 2014]) that describes quality assurance criteria for ozonesondes and SOP for ozonesonde operations. Given the developments described in the prior section and the expanding use of sonde data by the satellite, assessments, and modelling communities, our report is aimed at data users as well as data providers. Thus, although the topics follow those of [GAW Report No. 201, 2014], the chapters on uncertainties ([Chapter 3](#), [Annex C](#)) and data quality indicators ([Chapter 5](#)) are more extensive.

We begin with a description of the ozonesonde instrument ([Chapter 2](#)). The data quality goals ([Chapter 3](#)) summarize relevant experiments to date, key parameters for which standards are set, the level of performance desirable and achievable, and a detailed discussion of uncertainties. Three new concepts are introduced. First, the traditional “pump efficiency factors” used in processing sonde readings [*Komhyr, 1986; Komhyr et al., 1995*] are in fact empirical correction factors, not pump efficiencies, per se, as might be measured in the laboratory. Second, we require that all parameters reported reflect, to the extent that they are known, the actual physical and chemical processes taking place in the ozonesonde measurement. Related to the second concept, the nature of the so-called “background current” is considered in detail. The SOP, with recommendations on preparation steps, launching and data processing are given as before in [Chapter 4](#) and [Annex A](#), with the JOSIE-SHADOZ results and several follow-on field tests as the basis. Data quality indicators have been expanded with particular attention to the need for extensive and consistent metadata ([Chapter 5](#), [Annex B](#)), including ozonesonde and radiosonde serial numbers, the composition of the sensing solution, the final background current, and measurements of the laboratory conditions (i.e. pressure, temperature, humidity) during the ozonesonde preparation. These data are required for reprocessing and for users to understand the comparability of various datasets. [Annex C](#) provides recommendations for the reporting of uncertainties and [Annex D](#) details steps for the reprocessing of long-term datasets. Other supporting information appears in [Annexes E](#) (Acronyms) and [F](#) (ASOPOS 2.0 People Involved).

Table 1–1: Global ozonesonde station locations and approximate number of ozonesonde data records from 2005–2019.

*Denotes that the station is not currently active. Data for these stations are located at the WOUDC, NDACC, SHADOZ or NOAA GML archives

Site	Latitude (deg)	Longitude (deg)	No. of Profiles (#)
Alert, Canada	82.49	-62.34	646
Eureka, Canada	79.98	-85.94	910
Ny-Ålesund, Norway	78.92	11.93	1131
Thule, Greenland	76.53	-68.74	119*
Resolute, Canada	74.7	-94.96	532
Summit, Greenland	72.34	-38.29	634*
Scoresbysund, Greenland	70.48	-21.97	633
Sodankylä, Finland	67.37	26.65	262
Lerwick, UK	60.13	-1.18	765
Churchill, Canada	58.74	-94.07	409
Edmonton, Canada	53.54	-114.1	662
Goose Bay, Canada	53.31	-60.36	650
Legionowo, Poland	52.4	20.97	660
Lindenberg, Germany	52.21	14.12	512
DeBilt, Netherlands	52.1	5.18	723

Site	Latitude (deg)	Longitude (deg)	No. of Profiles (#)
Valentia, Ireland	51.94	-10.25	430
Uccle, Belgium	50.8	4.35	2105
Bratt's Lake, Canada	50.2	-104.7	363*
Praha, Czech Republic	50.01	14.45	715
Kelowna, Canada	49.93	-119.4	655
Hohenpeissenberg, Germany	47.80	11.02	2022
Payerne, Switzerland	46.49	6.57	2152
Egbert, Canada	44.23	-79.78	342*
Haute Provence, France	43.94	5.71	655
Yarmouth, Canada	43.87	-66.11	606
Sapporo, Japan	43.06	141.33	373*
Trinidad Head, California, USA	40.8	-124.16	760
Madrid, Spain	40.47	-3.58	668
Boulder, Colorado, USA	40	-105.25	804
Ankara, Turkey	39.95	32.88	138
Wallops Island, Virginia, USA	37.93	-75.48	753
Tateno (Tsukuba), Japan	36.06	140.13	470
Huntsville, Alabama, USA	34.72	-86.64	745
Esfahan, Islamic Rep. of Iran	32.51	51.7	75
Izana, Tenerife, Spain	28.3	-16.5	677
New Delhi, India	28.3	77.1	24
Naha, Japan	26.21	127.69	407*
Hong Kong, China	22.31	114.17	678
Hanoi, Vietnam	21.01	105.8	257
Hilo, Hawaii, USA	19.43	-155.04	716
Costa Rica	9.94	-84.04	605
Cotonou, Benin	6.2	2.2	97*
Paramaribo, Surinam	5.8	-55.21	504
Kuala Lumpur, Malaysia	2.73	101.27	258
San Cristobal, Ecuador	-0.92	-89.62	156*
Nairobi, Kenya	-1.27	36.8	585
Malindi, Kenya	-2.99	40.19	20*
Natal, Brazil	-5.42	-35.38	383
Watakosek, Java, Indonesia	-7.5	112.6	111*
Ascension Island, UK	-7.58	-14.24	379
Pago Pago, American Samoa	-14.23	-170.56	465
Suva, Fiji	-18.13	178.4	195
Réunion Island, France	-21.06	55.48	443
Irene, South Africa	-25.9	28.22	206
Broadmeadows, Australia	-37.69	144.95	658
Lauder, New Zealand	-45	169.68	715

Site	Latitude (deg)	Longitude (deg)	No. of Profiles (#)
Macquarie Island, Australia	-54.5	158.95	668
Marambio, Antarctica	-64.24	-56.62	851
Dumont d'Urville, Antarctica	-66.7	140	341
Davis, Antarctica	-68.58	77.97	460
Syowa, Antarctica	-69	39.58	706
Neumayer, Antarctica	-70.62	-8.37	1067
McMurdo, Antarctica	-77.85	166.67	152*
South Pole, Antarctica	-90	169.68	854

Table 1–2: JOSIE activities on ozonesonde procedures and related reports

Campaign	Objective
JOSIE-1996 GAW Report No. 130 [Smit and Kley, 1998]	<ul style="list-style-type: none"> Operating Procedures Profiling Capabilities Intercomparison sonde types (e.g. ECC, Brewer-Mast, KC79)
JOSIE-1998 GAW Report No. 57 [Smit and Straeter, 2004a]	<ul style="list-style-type: none"> ECC sonde manufacturer differences (SPC, ENSCI) Brand new sondes provided by sounding stations (randomly taken)
JOSIE-2000 GAW Report No. 158 [Smit and Straeter, 2004b] [Smit et al., 2007]	<ul style="list-style-type: none"> Operating Procedures Focus on ECC sonde Different sensing solution types Different manufacturers (SPC, ENSCI) Basis for a preliminary SOP-V1.0 adopted in April 2001 at a workshop at Geneva, Switzerland
BESOS-2004 [Deshler et al., 2008]	<ul style="list-style-type: none"> Testing Standard Operating Procedures (SOP V1.0) under flight conditions Focus on ECC sonde Different sensing solution types Different manufacturers (SPC, ENSCI) Unanimous agreement on SOP's by the ASOPOS 1.0 Panel – outcome of a Jülich Workshop in September 2004
ASOPOS 2002–2012 GAW Report No. 201	<ul style="list-style-type: none"> Define and establish Standard Operating Procedures for ECC sondes: Evolution of SOP-V1.0 into new SOP-V2.0
JOSIE-2009	<ul style="list-style-type: none"> Compared newly manufactured ECC sondes (SPC, ENSCI) Brand new sondes provided by sounding stations (randomly taken)
JOSIE-2010	<ul style="list-style-type: none"> Refurbished sondes

Campaign	Objective
JOSIE-2017-SHADOZ [Thompson et al., 2019]	<ul style="list-style-type: none"> • Tested manufactured ECC sondes (SPC, ENSCI) provided by participating sounding stations • Tested Standard Operating Procedures for ECC sondes • Preparatory Workshop was conducted in September 2016 at Edinburgh, UK, at Quadrennial Ozone Symposium
O3S-DQA Guidelines Report-2012 [Smit and O3S-DQA, 2012].	<ul style="list-style-type: none"> • Recommendations for Homogenization and Uncertainties • Basis was several workshops: <ul style="list-style-type: none"> (a) January 2009 at Jülich, Germany (b) October 2011 at Boulder, USA. (c) April 2012 at Washington, USA. (d) September 2012 at Toronto, Canada

2. OZONESONDE-ELECTROCHEMICAL CONCENTRATION CELL (ECC) (Herman G.J. Smit)

2.1. Introduction

The setup of a typical ozone sounding system is shown in **Figure 2–1**. During normal flight operation, ozonesondes are coupled via interfacing electronics to standard meteorological radiosondes for real time transmission of the measured ozone sensor current, pump temperature, plus standard aerological parameters: pressure, temperature, humidity, and GPS (Global Positioning System) determined position including the derived GPS-pressure plus wind direction and speed. The ozone data transmitted to the ground station are further processed (**Chapters 3** and **4**). The wind-finding capabilities of modern radiosondes are based on GPS satellite navigation [e.g. *Dabberdt et al.*, 2014; *Guide to Instruments and Methods of Observation* (WMO-No. 8 Report, Volume I), 2018].

The total weight of the ozonesonde-radiosonde package is about 1.5 kg, so it can be flown on a weather balloon; an 800-g balloon usually gives enough lift to reach 20 hPa (**Figure 2–1**). Normally data are taken during ascent to a balloon burst altitude of 30–35 km at a typical rise rate of ~5 m/s; some stations record descent data, as well, although the uncertainties and altitude resolution differ from the ascent measurement. The inherent response time of the ozonesonde is 18–28 s (**Chapter 4**) so that the effective vertical resolution of the ozone profile is ~100–150 m.

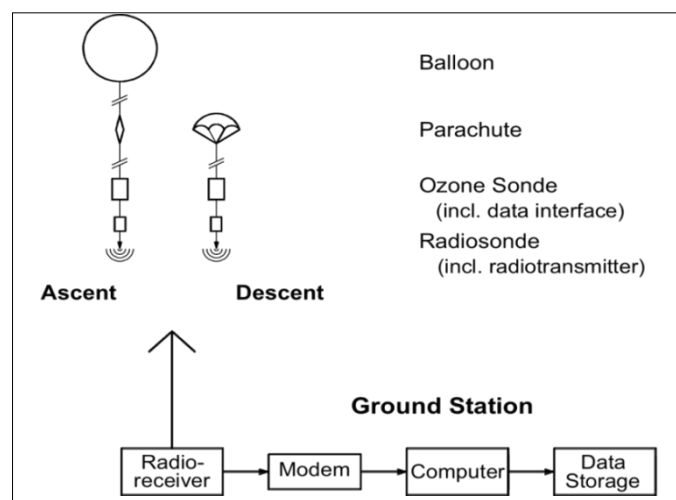


Figure 2–1: Set up of an ozone sounding system

In the past 50 years, there have been three main types of ozonesondes used in the global ozonesonde network [*Smit*, 2014]. All are based on an electrochemical method converting the sampled ozone into an electrical current: the electrochemical concentration cell (ECC) [*Komhyr*, 1969]; the Brewer-Mast (BM) [*Brewer and Milford*, 1960] and the carbon iodine cell (KC96) [*Kobayashi and Toyama*, 1966]. Although the principle of operation is similar for all three sonde types, the instrument layouts are significantly different for each sonde type [*GAW Report No. 201*, 2014].

In 2008 the Japan Meteorological Agency (JMA) stopped flying the KC96 and started to deploy ECC sondes at their sounding stations. Most stations flying BM sondes transitioned to the ECC in the early 1980s (Canadian stations) and in 1990s (Uccle, Belgium; Payerne, Switzerland; Bradmeadows and Macquarie Island, Australia). Only the Hohenpeissenberg, Germany, station still operates the BM ozonesonde in a time series that started in 1967. All other stations listed in **Table 1–1** are currently flying the ECC sonde instrument. This report deals only with the ECC ozonesonde. The BM and KC96 ozonesondes and their standard operating procedures (SOP's) are described in detail in the GAW Report No. 201 [*Smit and the ASOPOS Panel*, 2014].

Figure 2–2 shows examples of vertical ozone sounding profiles obtained at representative midlatitude, tropical and polar sites. Ozonesondes have a high vertical resolution of about 100 m in contrast to most remote sensing techniques.

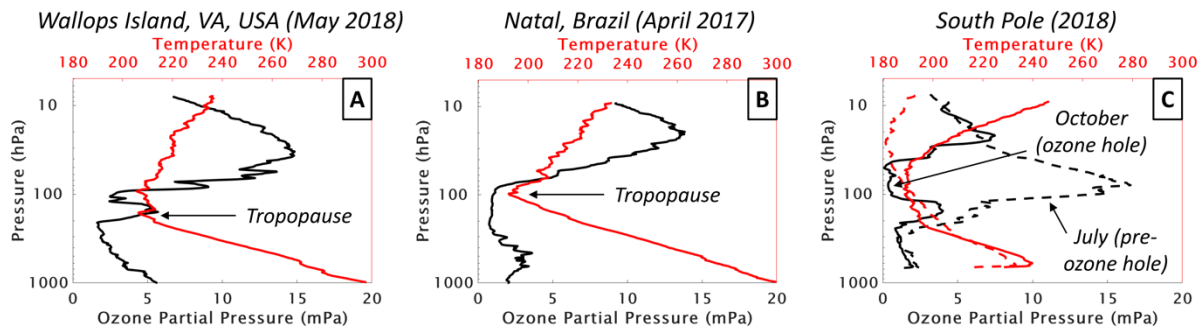
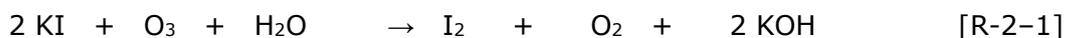


Figure 2–2: Examples of ozone sounding examples: (A) a midlatitude profile from Wallops Island, VA, USA (37.9 °N, 75.5 °W) showing a tropopause fold; (B) a tropical profile from Natal, Brazil (5.5 °S, 35.4 °W), showing low ozone partial pressures with a high tropopause; (C) the difference between the July and October 2018 high-latitude profiles from South Pole (90 °S, 169.7°E); the October profile shows the lower stratospheric depletion associated with the ozone hole

2.2. Principle of Operation and Instrument Design

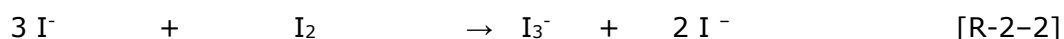
The ECC ozonesonde is based on the electrochemical method after [Komhyr, 1969]. The ozone measurement is based on the titration of ozone in a potassium iodide (KI) sensing solution according to the redox reaction:



The ECC ozone sensor uses an electrochemical cell consisting of two half cells, made of Teflon or moulded plastic, which serve as cathode and anode chambers. Both half cells contain platinum mesh electrodes, each one immersed in a KI-solution of different concentrations. The two chambers are linked together by an ion bridge (length ~ 0.5 cm and diameter ~ 0.2 cm) in order to provide an ion pathway and to prevent mixing of the cathode and anode electrolytes.

The ECC sensors do not require an external electrical potential. The ECC gets its driving electromotive force from the difference in the concentration of the KI-solution in the cathode and anode chambers, $0.03\text{--}0.06 \text{ mole L}^{-1}$ ($=0.5\%\text{--}1\%$ KI) and about 8 mole L^{-1} (KI-saturated) respectively. The schematics of the ECC ozone sensor are displayed in **Figure 2–3**. The sensor, size about $8 \times 8 \times 14$ cm, is enclosed in a Styrofoam flight box ($\approx 19 \times 19 \times 25$ cm).

A chemically inert gas sampling pump made of Teflon [Komhyr, 1967] bubbles ozone in ambient air through the cathode cell containing the lower concentration KI sensing solution, resulting in an increase of “free” iodine (I_2) according to the redox reaction [R-2-1]. Transported by the stirring action of the air bubbles the „free” I_2 makes contact with the cathode and is converted back to 2I^- through the uptake of two electrons, whereas at the surface of the Pt-anode, I^- is converted to I_2 through the release of two electrons. The overall cell reaction is:



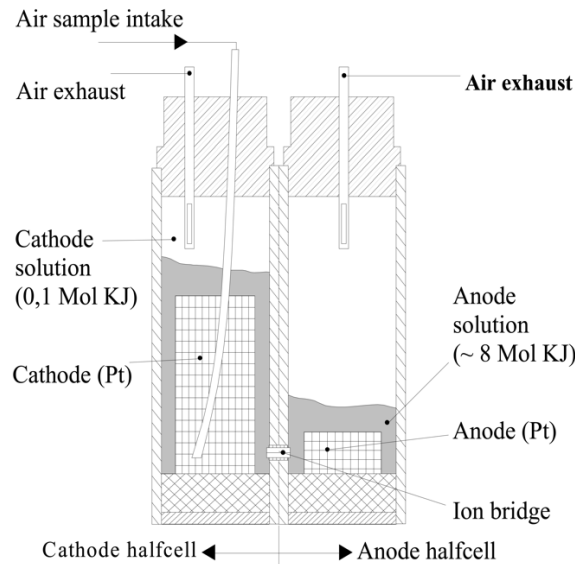


Figure 2–3: Schematic of the electrochemical concentration sensing cell. The KI-solution strength in the cathode and anode chambers are 0.03–0.06 mole L⁻¹ (=0.5%–1% KI) and about 8 mole L⁻¹ (KI-saturated), respectively

Thus, in principle, each ozone molecule causes two electrons to flow in the external electrical circuit. The electrical current is thus directly related to the uptake rate of ozone in the cathode chamber.

The electrical current I_M [μA] generated in the external circuit of the electrochemical cell is, after correction for a background current I_B [μA], directly related to the uptake rate of ozone in the sensing solution. By knowing the gas volume flow rate Φ_{P0} [cm^3s^{-1}] of the air sampling pump, its temperature T_P [K] and the total (i.e. overall) efficiency of the ozone sensor η_T , the measured ozone partial pressure P_{O3} [mPa] is determined by the conventional relation:

$$P_{O3} = 0.043085 * \frac{T_P}{(\eta_P * \eta_A * \eta_C * \Phi_{P0})} * (I_M - I_B) \quad [\text{E-2-1}]$$

The constant 0.043085 is determined by the ratio of the universal gas constant to two times the Faraday constant (because two electrons flow in the electrical circuit from Reaction R-2-2).

The total efficiency η_T consists of:

η_P = Pump flow efficiency as a function of pressure;

η_A = Absorption efficiency for the transfer of the sampled gaseous ozone into the liquid phase;

η_C = Conversion efficiency of the absorbed ozone in the cathode sensing solution into iodine and finally into the measured cell current I_M .

Basic Formula of ECC-Operation:

The number of moles of ozone, n_{O3} , sampled per second and cm^3 are

$$n_{O3} = \frac{(I_M - I_B)}{(\eta_P * \eta_A * \eta_C * 2 * F * \Phi_{P0})} \quad [\text{E-2-2}]$$

where F is Faraday's constant ($= 9.6487 \times 10^4 \text{ C mole}^{-1}$). By applying the ideal gas law, the corresponding partial pressure of ozone P_{O3} can be expressed as

$$P_{O3} = \frac{R}{2 * F} * \frac{T_P}{(\eta_P * \eta_A * \eta_C * \Phi_{P0})} * (I_M - I_B) \quad [\text{E-2-3}]$$

where R is the universal gas constant ($= 8.314 \text{ J K}^{-1} \text{ mole}^{-1}$)

Currently, there are two manufacturers of ECC ozonesondes, Science Pump Corporation and Environmental Science Corporation (**Table 2-1**), producing now the SPC-6A and ENSCI-Z ozonesonde types (**Figure 2-4**), respectively. The designs of both ECC types are somewhat similar but there are three differences:

- The material of the electrochemical cell: Teflon for SPC-6A and moulded plastic for ENSCI-Z;
- Ion bridges (details are not really known for either manufacturers [proprietary]);
- Layout of the metal frame: the electrochemical cell of the SPC-6A is mechanically more integrated with the metal frame of the sonde than is the ENSCI-Z sonde which is only mounted to the metal frame of the sonde.

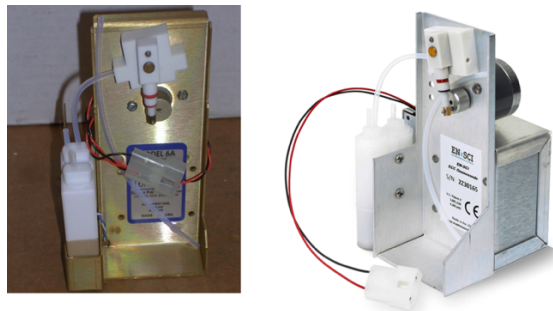


Figure 2-4: ECC ozonesonde types SPC-6A (left) and ENSCI-Z (right) manufactured by Science Pump Corporation (Camden, NJ, USA) and EN-SCI (Westminster, CO, USA), respectively

Table 2-1: Electrochemical concentration cell (ECC) ozonesonde models and manufacturers

Source: Johnson et al., 2002

Manufacturer	Model Number	Years Manufactured	Design Changes
Science Pump	1A	1968	Initial ECC ozonesonde model
Science Pump	3A	1968-1981	Rectangular pump
Science Pump	4A	1978-1995	Switch to cylindrical piston pump
Science Pump	5A	1986-1997	Start of digital data acquisition
Science Pump	6A	1995-present	Drilled hole in Teflon base of the pump for thermistor to measure internal pump temperature
EN-SCI, DMT, EN-SCI ¹	1Z & 2Z	1993-present	Moulded plastic sensor cell & drilled hole in the Teflon base of the pump for a thermistor to measure internal pump temperature

¹ EN-SCI started production in 1993. In early 2011 the EN-SCI was bought by Droplet Measurement Technologies (DMT, Boulder, USA), who continued to manufacture this sonde model under their name. In 2016, EN-SCI was spun off by DMT. A new company continues manufacturing these sondes under the name EN-SCI.

These small differences are probably responsible for the 4%–5% difference in performance between the two ECC types when they are flown under the same conditions with an identical sensing solution.

Since 2014, a modified ECC type instrument manufactured at the Institute of Atmospheric Physics (IAP), Beijing, China has been produced [Zhang *et al.*, 2014a,b]. However, only limited comparisons of the Chinese instrument with the more established SPC-6A and ENSCI model types have been carried out up to this time.

Details of the Electrochemical Process in the ECC

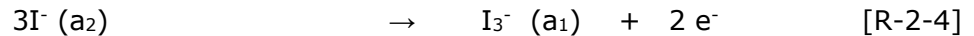
ECC sensors do not require an external electrical potential in contrast to the earlier Brewer-Mast electrochemical ozone sensor [Brewer and Milford, 1960]. The difference in the concentrations of the **KI** solutions in the cathode and anode chambers, 0.5%–1% **KI** (0.03–0.06 Mol/l) and saturated **KI** (8.0 Mol/l), respectively, delivers the electromotive force (**EMF**) for the ECC (for more details see Komhyr [1969]) as:

$$EMF = \frac{-R \cdot T}{2 \cdot F} * \ln(\beta) \quad [E-2-4]$$

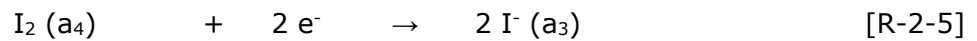
where

$$\beta = \left(\frac{(a_1)_{I_3^-}}{(a_2)_{I_3^-}} \right) * \left(\frac{(a_3)_{I^-}^2}{(a_4)_{I_2}} \right) \quad [E-2-5]$$

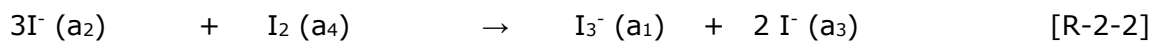
R is the universal gas constant; **F** is the Faradays constant and **T** the temperature of the sensing solutions in anode and cathode chambers; **a₁** and **a₂** are the activities of **I₃⁻** and **I⁻** in the anode chamber with the high **KI** concentration dominated by the oxidation reaction:



a₃ and **a₄** are the activities of **I⁻** and **I₂** in the cathode chamber with low **KI** concentration governed by the reduction reaction:



The overall cell reaction is then:



In an open circuit, **EMF** is approximately 0.13 V (at **T**=25 °C), while in a closed-circuit **EMF** changes such that:

1. **I⁻** ions at the surface of the anode will give up electrons to the anode
2. **I₂** molecules at the surface of the cathode will extract electrons from the cathode

Consequently, the activities **a₁** to **a₄** will change until **β = 1** and the **EMF** approaches zero. This means when ozone is pumped through the cathode sensing solution (lower **KI**-concentration), there will be an increase of **I₂** according the redox reaction (R-2-1). At the cathode surface the chemically formed "free" **I₂** is converted back to **I⁻** ions (R-2-5), while at the anode surface, **I⁻** ions are converted to **I₂**, (R-2-4). This means that **β ≠ 1** and the **EMF** will change from zero such that an electrical current will flow (in the external electrical circuit), which is proportional to the uptake rate of ozone in the sensing solution and chemically converted into "free" Iodine.

2.3. Aspects of Instrumentation and Different Sensing Solutions

During an ozone sounding the electrical cell current I_M and pump temperature T_P are measured by a current to voltage (I/V) converter and a thermistor, respectively. Both are integrated in the interfacing electronics between ECC sonde and radiosonde. The “background current” I_B and initial volumetric flow rate Φ_{PO} of the gas sampling pump of each sonde are determined in the laboratory at ambient air pressure during pre-flight preparations (Chapters 3 and 4). The nature of I_B has been a topic of concern for many years [Thornton and Niazy, 1982; 1983; Smit et al., 1994, Vömel et al., 2020, Tarasick et al., 2020] and is discussed in Section 3.3.6.

The pump efficiency η_P declines with decreasing pressure, as described by empirical efficiency tables that are obtained from pumpflow calibration experiments at pressures between 1000 and 3 hPa (Section 3.3.3). The efficiency of absorption η_A of gaseous O_3 sampled into the liquid sensing solution is close to 1.0 under most conditions (complete absorption; Section 3.3.4), whereas the conversion efficiency of O_3 into I_2 (i.e. the stoichiometry of the overall chemical conversion of O_3 into I_2) during normal operation is also about 1.0 at neutral pH [eg. Saltzman and Gilbert, 1959, Komhyr, 1969], so that from R-2-1, $\eta_c \approx 1$ (Section 3.3.5). Usually a sodium-hydrogen phosphate buffer is added to the cathode sensing KI-solution to keep the pH neutral at 7.0. Equations E-2-1 and E-2-3 assume that if (1) no-ozone is destroyed in the sampling system; (2) no reactions other than R-2-1 cause production or loss of iodine, then each ozone molecule produces two iodine molecules; (3) there are no interfering reactions in the solution from minor constituents other than ozone in the air sample [SPARC-IOC-GAW, 1998]. These assumptions, together with their associated uncertainties contributing to the overall uncertainty of the sonde measurement of P_{O_3} , are discussed in detail in Chapter 3.

Three different aqueous (distilled or highly purified water) sensing solution types are commonly used in the ECC sonde cathode cells; in all cases a KI-saturated cathode solution is employed in the anode cell (See Table 2-2). Laboratory studies by Johnson et al. [2002] found that, depending on the concentration of the cathode sensing solution, the stoichiometric ratio of the ozone to iodine conversion (R-2-1) can increase from 1.00 up to 1.05–1.20. Johnson et al. [2002] determined that this increase is caused primarily by the phosphate buffer and to a lesser extent depends on the KI concentration (Figure 2-5). No significant influence of KBr-concentration was observed, and its role is not well understood.

Table 2-2 lists the three most commonly used cathode sensing solution types (SST). SST1.0 (1.0% KI and full pH-buffer) is the conventional sensing solution based on the guidelines described by Komhyr [1986] and is most widely used for the ozonesonde types SPC-4A, -5A, and -6A [Science Pump Corporation, 1996]. SST0.5 (0.5% KI and half pH-buffer) is the sensing solution recommended by ENSCI Corporation [1996] since 1996 as the cathode solution for their sonde type. The third sensing solution, SST0.1, is a low buffered variant of the other two SST with 1.0% KI and 1/10th buffer. It has been in use at all NOAA/GML sites since 2005 [Sterling et al., 2018]. A non pH-buffered solution with no KBr, but with 2.0% KI for the cathode cell was deployed as described in Johnson et al, [2002] for the NOAA/GML ozonesonde sites from 1998 to 2005 but is no longer in use. Linked to the complex O_3 +KI-chemistry in the different sensing solutions are the different time response and background behaviour of the ECC sonde when operated with different sensing solutions as demonstrated in laboratory experiments by Vömel and Diaz [2010] (see Figure 2-6).

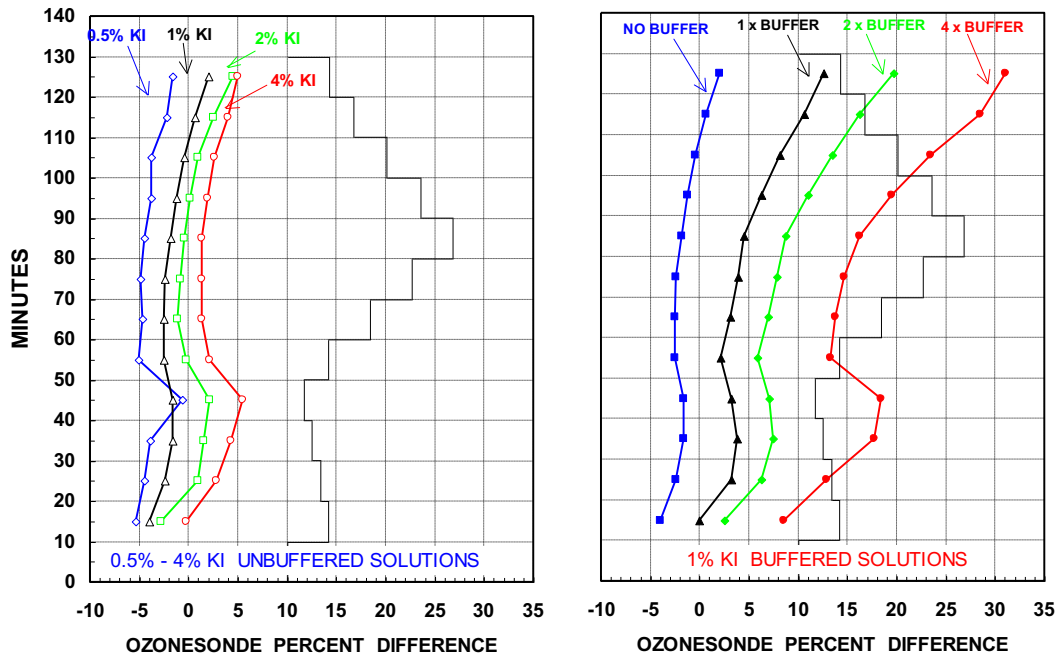


Figure 2–5: (left) Surface ozonesonde sensitivity tests of cathode sensor solutions using various unbuffered potassium iodide (KI) concentrations; (right) zero to four times the buffer concentration for the standard 1% KI buffered sensor solutions (black curve)

Source: Johnson et al. [2002]

Table 2–2: Most common Sensing Solution Types (SST) with chemical composition in aqueous (distilled or highly purified water) solution for ECC sonde cathode cells. For the anode sensing solution, a KI-saturated cathode solution is employed. The preparation of the SST’s is described in detail in Annex A

Sensing Solution Type (SST)	KI [g/L]	P _H -Buffer		KBr [g/L]
		NaH ₂ PO ₄ .H ₂ O [g/L]	Na ₂ HPO ₄ .12H ₂ O [g/L]	
SST1.0: 1.0% KI & full buffer ^(a)	10	1.250	5.0	25
SST0.5: 0.5% KI & half buffer ^(b)	5	0.625	2.5	12.5
SST0.1: 1.0% KI & 1/10th buffer ^(c)	10	0.1250	0.5	25

(a) Komhyr [1986], SPC-6A instruction manual [Science Pump Corporation, 1996]

(b) ENSCI-Z instruction manual [ENSCI Corporation, 1996]

(c) Sterling et al. [2018]

The background current is not a time invariant ECC property. Vömel and Diaz [2010] suggested that the time-varying background is most likely due to the fact that the ECC-chemistry has a fast but also an additional minor, slow reaction pathway (reaction time constant typically 20–30 min). This minor path leads to a memory effect caused by slow side reactions in the oxidation of iodide by ozone in the cathode sensing solution. In equilibrium this leads to an overall stoichiometry factor, S_{O_3/I_2} , larger than 1.0. The magnitude of the excess stoichiometry effect is strongly related to the strength of the phosphate buffer concentration in the cathode sensing solution [Johnson et al., 2002]. The memory effect by the slow reaction pathway causes the background current to be not only time-dependent but also

ozone exposure dependent. To resolve the time and ozone exposure dependent background signal of the ECC sonde new methodologies of post-flight processing are proposed by *Vömel et al. [2020]* and *Tarasick et al. [2021]* (See also [Chapter 3](#)).

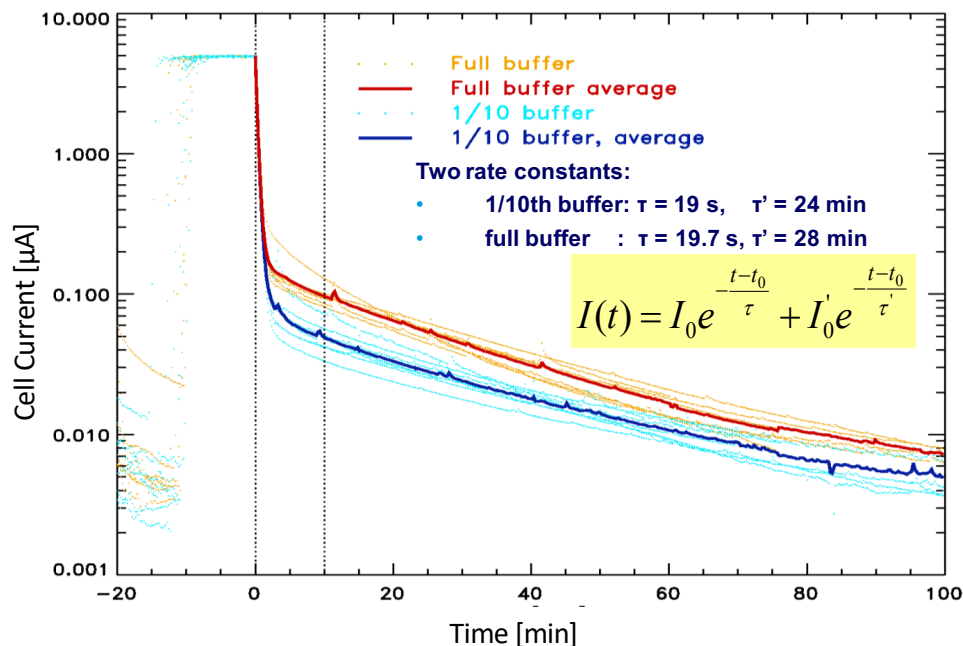


Figure 2–6: ECC ozone sensor current with purified air, as a function of time, before, during and after the ECC sensor has been exposed to about 170 ppbv ozone ($\sim 5\mu\text{A}$ cell current) for about 10 minutes. ECC sensors were charged with either 1%KI, full buffer (SST1.0) or 1%KI, 0.1(1/10) buffer.

Source: *Vömel and Diaz [2010]*

2.4. Ozonesonde and Radiosonde Systems

2.4.1. Comparison of Ozonesondes in the WCCOS (JOSIE Campaigns)

The JOSIE (Jülich Ozone Sonde Intercomparison Experiment) campaigns are a series of laboratory experiments that have been conducted in the environmental simulation chamber at the WCCOS (Research Centre Jülich, Germany: **Figure 1–4c**). The WCCOS chamber tests the profiling capabilities of ozonesondes by comparing their measurement to that of a UV ozone photometer (OPM) that has been referenced to the global standard at the National Institutes of Standards and Technology (NIST, Maryland, USA). The comparison is carried out during a simulated launch in which the chamber P, T and introduced O_3 amount follow the variation of an actual ascent through the atmosphere from surface to 35 km [*Smit et al., 2000*].

The experimental set up (**Figure 2–7, left**) consists of: (i) a pressure- and temperature-controlled vacuum chamber (P: 5–1000 hPa, T: 200–300 K); (ii) a fast dual-beam UV-photometer reference instrument (OPM; *Proffitt and McLaughlin, 1983*) with a 1-s response, precision = 0.025 mPa, uncertainty = 2%–3%; (iii) an ozone profile simulator (OPS): 0.1–30 mPa; (iv) an automatic data acquisition system (DAS). Different pressure, temperature, and ozone profiles (e.g. midlatitude or tropical) can be simulated for ozone soundings at a typical balloon ascent velocity of 5 m s⁻¹ (**Figure 2–7, right**). Four ozonesondes can be flown simultaneously and compared to the OPM-reference.

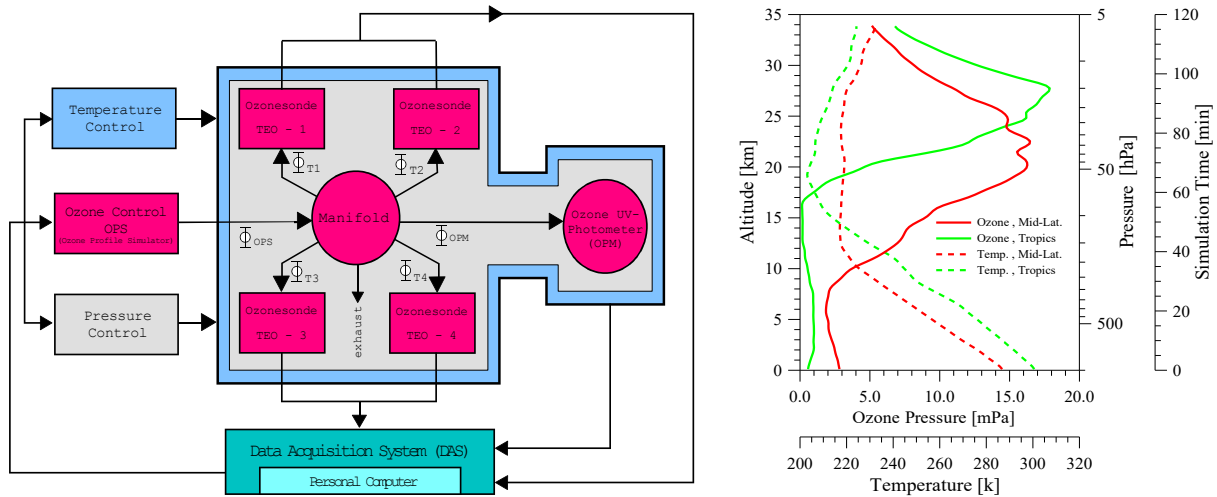


Figure 2-7: Left: Schematic of the JOSIE experimental setup at the environmental simulation facility at WCCOS, Jülich, Germany. Right: Profiles of the simulation of ozone pressure and temperature as function of air pressure (i.e. time or altitude of a simulated ascent rate of 5 m s^{-1}). Midlatitude and tropical profiles are illustrated

JOSIE campaigns over more than two decades have characterized and tested the performance of the various ECC sonde types charged with different sensing solutions operating in polar, midlatitude and tropical P, T and O_3 conditions. These intercomparison experiments constitute a series of calibrations of sondes against the OPM as reference standard; in this way the long-term quality and stability of the ECC sonde instruments produced by the two manufacturers are evaluated. The JOSIE campaigns also serve as a platform for (i) testing standard operating procedures (SOPs) and (ii) capacity building through training of ozonesonde field operators (**Section 1.3.2.2**).

2.4.2. Radiosonde Evolution

In the late 1960s through the 1980s, the ozonesonde instrument was coupled to the radiosonde using analog data techniques, with the humidity channel of the radiosonde being used for the transmission of the ozone signal. Radiotheodolites or terrestrial wind-finding systems such as Loran-C or Omega were employed to measure the horizontal wind velocity and direction. Since the early 1990s, the introduction of digital electronic interfaces between the ozonesonde and the radiosonde has allowed the simultaneous measurement of the different parameters of the ozonesonde and radiosonde. In addition, since ~ 2010 modern radiosondes have employed GPS navigation to detect in-flight the 3-D position, yielding a GPS altitude along with horizontal wind velocity and direction. The use of a digital ozonesonde interface enables the simultaneous measurements of the ozone sensor current and pump temperature plus the additional aerological parameters pressure, temperature, relative humidity, wind velocity, and wind direction. All signals are digitized in-flight and transmitted as a digital coded data stream to the ground station for further processing. The radiosondes may operate at a FM radio frequency band of 401–406 MHz or 1680 MHz, both reserved for meteorological purposes.

The interface allows in-flight measurements of additional parameters used to monitor the performance of the ozonesonde, throughout the sounding, including the pump motor current and battery voltage. Digital processing allows us to include pre-flight, in-flight, and other metadata automatically. Through storage of all measured (raw) data together with the essential metadata (**Chapter 5** and **Annex B**), the sonde data can in principle be reprocessed when necessary.

2.4.3. Air Pressure, Geopotential Height and Geometric Height

From the pressure **P** and temperature **T** and relative humidity **RH** measured with the radiosonde, the in-situ geopotential height **H** is calculated step-by-step as the cumulative sum of the height difference between two successive pressure **P** levels using the hydrostatic equation and the ideal gas law (e.g. *Curry and Webster, 1999*):

$$H = H_0 + \sum_{i=0}^{i=n} \Delta H_i = H_0 + \sum_{i=0}^{i=n} \frac{R_D}{g_0} \frac{T_{V,i+1} + T_{V,i}}{2} \ln \left(\frac{P_i}{P_{i+1}} \right) \quad [\text{E-2-6}]$$

Where **H₀** = height of launch platform in m above sea level
T_v = virtual temperature in K
g₀ = gravitational constant (after WMO standard: 9.80665 m s⁻²)
R_D = universal gas constant for dry air (287 J kg⁻¹ K⁻¹)

The virtual temperature can be derived from the temperature and relative humidity readings of the radiosonde

$$T_V = T * \left(1 + 0.378 * \frac{\frac{RH}{100} * e_{sat}(T)}{P} \right) \quad [\text{E-2-7}]$$

where **e_{sat}(T)** is the saturation pressure of water vapor as function of the temperature **T**.

For **e_{sat}(T)** there are several empirical formulas available, such as that by Magnus-Teten [Murray, 1967]:

$$\text{Log}_{10}(e_{sat}) = \frac{7.5 * t_{air}}{t_{air} + 237.3} + 0.7858 \quad (\text{E-2-8})$$

where **t_{air}** is the ambient air temperature in degrees Celsius [°C].

The starting point of **Eq. E-2-6** is the (geometric) altitude at the launch site and the surface pressure at the launch site. This pressure can be read from a local reference sensor (with a correction for the difference in height of this sensor and the ground at the launch site). In the absence of a reference sensor, the pressure shortly before launch can be used.

Modern radiosondes use GPS to determine the geometric height **Z** (*in m above sea level*), which is slightly different from the geopotential height (e.g. *WMO-No.8 Report, 2018: Section 12.3.6*), depending on the Earth radius **E** (*in m*), which varies with latitude.

$$E(\varphi) = 6378.137 * 10^3 / \left(1.0066803 - 0.006706 * (\sin(\varphi))^2 \right) \quad [\text{E-2-9}]$$

From the geometric height **Z** the geopotential height **H** can be calculated approximately

$$H = \frac{g(\varphi) * E * Z}{g_0 * E + Z} \quad [\text{E-2-10}]$$

where **g(φ)** is the normal gravity as a function of latitude **φ** taking into account the ellipsoidal shape of the Earth and the Earth's rotation, and where

$$g(\varphi) = 9.780325 * \left(\frac{\left(1 + 0.00193185 * (\sin(\varphi))^2 \right)}{\left(1 - 0.00669435 * (\sin(\varphi))^2 \right)^{0.5}} \right) \quad [\text{E-2-11}]$$

or vice versa the geometric height Z from the geopotential height H

$$Z = \frac{E * H}{\frac{g(\varphi) * E - H}{g_0}} \quad [E-2-12]$$

Usually, the geopotential height H is somewhat lower than the geometric height Z . At 30 km the height difference is about 0.2–0.7%, varying with latitude from the poles to the equator (**Figure 2–8**).

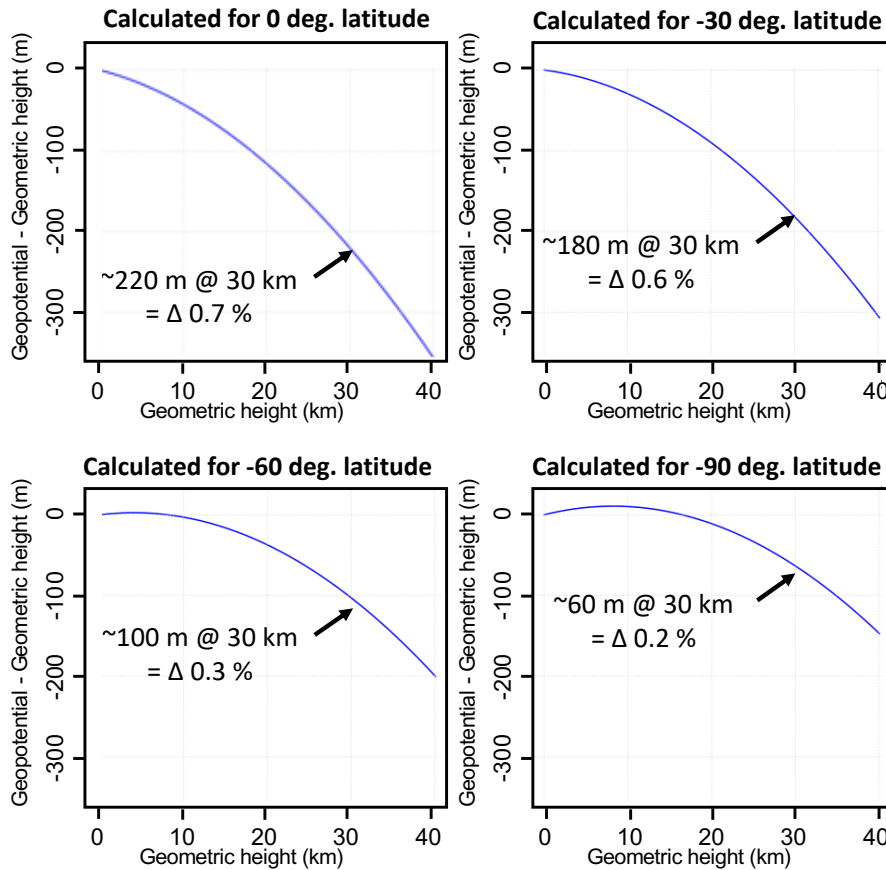


Figure 2–8: Difference between geometric height and geopotential height at different latitudes from 0 to 90 °S (same behaviour from the equator to the North Pole)

For each geometric height level, the corresponding geopotential height level can be calculated (E-2-7). Then from the hydrostatic equation, the corresponding pressure level P_{i+1} is derived from the previous pressure level P_i as

$$P_{i+1} = P_i * \text{Exp} \left[-\frac{g_0}{R_D} * \frac{2 * (H_{i+1} - H_i)}{T_{V,i+1} + T_{V,i}} \right] \quad [E-2-13]$$

This formulation allows a comparison of the performance of the radiosonde pressure sensor with the pressure derived from the reported GPS geometric altitude and calculated geopotential height [Stauffer *et al.* 2014]. Modern radiosondes often do not have a pressure sensor and use GPS altitude exclusively. In that case, the geopotential height is a derived quantity from **Eq. E-2-8** and so is the pressure (**Eq. E-2-13**). Depending on the radiosonde type used the GPS system deployed can be either an absolute GPS or a differential GPS. Both altitudes are part of the profile data segment of the ozonesounding data stored in the data archives.

The uncertainties of air pressure, geopotential and geometric heights depend strongly on the fact if the radiosonde can measure GPS (=geometric) altitude (Case B) or not (Case A).

Case A: Uncertainties for radiosonde without GPS altitude: H and Z derived from P_{Air} Measurement

The uncertainty of the air pressure readings and the corresponding uncertainty in the geopotential height H are listed in **Table 2–3** at different pressure (P_{Air}) levels. The pressure uncertainties ΔP_{Air} and the corresponding uncertainties of the geopotential height H (in gpm) are derived from *WMO-No.8 Report* (2018; Section **12.3: Tables 12.2 and 12.3**). The uncertainty ΔZ in the geometric altitude Z can be assumed to have same values as the corresponding uncertainty ΔH of the geopotential height H . The uncertainty in altitude (ΔH) resulting from the pressure uncertainty contributes to the uncertainty of the ozone partial pressure measurement because of the strong ozone gradient, and is the dominant factor above about 25 km.

Table 2–3: Radiosonde without GPS altitude: Uncertainty of P_{Air} measured at different pressure levels with the most common radiosonde types currently used in the global ozonesonde network, where the radiosonde lacks GPS altitude

Pressure P_{Air}	Uncertainty ΔP_{Air} (hPa)	Uncertainty ΔH (gpm)
1000	2	20
300	1–2	25–50
100	1	75
30	0.5–1	125–250
10	0.5	350

Case B: Uncertainties for radiosondes with GPS altitude Z : P_{Air} derived from Z

Where the GPS (geometric altitude Z) is measured, then the uncertainty ΔZ of the measured geometric altitude is of the order of 10 m and can be assumed to be constant between the surface and 35 km altitude. Further, assuming that the surface air pressure at the launch site is recorded with a barometer with an uncertainty of 1.0 hPa then the uncertainty of the air pressure P_{Air} (**Eq. E-2–1**) declines rapidly with altitude (**Table 2–4**).

Table 2–4: Radiosonde with GPS altitude Z : Uncertainty of P_{Air} derived from the GPS altitude measured with a radiosonde at different pressure levels assuming uncertainty $\Delta Z = 10\text{m}$, constant between the surface and 35 km altitude, and uncertainty of the surface pressure recording of 1 hPa

Pressure P_{Air}	Uncertainty ΔZ (m)	Uncertainty ΔP_{Air} (hPa)
1000	10	1
300	10	0.4
100	10	0.15
30	10	0.04
10	10	0.03

3. OZONESONDE MEASUREMENT AND UNCERTAINTY (David W. Tarasick, Gary A. Morris, Bryan J. Johnson)

3.1. Introduction

This Chapter explores a range of influences on ozonesonde data quality. It is based on the ASOPOS assessment reported in GAW Report No. 201 (2014; see also SPARC-IOC-GAW, 1998) and new information from analyses of JOSIE 2009/2010 (**Table 1–2**) and JOSIE 2017-SHADOZ [*Thompson et al.*, 2019] experiments. The goals are twofold: (1) to guide operators and data managers who seek objective evaluation of different techniques presently in use, and (2) to explain to the community of ozonesonde data users the origins of systematic variations in ozone profiles taken by different instruments and techniques. The first part (**Section 3.2**) reviews the uncertainty of measurements using the two major ECC sonde types, EN-SCI and SPC. **Section 3.3** presents the major factors influencing sonde performance and how each contributes to the overall uncertainty of the measurement. Recommendations are given for the treatment of each measured term in the calculation of the ozone partial pressure. These elements serve as background for the operational steps in [Chapter 4](#) and the recording of measurement parameters reviewed in [Chapter 5](#) and [Annex B](#).

3.2. Performance of the Sondes

3.2.1. Introduction

During the 90–120 minute ozonesonde ascent from the ground to balloon burst altitudes of up to 35 km, the ozone sensor and gas piston pump operate under wide ranges in ambient temperature (+40 C to -90 C) and pressure (1000 to 5 hPa). Above ~100 hPa the ozonesonde pump efficiency begins to decrease with height. Above ~25 hPa, the sensor solution may momentarily boil, but rapid evaporative cooling brings the sensor solution back to a stable condition. This sequence of events illustrates why the reliability of sounding data requires regular evaluation of performance SOPs under both actual atmospheric and simulated conditions. As noted in [Chapter 1](#), these evaluations are accomplished through intercomparison campaigns of multiple ozonesondes on balloon-borne payloads in field campaigns and in environmental simulation chamber experiments, ideally in both cases referencing the ozonesondes to an established ozone standard.

3.2.2. Instrument Biases

ECC ozonesondes have gone through several modifications of the instrument and procedures since they were first manufactured in the early 1970s [*Johnson et al.*, 2002]. Such changes may introduce systematic errors and affect trend estimates. The differences found between the ENSCI-Z ozonesonde and the SPC-6A ozonesonde found in the early JOSIE and BESOS experiments [*Smit et al.*, 2007; *Deshler et al.*, 2008] demonstrate that sonde response can be different for apparently modest differences in sonde construction, and so may be different for other changes in manufacture or in preparation.

The two types show about 5% difference, when the same cathode sensing solution is used. For both ECC types, the use of 1.0% KI and full buffer gives 5% larger ozone values compared with the use of 0.5% KI and half buffer. More recent experiments at WCCOS, with new (JOSIE 2009, JOSIE-SHADOZ-2017) and reconditioned sondes (JOSIE 2010) have confirmed these differences, with re-used sondes agreeing within 1%–2% with brand new sondes, although with a slightly lower precision of ~5%. These findings are in agreement with observations made in the field from dual balloon soundings [e.g. *Deshler et al.* 2017]. Although the reasons for these differences are not well understood, the biases are reasonably consistent and can be removed by the transfer function suggested by *Deshler et al.*, [2017], with an additional uncertainty of the conversion efficiency in **Eq. E-3–1 (Section 3.3.1)** of ±5%.

JOSIE-SHADOZ-2017, simulating only tropical profiles, also showed that errors in the sensitive near-tropopause region can be greatly reduced by use of the low-buffer solution variant adopted by NOAA: 1.0% KI with 0.1 buffer (SST0.1 in [Table 2–2](#)). This typically large error is

due to response time complications from longer time constants associated with secondary chemical reactions in the cathode cell that are described in detail below (**Section 3.3.6**). This error can be largely corrected in data processing through a modified procedure [**Section 3.3.6**; *Tarasick et al., 2021*; *Vömel et al., 2020*].

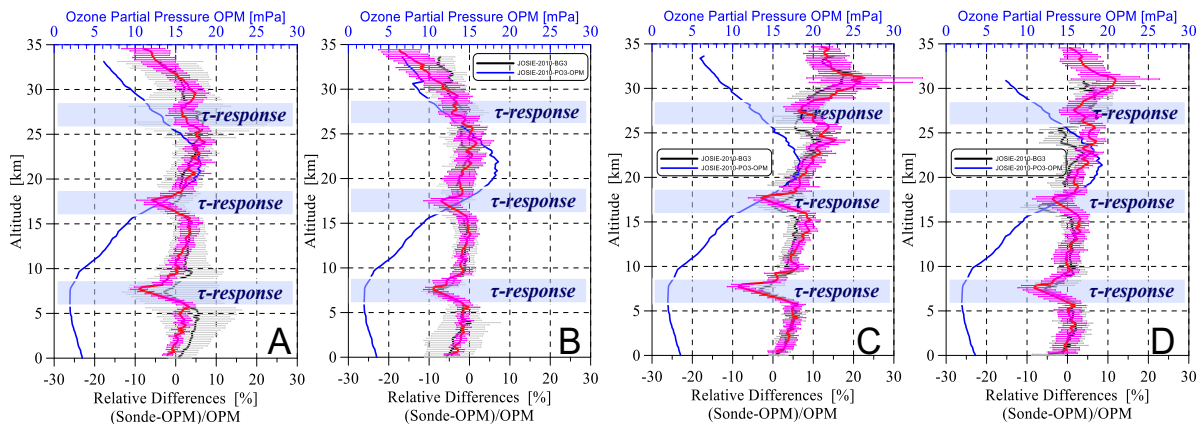


Figure 3–1: JOSIE-2009/2010: Comparison of 18 SPC-6A and 18 ENSCI ozonesondes with the ozone UV-photometer (OPM) at the WCCOS, testing two sensing solutions, SST1.0 and SST0.5. All sondes were prepared and processed following the SOP’s described in GAW Report No. 201 (2014). Relative differences of sonde readings compared to the OPM: SPC-6A & SST1.0 (Figure A, N=9); SPC-6A & SST0.5 (Figure B, N=9); ENSCI & SST1.0 (Figure C, N=9); ENSCI & SST0.5 (Figure D, N=9) for brand new sondes (JOSIE 2009, red solid line) and re-used sondes (JOSIE 2010, black solid line). Thin horizontal lines are standard deviation of the average relative differences of sondes to the OPM. The blue curve is the simulated ozone profile at midlatitude conditions. In the light blue shaded areas τ -response tests were done by setting ozone to zero for ~ 5 minutes then resuming the ozone profile

As noted in **Section 1.3.2.2**, recent ozonesonde-satellite comparisons indicate that there has been an apparent change of response since 2013 at a large number of stations using ENSCI sondes [*Stauffer et al., 2020*]. Causes are currently being investigated. Once characterized, it may be possible that the bias can be corrected by a transfer function to quantify the change of conversion efficiency, with an additional associated uncertainty. Bias changes need to be carefully tracked by the sonde community so that ozonesonde data remain reliable and free from artefacts or drifts. With ongoing monitoring of sondes, these instruments can be used as transfer standards for comparing and merging satellite time series, and for long-term trend analyses. The comprehensive analysis of *Hubert et al. [2016]*, comparing sonde results to 14 limb-measuring satellites and lidars, is a valuable approach that should be performed regularly. Comparisons with IAGOS aircraft data [*Stauffer et al., 2013; 2014; Zbinden et al., 2013; Tanimoto et al., 2015; Tarasick et al., 2019b*] can independently detect tropospheric biases. It is imperative that sonde intercomparisons continue on a regular basis and that the measurements are referenced [e.g. *Tarasick et al., 2019b*], via well calibrated UV-photometers, to the modern UV-absorption standard [*BIPM, 2019; Hodges et al., 2019*].

3.2.3. Stratospheric Performance

Field intercomparisons have been carried out since 1970 [e.g. *SPARC-IOC-GAW, 1998*]. Many of the earlier intercomparisons (e.g. *Attmanspacher and Dütsch [1970, 1981]; Kerr et al. [1994]*) included only ozonesondes without an independent reference profile. Other intercomparisons (e.g. *Hilsenrath et al. [1986]; Aïmedieu et al. [1987]; McDermid et al. [1990]; Komhyr et al. [1995]; Beekmann et al., [1994; 1995]*), used a reference profile measured by other techniques. In the JOSIE laboratory experiments [*Smit et al., 2007*] the sondes measure a simulated ascent ozone profile against the OPM, a fast response dual-beam UV-absorption photometer. Although the evidence is less firm before the 1990s, since at least 1990, properly prepared ECC ozonesondes show a precision of 3%–5% throughout most of the profile below ~ 28 km [*Smit et al., 2007; Kerr et al., 1994; Deshler et al., 2008; Liu et al.,*

2009]. Despite model changes, ECC sonde response has remained stable over the last 50 years, with the exception of differences between the EN-SCI and Science Pump models noted above. An additional reassurance is found in the fact that long-term stations do not in general show any trends against co-located total ozone spectrophotometer measurements.

Besides “snapshot” ozonesonde evaluation campaigns, many stations regularly monitor ozonesonde stratospheric performance through total column ozone (TCO) comparison with a ground-based instrument (Dobson spectrophotometer, Brewer, or Pandora) or with a satellite instrument. The so-called normalization ratio or normalization factor (**Section 3.3.11**) is the factor by which the sonde-estimated total ozone (the integrated ozone profile plus the estimated residual above burst altitude or designated cut off), must be multiplied to match the TCO measurement. Historically, the normalization ratio was used as a linear correction applied to the entire ozonesonde profile, essentially forcing a match in TCO values to the optical reference [e.g. *SPARC-IOC-GAW*, 1998]. This is no longer recommended, but the TCO comparison of sondes with the ground-based instruments serves as a data quality indicator, which continues to be useful to detect suspicious profiles or issues with sonde records (**Section 1.3.2.2**).

3.2.4. Tropospheric Performance

For decades, laboratory experiments have been used to assess the reliability of the ozonesonde instrument [*Powell and Simmons*, 1969; *Reid et al.*, 1996; *Tarasick et al.*, 2002; *Smit et al.*, 2007; *Thompson et al.*, 2007b; *Vömel and Diaz*, 2010]. Numerous field campaigns [*Attmannspacher and Dütsch*, 1970, 1981; *Hilsenrath et al.*, 1986; *Beekmann et al.*, 1994; *Kerr et al.*, 1994; *Margitan et al.*, 1995; *Deshler et al.*, 2008] concluded that, in the absence of significant levels of interfering gases, ECC ozonesondes have a precision of 3%–5% and an overall uncertainty of about 5%–10% in the troposphere, with differences in sonde manufacture and preparation introducing tropospheric biases of $\sim\pm 5\%$.

Tarasick et al. [2019b] reviewed intercomparison data back to the late 1960s. ECC ozonesondes display good agreement in the lower troposphere compared to UV-photometer measurements, with a mean small positive bias (1%–5%) over the entire record. Stations using ENSCI sondes with SST1.0 solution show additional positive biases of 4%–8% in the lower troposphere and 2%–6% in the upper troposphere. Because ozone concentrations in the troposphere are lower than in the stratosphere, the impact of instrumental errors and variability is larger. As a result, the historical WOUDC record shows larger uncertainties at the surface and near the tropopause [*Liu et al.*, 2009], as do field experiments [*Kerr et al.*, 1994; *Deshler et al.*, 2008; *Stübi et al.*, 2008].

When examining a time series of station records, it is important to note the local solar time of release of the balloon as diurnal cycles in surface boundary layer ozone concentration can produce significant variability in near-surface measurements [*Tarasick et al.*, 1995; *Petetin et al.*, 2016]. Particularly in urban regions, where NO_x is plentiful and ozone titration can be nearly complete, a sharp vertical gradient in the ozone concentrations often appears in the shallow morning boundary layer. For example, *Clain et al.* [2009] reported artefact trends in near-surface ozone based on Irene, South Africa, ozonesondes that had been launched at progressively later times of day [*Thompson et al.*, 2014]. Other causes of large near-surface sharp gradients include dry deposition and vertical mixing [*Tang et al.*, 2011; *Galbally*, 1968]. Because of the finite (~ 20 s) response time of the sonde, sharp gradients in ozone near the surface can also appear, as artefacts in the data record, if the sonde is not allowed to run for a few minutes prior to release, after removal of the ozone destruction filter.

Ozonesonde profiles have been compared to data from the measurements of ozone and water vapour by the in-service Airbus and aircraft (MOZAIC) project that uses BIPM-traceable UV dual-beam photometers onboard commercial aircraft to record concentrations of trace gases throughout a flight [*Thouret et al.*, 1998]. Since 2005, the MOZAIC program has been continued by the In-service Aircraft for a Global Observing System (IAGOS; <https://www.iagos.org>). The MOZAIC/IAGOS data record now includes tens of thousands of flights covering six continents [*Petzold et al.*, 2015]. *Staufer et al.* [2013] compared MOZAIC

ozone observations with Payerne ozonesondes for the period 1994–2009 using a trajectory matching technique. They found agreement within 5% between ECC ozonesondes and MOZAIC/IAGOS profiles. *Staufer et al.* [2014] expanded this study to include 28 ozonesonde sites, confirming that while considerable differences appeared between MOZAIC and ozonesondes in the mid-1990s, those differences have decreased to 5%–10% since 1998 for mid- and high-latitude locations.

Assessing these studies and the complete ozonesonde data record, *Tarasick et al.* [2019b] find differences of $5\pm 1\%$ in the lower troposphere, and $8\pm 1\%$ in the upper troposphere, consistent with $1\pm 5\%$ and $5\pm 5\%$ positive biases found for ECC sondes from the UV-referenced sonde intercomparisons. Whereas in the upper troposphere, ozone concentrations reported by the ozonesonde may be 5% high, in the tropical western Pacific, near-zero ozone has been reported [*Kley et al.*, 1996; *Rex et al.*, 2014]. These very low readings may be due to a combination of factors, including lofting of low ozone from near the surface over the ocean. In such cases, the background current subtracted in data processing becomes crucial [*Vömel and Diaz*, 2010; *Newton et al.* 2016] and the uncertainty due to the background current becomes quite large. This may be corrected through a modified data processing procedure, treating the background current as due to previous exposure to ozone (Sec. 3.3.6; *Tarasick et al.*, 2021; *Vömel et al.*, 2020), but this is not yet standard practice.

3.2.5. Artefacts/Interferences Due to Local Pollution including SO₂

Interference reactions in the cathode cell of the ozonesonde have been reported. SO₂ has an inverse effect on the cell chemistry, cancelling ozone mole for mole [*Schenkel and Broder*, 1982], while other oxidants such as NO₂ and H₂O₂ can produce iodine through their reaction with KI, similar to how O₃ reacts (R-2-1). This positive interference is generally a small effect: for NO₂ the response is only about 5%–10% of that for ozone [*Pitts et al.* 1976; *Volz and Kley* 1988; *Tarasick et al.*, 2000]. However, NO₂ is commonly produced from the reaction (titration) of ozone with local NO pollution to remove ozone. Generally, this is seen in or near urban regions or locations with high local emissions (e.g. airports) and can lead to actual ozone losses in the surface boundary layer.

Morris et al. [2010] described an approach that leverages the SO₂ interference reaction in a dual-sonde payload to measure O₃ and SO₂ simultaneously. For most stations, most of the time, SO₂ concentrations are much less than O₃ concentrations (2% or less), so ignoring this interference reaction does not cause a significant problem in the profile and is even less of a problem in the integrated column O₃ amounts determined from the profiles.

Figures 3–2 and **3–3** show cases with significant interferences. An ozonesonde profile from San Jose, Costa Rica, taken on 21 November 2014, as part of a dual-sonde payload flight shows the “raw” instrument reported “O₃” signal (blue) and the dual-sonde determined SO₂ concentrations (orange). The low O₃ signal at the surface is the result of overnight surface deposition of O₃ and titration of O₃ from local NO_x sources. However, the sharp gradient in the ozone profile at 2–4.5 km is the result of the sonde rising through a plume of volcanic emissions downwind of the Turrialba volcano, 30 km to the east of the launch site.

In **Figure 3–3** profiles from Jülich, Germany, show in the planetary boundary layer (Z=0–2 km) impacts of interferences from urban SO₂ and NO pollution. The measured NO₂ likely includes significant amounts produced from ozone that has reacted with locally emitted NO. The SO₂ does not react with ozone but acts as a “negative” ozone signal in the ECC sensor. It is noteworthy that the sum of boundary layer O₃, NO_x, and SO₂ is comparable in each case to the ozone value measured just above the boundary layer.

Costa Rica - 21 Nov. 2014

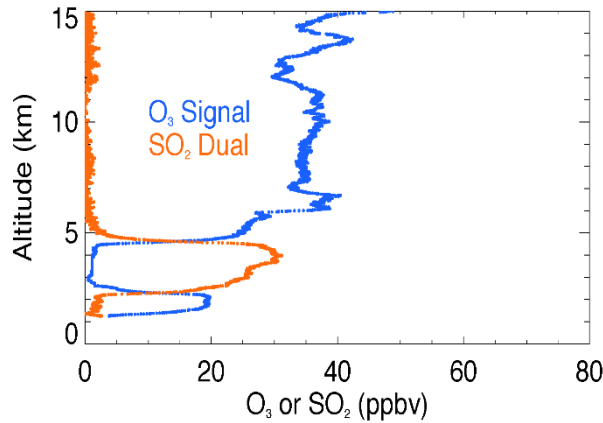


Figure 3–2: Profiles from a dual-sonde payload from University of Costa Rica. The O₃ profile (blue) shows a notch that results from interference of SO₂ (orange) as determined by the dual-sonde approach of *Morris et al. [2010]*

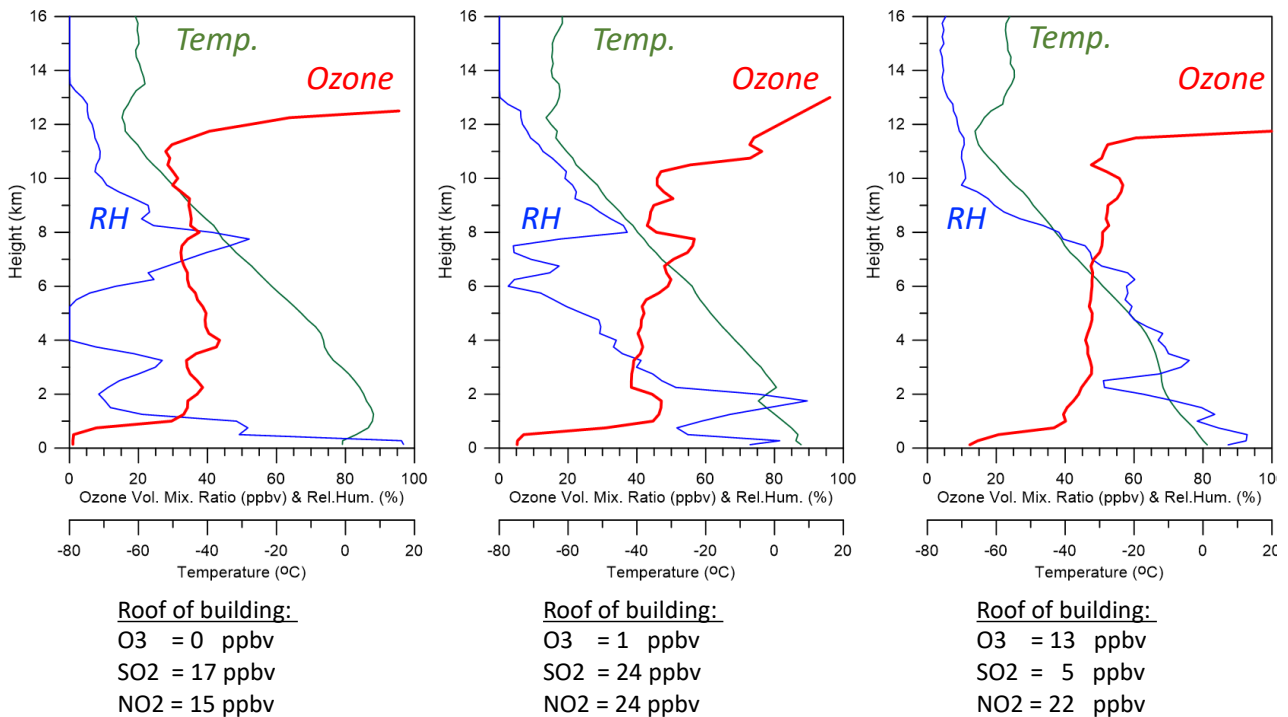


Figure 3–3: A series of profiles taken at FZ-Jülich in which ozone readings are modified by SO₂ and NO₂ interference in the surface boundary layer.

3.3. Factors Influencing Sonde Performance

3.3.1. Instrumental Uncertainties

The measured partial pressure of ozone P_{O_3} is dependent on several factors, as described in **Eq. E-2-1** in **Chapter 2**. Each of these parameters has an associated uncertainty, with systematic components, or biases, that do not vary from sounding to sounding, and random components that vary with each sounding. The systematic components can be measured or estimated, and so corrected, but the derived corrections will carry their own uncertainties.

To first order, it can be assumed that the uncertainties are random, uncorrelated, and normally distributed, so that the overall relative uncertainty of P_{O_3} can be expressed as the combined uncertainties of the variables determining P_{O_3} in **Equation E-2-1**:

$$\frac{\Delta P_{O_3}}{P_{O_3}} = \sqrt{\left(\frac{\Delta \eta_P}{\eta_P}\right)^2 + \left(\frac{\Delta \eta_A}{\eta_A}\right)^2 + \left(\frac{\Delta \eta_C}{\eta_C}\right)^2 + \frac{(\Delta I_M)^2 + (\Delta I_B)^2}{(I_M - I_B)^2} + \left(\frac{\Delta T_P}{T_P}\right)^2 + \left(\frac{\Delta \Phi_{P0}}{\Phi_{P0}}\right)^2 + \sum \varepsilon_i^2} \quad [\text{E-3-1}]$$

Here, the additional term in ε_i represents additional random uncertainties due to other causes: uncertainties associated with bias corrections applied to the other parameters, e.g. the transfer function of *Deshler et al.* [2017] noted in **Section 3.2.2**, and uncertainties in the pressure coordinate or time registration of the ozone signal, which in practice are expressed as uncertainties in ozone partial pressure.

The uncertainties described in **Eq. 3-1** vary randomly between soundings but are assumed to be constant or to vary in a predictable way within a sounding (e.g. with altitude, but not randomly with time). A few of these parameters also have a random uncertainty associated with the in-flight measurement: T_P , I_M , η_A (due to the stochastic nature of bubble formation), and possibly pump motor speed. From laboratory comparisons using a calibrated ozone source it can be estimated that these total <1%, and so can generally be neglected, except when differentiating the output signal (**Section 3.3.6**).

In the following sections, we describe these different uncertainties and how to derive their contributions from the metadata collected during the preparation.

3.3.2. Pump Flowrate at Ground (Φ_{P0})

The volumetric flow of the gas sampling pump of each ozonesonde is individually determined at the ground before flight, most commonly using a bubble flow meter at the gas outlet of the sensing cell.

$$\Phi_{PM} = \frac{100}{t_{100}} \quad [\text{E-3-2}]$$

where t_{100} is the time measured for a bubble to pass through 100 ml of volume.

The uncertainty $\Delta \Phi_{PM}$ of this measurement can be estimated from the standard deviations of recorded values for this measurement, of 0.1–0.3% [*Tarasick et al.*, 2016]. For automated measurement of Φ_{PM} with a commercial flow calibrator, standard deviations are about half as large, but drift can occur if the instruments are not cleaned or calibrated regularly. Differences between this laboratory measurement and the sonde manufacturer's flow rate determination are larger, with standard deviations of about 1%, suggesting operator-dependent biases, or pump motor speed variations of this magnitude. A conservative estimate of $\Delta \Phi_{PM}$ for moist air is therefore $\pm 1\%$ [*Tarasick et al.*, 2021].

The sampled air is typically non-saturated before it is forced through the sensing solution and into the bubble flow meter. Evaporation of water in the sensing solution or in the bubble flowmeter adds to the volume of the air that is sucked in by the pump. The measured pump

flow rate is corrected for this “moistening effect” [GAW Report No. 201, 2014; Tarasick et al., 2021] by a factor C_{PH} . The relative humidity of the sampled air (RH_{Lab}) at the intake of the pump, as well as air pressure (P_{Lab}) and temperature in the laboratory (T_{Lab}) are measured, so that this correction can be made with negligible uncertainty. However, when RH_{Lab} , P_{Lab} , and T_{Lab} are not well known, an estimate has to be made and the uncertainty of the correction cannot be neglected.

The pump piston temperature T_P , which most closely approximates the sampled air temperature, is about 2 K higher than the ambient air temperature, or T_{Lab} in this case. This difference will introduce an additional uncertainty of $\pm 0.3\%$ [Tarasick et al., 2021].

Recommendations for data processing:

The corrected pump flow rate Φ_{P0} at ground is

$$\Phi_{P0} = (1 + C_{PL} - C_{PH}) * \Phi_{PM} \quad [E-3-3]$$

1) Humidification Correction C_{PH}

$$C_{PH} = \left(1 - \frac{RH_{in}}{100}\right) \cdot \frac{e_{sat}(T_{Lab})}{P_{Lab}} \quad [E-3-4]$$

Where

P_{Lab} = Laboratory air pressure [hPa]

T_{Lab} = Laboratory air temperature [K]

$e_{sat}(T_{Lab})$ = Saturation vapor pressure [hPa] at T_{Lab}

RH_{in} = Relative Humidity of the airflow at the inlet of the cathode cell [%].

When the air intake is through a simple gas (ozone destruction) filter that does not dry the air, the RH_{in} equals RH_{Lab} . If more advanced gas filter techniques are used to obtain “zero ozone”, or if purified air is used, then the air will typically be dry, i.e. $RH_{in}=0$

For the saturation pressure of water vapor $e_{sat}(T_{Lab})$ there are several empirical formulas available, such as that by Magnus-Teten [Murray, 1967] (Section 2.4.3: Eq. E-2-7)

If RH_{Lab} and T_{Lab} have not been recorded, then an estimate of the range of RH_{Lab} (RH_{Low} to RH_{High}) and T_{Lab} (T_{Low} to T_{High}) is made to calculate C_{PH} and its uncertainty ΔC_{PH}

$$C_{PH,Average} = (C_{PH,High} + C_{PH,Low})/2 \quad [E-3-5]$$

$$\Delta C_{PH} = (C_{PH,High} - C_{PH,Low})/(2\sqrt{3}) \quad [E-3-6]$$

2) Pump Temperature Correction C_{PL} and its uncertainty ΔC_{PL}

$$C_{PL} = \frac{T_P - T_{Lab}}{T_{Lab}} \quad \text{whereby } T_P - T_{Lab} \cong 2K \quad [E-3-7]$$

$$\Delta C_{PL} = \frac{\Delta T_{PI}}{T_{Lab}} \quad [E-3-8]$$

where ΔT_{PI} is estimated to be about ± 0.5 K

From **Eq. E-3-3**, and because $C_{PH} \ll 1$ and $C_{PL} \ll 1$, the relative uncertainty of Φ_{P0} is

$$\frac{\Delta\Phi_{P0}}{\Phi_{P0}} = \sqrt{\left(\frac{\Delta\Phi_{PM}}{\Phi_{PM}}\right)^2 + (\Delta C_{PH})^2 + (\Delta C_{PL})^2} \quad [\text{E-3-9}]$$

3.3.3. Pump Efficiency (η_P)

At ambient air pressures < 100 hPa the efficiency of the gas sampling pump degrades, as a function of the ambient pressure. This change in efficiency is caused by pump leakage, dead volume in the piston of the pump and the back pressure exerted on the pump by the cell solution [Komhyr, 1967; Steinbrecht et al., 1998]. Johnson et al. [2002] summarize the results of a large number of pump calibrations. More recent measurements are generally consistent within statistical uncertainty but differ significantly from the Komhyr [1986] and Komhyr et al. [1995] values. Although they have historically been called “pump flow efficiencies” or “pump efficiency corrections”, these are now recognized as empirical curves, which combine pump efficiency and conversion efficiency for the standard buffered sensing solutions (see **Section 3.3.5**). For consistency with long-term data records, the values reported by Komhyr [1986] and Komhyr et al. [1995] are still recommended in practice as **K86-Efficiency**, and **K95-Efficiency**, respectively, but are no longer referred to as pump efficiencies.

Measured pump efficiencies, along with the Komhyr curves, as a function of ambient pressure for ECC ozonesondes, appear in **Figure 3.4** and **Table 3-1**. Measured standard deviations are also shown, which may be taken as the uncertainties of the corrections.

Whereas the uncertainty of the pump efficiency is modest below 20 km (1.1% at 100 hPa), it increases substantially at pressures below ~20 hPa, and thus contributes significantly to the overall uncertainty of the ozonesonde performance above 25–30 km altitude (2%–3% at 10 hPa, and 3%–4% at 5 hPa).

Recommendation for data processing:

For the two different ECC sonde types, the recommended efficiency tables should be used, depending on the sensing solution type:

- (a) Komhyr 1986 (**K86-Efficiency**) for SPC-6A sondes with SST1.0 or SST0.5;
- (b) Komhyr 1995 (**K95-Efficiency**) for ENSCI sondes with SST1.0 or SST0.5;
- (c) **NOAA/CMDL 2002** or **JMA 2016** for ENSCI sondes with SST0.1

*The corresponding pressure dependent uncertainties $\Delta\eta_P$ appear in **Table 3-1**.*

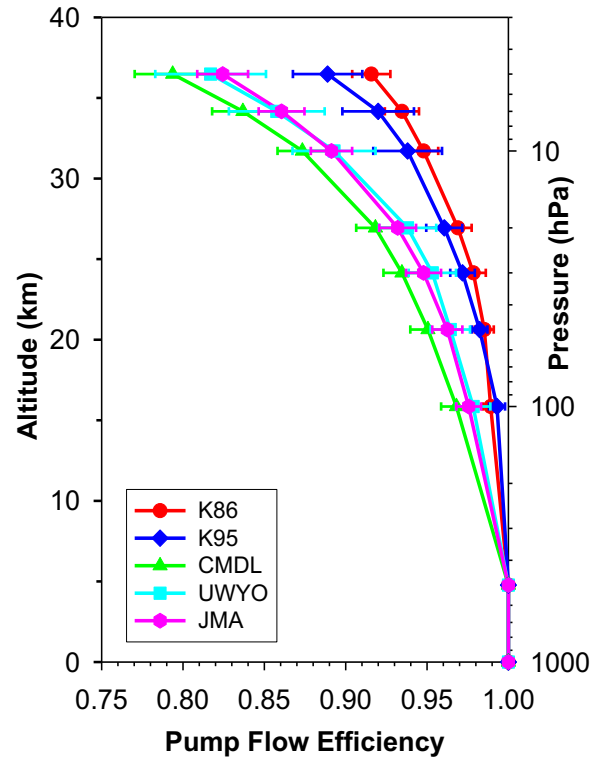


Figure 3–4: Pump flow efficiencies (η_p) as a function of air pressure for ECC ozone sondes reported by Komhyr (1986), Komhyr et al. (1995), and measured by Johnson et al. (2002): CMDL at NOAA & UWYO (=Univ.Wyoming), and measured by Nakano, personal communication, 2019 at JMA.

Table 3–1: Pump efficiencies (η_p) as a function of air pressure for ECC ozonesondes reported by (i) K86-Efficiency by Komhyr, 1986; (ii) K95-Efficiency by Komhyr et al., 1995; (iii) Johnson et al. 2002: CMDL at NOAA & UWYO=Univ.Wyoming; (iv) Nakano, personal communication, 2019 at JMA.

Note that the K86- and K95 Efficiency values reported by Komhyr are empirical correction curves, which actually are a combination of pump efficiency and conversion efficiency.

Pressure [hPa]	ECC (SPC-6a) Komhyr, 1986 K86-Efficiency	ECC (ENSCI) Komhyr et al., 1995 K95-Efficiency	ECC (CMDL) Johnson et al., 2002	ECC (UWYO) Johnson et al., 2002	ECC (JMA) Nakano, 2019
1000	1	1	1	1	1
100	0.989 ± 0.005	0.993 ± 0.005	0.968 ± 0.009	0.978 ± 0.011	0.976 ± 0.008
50	0.985 ± 0.006	0.982 ± 0.005	0.951 ± 0.011	0.964 ± 0.012	0.962 ± 0.009
30	0.978 ± 0.008	0.972 ± 0.008	0.935 ± 0.011	0.953 ± 0.015	0.948 ± 0.011
20	0.969 ± 0.008	0.961 ± 0.011	0.918 ± 0.012	0.938 ± 0.018	0.932 ± 0.011
10	0.948 ± 0.009	0.938 ± 0.021	0.873 ± 0.015	0.893 ± 0.026	0.891 ± 0.013
7	0.935 ± 0.010	0.920 ± 0.022	0.837 ± 0.019	0.858 ± 0.029	0.861 ± 0.014
5	0.916 ± 0.012	0.889 ± 0.021	0.794 ± 0.023	0.817 ± 0.034	0.824 ± 0.016

3.3.4. Absorption Efficiency (η_A)

The absorption efficiency η_A is the capture efficiency (i.e. mass transfer) of the sampled gaseous ozone into the liquid phase of the cathode solution. Although evaporation reduces the amount of the solution available for ozone uptake, η_A is not significantly affected by the changing liquid volume [Komhyr, 1971]. At higher altitudes the uptake of ozone appears to be more efficient due to much faster mass transfer (diffusion) at lower pressures [Davies *et al.*, 2003]. Thus, η_A stays at 1.00, with an uncertainty of $< \pm 1\%$ throughout the entire profile for ozonesondes containing 3.0 cm³ of cathode solution.

Recommendation for data processing:

1) Cathode cells charged with 3.0 cm³ of cathode solution.

$$\eta_A = 1.00 \quad \text{and} \quad \Delta\eta_A = 0.01 \quad [\text{E-3-10}]$$

2) Cathode cells containing 2.5 cm³ of solution require a small correction

$$\eta_A = 1.0044 - 4.4 \times 10^{-5} P_{\text{Air}} \quad \text{at } 100 \text{ hPa} < P_{\text{Air}} < 1050 \text{ hPa} \quad [\text{E-3-11-A}]$$

$$\eta_A = 1.00 \quad \text{at } P_{\text{Air}} \leq 100 \text{ hPa} \quad [\text{E-3-11-B}]$$

The correction adds an additional uncertainty of $\pm 0.01 * P_{\text{Air}}/P_0$ where P_0 is surface pressure such that

$$\Delta\eta_A = 0.01 + \frac{P_{\text{Air}}}{P_0} * 0.01 \quad [\text{E-3-11-C}]$$

3.3.5. Conversion Efficiency (η_C)

The efficiency of conversion of the absorbed ozone into the measured cell current, η_C , includes the stoichiometry of the conversion of iodide into I₂, as well as several possible loss processes. The stoichiometry of the neutral-buffered potassium iodide (NBKI) method may be different from 1.0 [Saltzman and Gilbert, 1959] due to simultaneous reactions other than **R-2-1**. The most important side reactions are those with the phosphate buffer [Johnson *et al.*, 2002]. Loss processes may include loss of ozone to the sensor walls, loss of I₂ through evaporation from solution, losses through the internal resistance of the cell, and in rare cases, loss of the solution itself via spraying through the exit tube.

Losses to the cell walls are likely negligible as the diffusion time constant for the sampled gas in solution is much less than the reaction time constant. Losses of I₂ are thought to be small, as most of the iodine in solution is in the form of I₃⁻ [Tarasick *et al.*, 2002]. In addition, iodine escaping from solution would also have been detected (as unabsorbed ozone) in the experiments of Davies *et al.* [2003]. Losses to internal resistance, i.e. the conductivity of the ion bridge between cathode and anode chambers, or of electron transfer at the Pt cathode surface, are not easily quantified. In practice, these loss processes may not be individually resolvable, but included in an empirically derived conversion efficiency.

Ozonesondes prepared and flown under similar conditions show a precision of 3%–5% throughout most of the profile below ~28 km [Smit *et al.*, 2007; Kerr *et al.*, 1994; Deshler *et al.*, 2008a; Liu *et al.*, 2009], suggesting that the random uncertainty of the stoichiometry of the NBKI method is less than 3%. However, the stoichiometry is observed to increase with flight time [Johnson *et al.*, 2002] because of the slower secondary reaction; this can bias results when sampling ozone in higher levels of the stratosphere. In addition, loss of water through evaporation during flight will concentrate both the KI and the buffer, and both effects will increase the stoichiometry. Both stoichiometry effects may increase the uncertainty of the stoichiometry i.e., conversion efficiency with altitude.

Most recent comparisons to UV photometry in environmental chambers or in balloon-based intercomparisons find average response ratios close to 1.0, and ECC sondes give results that

agree very well with coincident total ozone measurements. This is because, as noted above, the “pump efficiencies” used in past practice [Komhyr, 1986; Komhyr et al., 1995] in fact represent an overall correction that includes both the pump flow efficiency and an estimate of the stoichiometry increase over the flight [Sterling et al., 2018; Witte et al., 2018].

Figure 3-5 makes this clear; it shows ratios between the Komhyr [1986] “pump efficiencies” and the more recent, accurate determinations. These curves show an increase with altitude and represent the increase in conversion efficiency with time and ozone exposure discussed above. They agree well with the experimental results of Johnson et al. [2002] (reproduced in **Figure 2-5**), who found that the stoichiometry of R-2-1 over a typical 2-hour flight time for the sounding increased from 1.00 to 1.05 – 1.20, with the overall increase depending mainly on the concentration of the phosphate buffer and to a minor degree on the KI concentration.

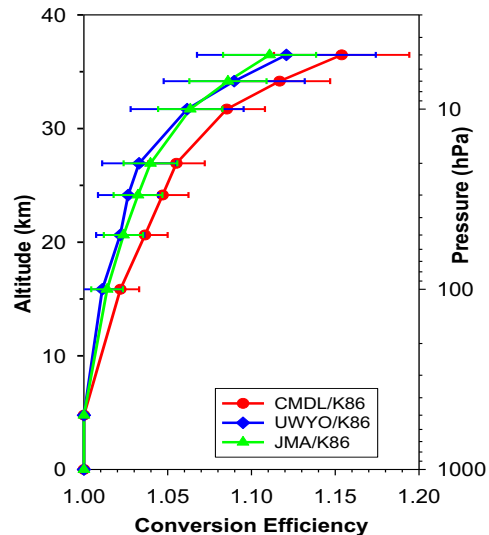


Figure 3-5: Estimated change in conversion efficiency during a typical ozonesonde flight, derived from the ratios of the three recent sets of measurements of pump efficiency (CMDL at NOAA and UWYO = Univ.Wyoming by Johnson et al., 2002, JMA by Nakano, personal communication, 2019) to the Komhyr [1986] values in Table 3-1

In other words, the low Komhyr pump corrections compensate for the increase in conversion efficiency during a flight due to an increase of stoichiometry caused by the slow side reactions. They do this quite well because the sondes have average total ozone column normalization factors close to 1.00. However, this is true only on average, as the actual pump efficiency is strictly a function of pressure and the increase in stoichiometry is a function of ozone exposure and time.

Recommendation for data processing:

While the curves in **Figure 3-5** may approximate average values for conversion efficiency, actual values will vary with sensor construction, KI-solution type, and the sensed ozone amounts. This is a topic of current research [e.g. Tarasick et al., 2021; Vömel et al, 2020]. A comprehensive analysis of results from JOSIE is expected to give a more direct evaluation of the stoichiometry in the cell and new empirical correction functions that will represent the variation and uncertainty of η_c with respect to altitude, sensor model, and preparation (Smit et al., paper in preparation). Until that time, in the interest of preserving the homogeneity of existing time series, the recommendation is that stations should NOT change their procedure, but (as in GAW Report No. 201, [2014]) continue to use the same empirical correction curves [Komhyr, 1986; Komhyr et al., 1995]. Within this context, $\eta_c = 1.00$. The published uncertainties of these empirical correction curves are given in **Table 3-1, Section 3.3.3**, but these do not include conversion efficiency uncertainty. Based on the discussion above and the estimates in **Figure 3-5**, it is recommended to add a stoichiometric uncertainty, independent of altitude, of $\Delta\eta_c = \pm 0.03$.

3.3.6. Cell Current I_M and Background Current I_B

The sensor current (I_M) measurement uncertainty is mainly determined by the accuracy of the current measurement with the current (I) to voltage (V) converter of the ozonesonde data interface board. For currents $>1.0 \mu\text{A}$, the uncertainty of I_M may be as low as $\pm 0.4\%$, and for currents $< 1 \mu\text{A}$, the uncertainty may be as low as $\pm 0.004 \mu\text{A}$, depending on the type of interface [Sterling *et al.*, 2018].

ECC ozonesondes exposed to ozone-free air are observed to produce a small current which varies with time, between sondes, and with their preparation. The nature of this current has been a subject of concern since the introduction of the ECC sonde in the 1960s. The “background current” concept was apparently introduced by Komhyr [1969], who suggested that it was due to reaction with oxygen. There is no evidence that this is the case; however, other oxidants such as NO_2 and H_2O_2 can produce iodine via **R-2-1** and may produce small fixed backgrounds of $\sim 0.01\text{--}0.03 \mu\text{A}$ [Tarasick *et al.*, 2021]. A leaky ion bridge, such that triiodide passes from one cell to the other, can also produce a constant “background current”.

In general, however, any measured current from ozone-free air is due to previous exposure to ozone [Smit *et al.*, 2007, Tarasick *et al.*, 2021; Vömel *et al.*, 2020]. This is clearly related to the time-dependent change in stoichiometry described in **Figure 3-5** and suggests that the ECC response to ozone can be treated as a first order response according to **R-2-1**, plus a time-varying component due to a slow reaction pathway of ozone with buffer components. Each of these is observed to approach a constant value with respect to the ozone input, asymptotically with time. For the fast response this ratio is ~ 1 , while for the slow response a range of estimates exists (Saltzman and Gilbert, 1959; Flamm, 1977; Johnson *et al.*, 2002; Tarasick *et al.*, 2002; Vömel and Diaz, 2010). If we consider that the sonde output, O_3^{sonde} , is the integral over time of its exposure to ozone, of two different processes, the change in O_3^{sonde} in response to an input of ozone, O_3^{true} , over a time interval Δt can be modelled as the sum of:

$$\Delta O_3^{\text{fast}}(t) = (O_3^{\text{true}} - O_3^{\text{fast}}) \left(1 - e^{-\frac{\Delta t}{\tau}}\right) \quad (\text{E-3-12})$$

and

$$\Delta O_3^{\text{slow}}(t) = 0.07 * (O_3^{\text{true}} - O_3^{\text{slow}}) \left(1 - e^{-\frac{\Delta t}{\zeta}}\right) \quad (\text{E-3-13})$$

where τ is the primary “fast” response time constant (~ 20 s) and ζ is the secondary “slow” response time constant (~ 20 min). The empirical value 0.07 for the magnitude of the slow response is taken from Johnson *et al.* [2002] and depends on the sensing solution type.

In the absence of noise, **Eq. E-3-12** can be used to retrieve the input ozone, O_3^{true} , from the output signal (differencing and dividing by the time response and subtracting the slow component). With a typical amount of noise, the differencing produces a result that removes the primary response lag (~ 20 s) but is several times noisier than the red curve in **Figure 3-6** [Vömel *et al.*, 2020]. However, **Eq. 3-13** can be used to accurately calculate the slow component. Assuming as a first guess $O_3^{\text{true}}(t) \approx O_3^{\text{sonde}}(t)$, a two-step iteration produces the green curve in **Figure 3-6**, and the blue curve is the derived ozone after subtraction of the green curve. The first order response of **Eq. 3-12** has not been corrected, but the slow response has been removed. This does not add appreciable noise because this component of the signal is slowly varying.

It is clear that the slow response represented by the green curve can explain the increase with time of the sonde response to a constant ozone input and also the slow decay of that response when the ozone input goes to zero. It therefore describes the behaviour of the time-varying component of the background current discussed above.

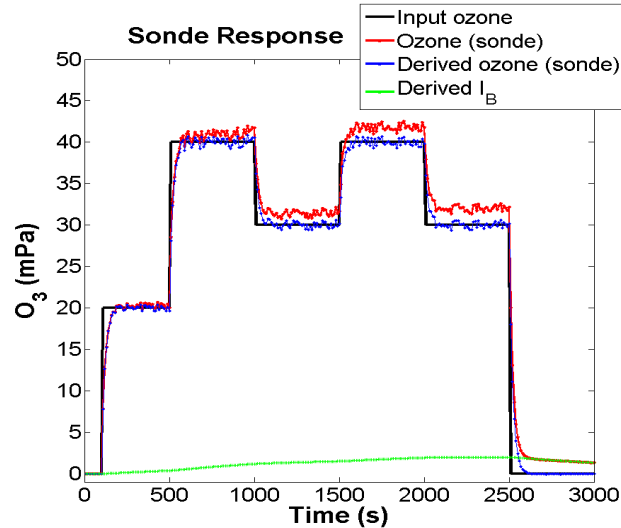


Figure 3-6: Modelled response of the ECC ozone sensor (red) to a changing input of ozone (black), for $\tau=20$ s and $\zeta=20$ min. The red curve, O_3^{sonde} , is the total of the fast and slow components from Eqs. 3-12 and 3-13, summed up to time t . An estimated component of random noise has been added. The blue curve is the derived ozone after subtraction of the green curve, the calculated slow response (background current)

Analysis based on previous JOSIE experiment data suggests that this may lead to improved accuracy (**Figure 3-7: Tarasick et al., [2021]** and **Figure 3-8: Vömel et al. [2020]**). These initial results present a promising avenue for improving the treatment of the background current in ozonesondes, but they need further testing to show how well they in fact model the behaviour of the background current, and to what extent the terms in **Eqs. E-3-12 and E-3-13** vary under flight (chamber) conditions, and/or from sonde-to-sonde. Investigations are presently ongoing using the JOSIE results.

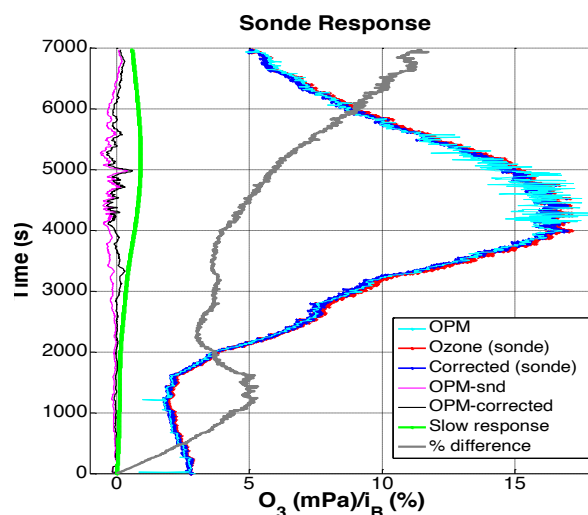


Figure 3-7: Response of an ECC ozone sensor in JOSIE-1996. The red curve is the original sonde profile with standard corrections for background current and pump efficiency (Komhyr, 1986). The blue curve is the derived profile after subtraction of the green curve, the calculated slow response, and using the CMDL pump efficiency corrections of Table 3-1. The agreement with the chamber OPM is significantly improved (pink and black curves), with changes of as much as 1 mPa in the regions of strong gradients. The grey curve is the ratio of the slow response to the total response [Tarasick et al., 2021]

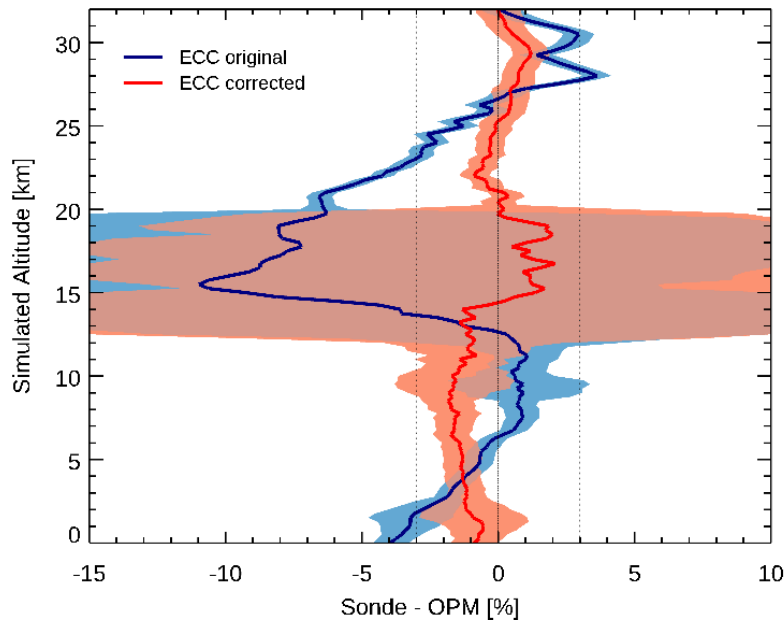


Figure 3–8: Comparison between ECC and OPM mixing ratio in 77 simulation experiments during JOSIE 2017. The originally reported difference is shown in blue; the difference calculated using the corrected data is shown in red. The shaded areas indicate the standard error. Dotted lines indicate $\pm 3\%$. [Vömel et al., 2020]

Recommendation for data processing:

1) Measured Cell Current I_M

The uncertainty of the measured sensor current (I_M) is mainly determined by the uncertainty of the current measurement made by the electronics (current to voltage converter) of the sonde data interface board, which is for current interfaces [Sterling et al., 2018]:

$$a. \Delta I_M = \pm 0.005 \mu A \quad \text{at } I_M < 1.00 \mu A \quad [E-14-A]$$

$$b. \Delta I_M = \pm 0.5\% \text{ of } I_M \quad \text{at } I_M > 1.00 \mu A \quad [E-14-B]$$

2) Background current correction I_B

As **Section 3.3.6** describes, the “background current” is not in general constant and may have several sources, so that the description of it as a background or offset may be improper. This is a topic of current research [e.g. Tarasick et al., 2021; Vömel et al., 2020], and the ASOPOS Panel’s recommendation for this correction is expected to change in future. It is important that stations archive cell current and pump temperature, as well as preparation metadata, so that data may be reprocessed in future. Until this issue is better understood and in the interest of preserving the homogeneity of existing time series for trend analysis, the recommendation is that stations should NOT change their procedure. i.e. continue as in GAW Report No. 201, [2014]. Following the conventional data processing procedure, a **constant** (i.e. air pressure independent) background current correction is applied, such that $I_B = I_{B1}$, i.e. the background current measured 10 min. after the ECC sonde has been exposed to a dose of ozone at a cell current of about $5 \mu A$ for 10 min. For a proper background measurement ($I_{B1} < 0.07 \mu A$) the uncertainty of the background correction I_B is estimated as $\Delta I_{B1} = \pm 0.02 \mu A$.

To track the evolution of the background current I_{B1} it is important to know the time span between the measurement of I_{B1} and the launch of the sonde.

3.3.7. Motor Speed

The ozonesonde Teflon piston pump is driven by an electric motor powered by a nominal 12–18 Volt lithium or wet battery cell pack. It is important that during balloon ascent the voltage remain above 12 V to maintain a constant **RPM** (rotations per minute) and deliver a stable flow rate Φ_{PM} . All SPC and ENSCI motors are set to operate in the range of 2350 to 2450 RPM although some have been measured by stroboscope RPM meter upwards of 2600 RPM. Good motors are observed to hold a steady RPM with less than $\pm 0.5\%$ drift during sonde preparation for flight and flow rate checks. Preliminary environmental chamber tests at NOAA (B.J. Johnson, personal communication) show that some motors may have a drift of $\pm 3\%$ – 4% when exposed to low temperatures and variable ambient pressure. Further testing and checking of ozonesonde RPM are being carried out as part of the investigations of the 3%–8% TCO “drop-off” problem (Stauffer *et al.* [2020]; **Section 3.3.11**). Ozonesonde manufacturers now offer instruments with an **RPM** controller to electronically maintain a constant RPM or a tachometer recording system to monitor RPM.

3.3.8. Temperature of Gas Sampling Pump (T_P)

The air mass flow rate through the sensor depends on the air temperature (**Eq. E-1-1**), which is measured by a thermistor in a hole drilled into the Teflon block of the pump. Over the course of a sounding the pump temperature can decline by 10–25 K. This measurement of the “internal pump temperature” has an estimated uncertainty of about 0.5 K. Laboratory measurements made in the WCCOS simulation chamber have shown that the so-called piston temperature, which is the best representative pump temperature T_P to be applied in **Eq. E-2-1**, is ~ 1 – 3 K larger than the measured internal pump base temperature (T_{PM}). This can introduce a negative bias of 0.5–1.0% in P_{O_3} that needs to be corrected.

Recommendation for data processing:

The corrected pump temperature T_P is

$$T_P = T_{PM} + 3.90 - 0.80 * \text{Log}_{10}(P_{Air}) \quad \text{at } P_{Air} > 3 \text{ hPa} \quad [\text{E-3-15}]$$

for P_{Air} in hPa. The uncertainty of this regression fit, and so of this correction, is about ± 0.5 K. When added to the uncertainty of the internal pump base temperature measurement, which is also ± 0.5 K, the sum of these uncertainties results in: $\Delta T_P = \pm 0.7$ K or $\pm 0.3\%$.

3.3.9. Sensor Response Time

The time delay due to the 18–28 s response time of the sonde leads to a slight upward shift and smoothing of atmospheric features during ascent and downward shift during descent. Different balloon ascent rates will therefore result in ozonesondes reporting somewhat differing ozone amounts, at a given altitude in regions where there is a vertical gradient of ozone [e.g. Imai *et al.*, 2013]. This difference is proportional to

$$\frac{\Delta O_3}{\Delta t} \text{Exp} \left[\frac{-\Delta t}{\tau} \right] \quad [\text{E-3-16}]$$

where Δt is the time interval between successive measurements, τ is the e^{-1} response time (~ 18 – 28 s), and $\frac{\Delta O_3}{\Delta t}$ is the change of ozone with respect to flight time, or $w * \frac{\Delta O_3}{\Delta z}$, where w is the rise rate of the sonde. The random uncertainty due to response time is then proportional to the random uncertainty in balloon rise rate. The typical variation of balloon rise rates adds modest uncertainty ($< 1\%$) at the sharp ozone gradients near the tropopause and mostly insignificant uncertainty elsewhere [Tarasick *et al.*, 2016; 2021].

Deconvolution of the ozone profile can remove biases due to sensor response time, rendering this source of random uncertainty negligible as well but at a cost of modest increase in random error [Tarasick *et al.*, 2021; Vömel *et al.*, 2020]. More research is required to evaluate the

effect of these deconvolution corrections in general and in particular, when compared to remote sensing observations from satellites, lidar and ground-based ozone observations.

3.3.10. Radiosonde Pressure Offsets

Pressure offsets appear frequently in data from radiosondes that use an onboard pressure sensor to calculate altitude [Stauffer et al., 2014; Inai et al., 2015]. These offsets impact ozone profiles in two ways: first, they shift the profile in altitude, displacing the ozone peak vertically; second, they change the ozone mixing ratio as computed from the ozone partial pressure and the ambient pressure. Pressure uncertainties can be quite important for older radiosondes. All current radiosondes use GPS sensors with typical height accuracies in the stratosphere of ± 20 m [Nash et al., 2006; 2011; da Silveira et al., 2006]. Using the GPS height to calculate the ambient pressure or to correct a measured pressure reduces this source of error to an insignificant range of 0.1–0.3% in ozone.

3.3.11. Total Ozone Normalization Factor (N_T)

Historically, ozonesonde profiles have often been normalized or scaled to an independent measurement of the Total Column Ozone, **TCO**. Normalization of ECC sonde profiles is no longer recommended, because it introduces the uncertainty of the total ozone measurement into the profile. This uncertainty can be considerable, because the amount of ozone above the balloon burst height can only be estimated, and because of the inevitable differences in the air masses being sampled by the two techniques. Normalization also renders the ozonesonde record dependent on the total ozone record, an important issue for trend studies [Morris et al., 2013], and is inconsistent with the goal of making all ozonesonde measurements traceable to the modern UV-absorption standard through the WCCOS-Ozone PhotoMeter (OPM).

However, the normalization factor provides a useful indicator for the quality of ozonesonde profile data. In routine operation, for ECC ozonesondes that reach at least 30 hPa (24 km), most normalization factors ($\sim 96\%$) are in the range 0.9–1.1, and 99% are within 0.8–1.2. The relative uncertainty of the N_T is typically in the range of 6%–10% [Tarasick et al., 2021].

Normalization ratios can also identify inconsistency in sonde data time series. For example, satellite and ground-based instrument **TCO** comparisons were key in identifying the global ozonesonde drop-off at several sites after 2013 when two sets of newly homogenized data were evaluated [Thompson et al., 2017; Sterling et al., 2018; Stauffer et al., 2020].

Because the balloon typically bursts at ~ 10 hPa, 15%–20% of the ozone column is above the profile recorded by the ozonesonde. Thus, a residual ozone column amount Ω_R , has to be added to obtain the sonde **TCO**. The oldest procedure for calculating the Ω_R was to assume a residual column based on a constant mixing ratio (CMR) equal to the measured value at the top of the sonde profile. Because satellite observations have shown that the ozone mixing ratio declines above 35 km, this means that the **TCO** from the sonde, Ω_T , is 2%–4% too high [SPARC-IOC-GAW, 1998]. Thus, nearly all ozone stations now use residual ozone column amounts obtained from satellite observations [McPeters and Labow, 2012].

Recommendation for data processing:

*The total ozone normalization factor (N_T) is defined as the ratio of an independent **TCO** measurement by a Dobson or Brewer spectrophotometer (Ω_C) and the **TCO** derived from the ozonesonde profile (Ω_T):*

$$N_T = \frac{\Omega_C}{\Omega_T} \quad [E-3-17]$$

*It is recommended **NOT** to apply N_T as a linear scaling factor of the vertical ozonesonde profile and only to use it as a quality indicator for the measured profile (**Section 5.2**).*

The sonde TCO (Ω_T) consists of the integrated ozonesonde column (Ω_S) plus an estimated residual ozone column (Ω_R) above burst altitude (Z_B):

$$\Omega_T = \Omega_S + \Omega_R \quad [E-3-18]$$

Ozone column abundances are expressed in Dobson units, where 1 DU = 2.69×10^{16} molecules per cm^2 at STP (Standard Temperature (=273.15 K) and Pressure (=1013.25 hPa) conditions (**1 DU = 1×10^{-3} atm.cm at STP**))

The integrated column of ozone from the sonde profile is:

$$\Omega_S = \frac{1}{n_0} \int_{\text{Surface}}^{\text{Burst}} n_{O_3}(z) \cdot dz = \frac{1}{n_0} \sum_{z_i=\text{Surface}}^{z_i=\text{Burst}} n_{O_3}(z_i) \cdot \Delta z_i \quad [E-3-19]$$

where $n_0 = 2.69 \times 10^{16}$ molecules per cm^2 at STP and $n_{O_3}(z)$ is the ozone concentration in molecules cm^{-3} from the sonde at altitude z .

The uncertainties described in the **sections 3.3.1–3.3.10** vary randomly among soundings but are assumed to be constant or to vary in a predictable way within a sounding. (e.g. with altitude, but not randomly with time). This implies that they are fully correlated in the vertical integral, and the uncertainty of the integral $\Delta\Omega_S$ is

$$\Delta\Omega_S = \frac{1}{n_0} \int_{\text{Surface}}^{\text{Burst}} \Delta n_{O_3}(z) \cdot dz = \frac{1}{n_0} \sum_{z_i=\text{Surface}}^{z_i=\text{Burst}} \Delta n_{O_3}(z_i) \cdot \Delta z_i \quad [E-3-20]$$

$$n_{O_3} = \frac{P_{O_3}}{k \cdot T_{\text{Air}}} \quad \text{and} \quad \Delta n_{O_3} = \frac{\Delta P_{O_3}}{k \cdot T_{\text{Air}}} \quad [E-3-21]$$

where k is the Boltzmann constant and T_{Air} is the temperature of the ambient air. Note that this neglects any uncertainties that vary randomly during the flights, such as electronic noise or those due to the stochastic nature of bubble formation. These uncertainty components are small and uncorrelated in the vertical integral, and so their contributions to the integral will be relatively small.

The residual ozone column above burst point to top of atmosphere (**TOA**) is:

$$\Omega_R = \frac{1}{n_0} \int_{\text{Burst}}^{\text{TOA}} n_{O_3}(z) \cdot dz = \frac{1}{n_0} \sum_{z_i=\text{Burst}}^{z_i=\text{TOA}} n_{O_3}(z_i) \cdot \Delta z_i \quad [E-3-22]$$

It is recommended to derive the residual ozone column from the satellite climatologies of McPeters and Labow [2012], which also give uncertainties for residual columns. The assumption that the ozone mixing ratio remains constant above the balloon burst should **NOT** be used to estimate the residual ozone above the top of the measured profile. This estimation introduces larger uncertainties compared to using satellite climatology.

The uncertainty of the normalization factor (N_T) is the sum of the total ozone column measurement ($\Delta\Omega_C$) uncertainty and the weighted sum of the uncertainty of the residual column estimate ($\Delta\Omega_R$) and the integral of the uncertainties in the ozone mixing ratio (or partial pressure) from the surface to the balloon burst height, $\Delta\Omega_S$

$$\frac{\Delta N_T}{N_T} = \sqrt{\left(\frac{\Delta\Omega_C}{\Omega_C}\right)^2 + \frac{(\Delta\Omega_S)^2 + (\Delta\Omega_R)^2}{(\Omega_S + \Omega_R)^2}} \quad [E-3-23]$$

3.3.12. Two Examples of Uncertainty Budgets

Table 3–2 lists estimated magnitudes of ozonesonde profile uncertainty from the sources considered above for sondes prepared according to the procedures recommended in this Report. Most of them are small. The estimated uncertainty of the background current subtraction represents only about 2%–3% in the midlatitude troposphere (**Figure 3–8**), although, it can be large near the tropical tropopause (**Figure 2–9**). The pump efficiency

correction uncertainty (η_P) is of similar size up to 10 hPa. Radiosonde pressure offsets, which caused errors in altitude registration for earlier sondes, are not generally a consideration because most modern radiosondes measure GPS altitude. However, to demonstrate the sensitivity of pressure uncertainty to the overall uncertainty budget we assume a pressure uncertainty of ± 1.0 hPa (Absolute pressure uncertainty for older radiosondes is of the order of 0.3 to 2 hPa [Nash *et al.*, 2006; da Silveira *et al.*, 2006; Steinbrecht *et al.*, 2008, Stauffer *et al.*, 2014; Inai *et al.*, 2015]). Pressure uncertainty is not included in the calculated uncertainty for the normalization factor. It is also assumed that RH_{Lab} , P_{Lab} and T_{Lab} are measured, so that the RH correction for pump efficiency is made with negligible uncertainty.

While the uncertainty of η_C (predominantly the stoichiometry) is estimated at only 3%, this is poorly known, and its variation with altitude, instrument model, and between sondes of the same model needs to be characterized (**Section 3.3.5**). Changes in sonde production or preparation can cause larger differences [Smit *et al.*, 2007; Deshler *et al.*, 2017; Stauffer *et al.*, 2020], which, even if corrected for average biases, may add significant uncertainty. The estimated uncertainty in the calculated total ozone normalization factor is the sum of these uncertainties integrated over the profile (**Figures 3–9 and 3–10**), with an estimated 3% uncertainty in the total ozone measurement (**Eq. E-3–21**).

Table 3–2: Sources of ozonesonde profile uncertainty and their estimated magnitudes for midlatitude station [Edmonton; Tarasick *et al.*, 2016] and tropical station [Watukosek, Witte *et al.*, 2018]. Total ozone normalization factor uncertainties are calculated for a balloon bursting at 30 km in June, and at 25 km in January (in parentheses). All quoted uncertainties are one standard deviation (1σ)

Source	Uncertainty (1σ)		
	Midlatitude (Edmonton)	Tropical (Watukosek)	Confidence
Stoichiometry η_C	$\pm 3.0\%$	$\pm 3.0\%$	low
T_P measurement	$\pm 0.3\%$	$\pm 0.5\%$	high
Φ_{PM} measurement	$\pm 1.0\%$	$\pm 1.0\%$	high
Φ_{PM} RH correction	$\pm 0.5\%$	$\pm 0.5\%$	moderate
Current measurement (interface)	$\pm 1.0\%$	$\pm 1.0\%$	high
η_P pump efficiency	JMA; see Figure 3–4	JMA; see Figure 3–4	high
η_A absorption efficiency	$\pm(1+ P/P_0)\%$ (2.5 ml solution) ^(a) $\pm 1\%$ (3.0 ml solution)	$\pm 1\%$	moderate
Background current	0.02 μ A (0.07 mPa)	0.02 μ A (0.07 mPa)	low
Ascent rate variation	$\pm 12\% \cdot \frac{\Delta O_3}{\Delta t} \text{Exp} \left[\frac{-\Delta t}{\tau} \right]$	$\pm 12\% \cdot \frac{\Delta O_3}{\Delta t} \text{Exp} \left[\frac{-\Delta t}{\tau} \right]$	high
Pressure uncertainty	± 1.0 hPa	± 1.0 hPa	moderate
Total ozone normalization factor	5.0% (7.9%)	4.8% (4.9%)	high

(a) P_0 is the surface pressure at the launch site

Correctum in Tarasick *et al.*, 2021:

Equation 10 should read: $\epsilon_{LT} = \frac{1}{O_3} \frac{\Delta w}{w} e^{-\Delta t/\tau} \nabla_t O_3 \Delta t$

Equation 11 should read: $\epsilon_{P0} = \frac{\Delta P}{O_3} \nabla_P O_3$

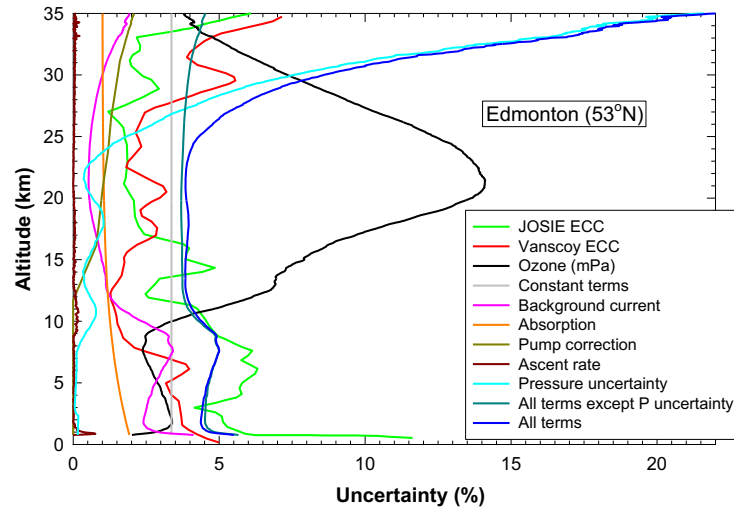


Figure 3–9: Uncertainty analysis for a northern midlatitude station (Edmonton, Canada; *Tarasick et al.*, 2016), showing the influence of different uncertainty terms, for the assumed values in Table 3–2. For older sondes without GPS altitude registration, the uncertainty due to pressure bias dominates at higher altitudes. Also shown are profiles of the standard deviation of differences from the midlatitude reference profile during the JOSIE 1996 intercomparison [*Smit et al.*, 2007] and the Vanscoy 1991 intercomparison [*Kerr et al.*, 1994]. These sondes were compared to a common pressure sensor, so these curves do not include any variance due to pressure offsets

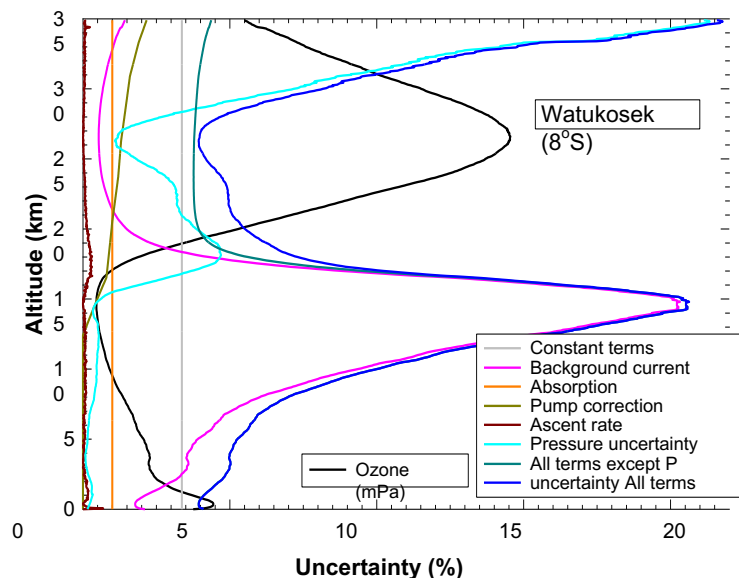


Figure 3–10: Uncertainty analysis for a tropical station (Watukosek, Java; *Witte et al.*, 2018), showing the influence of different uncertainty terms, for the assumed values in Table 3–2. Because of the very low ozone in the tropical upper troposphere, the uncertainty due to the background current without any time response correction dominates at these altitudes

4. ASSESSMENT OF STANDARD OPERATING PROCEDURES FOR OZONESONDES (ASOPOS) (Roeland Van Malderen, Peter von der Gathen & Richard Querel)

4.1. Introduction

Ozonesondes have been in wide use since the 1960s. The design and the principle of operation of a modern ECC ozonesonde are described in [Chapter 2](#). Published studies [*Smit et al., 2007, Deshler et al., 2008, and others*] show that ozone measured by ozonesondes should achieve an uncertainty of 5% or better when recommended procedures are carefully followed [*GAW Report No. 201, 2014*]. This Chapter provides a background on operational aspects of the ozonesonde instrument along with updated recommendations based on experiments with sondes in the laboratory and in the field, including:

- Updated Standard Operating Procedures (SOPs) for the preparation of ozonesondes to be followed by **new** stations and based upon our current best knowledge. In general, established stations should maintain existing practices unless they did not conform to prior recommended SOPs, after interaction with the ASOPOS Panel.
- Step-by-step recommendations for preparation of ECC ozonesondes, including procedures for the re-use of recovered ozonesondes (**Section 4.2**).
- The procedure for processing the sonde data according to the instrument-solution combination employed, consistent with the standards developed from JOSIE experiments (**Section 4.3**).
- A comprehensive list for logging metadata in various categories so that as new insights are gained from future experiments, data can be reprocessed at a later date (**Section 4.3.3**).

4.1.1. Ozonesonde Operations and the Need for SOP

Due to the wet chemical nature of the ozonesonde solutions, the initial preparation of an ozonesonde has to be performed within a month before launch with final steps completed the day before or immediately preceding the launch. This constraint means that preparation is not carried out by the manufacturer but is performed by station staff. Station operators and procedures may change over time, contributing to variability in sonde preparation and introducing artefacts into the station data record. At some stations, preparation and launch has been carried out by the same personnel for decades; at other stations, staff may change every year or more often. Instrumentation also changes over time. Therefore, long-term ozonesonde records from a single station may need to be reprocessed or “homogenized” before they can be used to estimate ozone trends [*Tarasick et al., 2016; Van Malderen et al., 2016, Witte et al., 2017; Sterling et al., 2018; Witte et al., 2018; Witte et al., 2019*]. Homogenization procedures are described in [Annex D](#).

4.1.2. Ozonesonde Testing as the Basis for Recommended SOP

Since 1996, activities to improve the quality of balloon-borne ozone soundings have been conducted at the World Calibration Centre for Ozonesondes (WCCOS) at FZ-Jülich (List in **Table 1–2**). The JOSIE (Jülich OzoneSonde Intercomparison Experiment: <http://www.wccos-josie.org/josie>) sonde simulation experiments demonstrate that caution must be exercised when making changes in instruments, preparation, or operational procedures [*Smit et al., 2007*]. The first set of SOP recommendations, published in the *GAW Report No. 201* [2014], was based on JOSIE experiments from 1996–2009, the WMO/BESOS (Balloon Experiment on Standards for Ozonesondes) campaign [*Deshler et al., 2008*], and additional work at other laboratories. The *GAW Report No. 201* represented a consensus review by the first Assessment of Standard Operating Procedures for Ozonesondes (ASOPOS) Panel of ozonesonde experts.

The first ASOPOS Panel focused on the performance of ECC sondes and KI-solution strength (SST1.0, SST0.5, SST2.0), how to handle the decrease of pump efficiency at low pressures,

which of the several measurements of “background current” made during instrument preparation to use in data processing, and the extent to which slight differences in instrument preparation and initial exposure could affect the final data. The ASOPOS 2.0 Panel has focused on the same issues, but with new information based on the 2017 JOSIE-SHADOZ [Thompson *et al.*, 2019] and follow-on tests at several laboratories. In addition, the new recommendations are based on uncertainty considerations described in [Chapter 3](#). In particular, we mention here the new insights about the Komhyr empirical pump efficiency corrections that combine the measured pump efficiency decrease and the increase in stoichiometry due to the slow side reactions during a flight (**Sections 3.3.3** and **3.3.5**) as well as the impacts on background current caused by a slow reaction pathway of ozone with buffer components (**Section 3.3.6**).

4.1.3. ASOPOS 2.0 Panel Summary SOP Recommendations

Based on the early JOSIE experiments, the first ASOPOS Panel [*GAW Report No. 201*, 2014] recommended different solution strengths for the ECC sonde types SPC-6A and ENSCI-Z (**Chapter 1.3**). The traceability and reliability of those recommendations were confirmed in JOSIE-SHADOZ-2017, which tested two other solution strengths that measured ~3%–5% less ozone than those prepared according to *GAW Report No. 201* [2014]. In **Section 3.3.3** and **3.3.5** the ASOPOS Panel describes new insights and potential modified practices with respect to the Komhyr empirical pump corrections, linking the correction tables to an absolute reference (the WCCOS OPM) and the traditional “background current”. However, the Panel agrees that implementation of all the new concepts in the data processing chain is premature. Therefore, the ASOPOS 2.0 Panel recommendations are mainly in line with the first ASOPOS Panel [*GAW Report No. 201*, 2014], but they anticipate the new concepts in the future SOP (**Section 4.2**) and metadata (**Section 4.3.3** and [Annex B](#)).

4.1.3.1. Recommendations for Existing Sonde Stations

1. Continue using ozonesonde type (SPC6A or ENSCI) with the same SST currently in use. Existing stations should avoid making any changes that might create a discontinuity in good long-term records.
2. The recommended combinations of sonde type and solution:
 - (a) Stations using the SPC-6A: 1.0% KI, full buffer (SST1.0);
 - (b) Stations currently using the ENSCI-Z: 0.5% KI, half buffer (SST0.5);
 - (c) Stations using the ENSCI-Z: 1% KI, 1/10th buffer (SST0.1) should continue with this.
3. Use the following empirical correction tables (see **Table 3-1**):
 - (a) SPC-6A (SST1.0: 1%KI,1.0B or SST0.5: 0.5%KI,0.5B): K86 [*Komhyr*, 1986];
 - (b) ENSCI (SST1.0: 1%KI,1.0B or SST0.5: 0.5%KI,0.5B): K95 [*Komhyr*, 1995];
 - (c) ENSCI (SST0.1: 1%KI,0.1B): CMDL at NOAA [*Johnson et al.*, 2002] or JMA [*Nakano*, personal communication, 2020).

Note that the K86 and K95 tables should no longer be referred to as “pumpflow efficiency” tables, but rather as “empirical correction” tables. Through the JOSIE experiments, the K86 and K95 tables are linked to the OPM, ensuring the traceability of each ozone reading to an absolute value. For ENSCI (SST1.0%KI, 0.1B) and use of CMDL or JMA tables, results from JOSIE 2017 can be used to provide “conversion efficiency” or “calibration” tables so that the profile data are traceable to the OPM.

4.1.3.2. Recommendations for New Sonde Stations

1. For stations joining the global ozonesounding network, the GAW Report No. 201 [2014] recommendations (SPC 1.0%KI 1.0B; ENSCI 0.5%KI 0.5B) with the corresponding empirical correction tables, remain in use;
2. For scientific research campaigns, the use of low buffered sensing solutions (SST0.1: 1.0% KI, 0.1B used in ENSCI sondes) might have some advantages (Chapter 3 and the JOSIE 2017 results, *Thompson et al.*, 2019). This combination must use the pump efficiency tables CMDL at NOAA (Johnson, 2002) or JMA (Nakano, personal communication, 2019) to ensure traceability across the global ozonesounding network;
3. Other types of ECC ozonesondes in use such as Chenfeng have not been tested in the WCCOS. ASOPOS recommends testing the newer sonde types in the laboratory and in the field [*Bak et al.*, 2020] to determine how they compare to SPC, ENSCI and the OPM.

4.2. Rationale for ASOPOS 2.0 Panel Recommendations on ECC Ozonesonde Preparation SOPs

4.2.1. Introduction

The full set of preparation steps appears in [Annex A](#), along with launch instructions. This section presents additional information on the preparation steps, including updates based on JOSIE-SHADOZ 2017 [*Thompson et al.*, 2019], where the preparation procedures of eight SHADOZ stations [*Thompson et al.*, 2003a; 2012] were compared and evaluated. [Annex A](#) provides a simple checklist based on these recommendations. A tutorial video on the new SOPs in practice is available at <https://www.wccos-josie.org/asopos> or <https://vimeo.com/niwanz/asoposprep>.

For example, one of the largest differences found during JOSIE-SHADOZ resulted from the use of an old model (SPC) test unit (one with a calibrator sonde) at some stations for which the corresponding SOPs (SPC Operator's Manual Model 6A ECC Ozonesonde, 1996) had been adopted by some manufacturers (e.g. Vaisala) in their ozonesonde operator's manual. **The ASOPOS 2.0 Panel recommends discontinuing use of this test unit model and SOPs.** JOSIE-SHADOZ found other more subtle differences among station SOPs in sensor response tests and whether or not the cathode chamber was bypassed during high ozone conditioning at the initial preparation 3 to 30 days ahead of the launch.

The aims of the ASOPOS 2.0 Panel update of the SOPs are threefold:

1. Further harmonization of SOPs within the global ozonesonde network, with a goal of better consistency across different stations;
2. Adoption of new SOPs that reflect the latest insights and understanding of the ECC ozonesonde measurement principles and pave the way for future modifications in data processing;
3. Simplification of SOPs, removing unnecessary steps and reducing the number of tasks performed when the caps are removed from the anode and/or cathode cells of the ozonesonde.

The SOPs given here are guidelines. Existing stations should carefully evaluate the impact of potential changes in SOPs on their data before adopting them so as not to lead to undesirable inhomogeneities or step discontinuities in their time series, particularly at stations with long data records. In case of doubt, station operators should contact members of the ASOPOS 2.0 Panel prior to making changes in SOPs. In particular, some prior procedures may already have been tested in a JOSIE or in the field. If not, a test in the WCCOS may be arranged before implementing procedural changes at operating stations. New ozonesonde stations, however, should follow the SOPs described below. These SOPs are valid both for new and recovered

ozonesondes, with **Section 4.2.3** giving guidelines on how to clean a recovered ozonesonde for re-use.

We also point out that the SOPs given here apply to the preparation of the ozonesondes only, and we do not consider any of the manipulations related to the preparation of and interaction with the radiosonde to which the ozonesonde is eventually coupled. These manipulations are out of the scope of the ASOPOS Panel although the Panel has frequent communication exchanges with the radiosonde manufacturers about integrating the SOPs and the ozonesonde metadata fields in their software packages.

4.2.2. Annotated SOP for Preparing ECC Ozonesondes

4.2.2.1 Preparation of Ozonesondes 3 to 30 Days Prior to Launch

The first steps in preparing the ECC sonde for use are a cleaning of some parts of the ozonesonde, checking the overall performance of the instrument and charging the sonde with the sensing solutions for the first time. All instructions below are displayed in the flow chart of **Figure 4-1**.

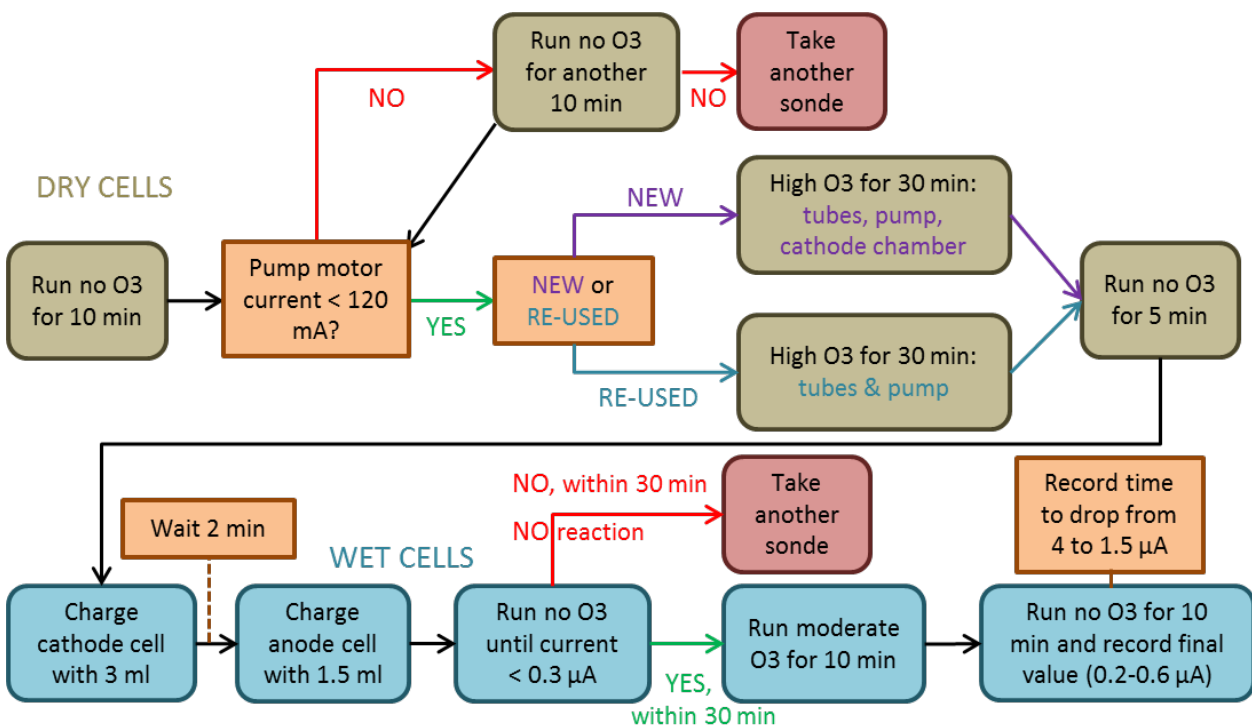


Figure 4-1: Flow chart summarizing the most important steps in the ozonesonde preparation procedure 3 days to one month before launch

- Run the ozonesonde on purified air free of ozone (“No-Lo O₃” port) for 10 minutes.

The performance of the motor has to be checked by looking at the pump motor current after 10 minutes of functioning. “Pump motor current” refers to the current of the pump motor only, not the combination of the pump motor current and the interface board current!

- Check the pump motor current. If the value is not < 120 mA
 - Run another 10 minutes.
 - If after 10 minutes, the motor current is still too high then take another sonde. After the sonde preparation, a methanol flush on the initial ozonesonde as described in **Section 4.2.3** should result in a reduction in the pump motor current. If no improvement is detected after up to five methanol flushes, this ozonesonde can also not be used at a future launch.

- Condition the following parts of the ozonesonde for 30 minutes with high ozone (> 10 ppmv):
 - Tubing (new and re-used sondes), including the tube attached to the cathode chamber cap.
 - Pump (new and re-used sondes).
 - Cathode chamber (new sondes only).

Additional cleaning of the Teflon tubes and the dry cathode chamber (only for new ozonesondes) is done by conditioning those parts with high ozone amounts (> 10 ppmv) for 30 minutes. The high ozone is generated by the UV lamp of the Ozonizer/Test Unit. The idea is to completely saturate any remaining pollutants in the sonde components with ozone, so that they will not destroy ozone molecules passing through the sonde during actual atmospheric measurements. For recovered ozonesondes (**Section 4.2.3**), only the tubes and the pump should be conditioned with high ozone, **not** the cathode chamber as it might destroy the optimum functioning of the (wet) ion bridge.

- Run on purified air free of ozone for at least 5 minutes.
- Charge the cathode cell with 3 ml of cathode solution.
- Wait 2 minutes. Then charge the anode cell with 1.5 ml of anode solution.

The sensor cathode must always be filled first. The waiting time before charging the anode cell allows the cathode solution to permeate the sensor's ion bridge, which prevents the saturated anode solution from leaking through the bridge into the cathode and changing the solution strength of the cathode.

- Run on purified (no-O₃) air. Wait until the current drops below 0.3 μA.
- If there is no reaction of the sensor or the current drops too slowly (taking > 30 minutes), set aside the sonde for a couple of hours with cell leads short circuited before rechecking the current on no-O₃ air.

The response of the charged cells is tested first by running ozone-free air through the cells. If the charged cells do not detect any current or never detect a current greater than 0.3 μA after 30 minutes sampling no-O₃ air (prior to which the cell was flushed with high ozone), it is likely that the ion bridge material is not completely saturated. In this case, the ozonesonde should be set aside for a couple of hours to ensure that the ion bridge is saturated.

- Run on moderate ozone (5 μA) for 10 minutes.
- Run on purified no-O₃ air. Record the time to drop from 4.0 to 1.5 μA.

The last test determines whether the response of the charged cells is fast enough (20–30 sec), after pumping ozone-free air through the cells following charging them with 5 μA of moderate ozone. The response time of the drop from 4.0 to 1.5 μA readings is recorded and corresponds to a direct measurement of the exponential decay time, $1/e = 0.368 \approx 1.5/4.0$.

- At the end of the 10 minutes of no-O₃, record the remaining current ("background current").

This remaining current value might give a first indication of the slow reaction pathway time constant. A typical range is between 0.2 and 0.6 μA for new ozonesondes and can be even lower for re-used ozonesondes (because its cells have not been conditioned with high ozone amounts).

- Short cell leads and return the sonde to its container. Store in a cool, dark, clean place, with a tissue under the cells until day of flight.

Prior to storage, the ECC sensor leads should be short circuited with a shorting plug. This allows a better electrochemical equilibration of the cell during storage. Never plug the sensor into the sonde's electronic interface board for storage because the unpowered board's input impedance may be high, and proper equilibration will not occur. Storing the ECC cells on a tissue – you might take the SPC cells out of their placeholder first – will allow for detection of leaking cells when the box is opened on day of flight. If a leak is detected by observing a discolouration of the tissue from the iodine in the solution, the sonde unit **should not be flown**.

Prepared ozonesondes can stay dormant for several weeks, even without refreshing the solutions in the meantime. In some cases, it has been observed that certain performance characteristics may improve with time. There is no need to refresh the solutions for ozonesondes during this storage.

4.2.2.2 Preparation of Ozonesondes 0–1 Day Prior to Launch

Both solutions are changed and the ozonesonde cells are checked during the flight preparations one day before or at the day of launch by re-measuring the time response of the sensor and currents. Additionally, some measurements are performed that immediately enter in the ozonesonde data processing code (flow rate, laboratory conditions at the time of this measurement, background current, and fast response time). A flow chart outlining this preparation procedure appears in **Figure 4–2**.

- Check the tissue under the cells for any leakage of the cells.

Leaking cells should not be used.

- Remove both cell caps and place on a clean surface. Make sure to leave space between the cathode and anode caps so they do not touch one another.
- Check that the cathode solution does not show any sign of contamination or crystals at the bottom.

If this is the case, there might be some leakage of anode solution in the cathode chamber through the ion bridge, and the ozone sensor should not be used.

- Remove and discard the anode and cathode solution. Make sure to prevent any contamination of the cathode cell with anode solution.
- Add 3 ml fresh cathode solution to the cathode cell.
- Wait 2 minutes and then add 1.5 ml fresh anode solution to the anode cell.
- Remove the electrical short on the cell leads; then connect the cell leads to the test unit.

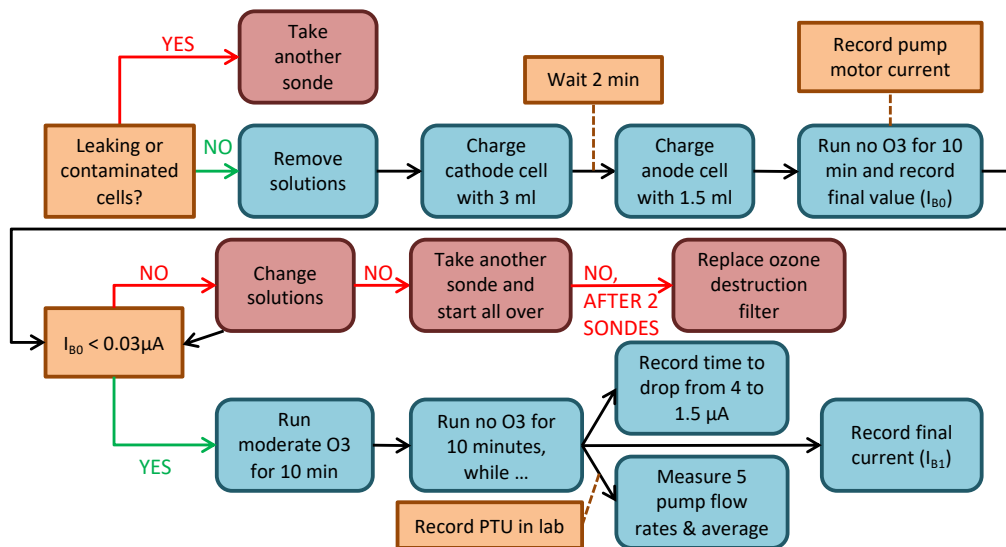


Figure 4–2: Flow chart summarizing the most important steps in the ozonesonde preparation procedure at the day before or at launch

Again, the sensor cathode must always be filled first, taking into account a long enough waiting time before charging the anode cell to allow the cathode solution to permeate the sensor’s ion bridge, thus preventing the “leaking” or “intruding” of the anode solution into the cathode chamber through the ion bridge. Keep track of the ID number of the sensing solutions that are used (see **Annex B-2.2.10**). In a site logbook (an example is given in **Annex A-3**), link the ID number of the sensing solution batch, to e.g. date of creation, the person making the solution, the recipe (**Annex B-2.1.10**), the reagent chemicals used for it.

- Run purified no-O₃ air for 10 minutes.
- Record the pump motor current (see **Annex B-2.3.8**).
- Record the cell background current (I_{B0} , see **Annex B-2.2.1**). This value must be < 0.03 μA (see also Table 5.1). If this limit is not reached, then
 - Change the solutions and repeat the test.
 - If $I_{B0} < 0.03 \mu\text{A}$ is still not reached with fresh solution, start over with a new ozonesonde.
 - If this upper limit of 0.03 μA still cannot be obtained with the new ozonesonde, replace the ozone destruction filter on the source of no-O₃ air entering the inlet of the pump (usually inside the test unit) (see **Annex B-2.2.11**).

After the pump motor has been running for a couple of minutes, record the pump motor current. This value can be compared with the recorded value during the 3 to 30 days prior to launch procedure. A first test to check the solutions is the measurement of the current generated by the cells after exposing the cells to no-O₃ air for at least 10 minutes. This current, previously defined as background current I_{B0} , should be very low ($I_{B0} < 0.03 \mu\text{A}$). If this value is exceeded, there might be a problem with the solutions or the source of the “no-O₃” air. You might change the solutions once more. If 0.03 μA is still not within reach, start all over with another ozonesonde. If the problem persists, the ozone destruction filter may be malfunctioning, requiring replacement. A proper ozone destruction filter is discussed in **Section 4.2.5**.

- Run on moderate ozone (5 μA) for 10 minutes.
- Switch to run on no-O₃ air.
- Record the time to drop from 4.0 to 1.5 μA .

The fast time response of the sensor (see **Annex B-2.1.14**) is measured after the cells have been exposed to a moderate ozone source ($5 \mu\text{A}$), timing the decay from 4.0 to $1.5 \mu\text{A}$ while being exposed to ozone-free air. This response time is typically between 18 and 28 seconds (see **Table 5-1**).

- Continue running the sonde on purified air. Connect tubing from the cathode exhaust port to the flowmeter. Allow a steady flow of bubbles to thoroughly wet the inside of the buret. Allow about 1 or 2 minutes for the temperature of the glass buret to stabilize.
- Measure and record the pump flow rate five times and calculate the average (see **Annex B-2.1.4**), which should be between 25 and 35 sec/100 ml. (see **Table 5-1**).
- Record the air temperature, pressure, and relative humidity (see **Annex B-2.1.8**) in the preparation room.

The pump flow rate directly enters the equation to convert the measured current of the ozonesonde sensor to ozone partial pressure (**Eq. E-2-1**). If measured with a bubble flow meter, a correction for humidification is required based on the environmental conditions (air temperature, pressure, and relative humidity) in the preparation room (**Section 3.3.2**). When using a well calibrated Gilibrator (**Section 4.2.5**) for the pump flow measurement, correction for the humidification effect is not required.

- After 10 minutes sampling of no- O_3 air, record the preparation current I_{B1} (see **Annex B-2.2.2**, should be $< 0.07 \mu\text{A}$) and the timestamp of this measurement (see **Annex B-2.2.3**)
- Turn off ozonesonde pump, short cell leads and store in the box

Do not launch the sonde sooner than 30 minutes after the measurement of I_{B1} . Otherwise, the surface ozone values measured by the ozonesonde might be biased high due to the remaining contributions of the ozone exposure prior to the I_{B1} measurement. By taking into account this storage time between the laboratory preparations and the actual launch, the preparation background current at the time of the launch should have decayed to the I_{B0} value. **Following this procedure, the background current (formerly I_{B2}) at the launch site should not be measured again.**

However, at sites with contamination from air pollution sources such as exhaust from local traffic, volcanic activity, or ammonia emissions from livestock, an ozone destruction filter should be used when switching on the ozonesonde pump after the I_{B1} measurement. During the last 5 minutes prior to launch, the ozonesonde should be unplugged from the filter even under contaminated conditions. **At ozonesonde sites without contamination sources the use of an ozone destruction filter is not recommended.**

Finally, during the 0–1 day before launch preparations, a calibrated ozone source in the laboratory (see **Annex B-2.3.4**) may provide added value. These devices are normally equipped with built-in ozone destruction filters and provide, if properly calibrated, an external reference for assessing the performance of the prepared ozonesonde. This requires that the ozonesonde measure exactly the air generated by the calibrator. Tests at fixed ozone amounts (50 ppb or 100 ppb) can give an extra ground check reference of the ozonesonde instrument. This manufacturer-independent ground check allows tracking of the performance of ozonesondes throughout a time series as long as proper calibration of the ozone reference instrument is maintained.

4.2.3. SOP for Re-Use of Recovered Sondes

Motivated by cost and environmental concerns, several stations launch reconditioned ozonesondes (see **Annex B-2.3.7**) routinely. Experiments at the environmental chamber at Jülich with re-used ozonesondes (JOSIE 2010, with ozonesondes used during the JOSIE 2009 campaign) confirmed proper functioning of those re-used ozonesondes (**Section 3.2.2, Figure 3-1**). Statistics from re-used sondes against new sondes at sites where recovery is

common (Payerne, Boulder, Uccle) show a similar performance, with very similar background currents, and only 1%–2% higher pump flow rates and 1%–2% less precision for recovered sondes.

Here we suggest procedures and tests that can help the operator recondition a used ozonesonde and decide whether a used ozonesonde is acceptable for re-use. The following steps focus on tasks that can be performed by non-expert operators and do not require significant labour. Refer to **Figure 4–3**. The two main parts of the ozonesonde that can be reconditioned are: (1) the pump motor assembly; (2) the electrochemical cells. If, for example, the pump and motor are operational, but the electrochemical cells are damaged, the cells could be replaced.

Pump and motor:

- First, make an initial visual assessment of the recovered ozonesonde. Is it rusty, dirty, or water damaged? If needed, rinse frame with tap water. Check if the plastic ring in the hole at the end of the piston is present and if both rubber bands around the pump cylinder are present. These rubber bands might be replaced by original rubber rings provided by the manufacturer. If the motor shaft rotates and the pump has not seized, then proceed.
- If electrically safe (i.e. no visible shorts or exposed wires) power the ECC with 12 VDC and measure the pump motor current.
- If the motor runs smoothly and the current < 120 mA, then proceed.
- If not, the fit between the piston and cylinder may be too tight and should be loosened.
- Disconnect the outlet tube from the cathode cell, then flush the pump with methanol briefly. Therefore, dip the inlet tube in a container with methanol to draw the methanol through the pump. Make sure that the output tube ejects the liquid into another container, not into the cathode cell. Monitor the motor current during this process. You may need to repeat the flush several times to achieve the desired reduction in pump motor current. However, if no improvement is detected if up to five methanol flushes, flushes not resulted in any improvement, then reject the pump for further use.
- Check the pressure and vacuum of the pump. Using a pressure/vacuum gauge, check the pump head pressure from the pump outlet (output pressure should be > 700 hPa excess to laboratory pressure) and pump vacuum from inlet port (“under” pressure should be more than 500 hPa lower than laboratory pressure). If within specifications, then the motor and pump can be considered for re-use.

Electrochemical cell:

- Open both the cathode and anode cell and rinse well with distilled water.
- Fill both cells with distilled water and let them soak for several hours to several days, to flush/clean the ion bridge.
- Rinse again with distilled water.
- Let the cells (and ion bridge) dry out for a couple of days before re-using. Dry them upside down, tilted somewhat, with the opening at the bottom (in particular in wet environments).
- Replace the Teflon inlet/outlet tubes with new ones if possible. If not, flush the old tubing and check the integrity of the tubing to make sure there are no cracks or leaks.
- Follow the SOPs for the preparation of ozonesondes 3 to 30 days prior to launch (**Section 4.2.2.1**).

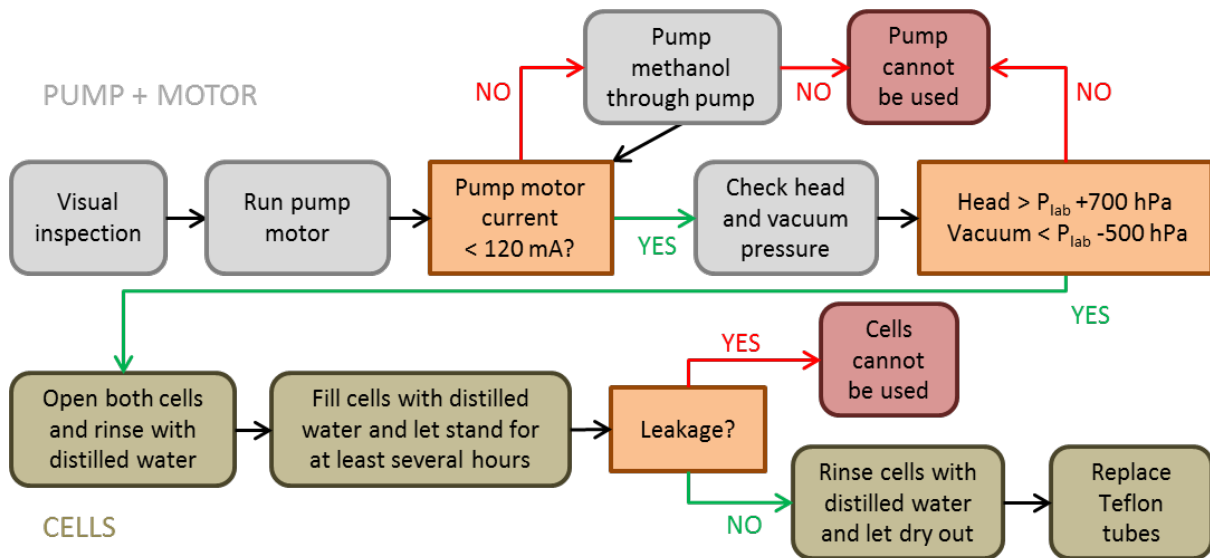


Figure 4–3: Flow chart with the most important steps to prepare recovered ozonesondes for re-use

For advanced sonde users, it is possible to disassemble the Teflon pump and clean the inner components of the piston unit, but this process is time consuming and carries a high risk for damage. Make a mark on the front side of the piston before disassembly. Reassemble then with the mark to the front. If the ozonesonde does not perform well after the minimally invasive steps described above, it may not be worth the additional time and cost to try to further clean and refurbish the unit. Advanced sonde users might also check the motor speed with a tachometer or an oscilloscope. It should be stable and within 2350–2450 RPM (40 Hz), see **Section 3.3.7**; this can be adjusted with a potentiometer on the motor using a small plastic screwdriver.

4.2.4. Issues to Avoid, Potential Pitfalls, and Troubleshooting.

We present here a far from complete list of issues to avoid and any potential pitfalls that might arise during the preparation of ozonesondes. These are just some examples, and we invite the community to post more of these on the ozonesonde’s operators and users blog (<https://www.wccos-josie.org/asopos>).

Incorrect Preparation of Solution by Neglecting Final Water Addition

At two stations in the the past, the cathode solution recipe was incorrectly applied. The usual recipe is to start with 500 ml distilled water in a 1 l bottle. After adding the chemicals, the bottle has to be shaken until the crystals become dissolved. In a final step, more distilled water has to be added to obtain a final total of 1 l of liquid. This last step has been listed in one manufacturer’s manual just below an eye-catching text block describing the chemicals. This part of the recipe may easily be overlooked. Beware!

Pump Flow Rate Measurements

Some station operators cover the top opening of the burette used for the pump flow measurement with a plastic film or a rubber stopper to avoid collecting dust, when not in use. Of course, when making the pump flow measurements, such covers/plugs must be removed. The burette must be open to the air when performing the pump flow measurement test.

Ruining the Cathode by Mixing in Anode Solution

Because the anode solution is prepared by saturating the cathode solution with KI, the introduction of even a small amount of anode solution into the cathode solution changes the KI concentration of the cathode solution significantly, making the ozone concentration

measurement highly uncertain and inaccurate. Consequently, inadvertent mixing of anode and cathode solution during the emptying and filling of the cells must be avoided. Use of separate syringes for the anode and cathode is required. If contamination occurs, discard this sonde and follow the process of preparing re-used sondes and launch the contaminated sonde some other time.

Ruining the Solutions by High ozone Exposure

During the 3 to 30 days prior to launch procedure, parts of the ozonesonde are exposed to high ozone concentrations (conditioning). If by accident, solutions in the ozonesonde cell were also exposed to these high ozone amounts, follow the procedure for preparing a recovered ozonesonde before the cells are used again.

Black Rubber Caps on Test Unit

The most recent ozonesonde test units come with black rubber caps on the NO-LO O₃ and HI-O₃ outlets of the test unit. Please remove these when the machine is in operation. If not, this may cause internal damage to the test unit.

4.2.5. Hardware to Prepare Ozonesondes

The steps on how to prepare and fly an ECC ozonesonde, including hardware and tools, are described in detail in [Annex A](#). In this section some criteria and recommendations are made on various components of the hardware.

Preparation Unit

The preparation unit for conditioning and checking out the ECC ozonesonde prior to flight needs to include the following:

- Provision for the flow of both purified and ozone-free air (500–1000 ml/min) through the use of an appropriate gas filter technique;
- High ozone source for conditioning (cleaning) of the inlet tube, pump, and (possibly) cathode cell;
- Low ozone source (variable) that supplies 0–250 ppbv ozone at 500–1000 ml/min;
- 12 V power to operate the pump motor;
- Measurement of applied voltage pump motor (0–20 V, uncertainty 0.05 V or better) and its current (0–250 mA, uncertainty 5 mA or better);
- Measurement of ECC cell current I_M (Range: 0–10 μA ; Resolution: 0.005 μA ; Uncertainty: 0.01 μA or better at $I_M < 1 \mu\text{A}$ and 1% of I_M or better at $I_M > 1.00 \mu\text{A}$).

The ASOPOS Panel does not recommend using the so-called calibrator cell with which some of the preparation units are equipped. A number of preparation units are commercially available (e.g. Ensci's KTU-3 or SPC's TSC-1), but not all stations maintain their units to these standards. It is strongly recommended that stations check their preparation unit to make sure that it has not deteriorated over time (see below).

Gas filter to obtain ozone-free and purified air

In **Sections 3.3.6 and 3.3.12** it was shown that background currents and their uncertainties are the dominating factors in ECC sonde performance near the tropopause, particularly in the tropics. During the day of launch preparation procedure (**Section 4.2.2.2**) in order to achieve low background currents $I_{B0} (\leq 0.03 \mu\text{A})$ and $I_{B1} (\leq 0.07 \mu\text{A})$, a good gas filter is essential.

From the stations that have homogenized their ozonesonde time series data following the guidelines given in [Annex D](#), it is clear that some stations reported background currents

significantly higher than the values recommended here, likely as a result of not using a sufficiently effective filter. These filters must be refurbished (every 2–3 months) or changed regularly (every 6–12 months). The commonly used commercial filters contain hopcalite (a mixture of copper and manganese oxides that catalyses the conversion of ozone to ordinary oxygen) or charcoal. However, these filters alone may not purify the ambient air sucked into the preparation unit. **Filters must first dry the air and then trap impurities as described in more detail in Annex A-8.**

Bubble flowmeter and automated versions (e.g. Gilibrator)

The bubble flowmeter that measures the rate of the soap film passing through 100 ml in the measured time t_{100} must be well calibrated. The 100 ml mark of the tube should be checked at least once to avoid errors in the measurements. For stations that use an automated version of the flowmeter, operators should be aware that these instruments can drift and should be checked regularly (i.e. monthly) against a calibrated bubble flowmeter, and the drift recorded. When drifts of more than 1% are noted, the instrument should be serviced.

Maintenance of ground equipment

To guarantee optimal performance of the ECC ozonesonde, the ground equipment needs regular check-ups to be sure it is in the best possible working order. Some specifics:

- Regular exchange of the gas filter, under humid conditions (e.g. in the tropics) at frequent intervals; a colour-indicating desiccant helps;
- The low ozone outlet should provide air with an ozone concentration of at least 300 ppbv (about 8 μA ECC cell current). If these ozone levels cannot be achieved anymore (cell currents above 8 μA), the UV lamp in the preparation unit has most likely degraded and should be replaced;
- In addition to the previous point, you should check the position of the ozone regulator tube for the moderate (5 μA) ozone amount. Check for drifts or jumps over time, which might indicate that it is time to replace the UV lamp;
- Check yearly the flow of the internal pump with a flowmeter (or e.g. the bubble flow meter). This flow at the outlet port "NO-LO-O3" should be at least twice or more than the flow generated by the ozone sonde pump;
- Open the Test Unit yearly and visually check that the tubes are connected firmly and that there is no leakage near the ozone destruction filter. Check if the glass of the UV lamp is still clear.

It is recommended that every 3–5 years an overall check by the manufacturer is performed on the test unit.

4.3. Data Processing and Archiving

4.3.1. Introduction

The overall goals of updates for archiving sonde data are (1) traceability to a common ozone reference (the WCCOS-OPM) and (2) for each data set to have a unique version number that denotes the processing status.

Access to high-resolution vertical profiles of ozone measured with ozonesondes is important for many data users. Primary ozonesonde data are archived at the WOUDC (<https://woudc.org>), NDACC (<https://www.ndacc.org>) and SHADOZ (<https://tropo.gsfc.nasa.gov/shadoz>) databases. These data may also be found in other archives in user-preferred formats or modified through assimilation or combination with other observations or model output. Because both the archiving process and the capacity to store ozonesonde profiles have greatly improved since the 1990s, it is easy to store full resolution sounding data and supporting documentation

(metadata) about the sounding origin, content, and quality that are needed to ensure permanent traceability.

The ASOPOS 2.0 Panel recommends a revision of the reported ozone sonde data for archiving with emphasis on the traceability of the data through (i) an extended suite of parameters obtained during pre-flight preparation; (ii) the complete ozone and pressure-temperature-humidity profiles, and (iii) the station characteristics (logbook of instrumental preparation and correction procedures). Reporting and retaining this information allow for reprocessing of ozone profiles from the original parameters (i.e. the raw ozonesonde cell current, pump temperature and flow rate) when any new recommendations are made.

To supply complete ozonesonde records, including missing, erroneous, pre-launch, descent and questionable results to a community that is accustomed to seeing only high quality 'clean' data, can be a challenge both for data provider and data user. However, the introduction of reliability flags (below) is intended to guide data users.

4.3.2. Processing Ozonesonde Data-Corrections and Uncertainties

The partial pressure of ozone P_{O_3} measured by the electrochemical sensor can be determined from the measured sensor current (I_M), the background current (I_B), the total efficiency (η_T), the temperature of the gas sampling pump (T_P) and the volumetric flow rate (Φ_{P0}) using the basic ozonesonde Eq. E-2-1. Also, it is essential to include the overall uncertainty of each P_{O_3} measurement. In Chapter 3, it was shown that the measurement of P_{O_3} is subject to a number of instrumental factors that can influence the sonde performance and contribute to the overall uncertainty of the measurement. Section 3.3 discussed the contributions of the individual uncertainties of the different instrumental parameters. After correcting for known bias effects, it is assumed that the remaining uncertainties are, to the first order, random, uncorrelated, and following Gaussian statistics. Eq. E-3-1 gives the overall relative uncertainty of P_{O_3} . Table 4-1 gives an overview of the recommended data processing procedures, including the correction steps required to resolve bias effects in the measured parameters that are used to derive P_{O_3} and its overall uncertainty. For details on each component of the recommended processing steps and the formulas to be applied, refer to Section 3.3 and Annex C.

Table 4-1: Summary of recommended data processing steps to derive P_{O_3} for the ECC ozonesonde from the corrected measured parameters (Φ_{P0} , I_M , I_B , T_P , η_A , η_B , η_C) applying Eq. E-2-1. Included are the individual correction steps and the individual uncertainty contributions to derive the overall uncertainty P_{O_3} (Eq. E-3-1).

Corrected Parameters In Eq. E-2-1	Correction Step	Processing Step	Absolute or Relative Uncertainties Contributing to Eq. E-3-1	Section
Φ_{P0}	$\Phi_{P0} = (1 + C_{PL} - C_{PH}) * \Phi_{PM}$ Φ_{PM} : t_{100} to flowrate C_{PH} : Humidification C_{PL} : Difference T_P to T_{Lab}	Eq. E-3-3 Eq. E-3-2 Eq. E-3-4 Eq. E-3-7	$\Delta\Phi_{P0}/\Phi_{P0}$ (Eq. E-3-9) $\Delta\Phi_{PM} = \pm 1\%$ of Φ_{PM} ΔC_{PH} (Eq. E-3-6) ΔC_{PL} (Eq. E-3-8)	3.3.2
I_M			$\Delta I_M = \pm 0.005 \mu A$ at $I_M \leq 1.00 \mu A$ (Eq. E-3-14-A) $\Delta I_M = \pm 0.5\%$ of I_M at $I_M > 1.00 \mu A$ (Eq. E-3-14-B)	3.3.6
I_B	$I_B = I_{B1}$ is constant		$\Delta I_{B1} = \pm 0.02 \mu A$	3.3.6
T_P	$T_P = T_{PM} + 3.90 - 0.80 * \text{Log}_{10}(P_{air})$	Eq. E-3-15	$\Delta T_P = \pm 0.7 K$	3.3.8
η_A	Cathode cell charged with sensing solution: 3.0 ml 2.5 ml	$\eta_A = 1.00$	$\Delta\eta_A = 0.01$ (Eq. E-3-10)	3.3.4

		Eq. E-3-11-A/B	$\Delta\eta_A$ (Eq. E-3-11-C)	
η_p	SPC-6A sondes with SST1.0 or SST0.5: K86-Efficiency (<i>Komhyr, 1986</i>) ENSCI sondes with SST 1.0 or SST0.5: K95-Efficiency (<i>Komhyr et al., 1995</i>) ENSCI sondes with SST0.1: NOAA/CMDL 2002 or JMA 2016	Table 3-1	Table 3.1	3.3.3
η_c		$\eta_c = 1.00$	$\Delta\eta_c = 0.03$	3.3.5

4.3.3. Metadata

Observations of ozone using ECC ozonesondes require additional information to properly describe the observations. This additional information, called metadata, characterizes the environment under which the ozone measurements were taken and the ozonesonde itself. Metadata are critical in describing the unique characteristics of each ECC sensor and provide a valuable record for tracking changes in preparation procedures and changes in the sensor itself. Consistent and complete record keeping is important for maintaining quality across the data record by guiding users and data managers in maintaining homogenized data records. We make a distinction between (i) *required* metadata and raw data, without which reprocessing is not possible, (ii) *essential* metadata, needed to understand the performance of the instrumentation, and (iii) *desired* metadata to fully understand all aspects regarding an ECC ozonesonde observation.

The metadata are best collected during sonde preparation and at the time of the relevant observations, when most information is readily available. Over time, commonly used parameters and coefficients, such as pump efficiency factors, solution recipe, or cell background current treatment, may change. It is vital that these changes are properly captured with the measured data so that the data record as a whole can be properly analysed and evaluated.

The standard operating procedures specified in the previous sections (**Section 4.2.2**) describe some metadata that are important for ozonesonde observations. However, from a historical point of view, this metadata checklist sheet information has often been incomplete. As a result, providers of software to collect ECC ozonesonde data have relied on historic and often obsolete metadata "checklists" that complicate the interpretation, troubleshooting, and reprocessing of ECC ozonesonde observations across networks.

In [Annex B](#) of this report, we provide guidelines on metadata that should be captured by sounding system software and made available to the end-user, so that the metadata can be analysed and processed further by researchers and data centres. These recommendations also serve as 'best practice' guidelines to the ozonesonde community on metadata reporting. Implementation of these recommendations is an essential step towards a homogeneous ozonesonde network.

4.3.4. Overview of Required Ozonesonde Data to be Archived

The primary purpose of the recommended format is to provide level 1.0 quality controlled vertical profile data to end users that are interested in ozone for scientific research. Secondly, these recommendations provide metadata to users who need to assess the performance of ozonesondes in detail (e.g. members of the satellite data and trends assessment communities). A file format designed for both types of requirements represents a compromise between the need for a simple summary and the need for as much secondary information as possible. Each stored ozone profile measurement record consists of:

1. Measured values;
2. Overall uncertainties in the physical quantities measured, which consists of the sum of all uncertainty contributions from the preparation and in-flight performance of the ozonesonde;
3. Flags giving: (i) the state of reliability, and optionally (ii) the identification of various conditions impacting the reliability of the measurements (e.g. functioning of the instrument, atmospheric conditions).

Data Flagging Scheme

The ozonesonde data flagging scheme needs to provide basic information on whether or not the data has been validated, the status or reliability of the data, and some higher-level explanatory details. Criteria to evaluate the reliability of the vertical ozone profiles are listed in **Table 5.1**. The following data flagging scheme fulfils these requirements, while avoiding too much complexity for the data user.

1. For each ozonesonde flight, a flag should be added to indicate whether the data has been checked by the PI, an algorithm, or not checked at all.

- 0 Raw
- 1 Preliminary (L1)
- 2 Final (L2)
- 3 Near Real Time (NRT)

2. For each measured ozonesonde data point, a first mandatory reliability flag should be added to each profile level (data record) using the WMO Code 0 33 020 convention (<https://codes.wmo.int/bufr4/codeflag/0-33-020>) , indicating the following conditions:

- 0 Good
- 1 Inconsistent
- 2 Doubtful
- 3 Wrong
- 4 Not checked
- 5 Has been changed
- 6 Estimated
- 7 Missing value

3. A second flag is added to each profile data record with explanatory codes for various specific conditions impacting the data reliability (see some criteria in **Table 5.1**).

- 0 Instrument behaving normally
- 1 Apparent ozone level suspicious but no other indication of an instrument problem
- 2 Suspected frozen sensing cell
- 3 Suspected pump seizure or pump battery failure
- 4 Other (details should be recorded in-flight comments)
- 5 Ground checks or total ozone normalization out of acceptable range
- 6 Telemetry or radiosonde failure (value missing or physically impossible)
- 7 Descent or pre-launch data

4. A third flag may be added to each profile data level with explanatory codes for various specific conditions impacting the data reliability (see some criteria in **Table 5-1**).

- 0 Instrument behaving normally
- 1 Specific comment to report in the Logbook Data Segment to document specific details on the sounding in "free style ascii text"

In cases where more than one condition is present, the higher value numeric code is used.

Overview of major specifications of requested ozonesonde data format

The required ozonesonde data content is categorized into four data segments as follows.

- (I) Overhead Data Segment: Administrative and instrumental information on data version number, data flag on level of processing, data provider, measuring platform, location, date and time of the launch (UTC).
- (II) Meta Data Segment: Specifications of the flown instrument (including radiosonde type, balloon size, etc.), data from the pre-flight instrument preparation, and information on the post-flight data processing approach/algorithm (see **Annex B-5.1**).
- (III) Profile Segment: Vertical profile data (including uncertainties and flags)

#PROFILE

- 1. *Duration* [second], i.e. elapsed flight time as primary variable
- 2. *Flag* [3-digits], i.e. status, reliability, and specifics of the data record
- 3. *Pressure* [hPa]
- 4. *O3PartialPressure* [mPa], i.e. ozone partial pressure after all corrections applied
- 5. *Temperature* [K]
- 6. *WindSpeed* [m/s], i.e. wind speed (if available)
- 7. *WindDirection* [degrees in 360, 0° = N, 90° = E], i.e. wind direction (if available)
- 8. *GPHeight* [masl = meter above mean sea level], i.e. geopotential height
- 9. *RelativeHumidity* [%], i.e. relative humidity (in percent) with respect to liquid water (even when temperature is lower than 0 °C)
- 10. *PumpTemperature* [K], i.e. temperature of air sampled by pump, usually the pump temperature
- 11. *CellCurrent* [microamps = 10⁻⁶ A], measured ozonesonde cell current (no corrections applied)
- 12. *PumpMotorCurrent* [mA] (if available), i.e. electrical current measured through the pump motor
- 13. *PumpMotorVoltage* [V] (if available), i.e. voltage measured across the pump motor
- 14. *Latitude* [-90 to +90 degrees] (if available), i.e. geographical latitude (e.g. GPS)

15. *Longitude* [-180 to + 180]) (if available), i.e. geographical longitude (e.g. GPS)
16. *GPSHeight* [masl = meter above mean sea level] (if available), i.e. geometric height

#PROFILE UNCERTAINTY

- Estimated uncertainty (if available) for each of the measured profile parameters as listed in #PROFILE segment.

Pre-Launch

- Pre-launch data (if available) for each of the measured parameters (listed in #PROFILE segment) as recorded 15–20 minutes before launch. At launch the duration is zero, whereas before launch the duration is relative to launch and consequently negative in sign.

Descent

- Descent data (if available) for each of the measured parameters (listed in #PROFILE segment).

(IV) Logbook Data Segment: Detailed Information on the sounding

A new feature added here is the possibility to link individual sounding data to the logbook of the station, in which links to web archives of Logbooks from stations may be available for some stations. The specific information on changes of sounding system, ozonesonde preparation procedures, or data processing procedures that are documented should be part of the data archives or require a DOI to be invariant to any changes of web links over time. Problems encountered during the sounding can be linked to the third Data Flag in the Profile segment. This information in the Logbook Data Segment can be done in free ascii text format.

5. DATA QUALITY INDICATORS (DQI) (Holger Vömel and Ryan M. Stauffer)

5.1. Introduction

The WOUDC has defined several ozone data products in the categories of total column ozone and vertical profile information from ozonesondes and Umkehr/Lidar retrievals from ground-based, stationary platforms. Ozonesondes have instrument specific-data content and quality indicators. The ozonesonde data format at WOUDC uses four major data sections: (i) Overhead (ii) Header, (iii) Profile, and (iv) Metadata (**Section 4.3.3**) that includes additional information to be used to process, reprocess, and evaluate the reliability of the data. The purpose of this Chapter is to provide some data quality indicators (**DQIs**) to the ozonesonde data user that may be applied to objective assessments of the quality of sounding data archived at the WOUDC. The **DQIs** may be used (i) to screen the sonde performance in individual vertical profiles, allowing an estimate of the measurement uncertainty that may be expected; (ii) to homogenize long-term records at single sounding stations or data records across different sounding stations, and (iii) to monitor more general aspects, such as station operators, station sounding practice, instrument and data traceability, data reprocessing, and data usage.

5.2. Screening individual vertical ozonesonde profiles

Typically, each ozone profile is measured with a new ozonesonde instrument, which is characterized and conditioned prior to the sounding; post-flight characterization is usually not possible. Therefore, DQIs rely exclusively on pre-flight and in-flight sounding data to evaluate the reliability of individual sounding profiles. **Table 5-1** contains quantitative criteria to evaluate the quality of an ozonesonde profile. These criteria do not guarantee an assumed measurement uncertainty but serve as indicators of the performance of the sonde and the reliability of the individual sounding data. Distributions of selected parameters in **Table 5-1** for SPC and ENSCI ECC ozonesondes are shown in **Figure 5-1**. We do not imply that data and metadata outside of the ranges in Table 5-1 should always be removed from the profile, rather that caution should be used with those data. See also recommendations for flagging profile data in **Section 4.3.4**.

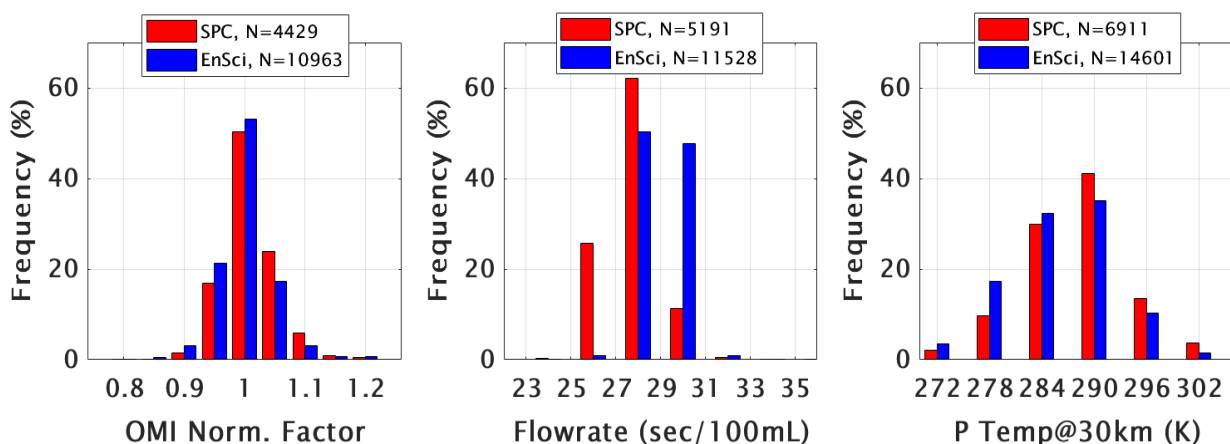


Figure 5-1: Example frequency histograms of total ozone normalization factor derived from the comparison with the Aura OMI satellite instrument, ECC pump flowrates, and pump temperatures at 30 km altitude from a set of SPC (red) and ENSCI (blue) ozonesondes.

Table 5–1: Criteria to evaluate the reliability of vertical ozonesonde profiles made using the two major ozonesonde types used in GAW-ozonesonde networks. The here marked indicators are independent of the sensing solution types used but are related to the ozonesonde types deployed (For details see text in Section 5.2).

Indicator	ECC SPC	ECC ENSCI-Z	Identifier in WOUDC
Total ozone normalization factor	0.9–1.1	0.9–1.1	TotalOzoneNormalizationFactor
Time to pump 100 ml [s]	25–35	25–35	FlowRateTime
Pump flowrate [ml/min]	170–240	170–240	PumpFlowRate
Response time (1/e) [s]	18–28	18–28	ResponseTimeFast
Pump temperature [K]	278–310	283–310	SampleTemperature
Background current before exposure to ozone [μ A]	< 0.03	< 0.03	I_{B0}
Background current after exposure to ozone [μ A]	< 0.07	< 0.07	I_{B1}
Pump motor current [mA]	50–120	50–120	PumpMotorCurrent
Pump motor voltage [V]	12–18	12–18	PumpMotorVoltage

5.2.1. Total Ozone Normalization Factor (See Section 3.3.11)

The ratio of total ozone column measured by a spectrophotometer (e.g. Dobson or Brewer) and total ozone column derived from an ozonesonde profile plus estimated residual above balloon burst height has historically been called total ozone normalization factor (**N_T**). A common practice is to integrate the ECC ozone to 10 hPa, and to apply the *McPeters and Labow* [2012] satellite ozone climatology above 10 hPa to calculate the total column ozone. The factor provides a good screening test for unreliable soundings using the criterion that the normalization factor may not deviate more than about ± 0.1 from 1.0. However, a normalization factor of one is not a guarantee that the profile is correct.

Ozonesonde profile data should not be normalized (i.e. the individual data points within an ozonesonde ozone partial pressure profile should not be scaled by the total ozone normalization factor, **N_T**). A total ozone normalization factor (**N_T**) may be reported as a negative value, indicating that the factor has not been applied to the vertical ozonesonde profile, consistent with earlier conventions. Thus, all data submitted to archives should report negative normalization factors if the data conform to these recommendations.

5.2.2. Pump Flow Rate (See also Section 3.3.2)

The volumetric flowrate of the air sampling pump is measured at surface conditions as part of the pre-flight preparation of each ozonesonde. If the flowrate of the pump is outside of the limits listed in **Table 5–1**, this could be indicative of an unstable motor and the ECC should be set aside and a new one prepared. At air pressures below 100 hPa, the pump efficiency of the gas sampling pump decreases as a known function of ambient pressure. The pump efficiencies listed in **Table 3–1** may represent a true pump efficiency or may include empirical pressure dependent efficiency factors, which are sonde type and solution specific. The uncertainty of the pump efficiencies presented increases substantially at pressures below about 20 hPa, which can contribute significantly to the overall uncertainty of the sonde performance above an altitude of 25 km. Great care must be taken that the appropriate pump efficiency tables are used based on the recommendations in **Chapter 3.3.3**.

5.2.3. Response Time (see also Section 3.3.9)

The in-flight response time to a step change in ozone is approximately 18–28 s for the ECC. The response time must be measured as part of the pre-flight preparation of the ozonesonde as the time during which the cell current decreases from 4 μA to 1.5 μA immediately following the 5 μA conditioning of the ECC. With a typical ascent velocity of 5 m/s, the ECC has an effective vertical resolution of about 100 m, with a slight displacement upward of the profile in the vertical relative to the actual atmospheric ozone distribution. Corrections for the lag in response should be applied to improve the resolution of finer structures, but the response time is typically not considered in the operational processing of ozonesonde profile data. (i.e. data submitted to archives do not account for this vertical shift). Response times larger than 30 s are an indication of malfunction or improper preparation of the ozonesonde, which are likely to produce unreliable data.

5.2.4. Pump Temperature (See also Section 3.3.8)

The air mass flow rate through the sensor depends on the temperature of the air flowing through the sensor, which is measured in-flight by a thermistor embedded in the Teflon body of the pump. Over the course of a sounding, the pump temperature typically varies by 10–25 $^{\circ}\text{C}$. In modern soundings, the temperature can be measured with an uncertainty of better than 1–2 $^{\circ}\text{C}$.

Temperature measurements at other locations inside the ozonesonde foam box are no longer in use. In older sounding systems (before the 1990s), it was not possible to report the actual pump temperature due to telemetry limitations of the analogue radiosondes. More recently, some historical sondes measured the temperature of the air inside the foam box or of the tubing into the cell. Historical soundings without a dedicated temperature measurement commonly used a constant pump temperature or an empirical table of the pump temperature as a function of the ambient air pressure. This can introduce uncertainties of 1%–7% in the ozone computations, particularly for the highest altitudes [SPARC-IOC-GAW, 1998].

The in-situ pump temperature should never be below 278 K (+5 $^{\circ}\text{C}$) for either SPC sondes or 283 K (+10 $^{\circ}\text{C}$) for ENSCI sondes, which is a few degrees above the freezing point of the sensing solution. The sensing solution is likely colder than the air flowing through it due to evaporative cooling. Thus, freezing of the sensing solution is likely if the pump temperature reaches these temperatures. Malfunction of the ozone sensor cell resulting from freezing solutions manifests as relatively fast decaying towards erratic low ozone data values, which should be flagged. On the other hand, high pump temperatures increase the evaporation rate of the sensing solution, which may introduce larger uncertainties in the conversion efficiency of the ozone sensor (**Section 3.3.5**). If this temperature range is frequently exceeded, then a change in the thermal management of the ECC sonde may be needed to increase or decrease the mean temperature inside the Styrofoam box.

5.2.5. Pump Motor Current

A 12 VDC electric motor drives the air sampling pump of the ozonesonde. The electrical current drawn by this motor should be maintained within the range shown in **Table 5–1**. Higher pump motor currents may indicate excessive frictional heating of moving parts of the pump causing a loss of pump efficiency. Lower pump motor currents may be symptomatic of pump leakage and loss of pump efficiency. In both cases, the ozonesonde data will tend to be too low, which may result in a total ozone normalization factor larger than 1.0. Current interface boards measure this current directly and transmit it as part of the telemetry stream. Ground equipment may measure the total of the motor current and the current required to operate the interface board. The contribution of the interface board should be subtracted when noting the motor current during the ground check.

5.2.6. Pump Motor Voltage

The ECC ozonesonde 12 VDC pump motor is powered by one of two types of batteries: dry or wet cells. For dry cell batteries, the ozonesonde pump motor voltage is supplied by two 9 V

alkaline batteries connected in series, supplying up to 18 V. For wet cells, the battery is activated with water just prior to launch to ensure sufficient voltage is supplied for the duration of the flight. The battery voltage should not drop below the rating of 12 V for the motor (**Section 3.3.7**); otherwise, the ozonesonde pump motor speed may slow down, affecting the ozone measurements. In some cases, if the battery voltage drops too low, the ozonesonde pump or the electronic interface may stop completely. The battery voltage should be checked at the ground site to ensure that proper voltage is being supplied to the pump motor (typically 16 V under load or more).

5.2.7. Background Current (See also Section 3.3.6)

As part of the pre-flight preparation of the sonde the cell current of each ozonesonde is individually recorded by forcing ozone-free air through sensor cell. The background current depends on the exposure to ozone and is measured in the laboratory before and after exposure of ozone (I_{B0} and I_{B1} respectively). The background current should be less than 0.03 μA before ozone exposure and is typically less than 0.05 μA after exposure to ozone. For instruments to be flown, the background current after exposure to ozone should not exceed 0.07 μA . Larger values indicate a problem during preparation or a malfunctioning ozonesonde. In ECC-soundings before about 1990, the background currents were generally about factor of four larger than after that date.

5.2.8. Sensing Solution Type (SST) and ECC sonde Type (See Sections 1.3 and 2.3.2)

Since 1995, two main manufacturers produce ECC ozonesondes. Science Pump Corporation (SPC) produces the SPC-6A series and Environmental Science Inc. (ENS-CI) produces the Z series. JOSIE 2000 and BESOS experiments [Smit *et al.*, 2007; Deshler *et al.*, 2008] demonstrated significant differences in ozone readings when sondes of the same type are operated with different cathode sensing solutions (**Table 2-2**). For each ECC manufacturer, the use of 1.0% KI and full buffer (SST1.0) gives approximately 5% larger ozone values compared to the use of 0.5% KI and half buffer (SST0.5) [Smit *et al.*, 2007]. JOSIE also demonstrated that the performance of the two ECC types differs significantly, even when operated under the same conditions. Particularly above 20 km the ENSCI-Z sondes tend to report 5%–10% more ozone than the SPC-6A sondes. SST variants other than SST1.0 and SST0.5 have been used at NOAA-operated sites. A 2.0% unbuffered solution (SST2.0) was introduced in the late 1990s to eliminate the secondary buffer reactions and the need to consider the solution conversion efficiency and ECC pump efficiency as two compensating factors [Johnson *et al.*, 2002]. However, JOSIE experiments noted that SST2.0 measured up to 10% too low in the stratosphere [Smit *et al.*, 2007].

The 1.0% 1/10th buffer solution (SST0.1) was introduced at NOAA sites (and Costa Rica) around 2005. JOSIE-SHADOZ in 2017 demonstrated that the differences in ozone measurements between sondes from the two manufacturers may be reduced when using SST0.1 [Thompson *et al.*, 2019], but further investigation is still needed.

Before 1995 the SPC-(3A, 4A, 5A) sonde types were mostly flown with 1.0% KI and full buffer (SST1.0). However, in the 1970s and early 1980s, ECC sondes were operated with higher concentration sensing solutions (1.5 or even 2.0 higher) than SST1.0. Therefore, it is important to recognize that there is a conversion efficiency, which depends primarily on the stoichiometry of the redox reaction of O_3 with KI in the different sensing solution types and sonde type, but also can include other underlying processes, which may also depend on the details of the sonde design and manufacture as shown in **Section 3.3.5**.

The recommendation of SSTs for existing stations remains the same as in GAW Report No. 201: SST1.0 for SPC, and SST0.5 for ENSCI. New ozonesonde stations should consult ASOPOS for solution recommendations and SOP. It is worth reiterating that existing network stations should not change SST or ozonesonde preparation.

5.2.9. Removal of Artefacts and Interferences

Occasionally, stratospheric ozonesonde profiles exhibit large, transient spikes (**Figure 5–2**). These spikes are characterized by the cell current jumping by up to one μA or more within one second, followed by a decay to a reasonable profile with a time constant of approximately 20 s. These spikes are unphysical responses to ozone. The cause of these spikes has yet to be determined. No rigorous investigation has yet taken place to better characterize the occurrence of these spikes. In addition to the spike, the ozone profile prior to the occurrence of the spike may show a low bias, which must be corrected as well. While detection of the spike is trivial, estimating the region and extent of low bias is more challenging.

Spikes may occur more than once in a profile. Expert opinion is required to evaluate how much these spikes may contribute to the uncertainty of the total ozone column. Rarely is the number of spikes in a profile sufficiently large to render a profile less useful. Spikes are generally not observed in tropospheric profiles. Ozone data in obvious spikes as in **Figure 5–2** should be flagged and not used for analysis. In some cases, stratospheric spikes may be less obvious, and require expert analysis for identification.

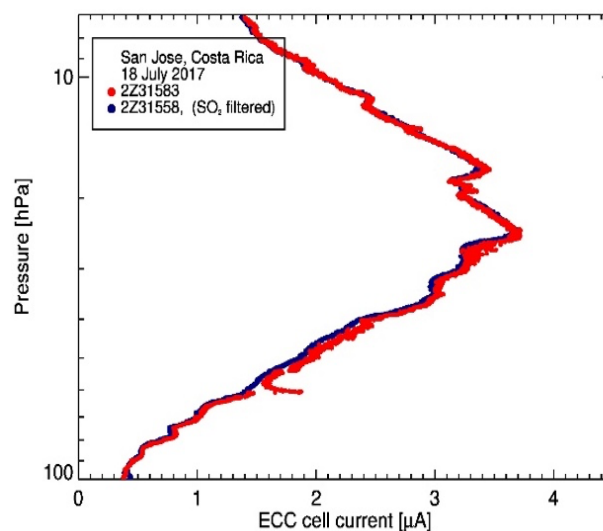


Figure 5–2: Example of an artificial ozone spike at Costa Rica from a dual flight. A spike (red profile) near 60 hPa level appears as a sharp increase in the stratospheric ozone which is very uncharacteristic of the rest of the profile. The second ECC (blue profile) shows no artificial ozone spikes in the stratosphere

Other trace gases such as SO_2 or NO_x may act as reducing agents and interfere with the reaction of ozone and iodide in solution, leading to artificially low-biased observations of ozone (see **Section 3.2.5**). Detailed knowledge about the local environment may be necessary to identify these interferences. Observations of low ozone should be flagged as unreliable if there is any suspicion for interferences from these trace gases.

5.2.10. Metadata Record

Ozonesonde data are submitted to large archives, such as the WOUDC, NDACC or SHADOZ. The metadata accompanying an ozonesonde profile should be complete. In addition to station information and launch date and time, the description of the sonde, the solution, and all processing steps must be included accurately. Incorrect metadata may reduce the utility of an

ozonesonde profile. [Annex B](#) provides a listing of all metadata that should accompany an ozonesonde profile. When a change at an ozonesonde station occurs, great care has to be taken to make sure that automatic routines capturing metadata are appropriately updated to properly reflect that change.

While handwritten notes are vital for documenting procedures at a station, electronic records are archived at the larger data centres. These electronic records must be consistent with the handwritten records, and duplicate written and electronic records are strongly recommended for all stations.

5.2.11. ECC Manufacturer Changes

In addition to intentional and well documented changes in the construction of the ECC ozonesonde (e.g. changes from SPC 3A-6A), inadvertent changes may be introduced that can affect the ozonesonde measurements. For example, the EN-SCI company was sold to Droplet Measurement Technologies (DMT) in 2011, and changed ownership again in 2016 with a rebranding back to EN-SCI. During this period, EN-SCI ozonesonde station operators began noticing changes in instrument response during the ECC preparation process, and subsequent drops in the ozonesonde measurements were documented [*Thompson et al., 2017; Sterling et al., 2018; Stauffer et al., 2020*]. Possible differences in the construction of the EN-SCI ozonesonde during 2011–2016 are currently being investigated. This example shows that careful record keeping of metadata and notes by the observers are vital for the evaluation of ozonesonde data regardless of documented changes to the ECC instrument or preparation process.

5.3. Homogenization of Temporal and Spatial Ozonesonde Records

JOSIE [*Smit et al., 2007*] showed that great caution has to be exercised in changing instrument configuration or operating procedures, any of which may negatively influence the ability to estimate long-term changes in atmospheric ozone. Changes in operating procedures for ozonesondes in historic records of some sounding stations require a variety of corrective methods. Quantitative tools are needed to homogenize long-term records of individual sounding stations, as well as sounding records between different stations [*Smit and O3S-DQA, 2012*]. Transfer functions [e.g. *Deshler et al. 2017*], which quantify the differences of sonde response depending on changes to the instrument or operating procedures, are based on empirical evidence and statistical analysis. Other factors requiring homogenization include changes to the cathode SST volume used, changes to how the background current is measured or applied during processing, and changes to the pump temperature and flowrate measurements. Guidelines for the homogenization of historical ozonesonde records are found in [Annex D](#). Extensive validation is required to verify the consistency of the homogenization and to ensure that no additional inhomogeneities are introduced. It is also important to recognize that no changes to site operation should be considered before carefully quantifying its potential impact to the long-term record.

Examples of the homogenization of individual site [e.g. *Van Malderen et al., 2016; Witte et al., 2019*] and network [e.g. the Canadian Network and SHADOZ; *Tarasick et al., 2016; Witte et al. 2017; Sterling et al., 2018*] ozonesonde data are found in recent literature. Emphasis is placed on the improved comparisons of the homogenized ozonesonde data against independent data, primarily total column ozone from ground-based (e.g. Brewers and Dobsons) and satellite instruments (e.g. Aura OMI), and satellite profiling instruments (e.g. Aura MLS). Validation of the homogenized SHADOZ data set is also found in *Thompson et al. [2017]*. To date about more than half (~40 stations) of regularly-reporting ozonesonde stations have homogenized their records.

5.4. General DQI's for Ozonesondes

General **DQI** are grouped in: (i) Station information and sounding practice; (ii) Traceability; (iii) Data reprocessing; and (iv) Data usage. General **DQI** are only qualitative and give valuable information about the profiling capabilities of an individual sounding station and its data quality, which is particularly relevant for the determination of long-term trends. However, these are only indirect indicators and need to be examined carefully in order to avoid subjectivity. The four major categories of general **DQI** are described in more detail below.

5.4.1. Station Information and Sounding Practices

In addition to geographical location, air quality (industrial or natural pollution) and other general information, the station information must include a description of the sounding system, practice of sonde preparation, operations, and post-flight processing. Details of sonde operations and processing are described in [Chapter 4](#) and [Annex A](#).

5.4.2. Traceability

Traceability is crucial, particularly for long-term sounding records. Intercomparison campaigns like JOSIE and BESOS have shown that small changes in instruments or operating procedures can have significant impact on long-term records of a sounding station and the long-term trend derived from these records. Important aspects of traceability are:

- (i) A long-term record of changes in the sounding system, details of preparation, operations, and post-flight processing is vital to identify when changes in the equipment or operations occurred. The latter may be scrutinized in detail for possible discontinuities in the long-term record;
- (ii) Where available, comparisons with other profiling techniques such as ground-based lidar or microwave profiling, or ground-based column ozone from spectrometers, should be performed to verify the consistency of the data provided by a station;
- (iii) Regular comparisons with satellite-based profiles during station overpasses are useful to identify possible inconsistencies that have not been detected using data recorded at the station alone and to provide an early warning for problems either in the sounding station or with satellite observations;
- (iv) The performance of the radiosonde, in particular the reported pressure measurements, affects the calculation of some ozone parameters [*Stauffer et al., 2014*]. Therefore, the operations and performance of the radiosonde need to be tracked with the same care as the ozonesonde.

5.4.3. Data Reprocessing

Documentation of data processing and data revisions is essential for long-term records. A unique version number should be assigned to the data sets and linked to the documentation of the data revision. This allows tracking the evolution of the data processing and possible influences on long-term trends derived from the time series of ozone soundings at the station.

5.4.4. Data Usage

Data usage may refer to the use of station sounding data for:

- (i) Scientific publications (especially in refereed journals);
- (ii) Technical publications assessing the performance of the sonde used at the station.

These publications may describe problems within a data set or simply demonstrate its high quality. It is important to know that a data record has already been analysed by others in an independent study, especially by experts, so that similar problems do not have to be "rediscovered". Inclusion of these data sets within the WOUDC and/or other archives (NDACC, SHADOZ, etc.) is also recommended.

REFERENCES

- Aimedieu, P., W.A. Matthews, W. Attmannspacher, R. Hartmannsgruber, J. Cisneros, W. Komhyr, D.E. Robbins, 1987: Comparison of in-situ stratospheric ozone measurements obtained during the MAP/Globus 1983 campaign, *Planetary Space Science*, 35, 563–585
- Attmannspacher, W. and H. Dütsch, 1970: *International Ozone Sonde Intercomparison at the Observatory of Hohenpeissenberg*, Berichte des Deutschen Wetterdienstes, 120
- Attmannspacher, W. and H. Dütsch, 1981: *2nd International Ozone Sonde Intercomparison at the Observatory of Hohenpeissenberg*, Berichte des Deutschen Wetterdienstes, 157
- Bak, J., K-H Baek, J-H. Kim, X. Liu, J. Kim, K. Chance, 2019: Cross-evaluation of GEMS tropospheric ozone retrieval performance using OMI data and the use of an ozonesonde data set over East Asia for validation, *Atmospheric Measurement Techniques*, 12, 5201–5215, 2019 <https://amt.copernicus.org/articles/12/5201/2019/amt-12-5201-2019.pdf>
- Basher, R. E., 1982: *Review of the Dobson Spectrophotometer and its Accuracy*, Global Ozone Research and Monitoring Project (GORMP), No. 13, World Meteorological Organization, Geneva
- Beekmann, M., G. Ancellet, G. Megie, H.G.J. Smit, and D. Kley, 1994: Intercomparison campaign for vertical ozone profiles including electrochemical sondes of ECC and Brewer-Mast type and a ground-based UV-differential absorption lidar, *Journal of Atmospheric Chemistry*, 19, 259–288
- Beekmann, M., G. Ancellet, D. Martin, C. Abonnel, G. Duverneuil, F. Eidelimen, P. Bessemoulin, N. Fritz, and E. Gizard, 1995: Intercomparison of tropospheric ozone profiles obtained by electrochemical sondes, a ground-based lidar and airborne UV-photometer, *Atmospheric Environment*, 29, 1027–1042
- Bevington, P.R. and D.K. Robinson, 1992: *Data Reduction and Error Analysis for the Physical Sciences*, McGraw-Hill Inc., New York
- BIPM, 2019: <http://www.bipm.org/en/bipm/chemistry/gas-metrology/ozone.html>, accessed 12/07/2019
- Brewer, A. and J. Milford, 1960: The Oxford Kew ozonesonde, *Proceedings of the Royal Society of London, Ser. A*, 256, 470
- Clain, G., J. L. Baray, R. Delmas, R. Diab, J. Leclair de Bellevue, P. Keckhut, F. Posny, J. M. Metzger, J. P. Cammas, 2009: Tropospheric ozone climatology at two southern hemisphere tropical/subtropical sites, (Réunion Island and Irene, South Africa) from ozonesondes, LIDAR, and in-situ aircraft measurements, *Atmospheric Chemistry and Physics*, 9, 1723–1734
- Cooper, O.R., A. Stohl, M. Trainer, A. Thompson, J.C. Witte, S.J. Oltmans, B.J. Johnson, J. Merrill, J.L. Moody, G. Morris, D. Trasick, G. Forbes, P. Nédélec, F.C. Fehsenfeld, J. Meagher, M.J. Newchurch, F.J. Schmidlin, S. Turquety, J.H. Crawford, K.E. Pickering, R.C. Cohen, T. Bertarm, P. Wooldrige, and W.H. Brune, 2006: Large upper tropospheric ozone enhancements above midlatitude North America during summer: In-situ evidence from the IONS and MOZAIC ozone monitoring network, *Journal of Geophysical Research*, 111, D24S05, doi: 10.1029/2006JD007306, 2006
- Cooper, O.R., M. Trainer, A.M. Thompson, S.J. Oltmans, D.W. Tarasick, J.C. Witte, A. Stohl, S. Eckhardt, J. Lelieveld, M.J. Newchurch, B.J. Johnson, R. W. Portmann, L. Kalnajs, M.K. Dubey, T. Leblanc, I.S. McDermid, G. Forbes, D. Wolfe, T. Carey-Smith, G.A. Morris, B. Lefer, B. Rappenglück, E. Joseph, F. Schmidlin, J. Meagher, F.C. Fehsenfeld, T.J. Keating, R.A. VanCuren, and K. Minschwaner, 2007: Evidence for a recurring eastern North America upper tropospheric ozone maximum during summer, *Journal of Geophysical Research*, 112, D23304, doi: 10.1029/2007JD008710, 2007

- Curry, J.A., and P.J. Webster, 1999: *Thermodynamics of Atmospheres & Oceans*, International Geophysics Series. Vol. 65, Academic Press, New York
- Dabberdt, W. F. and H. Turtiainen, 2014: Radiosondes, in *Encyclopedia of Atmospheric Sciences*, Second Edition, edited by G.R. North, J.A. Pyle, and F. Zhang, Vol 4, pp. 273–284, Academic Press, London
- Da Silveira, R. B., Fisch, G. F., Machado, L. A. T., Dall’Antonia, A. M., Sapucci, L. F., Fernandes, D., Marques, R., and Nash, J., 2006: *WMO intercomparison of GPS Radiosondes, Alcantara, Brazil, 20 May–10 June, 2001*, Instruments and Observing Methods, Report No. 90, WMO/TD-No. 1314, World Meteorological Organization, Geneva, https://library.wmo.int/doc_num.php?explnum_id=9322
- Davies, J., D. W. Tarasick, C. T. McElroy, J. B. Kerr, P. F. Fogal, and V. Savastiouk, 2000: Evaluation of ECC Ozonesonde Preparation Methods from Laboratory Tests and Field Comparisons during MANTRA, in *Proceedings of the 19th Quadrennial Ozone Symposium Sapporo, Japan, 2000*, R.D. Bojkov and S. Kazuo, eds., pp. 137–138
- Davies, J., C.T. McElroy, D.W. Tarasick and D.I. Wardle, 2003: Ozone capture efficiency in ECC ozonesondes: Measurements made in the laboratory and during balloon flights, EAE03-A-13703, in *Geophysical Research Abstracts*, Vol. 5, 13703, EGS-AGU-EUG Joint Assembly, Nice, France, 6–11 April 2003
- De Muer, D., and H. De Backer, 1992: The discrepancy between stratospheric ozone profiles and from other techniques: A possible explanation, in *Proceedings of the 17th Quadrennial Ozone Symposium Charlottesville, USA, 1992*, NASA Conf. Publ. 3266, 815–818
- Deshler, T., J. Mercer, H.G.J. Smit, R. Stübi, G. Levrat, B.J. Johnson, S.J. Oltmans, R. Kivi, J. Davies, A.M. Thompson, J. Witte, F.J. Schmidlin, G. Brothers, T. Sasaki, 2008: Atmospheric comparison of electrochemical cell ozonesondes from different manufacturers, and with different cathode solution strengths: The Balloon Experiment on Standards for Ozonesondes, *Journal of Geophysical Research*, 113, D04307, <https://doi.org/10.1029/2007JD008975>
- Deshler, T., Stübi, R., Schmidlin, F. J., Mercer, J. L., Smit, H.G.J., Johnson, B.J., Kivi, R. and Nardi, B., 2017: Methods to homogenize ECC ozonesonde measurements across changes in sensing solution concentration or ozonesonde manufacturer, *Atmospheric Measurement Techniques*, 10, 2012–2043, [doi:10.5194/amt-10-2012-2017](https://doi.org/10.5194/amt-10-2012-2017)
- Elliott, W. P., R. J. Ross, and W. H. Blackmore, 2002: Recent changes in NWS upper air observations with emphasis on changes from VIZ to Vaisala radiosondes. *Bulletin of the American Meteorological Society*, 83, 1003–1017.
- EN-SCI Corporation, 1994: *Instruction Manual, Model 1Z ECC-O3 Sondes*, EN-SCI Corporation, Boulder, USA
- EN-SCI Corporation, 1996: *Instruction Manual, Model 1Z ECC-O3 Sondes*, EN-SCI Corporation, Boulder, USA
- Fioletov, V. E., D.W. Tarasick and I. Petropavlovskikh, 2006: Estimating ozone variability and instrument uncertainties from SBUV(2), ozonesonde, Umkehr, and SAGE II measurements: Short-term variations, *Journal of Geophysical Research*, 111, D02305, <https://ui.adsabs.harvard.edu/abs/2006JGRD..111.2305F/abstract>
- Fioletov, V. E., G. Labow, R. Evans, E.W. Hare, U. Köhler, C. T. McElroy, K. Miyagawa, A. Redondas, V. Savastiouk, A.M. Shalamyansky, J. Staehelin, K. Vanicek and M. Weber, 2008: Performance of the ground-based total ozone network assessed using satellite data, *Journal of Geophysical Research*, 113, D14313, [doi:10.1029/2008JD009809](https://doi.org/10.1029/2008JD009809)
- Galbally, I., 1968: Some measurements of ozone variation and destruction in the atmospheric surface layer, *Nature*, 218, 456–457

- Garane, K., Lerot, C., Coldewey-Egbers, M., Verhoelst, T., Koukouli, M. E., Zyrichidou, I., Balis, D. S., Danckaert, T., Goutail, F., Granville, J., Hubert, D., Keppens, A., Lambert, J.-C., Loyola, D., Pommereau, J.-P., Van Roozendael, M., and Zehner, C., 2018: Quality assessment of the Ozone_cci Climate Research Data Package (release 2017) – Part 1: Ground-based validation of total ozone column data products, *Atmospheric Measurement Techniques*, 11, 1385–1402, <https://doi.org/10.5194/amt-11-1385-2018>, 2018
- GAW Report No. 86, 1993: *Global Atmosphere Watch Guide*, WMO Global Atmosphere Watch Report Series, No. 86, World Meteorological Organization, Geneva.
- GAW Report No. 104, 1995: *Report of the Fourth WMO Meeting of Experts on the Quality Assurance/Science Activity Centres (QA/SACs) of the Global Atmosphere Watch*, WMO Global Atmosphere Watch Report Series, No. 104, World Meteorological Organization, Geneva.
- GAW Report No. 201, 2014: Smit, H.G.J., and the ASOPOS Panel, *Quality Assurance and Quality Control for Ozone Sonde Measurements in GAW*, WMO Global Atmosphere Watch Report Series, No. 201, World Meteorological Organization, Geneva. [Available online at https://library.wmo.int/pmb_ged/gaw_201_en.pdf]
- GAW Report No. 228, 2017: *WMO Global Atmosphere Watch (GAW) Implementation Plan: 2016-2023*, WMO Global Atmosphere Watch report series, No. 228, World Meteorological Organization, Geneva.
- Hilsenrath, E., W. Attmannspacher, A. Bass, W. Evans, R. Hagemeyer, R.A. Barnes, W. Komhyr, K. Mauersberger, J. Mentall, M. Proffitt, D. Robbins, S. Taylor, A. Torres and E. Weinstock, 1986: Results from the balloon ozone intercomparison campaign (BOIC), *Journal of Geophysical Research*, 91, 13137–13152
- Hayashi, H., K. Kita, and S. Taguchi, 2008: Ozone-enhanced layers in the troposphere over the equatorial Pacific Ocean and the influence of transport of midlatitude UT/LS air, *Atmospheric Chemistry and Physics*, 8, 2609–2621
- Hodges, J.T., Viallon, J., Brewer, P.J., Drouin, B.J., Gorshchev, V., Janssen, C., Lee, S., Possolo, A., Smith, M.A.H., Walden, J., Wielgosz, R.I., 2019: Recommendation of a consensus value of the ozone absorption cross-section at 253.65 nm based on a literature review, *Metrologia*. 56: 034001. <https://iopscience.iop.org/article/10.1088/1681-7575/ab0bdd>
- Hu, D., Z. Guan, W. Tian, and R. Ren, 2018: Recent strengthening of the stratospheric Arctic vortex response to warming in the central North Pacific, *Nature Communications*, 9:1967, <https://doi.org/10.1029/2008JD009809>
- Hubert, D., J.-C. Lambert, T. Verhoelst, J. Granville, A. Keppens, J.-L. Baray, U. Cortesi, D.A. Degenstein, L. Froidevaux, S. Godin-Beekmann, K.W. Hoppel, B.J. Johnson, E. Kyrölä, T. Leblanc, G. Lichtenberg, M. Marchand, C.T. McElroy, D. Murtagh, H. Nakane, R. Querel, J.M. Russell III, J. Salvador, H.G.J. Smit, K. Stebel, W. Steinbrecht, K.B. Strawbridge, R. Stübi, D.P.J. Swart, G. Taha, D.W. Tarasick, A.M. Thompson, J. Urban, J.A.E. van Gijssel, R. Van Malderen, P. von der Gathen, K.A. Walker, E. Wolfram and J.M. Zawodny, 2016: Ground-based assessment of the bias and long-term stability of 14 limb and occultation ozone profile data records, *Atmospheric Measurement Techniques*, 9, 2497–2534, <https://repository.library.noaa.gov/view/noaa/18344>.
- IGACO, 2008: *IGACO Ozone and UV Radiation Implementation Plan*, WMO Global Atmosphere Watch Report Series, No. 182, World Meteorological Organization, Geneva
- Imai, K., M. Fujiwara, Y. Inai, N. Manago, M. Suzuki, T. Sano, C. Mitsuda, Y. Naito, F. Hasebe, T. Koide and M. Shiotani, 2013: Comparison of ozone profiles between Superconducting Submillimeter-Wave Limb Emission Sounder and worldwide ozonesonde measurements, *Journal of Geophysical Research*, 118(22), 12755–12765, <https://doi.org/10.1002/2013JD021094>

- Inai, Y., Shiotani, M., Fujiwara, M., Hasebe, F. and Vömel, H., 2015: Altitude misestimation caused by the Vaisala RS80 pressure bias and its impact on meteorological profiles, *Atmospheric Measurement Techniques*, 8, 4043–4054, 2015, <https://doi.org/10.1002/2013JD021094>
- IPCC, 2013: *Climate Change 2013: The Physical Science Basis. Contribution of Working Group I to the Fifth Assessment Report of the Intergovernmental Panel on Climate Change* [Stocker, T.F., D. Qin, G.-K. Plattner, M. Tignor, S.K. Allen, J. Boschung, A. Nauels, Y. Xia, V. Bex and P.M. Midgley (eds.)]. Cambridge University Press, Cambridge, United Kingdom and New York, NY, USA, 1535 pp
- Johnson, B.J., S.J. Oltmans, H. Vömel, H.G.J. Smit, T. Deshler and C. Kroeger, 2002: ECC Ozonesonde pump efficiency measurements and tests on the sensitivity to ozone of buffered and unbuffered ECC sensor cathode solutions, *Journal of Geophysical Research*, 107, D19 <https://doi.org/10.1029/2001JD000557>
- Kerr, J.B., H. Fast, C.T. McElroy, S.J. Oltmans, J.A. Lathrop, E. Kyro, A. Paukkunen, H. Claude, U. Köhler, C.R. Sreedharan, T. Takao, and Y. Tsukagoshi, 1994: The 1991 WMO International ozone sonde intercomparison at Vanscoy, Canada, *Atmosphere-Ocean*, 32, 685–716
- Kivi, R., E. Kyro, T. Turunen, N. R. P. Harris, P. von der Gathen, M. Rex, S. B. Andersen, and I. Wohltmann, 2007: Ozonesonde observations in the Arctic during 1989–2003: Ozone variability and trends in the lower stratosphere and free troposphere, *Journal of Geophysical Research*, 112, D08306, <https://doi.org/10.1029/2006JD007271>
- Kley, D., P.J. Crutzen, H.G.J. Smit, H. Vömel, S.J. Oltmans, H. Grassl, and V. Ramanathan, 1996: Observations of near-zero ozone levels over the convective Pacific: Effects on air chemistry, *Science*, 274, 230–233
- Kobayashi, J. and Y. Toyama, 1966: On various methods of measuring the vertical distribution of atmospheric ozone (III) – Carbon iodine type chemical ozonesonde, *Papers in Meteorology and Geophysics*, 17, 113–126
- Komhyr, W.D., 1967: Nonreactive gas sampling pump, *Review of Scientific Instruments*, 38, 981–983.
- Komhyr, W.D., 1969: Electrochemical concentration cells for gas analysis, *Ann. Geoph.*, 25, 203–210
- Komhyr, W.D. and T.B. Harris, 1971: *Development of an ECC Ozonesonde*, NOAA Technical Report, ERL 200-APCL 18
- Komhyr, W.D., 1986: *Operations handbook - Ozone measurements to 40 km altitude with model 4A-ECC ozone sondes*, NOAA Technical Memorandum, ERL-ARL-149
- Komhyr, W.D., R.A. Barnes, G.B. Brothers, J.A. Lathrop and D.P. Opperman, 1995: Electrochemical concentration cell ozonesonde performance evaluation during STOIC 1989, *Journal of Geophysical Research*, 100, 9231–9244
- Komhyr, W.D. and Evans R D., 2008: *Operations Handbook-ozone Observations with a Dobson Spectrophotometer*, WMO Global Atmosphere Watch Report Series, No. 183, World Meteorological Organization, Geneva
- Kotsakis, A., G.A. Morris, B. Lefer, W. Jeon, A. Roy, K. Minschwaner, A.M. Thompson and Y. Choi, 2017: Ozone production by corona discharges during a convective event in DISCOVER-AQ Houston, *Atmospheric Environment*, 161, 13–17
- Kuang, S., M.J. Newchurch, J. Burris, L. Wang, K. Knupp and G. Huang, 2012: Stratosphere-to-troposphere transport revealed by ground-based lidar and ozonesonde at a midlatitude site, *Journal of Geophysical Research*, 117, <https://doi.org/10.1029/2012JD017695>

- Kuttippurath, J. and P.J. Nair, 2017: The signs of Antarctic ozone hole recovery, *Scientific Reports*, 7 (1): 585, doi:10.1038/s41598-017-00722-7
- Liu, G., D. W. Tarasick, V. E. Fioletov, C. E. Sioris, and Y. J. Rochon, 2009: Ozone correlation lengths and measurement uncertainties from analysis of historical ozonesonde data in North America and Europe, *Journal of Geophysical Research*, 114, D04112, doi:10.1029/2008JD010576
- Lippmann, M., 1989: Health effects of ozone: A Critical Review, *JAPCA*, 39:5, 672–695, DOI: 10.1080/08940630.1989.10466554 (<https://dx.doi.org/10.1080/08940630.1989.10466554>)
- Luers, J. K. and R. Eskridge, 1995: Temperature corrections for the VIZ and Vaisala radiosondes, *Journal of Applied Meteorology*, 34, 1241–1253
- Margitan, J.J., R. A. Barnes, G. B. Brothers, J. Butler, J. Burris, B. J. Connor, R. A. Ferrare, J. B. Kerr, W. D. Komhyr, M. P. McCormick, I. S. McDermid, C. T. McElroy, T. J. McGee, A. J. Miller, M. Owens, A. D. Parrish, C. L. Parsons, A. L. Torres, J. J. Tsou, T. D. Walsh and D. Whiteman, 1995: Stratospheric Ozone Intercomparison Campaign (STOIC) 1989: Overview, *Journal of Geophysical Research*, 100, 9193–9208
- McDermid, I.S., S. Godin, R.A. Barnes, C.L. Parsons, A. Torres, M.P. McCormick, W.P. Chu, P. Wang, J. Butler, P. Newman, J. Burris, R. Ferrare, D. Whiteman and T.J. McGee, 1990: Comparison of ozone profiles from ground-based lidar, Electrochemical Concentration Cell balloon sonde, ROCOZ-A rocket ozonesonde, and Stratospheric Aerosol and Gas Experiment satellite measurements, *Journal of Geophysical Research*, 95, 10037–10042
- McPeters, R.D., G.J. Labow and B.J. Johnson, 1997: A satellite-derived ozone climatology for balloonsonde estimation of total column ozone, *Journal of Geophysical Research*, 102, 8875–8886, 10.1029/96JD02977
- McPeters R.D., G.J. Labow and J.A. Logan, 2007: Ozone climatological profiles for satellite retrieval algorithms, *Journal of Geophysical Research*, 112, D05308, <https://doi.org/10.1029/2005JD006823>
- McPeters, R.D. and G.J. Labow, 2012: Climatology 2011: An MLS and sonde derived ozone climatology for satellite retrieval algorithms, *Journal of Geophysical Research*, 117, D10303, doi: 10.1029/2011JD017006
- Morris, G. A., G. Labow, H. Akimoto, M. Takigawa, M. Fujiwara, F. Hasebe, J. Hirokawa and T. Koide, 2013: On the use of the correction factor with Japanese ozonesonde data, *Atmospheric Chemistry and Physics*, 13(3), 1243–1260, doi:10.5194/acp-13-1243-2013
- Morris, G.A., W. Komhyr, J. Hirokawa, J. Flynn, N. Krotkov and B. Lefer, 2010: A balloon sounding technique for measuring SO₂ plumes, *Journal of Atmospheric and Oceanic Technology*, 27 (8), 1318–1330
- Murray, F.W., 1967: On the computation of saturation vapour pressure, *Journal of Applied Meteorology*, 6, 203–204, <https://journals.ametsoc.org/jamc/article/6/1/203/351803/>
- Nash, J. and F. J. Schmidlin, 1987: *WMO International Radiosonde Comparison (UK 1984, USA 1985)*. WMO/TD–No. 195, 103 pp, World Meteorological Organization, Geneva
- Nash, J., R. Smout, T. Oakley, B. Pathack and S. Kurnosenko, 2006: *WMO Intercomparison of Radiosonde Systems, Vacoas, Mauritius, 02–25 February 2005*, WMO/TD–No.1303, 115 pp., World Meteorological Organization, Geneva, https://library.wmo.int/doc_num.php?explnum_id=9312
- Nash, J., T. Oakley, H. Vömel and L. Wei, 2011: *WMO Intercomparison of High Quality Radiosonde Systems, Yangjiang, China, 12 July-3 August 2010*, WMO/TD–No. 1580, 248 pp., World Meteorological Organization, Geneva, https://library.wmo.int/doc_num.php?explnum_id=9467

- Newton, R., G. Vaughan, H. M. A. Ricketts, L. L. Pan, A. J. Weinheimer and C. Chemel, 2016: Ozonesonde profiles from the West Pacific Warm Pool: Measurements and validation, *Atmospheric Chemistry and Physics*, 619–634, doi:10.5194/acp-16-619-201
- O'Connor, F.M., G. Vaughan, Murphy, G., 1998: Box and pump temperature measurements and the possible bias between Science Pump Corporation and ENSCI-type sondes, in *Polar stratospheric ozone 1997*, EC Air Pollution Report 66, 712–15
- Petzold, A., V. Thouret, C. Gerbig, A. Zahn, C.A.M. Brenninkmeijer, M. Gallagher, M. Hermann, M. Pontaud, H. Ziereis, D. Boulanger, J. Marshall, P. Nédélec, H.G.J. Smit, U. Frieß, J.-M. Flaud, A. Wahner, J.-P. Cammas, A. Volz-Thomas and IAGOS-Team, 2015: Global-scale atmosphere monitoring by in-service aircraft – Current achievements and future prospects of the European Research Infrastructure IAGOS, *Tellus B*, 67, 28452, <https://doi.org/10.3402/tellusb.v67.28452>
- Pitts, J.N., J.M. McAfee, W.D. Long and A.M. Winer, 1976: Long-path infrared spectroscopic investigation at ambient concentrations of the 2% neutral-buffered potassium iodide method for determination of ozone, *Environmental Science and Technology*, 10, 787–793
- Powell, D.B.B. and E.L. Simmons, 1969: Some laboratory and field investigations of the accuracy of Brewer-Mast ozone sensors, *Ann. Geophys.*, 25, 323–327
- Proffitt, M.H. and R.J. McLaughlin, 1983: Fast response dual-beam UV-absorption photometer suitable for use on stratospheric balloons, *Review of Scientific Instruments*, 54, 1719–1728
- Reid S.J., G. Vaughan, A.R. Marsh and H.G.J. Smit, 1996: Intercomparison of ozone measurements by ECC sondes and BENDIX chemiluminescent analyser, *Journal of Atmospheric Chemistry*, 25, 215–226
- Rex, M., I. Wohltmann, T. Ridder, R. Lehmann, K. Rosenlof, P. Wennberg, D. Weisenstein, J. Notholt, K. Krüger, V. Mohr and S. Tegtmeier, 2014: A tropical West Pacific OH minimum and implications for stratospheric composition, *Atmospheric Chemistry and Physics*, 14, 4827 – 4841, 2014, <https://doi.org/10.5194/acp-14-4827-2014>
- Richner, H. and P. D. Phillips, 1981: Reproducibility of VIZ radiosonde data and some sources of error, *Journal of Applied Meteorology*, 20, 954–962
- Saltzman, B.E. and N. Gilbert, 1959: Iodometric micro-determination of organic oxidants and ozone, resolution of mixtures by kinetic colorimetry, *Analytical Chemistry*, 31, 1914–1920
- Schenkel, A. and B. Broder, 1982: Interference of some trace gases with ozone measurements by the KI method, *Atmospheric Environment*, 16, 2187–2190
- Science Pump Corporation, 1996: *Operator's Manual Model 6A ECC OzoneSonde*, Science Pump Corporation, Camden, USA
- Schmidlin, F. J., 1988: *WMO International Radiosonde Intercomparison. Phase II: Wallops Island, Virginia, USA, 1985*, WMO/TD–No. 312, 113 pp, World Meteorological Organization, Geneva.
- Smit, H.G.J., W. Sträter, D. Kley and M.H. Profitt, 1994: The evaluation of ECC ozonesondes under quasi flight conditions in the environmental simulation chamber at Jülich, in *Proceedings of Eurotrac symposium 1994*, edited by P.M. Borell et al., SPB Academic Publishing B.V., The Hague, The Netherlands, 349–353
- Smit, H.G.J., W. Sträter, M. Helten, D. Kley, D. Ciupa, H.J. Claude, U. Köhler, B. Hoegger, G. Levrat, B. Johnson, S.J. Oltmans, J.B. Kerr, D.W. Tarasick, J. Davies, M. Shitamichi, S.K. Srivastav and C. Vialle, 1996: JOSIE: The 1996 WMO international intercomparison of ozonesondes under quasi-flight conditions in the environmental chamber at Jülich, in *Atmospheric Ozone, in Proceedings of the 16th Quadrennial O3 Symposium, l'Aquila*,

- Italy, 1996*, edited by R. D. Bojkov and G. Visconti, pp. 971–974, Parco Sci. e Tecnol. d'Abruzzo, Italy
- Smit H.G.J and D. Kley, 1998: *JOSIE: The 1996 WMO International Intercomparison of Ozonesondes Under Quasi Flight Conditions in the Environmental Simulation Chamber at Jülich*, WMO Global Atmosphere Watch Report Series, No. 130, WMO/TD No. 926, World Meteorological Organization, Geneva
- Smit H.G.J., W. Sträter, M. Helten and D. Kley, 2000: *Environmental Simulation Facility to Calibrate Airborne Ozone and Humidity Sensors*. Jül Berichte, No. 3796, Forschungszentrum Jülich
- Smit, H.G.J., 2014: Ozonesondes, in *Encyclopedia of Atmospheric Sciences*, Second Edition, edited by G.R. North, J.A. Pyle, and F. Zhang, Vol 1, pp. 372–378, Academic Press, London
- Smit, H.G.J., and W. Straeter, 2004a: *JOSIE-1998, Performance of ECC Ozone Sondes of SPC-6A and ENSCI-Z Type*, WMO Global Atmosphere Watch Report Series, No. 157, WMO/TD No. 1218, World Meteorological Organization, Geneva
- Smit, H.G.J., and W. Straeter, 2004b: *JOSIE-2000, Jülich Ozone Sonde Intercomparison Experiment 2000, The 2000 WMO International Intercomparison of Operating Procedures for ECC Ozonesondes at the Environmental Simulation Facility at Jülich*, WMO Global Atmosphere Watch Report Series, No. 158, WMO TD No. 1225, World Meteorological Organization, Geneva
- Smit, H.G.J., W. Straeter, B. Johnson, S. Oltmans, J. Davies, D.W. Tarasick, B. Hoegger, R. Stübi, F. Schmidlin, T. Northam, A. Thompson, J. Witte, I. Boyd and F. Posny, 2007: Assessment of the performance of ECC ozonesondes under quasi-flight conditions in the environmental simulation chamber: Insights from the Jülich Ozone Sonde Intercomparison Experiment (JOSIE), *Journal of Geophysical Research*, 112, D19306, [doi:10.1029/2006JD007308](https://doi.org/10.1029/2006JD007308)
- Smit, H. G. J., and O3S-DQA, 2012: *Guidelines for Homogenization of Ozone Sonde Data, SI2N/O3S-DQA Activity as part of "Past Changes in the Vertical Distribution of Ozone Assessment"*, available at <https://www.wccos-josie.org/o3s-dqa/>
- SPARC-IOC-GAW, 1998, *Assessment of Trends in the Vertical Distribution of Ozone*, SPARC Report No. 1, WMO Global Ozone Research and Monitoring Project Report, No. 43, World Meteorological Organization, Geneva
- SPC, 1999: *Science Pump Corporation Operator's Manual Model 6A ECC Ozone Sonde*, <https://www.vaisala.com/sites/default/files/documents/Ozone%20Sounding%20with%20Vaisala%20Radiosonde%20RS41%20User%27s%20Guide%20M211486EN-C.pdf>, accessed 22 Jan 2019
- Stauffer, J., J. Staehelin, R. Stübi, T. Peter, F. Tummon and V. Thouret, 2013: Trajectory matching of ozonesondes and MOZAIC measurements in the UTLS – Part 1: Method description and application at Payerne, Switzerland, *Atmospheric Measurement Techniques*, 6, 3393– 3406
- Stauffer, J., J. Staehelin, R. Stübi, T. Peter, F. Tummon and V. Thouret, 2014: Trajectory matching of ozonesondes and MOZAIC measurements in the UTLS – Part 2: Application to the global ozone sonde network, *Atmospheric Measurement Techniques*, 7, 241–266, <https://doi.org/10.5194/amt-7-2411-2014>
- Stauffer, R. M., Morris, G. A., Thompson, A. M., Joseph, E., Coetzee, G. J. R. and Nalli, N. R., 2014: Propagation of radiosonde pressure sensor errors to ozone sonde measurements, *Atmospheric Measurement Techniques*, 7, 65–79, <https://doi.org/10.5194/amt-7-65-2014>
- Stauffer, R.M., A.M. Thompson, D.E. Kollonige, J.C. Witte, D.W. Tarasick, J.M. Davies, H. Vömel, G.A. Morris, R. Van Malderen, B.J. Johnson, R.R. Querel, H.B. Selkirk, R. Stübi and H.G.J. Smit, 2020: A post-2013 drop-off in total ozone at a third of global

- ozonesonde stations: Electrochemical Concentration Cell instrument artefacts?, *Geophysical Research Letters*, 47, <https://doi.org/10.1029/2019GL086761>
- Steinbrecht W., R. Schwartz and H. Claude, 1998: New pump correction for the Brewer-Mast ozone sonde: Determination from experiment and instrument intercomparisons, *Journal of Atmospheric and Oceanic Technology*, 15, 144–156
- Steinbrecht, W., H. Claude, F. Schönenborn, U. Leiterer, H. Dier and E. Lanzinger, 2008: Pressure and temperature differences between Vaisala RS80 and RS92 radiosonde systems, *Journal of Atmospheric and Oceanic Technology*, 25, 909–927, <https://doi.org/10.1175/2007JTECHA999.1>
- Sterling, C.W., B.J. Johnson, S.J. Oltmans, H.G.J. Smit, A.F. Jordan, P.D. Cullis, E.G. Hall, A.M. Thompson and J.C. Witte, 2018: Homogenizing and estimating the uncertainty in NOAA's long-term vertical ozone profile records measured with the electrochemical concentration cell ozonesonde, *Atmospheric Measurement Techniques*, 11, 3661–3687, <https://doi.org/10.5194/amt-11-3661-2018>
- Tang, W., D.S. Cohan, G.A. Morris, D.W. Byun and W.T. Luke, 2011, Influence of vertical mixing uncertainties on ozone simulation in CMAQ, *Atmospheric Environment*, 45, 2898–2909
- Tanimoto, H., R.M. Zbinden, V. Thouret and P. Nédélec, 2015: Consistency of tropospheric ozone observations made by different platforms and techniques in the global databases, *Tellus A*, 67:1–20 <https://doi.org/10.3402/tellusb.v67.27073>.
- Tarasick, D.W., J. Davies, K. Anlauf and M. Watt, 2000: Response of ECC and Brewer-Mast ozonesondes to sulfur dioxide interference, in *Proceedings of the 17th Quadrennial Ozone Symposium Sapporo, Japan*, R.D. Bojkov and S. Kazuo, eds., pp. 675–676
- Tarasick D.W., J. Davies, K. Anlauf, M. Watt, W. Steinbrecht and H.J. Claude, 2002: Laboratory investigations of the response of Brewer-Mast ozonesondes to tropospheric ozone, *Journal of Geophysical Research*, 107, 4331, <https://doi.org/10.1029/2001JD001167>
- Tarasick, D.W., V.E. Fioletov, D.I. Wardle, J.B. Kerr and J. Davies, 2005: Changes in the vertical distribution of ozone over Canada from ozonesondes: 1980–2001, *Journal of Geophysical Research*, 110, D02304, doi:10.1029/2004JD004643
- Tarasick, D.W., J.J. Jin, V.E. Fioletov, G. Liu, A.M. Thompson, S.J. Oltmans, J. Liu, C.E. Sioris, X. Liu, O. R. Cooper, T. Dann and V. Thouret, 2010: High-resolution tropospheric ozone fields for INTEX and ARCTAS from IONS ozonesondes, *Journal of Geophysical Research*, 115, D20301, <https://doi.org/10.1029/2009JD012918>
- Tarasick, D.W., J. Davies, H.G.J. Smit and S.J. Oltmans, 2016: A re-evaluated Canadian ozonesonde record: measurements of the vertical distribution of ozone over Canada from 1966 to 2013, *Atmospheric Measurement Techniques*, 9, 195–214, doi:10.5194/amt-9-195-2016
- Tarasick, D.W., T.K. Carey-Smith, W.K. Hocking, O. Moeini, H. He, J. Liu, M. Osman, A.M. Thompson, B. Johnson, S.J. Oltmans and J.T. Merrill, 2019a: Quantifying stratosphere-troposphere transport of ozone using balloon-borne ozonesondes, radar windprofilers and trajectory models, *Atmospheric Environment*, 198, 496–509, <https://doi.org/10.1016/j.atmosenv.2018.10.040>
- Tarasick, D., I.E. Galbally, O.R. Cooper, M.G. Schultz, G. Ancellet, T. Leblanc, T.J. Wallington, J. Ziemke, X. Liu, M. Steinbacher, J. Staehelin, C. Vigouroux, J.W. Hannigan, O. García, G. Foret, P. Zanis, E. Weatherhead, I. Petropavlovskikh, H. Worden, M. Osman, J. Liu, K.-L. Chang, A. Gaudel, M. Lin, M. Granados-Muñoz, A.M. Thompson, S.J. Oltmans, J. Cuesta, G. Dufour, V. Thouret, B. Hassler, T. Trickl and J.L. Neu, 2019b: Tropospheric Ozone Assessment Report: Tropospheric ozone from 1877 to 2016, observed levels, trends and uncertainties. *Elementa: Science of the Anthropocene*, 7:39. <https://doi.org/10.1525/elementa.376>

- Tarasick, D.W., H.G.J. Smit, A.M. Thompson G.A. Morris, J.C. Witte, J. Davies, T. Nakano, R. van Malderen, R.M. Stauffer, T. Deshler, B.J. Johnson, R. Stübi, S.J. Oltmans and H. Vömel, 2021: Improving ECC ozonesonde data quality: Assessment of current methods and outstanding issues, *Earth and Space Science*, 8, e2019EA000914, <https://doi.org/10.1029/2019EA000914>
- Thompson, A.M.:1992: The oxidizing capacity of the Earth's atmosphere: Probable past and future changes. *Science*, 256, 1157–1165 [doi: [10.1126/science.256.5060.1157](https://doi.org/10.1126/science.256.5060.1157)]
- Thompson, A.M., J.C. Witte, R.D. Hudson, H. Guo, J.R. Herman and M. Fujiwara, 2001: Tropical tropospheric ozone and biomass burning, *Science*, 291, 2128–2132
- Thompson, A.M., J.C. Witte, R.D. McPeters, S.J. Oltmans, F.J. Schmidlin, J.A. Logan, M. Fujiwara, V.W.J.H. Kirchhoff, F. Posny, G.J.R. Coetzee, B. Hoegger, S. Kawakami, T. Ogawa, B.J. Johnson, H. Vömel and G. Labow, 2003a: Southern Hemisphere Additional Ozonesondes (SHADOZ) 1998–2000 tropical ozone climatology 1. Comparison with Total Ozone Mapping Spectrometer (TOMS) and ground-based measurements, *Journal of Geophysical Research*, 108, 8238, doi: [10.1029/2001JD000967](https://doi.org/10.1029/2001JD000967)
- Thompson, A.M., J.C. Witte, S.J. Oltmans, F.J. Schmidlin, J.A. Logan, M. Fujiwara, V.W.J.H. Kirchhoff, F. Posny, G.J.R. Coetzee, B. Hoegger, S. Kawakami, T. Ogawa, J.P.F. Fortuin and H.M. Kelder, 2003b: Southern Hemisphere Additional Ozonesondes (SHADOZ) 1998–2000 tropical ozone climatology. 2. Tropospheric variability and the zonal wave-one, *Journal of Geophysical Research*, 108, 8241, doi: [10.1029/2002JD002241](https://doi.org/10.1029/2002JD002241)
- Thompson, A.M., J.C. Witte, S.J. Oltmans and F.J. Schmidlin, 2004: SHADOZ (Southern Hemisphere Additional Ozonesondes): A tropical ozonesonde-radiosonde network for the atmospheric community, *Bulletin of the American Meteorological Society*, 85, 1549–1564
- Thompson, A.M., J.B. Stone, J.C. Witte, S.K. Miller, R.B. Pierce, R.B. Chatfield, S.J. Oltmans, O.R. Cooper, A.L. Loucks, B.F. Taubman, B.J. Johnson, E. Joseph, T.L. Kucsera, J.T. Merrill, G.A. Morris, S. Hersey, G. Forbes, M.J. Newchurch, F.J. Schmidlin, D.W. Tarasick, V. Thouret and J.-P. Cammas, 2007a: Intercontinental Chemical Transport Experiment Ozonesonde Network Study (IONS) 2004: 1 Summertime upper troposphere/lower stratosphere ozone over northeastern North America, *Journal of Geophysical Research*, 112, D12S12, doi:[10.1029/2006JD007441](https://doi.org/10.1029/2006JD007441), 2007
- Thompson, A.M., J.C. Witte, H.G.J. Smit, S.J. Oltmans, B.J. Johnson, V.W.J.H. Kirchhoff and F.J. Schmidlin, 2007b: Southern Hemisphere Additional Ozonesondes (SHADOZ) 1998–2004 tropical ozone climatology: 3. Instrumentation, station-to-station variability, and evaluation with simulated flight profiles, *Journal of Geophysical Research*, 112, D03304, doi:[10.1029/2005JD007042](https://doi.org/10.1029/2005JD007042)
- Thompson, A.M., S.J. Oltmans, D.W. Tarasick, P. von der Gathen, H.G.J. Smit and J.C. Witte, 2011: Strategic ozone sounding networks: Review of design and accomplishments, *Atmospheric Environment*, 45, 2145–2163, doi:[10.1016/j.atmosenv.2010.05.002](https://doi.org/10.1016/j.atmosenv.2010.05.002)
- Thompson, A.M., S.K. Miller, S. Tilmes, D.W. Kollonige, J.C. Witte, S.J. Oltmans, B.J. Johnson, M. Fujiwara, F.J. Schmidlin, G.J.R. Coetzee, N. Komala, M. Maata, M. 'bt Mohamad, J. Nguyo, C. Mutai, S-Y. Ogino, F.R. da Silva, N.M. Paes Leme, F. Posny, R. Scheele, H.B. Selkirk, M. Shiotani, R. Stübi, G. Levrat, B. Calpini, V. Thouret, H. Tsuruta, J. Valverde Canossa, H. Vömel, S. Yonemura, J.A. Diaz, N.T. Tan Thanh and H.T. Thuy Ha, 2012: Southern Hemisphere Additional Ozonesondes (SHADOZ) tropical ozone climatology: Tropospheric and tropical tropopause layer (TTL) profiles with comparisons to OMI based ozone products, *Journal of Geophysical Research*, 117, D23301, doi: [10.1029/2010JD016911](https://doi.org/10.1029/2010JD016911)
- Thompson, A.M., N.V. Balashov, J.C. Witte, G.J.R. Coetzee, V. Thouret and F. Posny, 2014: Tropospheric ozone increases in the southern African region: Bellwether for rapid growth in southern hemisphere pollution?, *Atmospheric Chemistry and Physics*, 14, 9855–9869

- Thompson, A.M., J.C. Witte, C. Sterling, A. Jordan, B.J. Johnson, S.J. Oltmans, M. Fujiwara, H. Vömel, M. Allaart, A. PETERS, G.J.R. Coetzee, F. Posny, E. Corrales, J. Andres Diaz, C. Félix, N. Komala, N. Lai, M. Maata, F. Mani, Z. Zainal, S.-Y. Ogino, F. Paredes, T. Luiz Bezerra Penha, F.R. da Silva, S. Sallons-Mitro, H.B. Selkirk, F.J. Schmidlin, R. Stübi and K. Thiongo, 2017: First reprocessing of Southern Hemisphere Additional Ozonesondes (SHADOZ) ozone profiles (1998–2016). 2. Comparisons with satellites and ground-based instruments, *Journal of Geophysical Research*, 122, <https://doi.org/10.1002/2013JD019771>
- Thompson, A.M., H.G.J. Smit, J.C. Witte, R.M. Stauffer, B.J. Johnson, G.A. Morris, P. von der Gathen, R. van Malderen, J. Davies, A. PETERS, M. Allaart, F. Posny, R. Kivi, P. Cullis, Nguyen T.H. Ahn, E. Corrales, T. Machinini, F.R. daSilva, G. Paiman, K Thiong'o, A. Zainal, G.B. Brothers, K.R. Wolff, T. Nakano, R. Stübi, G. Romanens, G.J.R. Coetzee, J.A. Diaz, S. Mitro, M. 'bt Mohamad and S.-Y. Ogino, 2019: Ozone sonde quality assurance: The JOSIE-SHADOZ (2017) experience, *Bulletin of the American Meteorological Society*, 100, <https://pubmed.ncbi.nlm.nih.gov/33005057/>
- Thornton, D.C., and N. Niazy, 1982: Sources of background current in the ECC ozonesonde: Implication for total ozone measurements, *Journal of Geophysical Research*, 87, 8943–8950
- Thornton, D.C. and N. Niazy, 1983: Effects of solution mass transport on the ECC ozonesonde background current, *Geophysical Research Letters*, 10, 148–151
- Thouret, V., A. Marenco, J.A. Logan, P. Nédélec and C. Grouhel, 1998: Comparisons of ozone measurements from the MOZAIC airborne program and the ozone sounding network at eight locations, *Journal of Geophysical Research*, 103, 25,695–25,720
- Torres, A.L., 1981: *ECC Ozonesonde Performance at High Altitude: Pump Efficiency*, NASA Technical Memorandum 73290, 10 pp., NASA Wallops Flight Center, Wallops Island, USA
- Van Malderen, R., M.A.F. Allaart, H. De Backer, H.G.J. Smit and D. De Muer, 2016: On instrumental errors and related correction strategies of ozonesondes: possible effect on calculated ozone trends for the nearby sites Uccle and De Bilt, *Atmospheric Measurement Techniques*, 9, 3793–3816, doi:10.5194/amt-9-3793-2016
- Volz, A. and D. Kley, 1988: Evaluation of the Montsouris series of ozone measurements made in the nineteenth century, *Nature*, 332, 240–242
- Vömel, H. and K. Diaz, 2010: Ozone sonde cell current measurements and implications for observations of near-zero ozone concentrations in the tropical upper troposphere, *Atmospheric Measurement Techniques*, 3, 495–505, doi:10.5194/amt-3-495-2010, <http://www.atmos-meas-tech.net/3/495/2010/>
- Vömel, H., H.G.J. Smit, D. Tarasick, B.J. Johnson, S.J. Oltmans, H. Selkirk, A.M. Thompson, R.M. Stauffer, J.C. Witte, J. Davies, R. Van Malderen, G.A. Morris, T. Nakano and R. Stübi, 2020: A new method to correct the ECC ozone sonde time response and its implications for “background current” and pump efficiency, *Atmospheric Measurement Techniques*, 13, 5667–5680, <https://amt.copernicus.org/articles/13/5667/2020/>
- Wang, J. and K. Young, 2005: Comparisons of 7-year radiosonde data from two neighbouring stations and estimation of random error variances for four types of radiosondes, in *13th Symposium on Meteorological Observations and Instrumentation*, 19–23 June 2005, Savannah, GA, USA
- Witte, J.C., A.M. Thompson, H.G.J. Smit, M. Fujiwara, F. Posny, G.J.R. Coetzee, E.T. Northam, B.J. Johnson, C.W. Sterling, M. Mohamad, S.-Y. Ogino, A. Jordan and F.R. da Silva, 2017: First reprocessing of Southern Hemisphere Additional Ozonesondes (SHADOZ) profile records (1998–2015): 1. Methodology and evaluation, *Journal of Geophysical Research*, 122, 6611–6636, <https://doi.org/10.1002/2016JD026403>
- Witte, J.C., A.M. Thompson, H.G.J. Smit, H. Vömel, F. Posny and R. Stübi, 2018: First reprocessing of Southern Hemisphere Additional Ozonesondes profile records: 3.

- Uncertainty in ozone profile and total column. *Journal of Geophysical Research*, 123, 3243–3268. <https://doi.org/10.1002/2017JD027791>
- Witte, J.C., A.M. Thompson, F.J. Schmidlin, E.T. Northam, K.R. Wolff and G.B. Brothers, 2019: The NASA Wallops Flight Facility digital ozonesonde record: Reprocessing, uncertainties, and dual launches. *Journal of Geophysical Research*, 124, 3565–3582, [doi:10.1029/2018JD030098](https://doi.org/10.1029/2018JD030098)
- World Meteorological Organization, 1982: *Report of the WMO Meeting of Experts on Sources of Errors in Detection of Ozone Trends*, WMO/TD No. 12, Geneva
- WMO-No.8 Report, 2018: *Guide to Instruments and Methods of Observation, Vol.I: Measurement of Meteorological Variables*, World Meteorological Organization, Geneva. [Available online at https://library.wmo.int/doc_num.php?explnum_id=10179]
- WMO/UNEP, 1991: *Scientific Assessment of Ozone Depletion: 1990*, Global Ozone Research and Monitoring Project – Report No. 25, World Meteorological Organization, Geneva
- WMO/UNEP, 1995: *Scientific Assessment of Ozone Depletion: 1994*, Global Ozone Research and Monitoring Project – Report No. 37, World Meteorological Organization, Geneva
- WMO/UNEP, 1999: *Scientific Assessment of Ozone Depletion: 1998*, Global Ozone Research and Monitoring Project – Report No. 44, World Meteorological Organization, Geneva
- WMO/UNEP, 2003: *Scientific Assessment of Ozone Depletion: 2002*, Global Ozone Research and Monitoring Project – Report No. 47, World Meteorological Organization, Geneva
- WMO/UNEP, 2007: *Scientific Assessment of Ozone Depletion: 2006*, Global Ozone Research and Monitoring Project – Report No. 50, World Meteorological Organization, Geneva
- WMO/UNEP, 2011: *Scientific Assessment of Ozone Depletion: 2010*, Global Ozone Research and Monitoring Project – Report No. 52, World Meteorological Organization, Geneva
- WMO/UNEP, 2015: *Scientific Assessment of Ozone Depletion: 2014*, Global Ozone Research and Monitoring Project – Report No. 55, World Meteorological Organization, Geneva
- WMO/UNEP, 2019: *Scientific Assessment of Ozone Depletion: 2018*, Global Ozone Research and Monitoring Project – Report No. 58, World Meteorological Organization, Geneva
- Wohltmann, I., P. von der Gathen, R. Lehmann, M. Maturilli, H. Deckelmann, G.L. Manney, J. Davies, D. Tarasick, N. Jepsen, R. Kivi, N. Lyall and M. Rex, 2020: Near complete local reduction of Arctic stratospheric ozone by record chemical loss in spring 2020, *Geophysical Research Letters*, 47, <https://doi.org/10.1029/2020GL089547>
- Zbinden, R. M., V. Thouret, P. Ricaud, F. Carminati, J.-P. Cammas and P. Nédélec, 2013: Climatology of pure tropospheric profiles and column contents of ozone and carbon monoxide using MOZAIC in the mid-northern latitudes (24°N to 50°N) from 1994 to 2009, *Atmospheric Chemistry and Physics*, 13, 12363–12388. DOI: <https://dx.doi.org/10.5194/acp-13-12363-2013>
- Zhang, J., Y. Xuan, X. Yan, M. Liu, H. Tian, X. Xia, L. Pang and X. Zheng, 2014a: Development and preliminary evaluation of a double-cell ozonesonde, *Advances in Atmospheric Sciences*, 31, 938–947
- Zhang, J.-Q., X.-J. Xuan, X.-A., Xia, M.-Y. Liu, X.-L. Yan, L. Pang, Z.-X. Bai, and X.-W. Wan, 2014b: Performance evaluation of a self-developed ozonesonde and its application in an intensive observational campaign, *Atmospheric and Oceanic Science Letters*, 7, 175–179

Acknowledgements

The Editors are grateful for support from FZ-Jülich, NASA, to the UNEP Vienna Convention Trust Fund for sponsorship of JOSIE-SHADOZ-2017, to the many organizations represented by

the ASOPOS team, to the Royal Meteorological Institute (Belgium) for hosting the 2019 ASOPOS authors meeting. We also acknowledge the Report reviewers, the sponsorships of WMO/GAW and the GAW Ozone Programme (Ms S. Netcheva), the International Ozone Commission and the Network for the Detection of Atmospheric Composition Change (NDACC).

Further thanks to Ms Penny Smale (National Institute of Water and Atmospheric (NIWA), New Zealand) for preparing the tutorial video on SOP's for ozonesondes in practice.

**Standard Operating Procedures for ECC Ozonesondes:
A practical guide**

Lead authors

Bryan J. Johnson (NOAA/GML, Boulder, USA)

Patrick Cullis (CIRES/NOAA/GML, Boulder, USA)

Jonathan Davies (ECCC, Toronto, Canada)

Table of Contents

A-1	Basic ECC Ozonesonde Station Setup	92
A-2	ECC Ozonesonde General Guidelines: Avoiding Problems	93
A-3	ECC Sensor Solution Preparation: Cathode and Anode	94
A-4	Advanced Ozone Preparation (3–30 days before flight)	97
A-4.1	High ozone conditioning	97
A-4.2	Add sensing solutions	100
A-4.3	Decay (response) test	100
A-4.4	Record background and prepare sonde for storage	101
A-5	Final Pre-flight Preparation (0–1-day preparation for launch)	101
A-5.1	Change the sensing solutions	101
A-5.2	Connect the ozonesonde to the ozonizer test unit for pre-flight testing	102
A-5.3	Decay (response) test	103
A-5.4	Flowrate and final background measurement	103
A-5.5	Prepare the ozonesonde box for flight	105
A-5.6	Turn on radiosonde and ozonesonde pump power at launch site	106
A-5.7	Surface ozone measurements at launch site	106
A-5.8	Ready for launch	106
A-6	Balloon Train and Launching	107
A-7	Trouble Shooting	108
A-8	Alternative Sources of Filtered or Zero Air (free of ozone)	109
A-9	ECC Ozonesonde Checklist for Ozonesonde Conditioning and Pre-Flight Preparation	110
A-9.1	ECC Ozonesonde Example Checklist with Sample Answers and Notes	111
A-9.2	ASOPOS 2.0 ECC Ozonesonde Blank Checklist Sheet	114

A-1 Basic ECC Ozonesonde Station Setup

The ozonesonde Standard Operating Procedure (**SOP**) is designed to obtain accurate and reproducible ozonesonde measurements by following a consistent procedure for each ozonesonde prepared for regular launches.

A typical ozonesonde station requires relatively little space for the sonde testing, electronic test equipment, and storing ozonesonde supplies. However, high-pressure helium cylinders or a hydrogen gas source are often housed in a separate building that may also be used for balloon inflation. The primary components of a basic receiving station setup will consist of the following:

1. Receiving Station

- Receiver (typically 400–405 mHz)
- Computer with telemetry and ozonesonde data acquisition software. The laptop should be set to GMT time.
- Antenna and cables
- Ozonizer test unit
- Flow meter (soap bubble graduated cylinder glass tube or calibrated device).
- Sensor solutions (stored in dark)
- Purified water (deionized or HPLC) and chemicals for making sensor solutions
- Rinse water (distilled)
- Cathode and anode syringes (3 cm³)
- Storage space for ozonesondes, radiosondes, balloons, parachutes, and payout reels
- Miscellaneous tools:
 - Small pliers for grasping cathode and anode caps
 - Kim Wipe tissues to provide a clean surface to lay the caps and tubing on when adding or replacing solutions
 - Stopwatch
 - Emery cloth for grasping Teflon intake tube
 - Shorting plugs – electrical short connecting the blue & white leads when stored with sensor solutions in place

2. Balloon Filling Facility:

- Storage for helium tanks or hydrogen gas source fitted with pressure regulators
- Fill nozzle and hose connections for balloon filling
- Floor or Ground Tarp for protecting the balloon during inflation
- Weigh-off weights or lift sensors to determine proper inflation
- Duct tape (for securing the ozonesonde lid)
- Double stick tape (for attaching radiosonde)

A-2 ECC Ozonesonde General Guidelines: Avoiding Problems

Ideal laboratory conditions for preparation of ozonesondes are not always possible. However, by following a few simple and important guidelines in this section will help with the success in consistent and accurate ozonesonde performance when following the step-by-step instructions in **Sections A-4** and **A-5**.

1. Preparing Sensor Solutions.

- Prepare solutions with reagent grade chemicals and high purity deionized water.
- Weigh chemicals with a scale accurate to within ± 0.01 grams.
- Use a test weight, for example a standard 10.00-gram weight, to check scale accuracy before weighing chemicals.
- Place a new or clean weigh paper or weigh boat on the scale. Zero the scale before weighing the chemical reagents.
- Prepare anode solution from the freshly prepared cathode solution. The saturated potassium iodide (KI) anode solution will require a ratio of about 10 grams of KI per 6 ml of cathode solution. Crystals of KI should still be present in the anode solution at the bottom of the anode bottle after at least one day of storage – indicating full saturation.

2. Sensor Solution Storage and Syringes.

- Solutions should be kept in dark Nalgene or amber glass bottles, preferably at room temperature (20–25 °C).
- Label Cathode and Anode solution bottles with date of preparation.
- Use the same batch # for cathode and anode solutions when charging the cathode and anode sensor cells during the ozonesonde preparation.
- Always use separate syringes for cathode and the anode solutions.
- Rinse syringes with clean, distilled or deionized water after finished with the ozonesonde preparation.

3. Ozonizer/Test Unit Operation Checks.

- UV lamp is working (blue light visible from the pin hole in ozone lamp shield).
- A reading of 5 μA is easily attained when the ozonesonde is sampling the no-low ozone source during ozonesonde checkout; the UV lamp shield is partially out, exposing UV light to air source.
- Test unit air pump provides a minimum flow of 500 ml/min (this is about twice the flow rate of an ozonesonde).
- The air filters or clean-air source provides ozone-free air – the ozonesonde will read $< 0.05 \mu\text{A}$ when sampling the ozone-free air source during the day of flight preparation.

4. During Ozonesonde Preparation.

- Avoid contamination of sensor cells, piston pump and tubing from: random droplets of anode solution accidentally falling into the cathode sensor or on the pump and tubing. Also be cautious when grasping tubing with the emery cloth so that tiny flakes of abrasive from the cloth do not fall into sensor cell or pump.
- If cathode and anode sensor solutions are accidentally added to wrong cells, then rinse cells with deionized water, and add proper solutions and store sonde for at least one day with cell leads shorted.

- High ozone is only run through dry cells during the first step of the 3–30-day advanced preparation (**Section A-4**). Thereafter, when the ozonesonde is charged with sensor solutions, only use the no-low ozone port from the test unit. Any brief sampling of high ozone through sensor cell at this time will result in an “off-scale” high microamp output from the cell. In that case solutions should be replaced, and cell leads shorted and allowed to sit for 30–60 minutes to equilibrate. Then repeat ozonesonde checkout.
- Carefully record all the key information and metadata during steps during the ozonesonde preparation on a check sheet. An example checkout sheet is provided in **Annex B-4**. The checkout sheet is not only an archive of the pre-flight and day of flight preparation steps and manufacturer information, but also provides a step-by-step guideline to follow rather than reading through all of the detailed steps with the SOP instructions.

A-3 ECC Sensor Solution Preparation: Cathode and Anode

To make 1 litre of 0.5% KI Buffered CATHODE SOLUTION:



1. Add ~ 500 ml of distilled, deionized water to a clean 1000 ml volumetric flask;
2. Use an accurate scale or balance (~ ± 0.01 grams accuracy). Place a sheet of weighing paper or a weighing boat on the scale and tare to zero grams;
3. Measure 5.00 (± 0.10) grams of **KI (potassium iodide)** on the tared weigh paper. Then transfer (pour or add) the 5.00 grams of KI to water in the volumetric flask;
4. Add few ml of distilled, deionized water to flush any KI that may be sticking to the inside of the flask neck;
5. Weigh and add 12.50 (± 0.10) grams of **KBr (potassium bromide)** to the flask;
6. Weigh and add 0.63 (± 0.05) grams of **NaH₂PO₄ • H₂O (sodium phosphate monobasic monohydrate)** to the flask;
7. Weigh and add 2.50 grams (± 0.05 g) of **Na₂HPO₄ • 12H₂O (sodium phosphate, dibasic, dodecahydrate)** to the flask;

CAUTION: NOTE THE CHEMICAL FORMULA (Molecular Weights) OF THE SODIUM PHOSPHATE HYDRATES ON THE REAGENT BOTTLES FOR PROPER QUANTITY WEIGHED:

0.63 grams of NaH₂PO₄ • H₂O (MW=137.99 grams/mole)

May be replaced with -

0.71 grams of NaH₂PO₄ • 2H₂O (MW=156.01 grams/mole)

2.50 grams of Na₂HPO₄ • 12H₂O (MW=358.14 grams/mole)

May be replaced with -

1.87 grams of Na₂HPO₄ • 7H₂O (MW=268.07 grams/mole)

8. Rinse in all chemicals that may be sticking to neck of flask. Then swirl flask around to dissolve most of chemicals;
9. Add distilled, deionized water exactly up to the 1000.0 ml mark of the volumetric flask;
10. Invert flask several times to thoroughly mix solution. Allow cathode solution to sit in the dark in the volumetric flask for ~10 minutes and invert a couple more times to be sure all the salts are dissolved before transferring to labelled cathode bottles;

NOTE: you may check the pH of a small 10 ml sample of the solutions if desired. It should be between 6.8–7.0.

11. Place a label on clean, amber Nalgene or dark glass sample bottles (typically 500 ml volume). Write the solution reference number and/or date of preparation on the label;
12. Transfer cathode solution to the cathode bottles.

To prepare 125 ml of ANODE SOLUTION (cathode solution that is saturated with KI):

1. Rinse an empty, clean, dry anode bottle (typically 125 ml volume) with a few ml. of cathode solution.
2. Discard the cathode rinse.
3. Tare to zero on the scale: the empty anode bottle and wide-mouth funnel.
4. Add ~ 120–130 grams of KI to labelled wide-mouth amber Nalgene or glass bottles.
5. Tare to zero – the anode bottle and KI on the scale.

NOTE: Taring to zero here makes it easier to add the desired weight of cathode solution in the next step.

6. Carefully pour in about 75 to 80 grams (or ml) of cathode solution to anode bottle. If you go over 80 grams (ml) then you should add 10–20 more grams KI to be sure it is saturated.

NOTE: It is fine to carefully pour cathode solution into the wide-mouth anode bottle without the use of the funnel.

7. By the next day, the anode solution will be KI-saturated. There should be crystals of KI visible at the bottom of the anode solution bottle to indicate it is fully saturated.
8. Store the solutions for about 1–2 weeks before first use. Anode solution will develop a yellow tint.
9. Properly stored solutions will be good for a year if stored in sealed, amber bottles at room temperature. The anode solution may develop a deeper yellow, or rusty colour after several months.
10. Keep a Sensor Solution Logbook: Record a reference number, date and all quantities measured into a logbook (example given below).

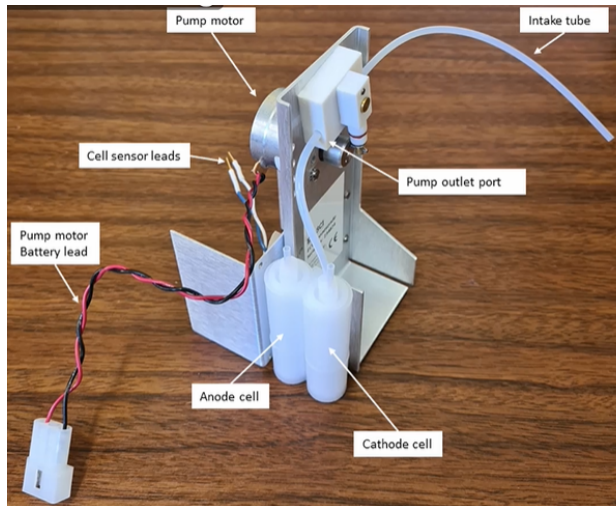


Sensor Solutions Record/Log Book								
Label cathode and anode bottles with Date, Solution Recipe, and Solution Number						Sodium phosphate	Sodium phosphate	
				potassium	potassium	dibasic dodecahydrate	monobasic monohydrate	
				iodide	bromide	Buffer - 2 sodium (dibasic)	Buffer - 1 sodium (acidic)	~10 ml sample
DATE	Solution Recipe	Solution #	Liters H ₂ O	KI	KBr	Na ₂ HPO ₄ ·12H ₂ O	NaH ₂ PO ₄ ·H ₂ O	pH
2019 Mar 23	1/2% EnSci	237	1.00	0.50	12.52	2.50	0.63	6.97
2020 Jan 15	1% Full Buffer	238	1.00	10.09	25.11	5.00	1.26	6.95
2020 Jul 21	1% 0.1 Buffer NOAA	239	1.00	10.02	24.98	0.50	0.13	6.93

Standard Operating Procedures:

Preparing ECC Ozonesondes

The Standard Operating Procedures described here are also visualized in an accompanying tutorial video available at: <https://www.wccos-josie.org/asopos> or <https://vimeo.com/niwanz/asoposprep> .



ENSCI-Z

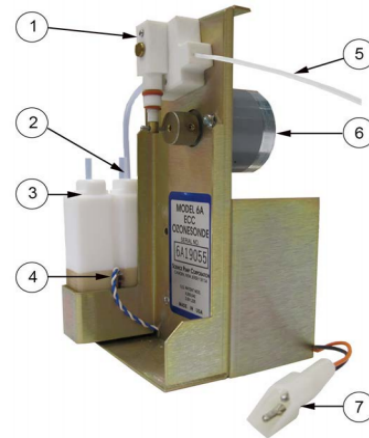


Figure 2 SPC ECC-6A Ozone Sensor Parts

- 1 Gas sampling pump
- 2 Ozone sensor cathode
- 3 Ozone sensor anode
- 4 Wires for interface
- 5 Air intake tube
- 6 Motor
- 7 Connector for pump battery

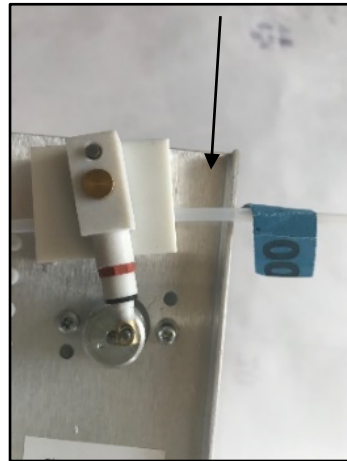
SPC6A

A-4 Advanced Ozonesonde Preparation (3–30 days before launch)

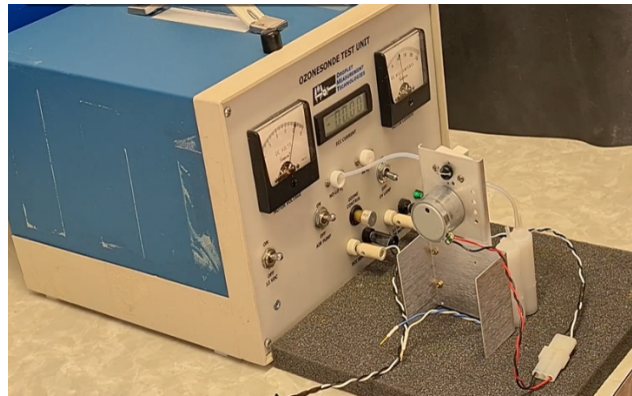
The primary purpose of the advanced preparation is twofold: to initially clean the Teflon tubing and piston by running the pump with the intake tube connected to the high ozone port of the test unit for 30 minutes. Secondly, to add the sensor solutions in order to saturate the ion bridge that links the anode and cathode cells. Adding the sensor solutions, several days before the actual balloon flight, allows the cell to attain a low background current ($<0.05 \mu\text{A}$); the sensor solutions are changed on the day of flight preparation. Electrically shorting the cell leads during instrument storage also aids in reducing the background. In addition, the advanced preparation may identify issues with the electrical connections and pump motor current.

A-4.1 High ozone conditioning

1. Begin a new ozonesonde checksheet: Record Sonde number, date, and record additional information while following the steps listed below.
2. Switch 'ON' the ozonizer/test unit power and air pump to begin zero ozone air flow.
3. Remove the ozonesonde from the white polystyrene box. Connect the ozonesonde intake tube to the pump intake port side of the ozonesonde Teflon pump. Use a piece of emery cloth to grasp the intake tube near the end that will be inserted into the pump port.



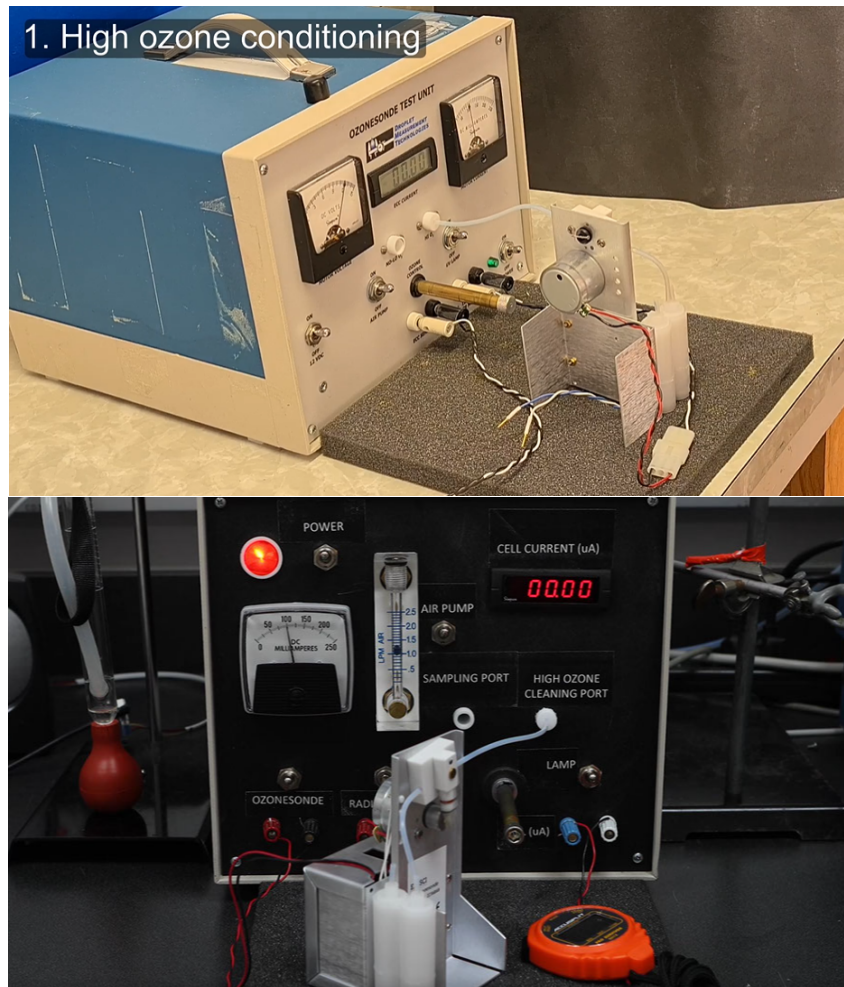
4. Connect the ozonesonde pump motor leads to ozonizer/test unit 12-volt DC power terminals. Insert the intake tube into the no/low ozone outlet. Switch on ozonesonde power and run for 10 minutes sampling clean, zero ozone air. At the end of this period RECORD the initial motor current (proper current should be < 120 mA).



If the current is higher than 120 mA:

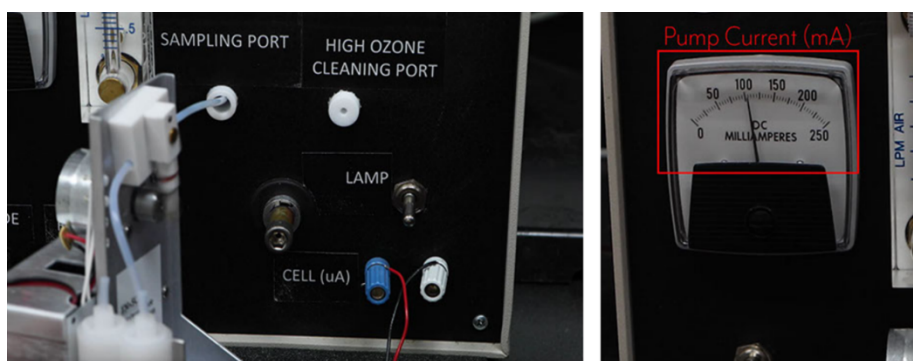
- (a) Run another 10 minutes.
If pump current remains > 120 mA then:
- (b) Clean the internal gas path with a methanol flush and put the ozonesonde aside. Start the preparation again with another ozonesonde.

5. Insert the intake tube firmly into the high ozone port of the ozonizer/test unit. Turn on the UV lamp and fully pull out the ozone control/shield tube. Turn on the ozonesonde pump and sample high ozone for 30 minutes to condition the intake tube, pump, cathode tubing and cathode cell chamber for new ozonesondes.



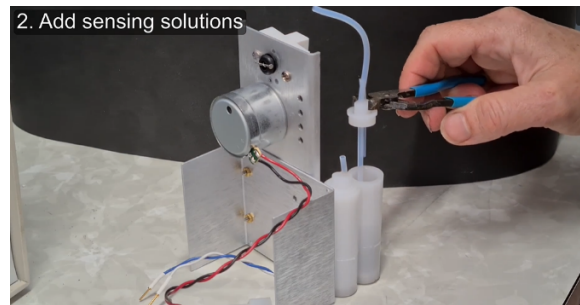
NOTE: For recovered ozonesondes, only the intake tube, pump, and cathode tubing should be conditioned; the cathode cap is removed from the cell and reconnected to the pump exhaust to bypass the cathode chamber. Avoid breathing the high ozone air exhaust by preparing the sonde in a well-ventilated large open laboratory room, under a laboratory hood, or connect the high ozone exhaust tubing to an old filter or Drierite desiccant column. This filter should be reserved as a high ozone destruction filter. Test unit air pump can be off during 30 minutes of high ozone.

- Turn the ozonizer/test unit air pump back on. Turn off the UV lamp and push the ozone control shield all the way back in. Withdraw the intake tube from the high ozone outlet and move into the no/low ozone outlet. Run for 5 minutes sampling clean, zero ozone air.

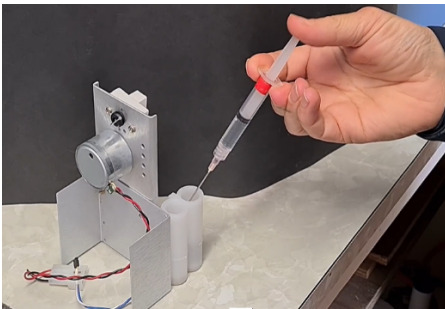


A-4.2 Add sensing solutions

- Use a small pliers to grasp and remove the cathode and anode caps and place them on a clean surface or Kim Wipe tissue, taking care not to handle the lower parts of the tubing below the cap.



- Using a designated cathode syringe or constant volume pipettor, add 3 ml of fresh cathode solution to the cathode cell. Wait 2 minutes to allow the cathode solution to begin permeating the ion bridge.



- Replace the cathode cap by carefully sliding the long section of the tubing over the Teflon rod protruding up from the bottom of the cell. Reconnect the tubing to the pump outlet.
- Then add 1.5 ml of anode solution to the anode cell using a separate syringe reserved for anode solution. Replace the anode cap.
- Disconnect the cell sensor leads from the electronic interface board and connect to the ozonizer/test unit microammeter leads. Run the ozonesonde for 10 minutes while sampling clean, zero ozone air. The cell current will typically begin high and slowly decline. Continue to monitor the background current until it drops below $0.3 \mu\text{A}$.

Note: If it takes longer than 30 minutes to reach $0.3 \mu\text{A}$, or the cell is not showing any current reading, then the ozonesonde should be set aside with the cell leads shorted to allow more time for the ion bridge to saturate. After 1–2 hours, resume cell current monitoring on zero air until $<0.3 \mu\text{A}$.

A-4.3 Decay (response) test

- While the ozonesonde continues to sample air from the no/low ozone port, turn on the UV lamp on the ozonizer test unit and pull out the ozone control shield about 3 to 4 cm. Make additional adjustments to the position of the ozone control shield until a relatively steady current of $5 \mu\text{A}$ is observed on the microammeter. Continue sampling for 10 minutes making small adjustments to the ozone control shield as necessary.
- After 10 minutes have elapsed then SIMULTANEOUSLY turn off the UV lamp and push in the UV lamp shield. Be ready with the stopwatch to record the rapid decline in the cell current (displayed on the test unit) by measuring the time to drop from $4 \mu\text{A}$ to $1.5 \mu\text{A}$. RECORD the decay time.



A-4.4 Record background and prepare sonde for storage

14. Continue sampling clean, zero ozone air for 10 minutes. The microammeter reading will slowly decay to values within the 0.2 to 0.6 μA range. RECORD the final background current.
15. Remove the intake tubing and place into the frame of the ozonsonde. SHORT circuit the sensor cell leads with a shorting plug. Return the sonde to the plastic bag. Place a piece of tissue just below the sensor cells before putting the sonde back into the plastic bag and inside the Styrofoam box compartment.



Short cell leads

16. Turn off all ozonizer/test unit switches.
17. Rinse syringes with distilled water after use. Place the bottle caps back on cathode and anode solution bottles immediately after use.

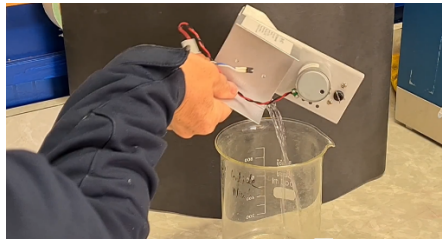
A-5 Final Pre-Flight Preparation (0–1 Day Preparation for Launch)

These final pre-flight procedures are to be completed less than 24 hours before the sonde is launched but in case of a delay can be repeated. It is helpful to have an extra sonde available that has gone through the 3–30-day high ozone conditioning step if problems with the day of flight sonde occur.

A-5.1 Change the sensing solutions

18. Remove the sonde from the Styrofoam flight box. Check that the tissue is not yellow or brown in colour nor has any salt residue from potential leakage during the storage. A clean tissue indicates that the cell is ready for the 0–1-day preparation. Disconnect the shorting plug. Before removing the cell caps, inspect the cell caps for KI salt crystals or white film. Rinse any presence of KI salt with distilled water and dry the anode and cathode caps with a Kim Wipe.
19. Disconnect the cathode tubing from the outlet (exhaust) port of the Teflon pump, then using a pair of small pliers, remove the cathode cap from the cell.
20. Place the cathode cap on a clean surface/tissue, again taking care not to handle the lower parts. Remove the anode cap and also place on a clean surface.

21. Remove and discard the anode and cathode solutions. This can be done by carefully dumping by inverting the sonde over a suitable waste container. Take care not to spill solution on other parts of the instrument while doing this and gently coax some of the last clinging droplets out with a gentle shake of the inverted sonde.



22. **ADDING CATHODE SOLUTION:** add 3 ml of fresh cathode solution to the cathode cell chamber.
23. Replace the cathode cap into the cell chamber by carefully sliding the long cathode tube over the Teflon rod protruding up from the bottom of the cell. Wait 2 minutes.
24. **ADDING ANODE SOLUTION:** add 1.5 ml of fresh anode solution to the anode cell chamber.
25. Replace the anode cap.
26. Cap and store sensor solution bottles. Flush the syringes with distilled water before storing.

Note: From this point on the ozonesonde must always remain upright!

A-5.2 Connect the ozonesonde to the ozonizer test unit for pre-flight testing.

27. Turn on the ozonizer test unit and the air flow to allow it to warm up and flush the internal filter for 3–5 minutes before the ozonesonde performance checks begin.
28. Connect the sonde power and cell leads to the test unit:
- Plug in to the 12 VDC power source from the test unit
 - Disconnect the cell sensor leads from the shorting plug and connect to the ozonizer/test unit microammeter leads
 - Insert the intake tube a few cm into the no-low ozone port of the test unit

The cell current will typically spike up to about 1 μA and rapidly decrease after the leads are connected to the microammeter.

29. After 10 minutes on zero ozone air.
- **RECORD:** the pump motor current
 - **RECORD:** the background current

If the background is larger than 0.03 μA , change the cathode and anode solutions and repeat this test. If, the 0.03 μA threshold is still not reached with fresh solutions, the ozone destruction filter may need replacement.



A-5.3 Decay(response) test

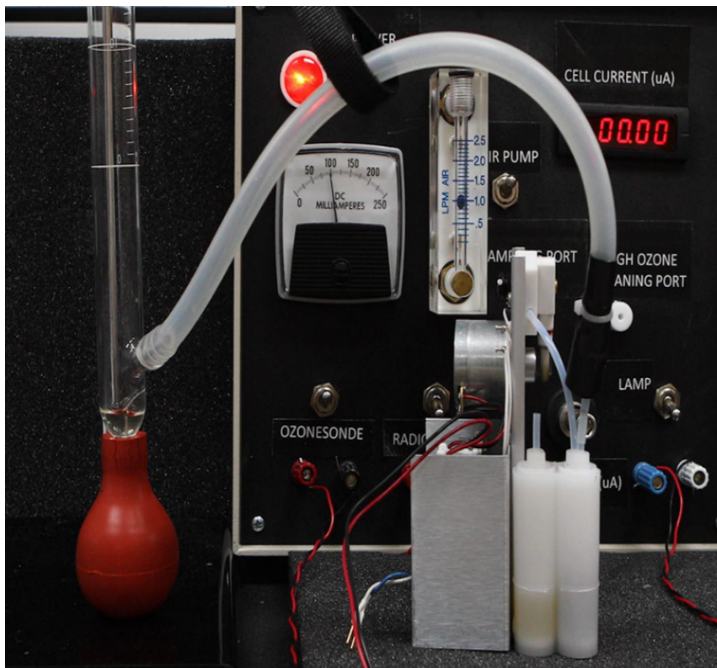
30. While the sonde motor is running and sampling air from the no/low ozone port, turn on the UV lamp on the ozonizer test unit and pull out the ozone control shield slightly. Make small adjustments to the position of the ozone control shield until a fairly steady current of $5 \mu\text{A}$ is observed on the microammeter.
- Run on moderate ozone ($5 \mu\text{A}$) for 10 minutes
 - Have a stopwatch in hand
 - Turn off the UV lamp and push in shield to run sonde on filtered zero ozone air
 - Time the response time (seconds) to drop from 4 to $1.5 \mu\text{A}$. RECORD the decay time, which is typically between 18 and 30 seconds

Continue to run on zero ozone air for flow rate measurements.

A-5.4 Flow rate and final background measurement



31. After a successful ozonesonde response (decay) test, continue running the instrument on zero ozone air. Connect the 100 mL soap bubble flow apparatus to the exhaust port of the cathode cell. Slowly squeeze the flow apparatus bulb until a steady column of soap bubbles are flowing up the glass burette tube. Continue until the entire glass column is thoroughly wetted.



32. Once the inside walls of the glass column are clear of bubbles, allow 1 or 2 minutes for the glass burette temperature to stabilize. Measure five flowrates (t_{100}) in (seconds per 100 mL/cm³) to the nearest hundredth of a second using a stopwatch. A calibrated electronic flowmeter or Gilibrator measurement device may also be used but be aware of flow rate units displayed and convert if necessary to match Φ_p in **Eq. E-2-1**.

- RECORD: All five flow rates and compute the average (typically between 25 and 35 sec/100mL)

FLOWRATE #1:	28.83	sec
FLOWRATE #2:	28.87	sec
FLOWRATE #3:	28.84	sec
FLOWRATE #4:	28.81	sec
FLOWRATE #5:	28.85	sec
AVERAGE T100:	28.84	

- RECORD: Room Temperature and Room Relative Humidity on the checkout sheet – This may be used to correct the flow rate for the moistening effect

33. Note: The Pump Volume Flow Rate Φ_{p0} in **Eq. E-2-1** requires units of (cm³/s). Therefore, the t_{100} time measured above assumes that a 100 mL glass burette tube is used. Conversion from t_{100} to Φ_{PM} (cm³/s same as ml/s) is:

$$\Phi_{PM} = 100/t_{100}$$

Φ_{p0} (**Eq. E-3-3**) is the actual flow after correcting Φ_{PM} for humidity and temperature.

- RECORD: The background current (I_{B1}) after 10 minutes on zero ozone air. (which should be < 0.07 μ A). Record the timestamp.

34. Turn OFF the 12 VDC SONDE MOTOR power and disconnect the bubble flow apparatus. Disconnect the sensor leads from the ozonizer/test unit and connect the leads to the sonde electronics interface board.
35. Depending on the radiosonde system and telemetry software. The initial check of transmission of data and the radiosonde can be done in the laboratory before assembling the ozonesonde box for flight.
 - Connect the radiosonde to the interface board of the ozonesonde
 - Connect power to radiosonde and ozonesonde (test unit may be able to supply the proper voltage/power to the radiosonde)
 - The ozonesonde will be sampling zero ozone air from the test unit
 - Turn on Telemetry software and enter required meta data
 - Turn on power to radiosonde. Tune into radiosonde frequency
 - Check Data: Pressure, temperature, ozone, pump temperature, etc.

A-5.5 Prepare the ozonesonde box for flight

The following final steps assumes dry lithium cell batteries are used for the radiosonde power and ozonesonde power. Wet cell batteries will require a slightly different procedure. Filling the balloon and preparing the balloon train (**Section A-6**) can be done any time during the final sonde preparation. This depends if the filled balloon can be housed in a shelter (out of the wind) and how finishing the final preparation of the ozonesonde box proceeds before it is time to connect to the balloon train and launch.

36. Turn on Computer:
 - Start telemetry software
 - Enter the check sheet data required by the telemetry software
 - Be sure that the antenna is connected to receiver and positioned ready to receive data
37. Assemble the Ozonesonde Package:
 - Attach the meteorological radiosonde to the side of the polystyrene box with double stick and/or other tape or in its placeholder
 - The radiosonde attaches on the side of the white Styrofoam box that has a small tab near the top edge of the box
 - Connect the radiosonde interface cables to the ozonesonde board
 - Place a small piece of double stick tape on the bottom of the pump battery and adhere the battery to the base of the sonde frame or at the back of the external battery compartment
 - Check that the intake tube is firmly in the pump inlet port using a small piece of emery cloth to grasp the tubing close to the end that will be inserted into the pump inlet hole
 - Now place the sonde inside the box with the intake tube resting in the angled slot in the box. Warning: Do not tape the intake tube into the slot on the Styrofoam box. Movement during launch could remove the inlet from the pump block
 - Extend the leads from both the battery and the pump motor outside the box so power can be connected and disconnected once the lid is taped closed.
 - Be sure the battery lead wires do not interfere with the movement of the piston

38. Open the radiosonde flap to release the temperature sensor and gently position the sensor boom. Avoid handling or touching of the sensitive sensor boom and be careful not to touch the temperature and humidity sensors.

A-5.6 Turn on radiosonde and ozonesonde pump power at launch site

39. Perform a final visual check inside the sonde compartment of the box to be sure that the ozonesonde tubing is firmly in place and no wires or cables are interfering with the sonde piston pump.
40. Position the box lid and attach by wrapping two full lengths (about 100 cm) of tape all the way around the outside edges of the sonde to hold the lid and radiosonde support tape firmly in place. The tape must overlap to remain secure in cold atmospheric temperatures.
41. Turn on radiosonde and plug in ozonesonde battery power. Check the signal strength and telemetry data on computer.

NOTE: At this stage an ozone filter is not needed. The background current has already been measured previously. Therefore, the ozonesonde will be sampling outside surface air for 5 minutes before it is attached to the balloon train. However, in the rare case there is polluted or smokey air nearby then attach an external filter to the intake tube until the sonde can be carried to a clean location for 5 minutes of surface sampling and launch.

A-5.7 Surface ozone measurements at launch site

42. Suspend the sonde about 1.5 meters above ground level. Run for 5 minutes to measure surface ozone.
43. RECORD the surface pressure from a nearby standard ground measurement that is at approximately the same altitude level as the ozonesonde.

A-5.8 Ready for launch (at least 30 minutes since the measurement of I_{B1})

44. Check the incoming data once more. Then connect the ozonesonde to the balloon train.
45. LAUNCH OZONESONDE BALLOON



46. RECORD Local and UTC date and time of launch on checkout sheet.

NOTE: Check the pump temperature when the balloon gets close to burst altitude. The pump temperature should be around 10–20 °C at the end of the balloon ascent. If it is warmer than about 20 °C then subsequent flights may need ventilation holes (about 0.5 cm diameter) bored into the side of the Styrofoam box. If the pump temperature at burst is cooler than 10 °C then the instrument and sensor cell may be getting too cold and will require a small battery heater placed next to the sonde frame.

A-6 Balloon Train and Launching

The ozonesonde instrument is carried aloft by a rubber balloon filled with hydrogen or helium. In dark polar regions, temperatures $< -80\text{ }^{\circ}\text{C}$ may result in early burst of the balloon. Rubber balloons can be treated by kerosene dipping at the surface. Another option is using polyethylene film balloons ($<0.3\text{ mm}$ film thickness). These are expensive and require two people to launch.

The ascent rate of the ozonesonde and balloon burst altitude are related to the weight of the entire ozonesonde balloon train, the amount of lifting gas used to inflate the balloon, balloon size, and environmental conditions (temperature, stability, and sunlight). The typical rise rate ranges from 250–350 meters per minute, with burst occurring between 28 and 35 km altitude.

The typical balloon train consists of:

1. The ozonesonde instrument;
2. A payout reel (ratchet-type or unwinder with approximately 30–40 meters of string);
3. A parachute to slow the descent after balloon burst;
4. Rubber balloon (typical sizes are 600, 1000, 1200, and 1500 grams).

The proper amount of lifting gas for inflation of the balloon should be approximately 35%–50% in excess of the weight of the entire ozonesonde balloon package and train weight (ozonesonde + balloon + payout reel, etc.). This can be adjusted depending on local conditions and experience with previous rise rates and burst altitudes attained. The lifting gas volume needed is determined by two methods

1. The volume of gas is measured by a gas meter or the pressure drop measured from the source lifting gas tank pressure gauge;
2. A dummy weight (weigh-off weight) is used. The lifting gas inflates the balloon until the dummy weight is just lifted (floated) off the floor. This is difficult if done outside under windy conditions.

An example of the dummy weight calculation using 40% lift is given below:

Weight of ozonesonde + radiosonde	=	800 grams
Weight of payout reel + string	=	130 grams
Weight of parachute	=	80 grams
Total Weight of Package	=	1010 grams
+		
Weight of balloon	=	1200 grams
Total Weight of entire sonde balloon train	=	2210 grams

$$\begin{aligned} \text{Dummy weight} &= (\text{Total Weight} + 40\%) - (\text{weight of balloon}) \\ &= 2210 \times 1.4 - (1200) = 3094 - 1200 = \underline{1894 \text{ grams}} \end{aligned}$$

Each station may have different routines for balloon train preparation and launching. Here are some general suggestions.

- Always check that the payout reel or unwinder will not jam and will release the line in a steady, slow manner. A typical ratchet payout reel will have one loop of the string going around a cylindrical bar to slow the speed of the line release
- The typical weather radiosonde unwinder is designed for the small weight of a single radiosonde and should **not** be used with the ozonesonde package, which

typically weighs up to 1 kg. The fast release of unwinder line often leads to the instrument crashing to the ground after launch

- Remove rings, watches or other objects that may scratch the rubber balloon during inflating and handling
- The balloon can be launched by one person when winds are less than about 15–20 knots. It is best to hold the rubber neck of the balloon and top of parachute in one hand and the sonde and payout reel in the other when carrying the ozonesonde out of the inflation facility. Slowly let the string and chute up until line is tight at the payout reel and sonde. If the wind is brisk you may have to run with the wind for a few meters just before release
- Be careful not to make contact with the radiosonde temperature-humidity sensor boom with your hands, arms, or string while handling the balloon train during launch

A-7 Troubleshooting

(a) No data coming in

Loose or poor connections from the antenna to the receiver are the most common problem.

- Check all connections
- Make sure Receiver is adjusted properly for band tuned to the strongest signal and that the attenuate button is Off
- With a directional antenna, make sure it is pointing towards the balloon payload

(b) High Background (greater than about 0.03 microamps)

Change both cathode and anode solutions as outlined in the day of preparation procedure. Run on filtered air for several minutes. If the background is still high, then try ozonesonde on another source of zero ozone air or a different filter. If the background is still high, consider preparing another ozonesonde.

(c) Lots of interference at your frequency

You may have to tune the radiosonde frequency up or down from your frequency to a cleaner region in the allowed 400 to 406 MHz range to shift away from other possible signals.

(d) Pump temperature does not show a typical value or shows no value

Check that the pump temperature thermistor is plugged into the interface board and that there are no broken wires or disconnected leads to the thermistor.

(e) Pump temperature is too cold or too warm (outside a range of 5 to 30 °C)

The pump temperature should be between 25–35 °C at launch and 10–20 °C at burst altitude. If pump temperature at burst has been greater than 20 °C then make one or two small ventilation holes (~1/2 cm diameter) in the side of the box.

If the pump temperature at burst altitude is less than 10 °C:

- Add a sealed, non-leaking, air free water bag or a resistor heater and battery next to the sonde frame
- Make sure the lid is sealed well
- Be sure that the starting pump temperature is around 29 to 35 °C or warmer

A-8 Alternative Sources of Filtered or Zero Air (free of ozone)

Filtered or zero ozone air is used during various stages of the ozonesonde conditioning and performance checks. It is important to use high quality ozone-free air, especially during the sensor background measurements. The ozonizer/test unit provides a very good source of zero ozone air. When the test unit air pump is switched on, ambient air is pumped through a particulate filter and chemical cartridge at approximately 1 litre per minute. The series of cartridges remove nearly all aerosols, dust, ozone, and other trace gases that may affect the ozonesonde sensor. The cartridges are considered to be good for several years when operating in a clean, relatively dry, non-smoking room. However, other zero ozone air sources should be considered if the ECC ozonesonde backgrounds have been drifting higher than normal compared to previous flight preparations. This may occur, for example, at tropical sites where the test unit exposure to high humidity air may eventually reduce the effectiveness of the filter cartridges.

In this case other zero ozone options that may be considered are 1) external pump and canister filters 2) zero air cylinders.

The external pump and canister filters setup shown below consists of a charcoal column used in series with a calcium sulfate (purchased commercially as Drierite) desiccant column that extracts water vapor to give a dry zero ozone source of air. The output flow rate should be at least 0.6 litres/min, which is about three times the flowrate of the ozonesonde (~ 215 ml/min). Higher flow through the desiccant column is normal but will require more frequent regeneration of the Drierite desiccant. As the indicating Drierite granules absorb moisture they turn pink in colour. Regeneration is done by spreading out the granules onto a tray and drying in a warm (~ 200 C) oven for 1 to 4 hours. Each of the columns are approximately 25 to 30 cm in height. An aluminum grating plate and fiber filters are used to hold the desiccant or charcoal granules in place and filter out any smaller particles before the output flow.

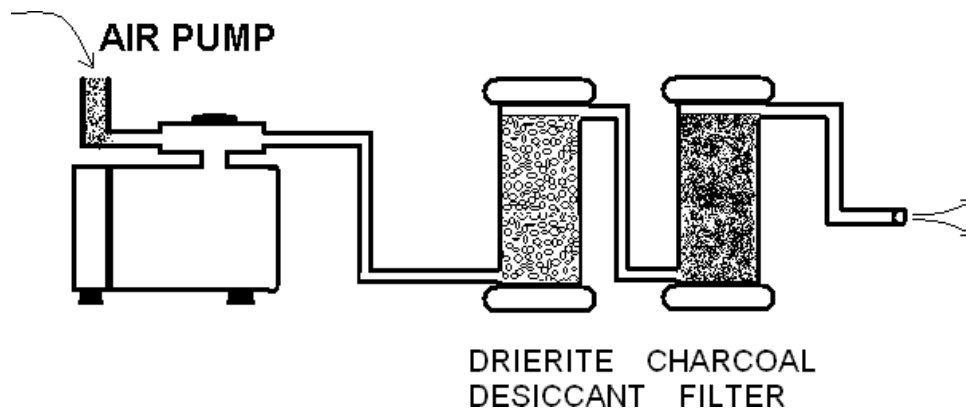


Figure A-2: Set up of air purification

- (1) The Zero Air Cylinder setup is shown below. Zero air tanks can be obtained from most gas suppliers (tanks may be rented or purchased). Additional items required are a properly sized pressure regulator and a gas flow meter.

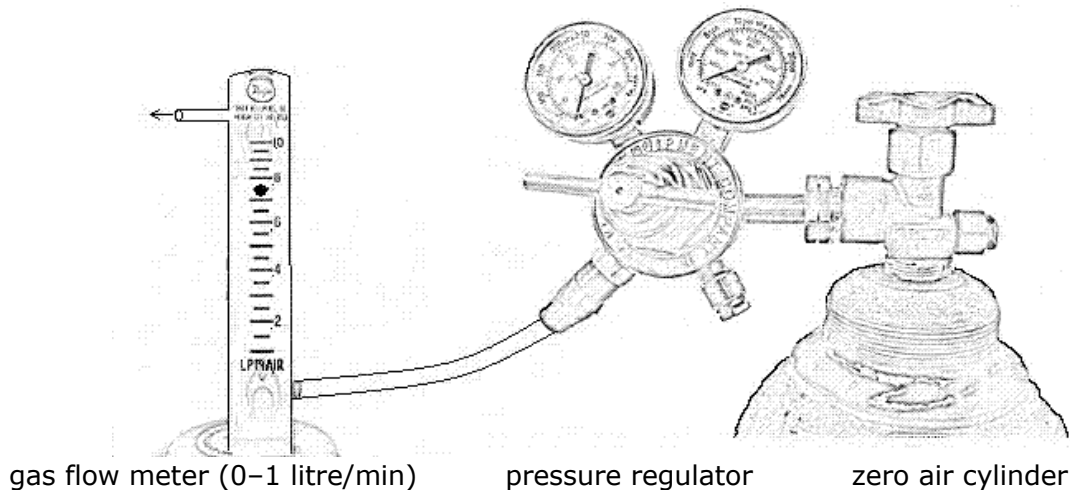


Figure A-3: Zero air supply from storage cylinder

- (2) The tanks can be filled (~ 2000 psi, or 13,800 KiloPascals) with:
- (3) Standard Zero Air which typically has zero ozone, 3 ppm water, and a maximum of 0.5 ppm hydrocarbons (HC).
- (4) Ultra-High Purity (UHP) zero air. UHP zero air is the highest grade zero air but not needed for ECC background use. This air (< 0.1 PPM HC) goes through an additional cleaning process to take out a little extra water vapor and HC, therefore it may cost approximately twice as much as standard zero air.
- (5) The high cost of shipping pressurized cylinders is a disadvantage of this method. Therefore, extra care must be used to conserve the gas. One option is to only use the zero air for 3–5 minutes when obtaining the final ozone background. Also be sure to immediately CLOSE the cylinder valve and turn the gas flow off when finished.

A-9 ECC Ozonesonde Checklist for Ozonesonde Conditioning and Pre-Flight Preparation

The following is an example metadata checklist of ECC sensor operating procedures that is filled in by the operator(s) during sonde preparation. The checklist reflects the required metadata in [Annex B](#) and describes, step-by-step, the operating procedures at the station. Stations should record procedures that diverge from this checklist, particularly if there are additional procedures, procedures that skip or change parts of the standard recommended procedures, or differences in the sequence of the standard recommended procedures. The checklist in its current iteration represents operating procedures largely followed by SHADOZ and NDACC member stations. Stations whose operating procedures perform a calibration of the ECC ozonesonde against an independent source of ozone, such as a TEI or TECO ozone analyser, should amend the checklist to record these values. The actual sequence of procedures and how the calibration is performed are important. They should not change throughout the ozonesonde record, but if they do, it is important that the data record clearly indicates when they changed and how they changed so that impacts on the long-term data record can be better understood.

There are two checklists that follow: (1) an example with sample answers and helpful notes and (2) a blank checklist that can be used by the operator. Not all metadata is captured by this checklist, which highlights the need for the software to capture and provide the missing metadata to the user.

A-9.1 ECC Ozonesonde Example Checklist with Sample Answers and Notes Version June 2021

SAMPLE METADATA ANSWERS IN RED BELOW

Pre-conditioning (prepared 3 to 30 days before flight)

1. Date of pre-conditioning: YYYYMMDD **See Step A-4.1 #1**
2. Operator Initials: JCW
3. Station ID: San Pedro, Costa Rica
4. ECC serial number: 2Z00000 or 6A00000
5. Manufacture Date: YYYYMM or YYYYMMDD
6. Manufacturer pump motor voltage (DC): 12.3
7. Manufacturer pump motor current (mA): 67 < 120 **See Step A-4.1 #4**
8. Manufacturer pump flowrate (s/100ml): 27.1/26.1
9. Sensing Solution/Buffer: 0.5% Half Buffer or 1% Full Buffer, or other
10. Sensing Solution Identifier: Batch date (yyyymmdd), ID number, or other
11. Run 10 min of no-Ozone air: ✓ **See Step A-4.1 #4**
12. Bypass Cathode chamber: Yes ___ or No ✓
13. Run 30 min on High Ozone: ✓ **See Step A-4.1 #5**
14. Run 5 min on no-Ozone air: ✓ **See Step A-4.1 #6**
15. Add Cathode solution (wait minimum 2 min): 3.0cc ✓ **See Step A-4.2 #8**
16. Add 1.5cc Anode solution: ✓ **See Step A-4.2 #10**
17. Run on no-Ozone air until the current drops below 0.3 μ A within less than 30 min ✓
18. Run 10 min on 5 μ A Ozone: ✓
19. Switch to no-Ozone air and record time to drop from 4 to 1.5 μ A (s): 25
See Step A-4.3 #13
20. Run 10 min on no-Ozone air: ✓ Record Ozone Current (μ A): 0.07
See Step A-4.3 #14
21. Short cell leads: ✓ **See Step A-4.3 #15**
22. Store in sonde box, with tissue under the cells, and store at dark place: ✓

Final conditioning for 0–1 day prior to launch

1. Date: YYYYMMDD
2. Operator Initials: HV
3. Check tissue under the cells for any leakage: ✓ **See Step A-5.1 #18**
4. Remove original Cathode and Anode solution: ✓ **See Step A-5.1 #21**
5. Add Cathode solution (wait minimum 2 min): **3.0cm³** ✓ **See Step A-5.1 #22 & 23**
6. Add **1.5cm³** Anode solution: ✓ **See Step A-5.1 #24**
7. Run 10 min of NO-Ozone air: ✓
8. Record ECC current (I_{B0}) (μA): 0.02 < 0.03 **See Step A-5.2 #29**
9. Run 10 min at 5 μA Ozone: ✓
10. Switch to no-Ozone air and record time to drop from 4 to 1.5 μA (s): 25
See Step A-5.3 #30
11. Run on no-Ozone air: ✓
12. Record 5 t_{100} times (s/100ml) to determine flow rate: **See Step A-5.4 #31**
 - a. 28.10
 - b. 28.30
 - c. 28.00
 - d. 28.40
 - e. 28.20
13. Average t_{100} time (s/100ml) for flowrate: 28.20 (should be between 25 and 35 sec/100 ml)
14. Lab. Temperature T_{Lab} ($^{\circ}\text{C}$): 274.5 **See Step A-5.4 #32**
15. Lab. Relative Humidity RH_{Lab} (%): 55
16. Lab. Pressure P_{Lab} (hPa): 850.5
17. After 10 min on NO-Ozone air, record Cell Current (I_{B1}) (μA): 0.02 < 0.07
See Step A-5.4 #33
18. Pump Motor Current (mA): 105
19. End time of preparation (**UTC**): HH:MM:SS

If the sonde package is not flown during final conditioning procedures:

1. Short cell leads: ✓
2. Store in sonde box, with tissue under the cells, at dark place: ✓

Day of Flight Metadata

1. Operator Initials: HV
2. Radiosonde Type: Vaisala **See Step A-5.5 #36**
3. Radiosonde Serial Number: G00000000 or other
4. Interface type: OIF411 or V7 or other depending on the radiosonde software system
5. **I_{Bo}**-Background current (before exposure to ozone) entered into the software (μ A): 0.02
6. Remove ozone filter and allow sonde to acclimate to ambient launch site conditions: ✓
7. Sample ambient air for 5 minutes prior to flight. ✓ **See Step A-5.7 #42**
8. Surface ozone measurement of sonde before release (ppbv) _____
9. Simultaneous surface ozone measurement of validating instrument (e.g. TECO 49i) – optional (ppbv) _____
10. Launch Date: YYYYMMDD
11. Launch Time (Local): HH:MM:SS Launch Time (**UTC**): HH:MM:SS
12. Surface Pressure Launch Site **P_{Surf}** (hPa): 1010
13. Surface Temperature Launch Site **T_{Surf}** (°C): 15.6
14. Surface Rel. Humidity Launch Site **RH_{Surf}** (%): 65

**A-9.2 ASOPOS 2.0 ECC Ozonesonde Blank Checklist Sheet
Version June 2021**

Pre-conditioning (prepared 3 to 30 days before flight)

1. Date of pre-conditioning (YYYYMMDD): ___
 2. Operator Initials: ___
 3. Station ID: ___
 4. ECC serial number: ___
 5. Manufacture Date (YYYYMMDD): ___
 6. Manufacturer pump voltage (V): ___
 7. Manufacturer pump current (mA): ___
 8. Manufacturer flowrate (s/100ml): ___
 9. Sensing Solution/Buffer: ___
 10. Sensing Solution Identifier: ___
 11. Run 10 min of NO-Ozone air: ___
 12. Bypass Cathode chamber: Yes ___ No ___
 13. Run 30 min on High Ozone: ___
 14. Run 5 min on NO-Ozone air: ___
 15. Add 3.0 cm³ Cathode solution (wait 2 min): ___
 16. Add 1.5 cm³ Anode solution: ___
 17. Run on no-Ozone air until the current drops below 0.3µA: ___
 18. Run 10 min at 5 µA Ozone: ___
 19. Switch to no-Ozone air and record time to drop from 4 to 1.5 µA (s): ___
 20. Run 10 min on NO-Ozone air: ___ Record Ozone Current (µA): ___
 21. Short cell leads: ___
 22. Store in sonde box, with tissue under the cells: ___
-

Final conditioning for 0–1 day prior to launch

1. Date (YYYYMMDD): _____
2. Operator Initials: ____
3. Check tissue under the cells for any leakage: ____
4. Remove original Cathode and Anode solution: ____
5. Add 3.0 cm³ cathode solution (wait minimum 2 min): ____
6. Add 1.5 cm³ anode solution: ____
7. Run 10 min of no-Ozone air: ____
8. Record Ozone current (***I*_{Bo}**) (μA): ____
9. Run 10 min at 5 μA Ozone: ____
10. Switch to NO-Ozone air and record time to drop from 4 to 1.5 μA (s): ____
11. Run on NO-Ozone air: ____
12. Record 5 times ***t*₁₀₀** inverse flow rates (s/100ml):
 01. _____
 02. _____
 03. _____
 04. _____
 05. _____
13. Average ***t*₁₀₀** time (s/100ml) inverse flowrate: _____
14. Lab Temperature ***T*_{Lab}** (°C): _____
15. Lab Relative Humidity ***RH*_{Lab}** (%): _____
16. Lab Pressure ***P*_{Lab}** (hPa): _____
17. After 10 min on NO-Ozone air, record Ozone Current (***I*_{B1}**) (μA): _____
18. Pump Motor Current (mA): _____
19. *End time of preparation* (**UTC**): HH:MM

If the sonde package is not flown during final conditioning procedures:

20. Short cell leads: ____
 21. Store in sonde box: ____
-

Day of Flight Metadata

1. Operator Initials: ___
 2. Radiosonde Type: ___
 3. Radiosonde Serial Number: ___
 4. Interface type: ___
 5. ***I_{BO}***-Background current (before exposure to ozone) entered into the software (μA): ___
 6. Remove ozone filter and allow sonde to acclimate to ambient launch site conditions: ___
 7. Sample ambient air for 5 minutes prior to flight. ___
 8. Surface ozone measurement of sonde before release (ppbv) _____
 9. Simultaneous surface ozone measurement of validating instrument (e.g. TECO 49i) – optional (ppbv) ___
 10. Launch Date (YYYYMMDD): ___
 11. Launch Time (Local, HH:MM): _____ Launch Time (UTC, HH:MM): _____
 12. Surface Pressure Launch Site ***P_{Surf}*** (hPa): _____
 13. Surface Temperature Launch Site ***T_{Surf}*** (°C): _____
 14. Surface Rel. Humidity Launch Site ***RH_{Surf}*** (%): _____
-

Metadata
(Extended Version)

Lead authors

Holger Vömel and Jacquie C. Witte, NCAR, Boulder, USA

Table of Contents

B-1	Background	120
B-2	Metadata Fields	120
B-2.1	Required Metadata Fields	121
B-2.1.1	Background Current (I_B) Used in Processing	121
B-2.1.2	Type of Background Current Used in Processing	121
B-2.1.3	Background Current Correction Method	121
B-2.1.4	Measured Mean Flowrate Time	122
B-2.1.5	Pump Flowrate Humidity Correction	122
B-2.1.6	Pump Flow Temperature Correction	122
B-2.1.7	Corrected Flowrate	122
B-2.1.8	Lab Conditions During Flow Rate Measurement	122
B-2.1.9	Pump Efficiency Correction Factors	123
B-2.1.10	Sensing Solution Recipe	123
B-2.1.11	Cathode Solution Volume	124
B-2.1.12	Absorption Efficiency	124
B-2.1.13	Conversion Efficiency	124
B-2.1.14	Response Time from 4 to 1.5 μ A	124
B-2.1.15	Slow Reaction Response Time	124
B-2.2	Essential Metadata	125
B-2.2.1	Background Current Prior to Ozone Exposure: IB0	125
B-2.2.2	Background Current After Exposure of Ozone: IB1	125
B-2.2.3	Time Stamp of IB1	125
B-2.2.4	Pump Temperature During Flow Rate Measurement	125
B-2.2.5	ECC Sonde Serial Number	125
B-2.2.6	ECC Sonde Manufacturer	125
B-2.2.7	Radiosonde Manufacturer	125
B-2.2.8	Radiosonde Model	125
B-2.2.9	Radiosonde Serial Number	126
B-2.2.10	Sensing Solution Identifier	126

B-2.2.11 Source of Ozone-filtered or Ozone-free air	126
B-2.2.12 Comments and Remarks	126
B-2.3 Desirable Metadata	127
B-2.3.1 ECC Interface Board Model	127
B-2.3.2 ECC Interface Board Serial Number	127
B-2.3.3 Processing Software and Version Number	127
B-2.3.4 Ground Check	127
B-2.3.5 ECC Sonde Model	127
B-2.3.6 Date of First Solution	128
B-2.3.7 Date of Previous Launch	128
B-2.3.8 Motor Current at Ground	128
B-2.3.9 Manufacturer Reported Flow Rate	128
B-2.3.10 Battery Type	128
B-2.3.11 Sonde Heater	128
B-2.3.12 Reference for Pump Efficiency Correction Factors	128
B-2.4 Obsolete Metadata	128
B-2.4.1 Background Prior to Launch: <i>IB2</i>	129
B-2.4.2 Head Pressure and Vacuum Pressure	129
B-3 Suggested Naming Convention	129

B-1 Background

Observations of ozone using Electrochemical Concentration Cell (ECC) ozonesondes require additional information to calculate ozone concentrations from the raw data and to describe the observations. This additional information, called metadata, characterizes the environment under which ozone measurements were taken, the ozonesonde itself, and how it was used. Metadata are essential to describing the unique characteristics of each ECC sensor and provide a critical record for identifying changes in preparation procedures and changes in the sensor itself that may lead to discontinuities in long-term records. Consistent and complete record keeping is important for maintaining quality across the data record by guiding users and data managers in maintaining homogenized data records.

This metadata is best collected during sonde preparation and at the time of observation when most information is readily available. Over time, commonly used parameters and coefficients, such as pump efficiency factors, solution recipe, or background treatment, may change. It is vital that these changes are properly captured with the measured data so that the data record as a whole can be properly analysed and evaluated.

The standard operating procedures specified in this report ([Chapter 4](#)) describe metadata. To be able to automatically process ECC ozone sonde data, metadata need to be defined as precisely as possible and at the same time need to be practical for station operators. Software providers should not need to rely on historic and often obsolete metadata 'checklists', which in the past has impeded the interpretation, trouble shooting, and reprocessing of ECC ozonesonde observations across networks. Networks such as the Southern Hemispheric Additional Ozonesondes (SHADOZ), the Network for the Detection of Atmospheric Composition Change (NDACC) or the larger ozonesonde community, which archives data at the World Ozone and Ultraviolet Radiation Data Centre (WOUDC), already provide significant parts of this metadata catalog. The GCOS Reference Upper Air Network (GRUAN) is implementing ozonesonde observations based on the recommendations by the Global Climate Observing System (GCOS) and will base its recommendations on this guide as well.

Here, we provide guidelines on metadata that should be captured by sounding system software and available to the end-user, such that it can be analysed and processed further by researchers and data centres. These recommendations also serve as a 'best practice' guideline to the ozonesonde community on metadata reporting. Implementation of these recommendations is an essential step towards a homogeneous ozonesonde network.

B-2 Metadata Fields

In addition to metadata, all raw data required to process ozonesonde data should be also stored by the sounding systems for the ozonesondes and be included in the data archives to allow reprocessing. The expert-led ozonesonde community has reprocessed existing ozonesonde observations multiple times to incorporate new scientific understanding of the instrumentation and results from WMO-sponsored intercomparisons, such as the Jülich Ozone Sonde Intercomparison Experiments (JOSIE).

As a lesson from this experience, here we define three levels of metadata:

- Required metadata are defined as those without which reprocessing of the raw data is not possible
- Essential metadata to understand the performance of the instrumentation, which describe most aspects of the ozonesonde preparation and its behaviour during preparation
- Desired metadata are needed to fully understand all aspects regarding an ECC ozonesonde observation

As technology and scientific understanding of the ECC sensors and their performance in the atmosphere progresses, new metadata fields may be needed in the future. All software providers should consider keeping their software flexible, such that new metadata fields, which have not yet been defined, may be easily included through future releases of the software.

Currently, no other known metadata definitions exist for the metadata fields described here. Providers may use the metadata definitions listed in **Section B-3** for implementation in their software. A sample checklist similar to those in use at SHADOZ and NDACC stations is provided in **Section A-9** of [Annex A](#). The metadata listed in this operator's checklist reflect those captured by the operator, but it is incomplete. The missing metadata are in the configuration of the software, which need to be provided by the software itself.

B-2.1. Required Metadata Fields

Required metadata fields defined in this document are those variables that appear in the ECC equation and describe the conversion from the measured raw cell current to ozone partial pressure using the basic ECC ozonesonde **Eq. E-2-1 (Chapter 2.2)**.

B-2.1.1 Background Current (I_B) Used in Processing

Historically, a background current is subtracted from the measured cell current. This current was typically measured prior to launch but in practice it has been shown that the operating procedures at different sites and at different times have defined this background current differently [Witte *et al.*, 2017]. The contribution of the background current to the ozonesonde uncertainty budget may be significant. Therefore, it is critical that documentation of the type of background current used in the processing be clearly defined. The background current is given in μA .

Recently, a new method to process ECC ozonesondes has been proposed [Vömel *et al.*, 2020] which does not use any prescribed background. If this algorithm is used, a background of '0' needs to be entered and the background current correction method "calculated" should be selected.

B-2.1.2 Type of Background Current Used in Processing

The type of background current describes how the background current was obtained. The following options are currently in use:

- Background current measured prior to the high ozone conditioning of the cell, during day of launch procedures (I_{B0})
- Background current measured 10 min after the high conditioning of the cell, during day of launch procedures (I_{B1})
- Background current measured just prior to launch (I_{B2})
- Default value, a climatological mean value or lab definition which has not been measured due to questionable filter performance (I_{BC})
- No background current is used

B-2.1.3 Background Current Correction Method (Constant/Pressure-dependent/Calculated)

The recommended standard operating procedures require that the background current, which is subtracted from the measured cell current, is constant throughout the profile, and that it does not depend on any other parameter (see **Section 3.3.6**). Some non-standard operating procedures treat this background current as a pressure dependent background. The software must indicate whether the background is treated as constant, as pressure dependent, or calculated.

Science Pump Corp. [SPC, 1999] incorrectly recommends a pressure dependence equation for the background measured at the surface. This equation has been implemented by Vaisala for Science Pump ECC sondes only. **It should not be used by any new station and no existing station should switch to this method.** Stations using this method should continue doing so and should properly track their use of this method.

Vömel *et al.* [2020] proposed a new method to process ECC ozonesondes, assuming that what has been called “background” is, in fact, attributable to a slow reaction pathway. This secondary reaction is explicitly calculated as part of the algorithm and subtracted from the measured cell current. If this method is used in future processing software, the calculated slow reaction pathway replaces what has been called “background”. For consistency, the metadata field should indicate that it has been “calculated”.

B-2.1.4 Measured Mean Flowrate Time (t_{100} , Section 3.3.2)

The pump flowrate time, following standard operating procedures, is measured at the outlet of the cathode cell using a bubble flow meter. t_{100} is the mean time in seconds to pump 100 ml of air under laboratory conditions during normal sonde preparation. The time given in the metadata is not corrected for any humidity dependent deviations caused by flowing drier air through the cathode cell.

B-2.1.5 Pump Flowrate Humidity Correction (C_{PH} , Section 3.3.2, Annex C-6.1.2.1)

This correction factor accounts for the increase in the flowrate due to evaporation inside the cathode cell and the bubble flow meter and applies only for flowrates measured using this method. Under dry conditions, this value can be as high as 2%–3%. The pump flow rate humidity correction factor C_{PH} can be calculated with **Eq. E-3-4**, using the relative humidity (RH_{Lab}), pressure (P_{Lab}) and temperature (T_{Lab}). For stations that measure the humidity dependent correction directly, the correction factor value provided by the operator is stored “as is” and used in place of the calculated flowrate correction. The values of C_{PH} provided by the operator may range between 0 and 0.03 with an uncertainty $\Delta C_{PH} = 0$. However, when P_{Lab} , T_{Lab} , & RH_{Lab} , are not recorded an average estimation for C_{PH} and its uncertainty ΔC_{PH} are made (**Section 3.3.2: Eqs. E-3-5 & E-3-6 & Annex C-6.1.2.1**). For stations that measure the humidity dependent correction directly, the correction factor *rate humidity correction source* specifies whether the flowrate correction was calculated following **Eq. E-3-4**, or whether it was provided by the operator. The possible entries for this field are:

- Calculated
- Operator provided

If no flowrate humidity correction has been applied, then the value of 0 must be used. This value must be described as *operator provided*.

B-2.1.6 Pump Flow Temperature Correction (C_{PL} , Section 3.3.2, Annex C-6.1.2.2)

This correction factor accounts for the small decrease in the flowrate through the slightly higher temperature inside the Teflon pump base of about 2 K compared to the laboratory temperature T_{Lab} . The pump flow temperature correction factor C_{PL} is calculated using **Eq. E-3-7** based on the the recorded laboratory temperature (T_{Lab}). C_{PL} values are typically about 0.007, while its uncertainty ΔC_{PL} is about 0.002.

B-2.1.7 Corrected Flowrate (Φ_{p0} , Section 3.3.2, Annex C-6.1.2)

The corrected flowrate Φ_{p0} in ml/s specifies the flow of gas through the cell and has been corrected for the humidification effect of the bubble flow meter during the flow rate measurement following **Eq. E-3-3**. The corresponding uncertainty $\Delta \Phi_{p0}$ is calculated from **Eq. E-3-9**. For most stations, the software must calculate this field based on the other metadata provided. At stations that measure the final corrected flowrate directly (Gilibrator or mass flow meter), this value is provided without further corrections.

B-2.1.8 Lab Conditions During Flow Rate Measurement (RH_{Lab} , T_{Lab} , P_{Lab})

The ambient air conditions in the laboratory (i.e. pressure, temperature, and relative humidity) during the flowrate measurement using a bubble flowrate meter enter the calculation of the flowrate humidity correction and must be stored:

- RH_{Lab} Relative humidity in the laboratory during flowrate measurement [%]
- T_{Lab} Temperature in the laboratory during flowrate measurement [°C]
- P_{Lab} Pressure in the laboratory during flowrate measurement [hPa]

If a station uses a filter with a well-maintained desiccant filter in front of the ECC pump intake during the flowrate measurement, then the laboratory humidity must be entered as zero and used in calculating the pump flowrate humidity correction.

B-2.1.9 Pump Efficiency (Section 3.3.3, C-6.6)

The pump efficiency takes into account the degradation in the performance of the Teflon pump to move air through the cell at low pressures and may take into account other empirical corrections. At pressures typically below 100 hPa, measured flow rates decrease and require corrections to the ozone profile measurements, which reach their maximum at balloon burst. Several research groups have published measured pump efficiencies (e.g. **Table 3.1**), which are used in the processing software. The software must provide these efficiencies with their uncertainties as part of the metadata and must refer/adapt to the table used in the original publication.

The pump efficiencies $\eta_P(\mathbf{P})$ and their uncertainties $\Delta\eta_P(\mathbf{P})$ are to be stored as an array, e.g.

$\eta_P(\mathbf{P})$: 1.0000, 0.989, 0.985, 0.978, 0.969, 0.948, 0.935, 0.916

$\Delta\eta_P(\mathbf{P})$: 0.0, 0.005, 0.006, 0.008, 0.008, 0.009, 0.010, 0.012

and must be accompanied by the corresponding pressures [hPa] at which they were reported.

The efficiency correction factor pressures must be stored as an array in the same order and with the same number of elements as the corresponding pump efficiency correction factors, e.g.

\mathbf{P} : 1000, 100, 50, 30, 20, 10, 7, 5

Different tables are in use, which report efficiencies at different pressures. The pressure levels and efficiencies reported by the original study must be reported in the metadata.

To avoid any misunderstanding, in literature often pump efficiency correction factors are reported, which are the inverse values of the corresponding pump efficiencies.

B-2.1.10 Sensing Solution Recipe (SST, Section 2.3)

Different recipes for the standard sensing solution exist (See also [Chapter 2, Table 2–2](#)). The exact recipe used for the sensing solution must be given. Options for the value of this metadata field are:

- SST0.5: 0.5% Half Buffer (5 g/L KI, 12.5 g/L KBr, 2.5 g/L Na₂HPO₄ 12H₂O, 0.625 g/L NaH₂PO₄ H₂O)
- SST1.0: 1%, Full Buffer (10 g/L KI, 25 g/L KBr, 5.0 g/L Na₂HPO₄ 12H₂O, 1.25 g/L NaH₂PO₄ H₂O)
- SST0.1: 1%, 1/10th Buffer (10 g/L KI, 25 g/L KBr, 0.5 g/L Na₂HPO₄ 12H₂O, 0.125 g/L NaH₂PO₄ H₂O)

The software needs to allow operators to enter different recipes for stations that use solutions not listed here. To be consistent with the above description and to minimize misinterpretations, the recipe should be entered with a short descriptive name, followed by the complete mixture in brackets. Listing the complete recipe helps identify problems at some

stations that may not have access to the full literature regarding the composition of the sensing solutions. The standard terminology for the Sensing Solution Type (SST) should be included.

B-2.1.11 Cathode Solution Volume (Section 3.3.4)

The default solution amount of cathode solution is 3.0 ml. Some non-standard operations use a smaller i.e. amount (typically, 2.5 ml) of cathode solution. The solution amount used in the sounding must be included in the metadata. For some existing software, the solution volume influences the calculations and is therefore required in order to process the data.

B-2.1.12 Absorption Efficiency (η_A , Section 3.3.4, Annex C-6.5)

For stations that use less than the standard recommended amount (3.0 ml) of sensing solution in the cathode, some of the ozone pumped into the solution may not be taken up by the solution, resulting in a low bias of ozone measurements recorded at higher pressures (1000–500 hPa). The absorption efficiency corrects for this effect. For the stations using 2.5 ml of sensing solution, the absorption efficiency $\eta_A(P_{Air})$ is calculated using Eq. E-3-11-A/B and for its corresponding uncertainty $\Delta\eta_A(P_{Air})$ from Eq. E-3-11-C, while for stations using 3.0 ml, the absorption efficiency $\eta_A = 1.00$ and its uncertainty $\Delta\eta_A = 0.01$ through the entire profile. The metadata should capture whether an absorption efficiency correction has been applied to the data or not.

Possible entries to this field are “yes” and “no”.

B-2.1.13 Conversion Efficiency (η_c , Section 3.3.5, Annex C-6.7)

It is well known that different combinations of sensing solution types and ECC ozonesonde types (SPC or ENSCI) provide slightly different measurements of ozone. These factors have not yet been defined and are under investigation as of this writing. In the meantime, software may assume a conversion efficiency $\eta_c = 1.00$ for all solution types and the corresponding uncertainty $\Delta\eta_c = 0.03$

However, this is subject to change in the future; however, metadata fields are already implemented here. The conversion efficiency refers to the generation of excess cell current under steady state conditions (steady state bias). This value may be used in processing when correcting for response time of the slow reaction pathway as proposed by *Vömel et al.* [2020].

B-2.1.14 Response time from 4 to 1.5 μA (τ_{fast})

Taken during day of flight sonde preparation, the decay time of the cell current from 4.0 μA to 1.5 μA (after 10 minutes of exposure to ozone resulting in cell current of 5 μA) indicates the response time of the ECC ($\frac{1}{e} = 0.368 \approx \frac{1.5}{4.0}$).

Using this interval avoids any imperfections in switching to a source of ozone-free air and flushing of tubing. The response time (τ_{fast}) is recorded in units of seconds.

This value may be used in processing when correcting for response time lag of the fast reaction pathway as proposed by *Vömel et al.* [2020].

B-2.1.15 Slow Reaction Response Time (τ_{slow})

Vömel et al. [2020] proposed a correction algorithm that considers the response times of both the slow and the fast reaction pathways occurring in an ECC. The fast response time constant is measured and reported as the time during which the cell current decays from 4 to 1.5 μA . The slow reaction time constant (τ_{slow}) is not measured during the normal preparation but has been reported in literature. If the background current is calculated explicitly based on the algorithms proposed by *Vömel et al.* [2020], then a slow reaction time constant of about 25

min should be used. If a constant background current is used, then this parameter should be set to "missing".

B-2.2 Essential Metadata

Essential metadata are defined in this document as metadata used to understand the performance of the instrumentation and which describe most aspects of the ozonesonde preparation. The essential metadata must be consistent with the sonde preparation procedures at the site. Differences between most operating procedures are minor and may be captured by the following essential metadata fields.

B-2.2.1 Background Current Prior to Ozone Exposure: I_{B0} (Section 3.3.6)

Taken during day of flight sonde preparation, a cell current is recorded after the sensor has run for 10 min on ozone-free air but before it is exposed to ozone amounts of 5 μA . The cell current reading prior to ozone exposure has historically been referred to as I_{B0} and must be recorded.

B-2.2.2 Background Current After Exposure of Ozone: I_{B1} (Section 3.3.6)

Taken during day of flight sonde preparation, a cell current is recorded 10 min **after** exposure to ozone of 5 μA while being exposed to ozone-free air. The cell current reading after ozone exposure has historically been referred to as I_{B1} and must be recorded. This reading gives some indication about the performance of the ozonesonde cell.

B-2.2.3 Time Stamp of I_{B1} (Section 4.2.2.2)

The time stamp in UTC (Coordinated Universal Time) when I_{B1} is measured should be recorded (**Section 4.2.2.2, Figure 4-2**). This time relates the conclusion of the sonde preparation with the launch of the sounding and is used to evaluate the time response of the ECC during launch.

B-2.2.4 Pump Temperature During Flow Rate Measurement (Section 3.3.2)

The elevated temperature of the ECC pump during the flowrate measurement contributes a small correction to the measurement of the flow rate and should be recorded (**Eq. E-3-8**). If it has been recorded, then it is assumed that the calculated flowrate has been corrected using this value.

B-2.2.5 ECC Sonde Serial Number

The sonde serial number is essential to evaluate potential manufacturer induced production variability. The sonde serial number must be stored with all prefixes and suffixes provided.

B-2.2.6 ECC Sonde Manufacturer

The sonde manufacturer must be stored in the metadata. Currently two sonde manufacturers dominate the market: ENSCI and Science Pump Corp.

B-2.2.7 Radiosonde Manufacturer

The processing software for ECC ozonesondes is typically provided by the radiosonde manufacturer. It is essential that the radiosonde manufacturer is stored in the metadata.

B-2.2.8 Radiosonde Model

It is essential that the radiosonde model is stored in the metadata, since some radiosonde models directly affect the ozonesonde uncertainties.

B-2.2.9 Radiosonde Serial Number

The radiosonde serial number may be used to identify the production vintage of the radiosonde and to characterize possible biases that may have been introduced by the radiosonde sensors.

B-2.2.10 Sensing Solution Identifier

Stations should keep track of the preparation of the sensing solutions used in their ozonesondes. This should be done through record keeping of the solution mixtures, providers of the chemicals and methods used in the preparation of the solutions. Sensing solutions from the same batch may be identified by a serial number or a date when the solutions were prepared. This identifier is stored as part of the metadata and should correspond to the station's record of solution preparations.

B-2.2.11 Source of Ozone-filtered or Ozone-free air

The measurement of the cell current before and after the exposure to ozone is often affected by the source of ozone-free air. The source of ozone-free air should be stored as part of the metadata. Currently used sources of ozone-filtered or ozone-free air are

- Charcoal filtered air
- Air taken from the Ozonizer unit
- Air taken from calibrated ozone reference instrument with built-in filter
- Compressed synthetic or purified air
- Air passed through Drierite filters
- Other

Many different types of filters are in use, but the list above should capture the majority of filters. Therefore, the metadata field should list one of these six options. Charcoal filters are in widespread use at stations and consist of a small container filled with charcoal that destroys ozone. These containers may be in the form of small metal cartridges or glass vials. In these filters, charcoal may or may not be easily replaced. Ozonizer units have built-in ozone filters, the type and condition of which are generally not known to the user. Although they should be replaced as part of routine maintenance, they rarely are. Compressed synthetic or purified air may be provided in small compressed gas cylinders or may be provided centrally in some laboratories. Compressed synthetic or purified air is considered free of ozone and is most reliable for making background current measurements. However, it is also the most resource intensive to provide and may not be feasible at many stations.

Drierite[®] filters combine a desiccant stage and a charcoal stage in a large plastic cartridge. The desiccant dries the air before it passes through the charcoal to remove ozone. These filters are considered most suitable for high quality stations. The condition of the desiccant is indicated by its colour. During routine maintenance procedures, station operators should change the desiccant and the charcoal when indicated by the operator. Other filters may be in use, which do not fall in the categories above. The metadata should allow a short description of the type of filter that may be in use at a site.

B-2.2.12 Comments and Remarks

The operator may make noteworthy observations. These notes should be stored with the metadata and should be available to the user. The comments field should be a free text string field of arbitrary length.

B-2.3 Desirable Metadata

Some metadata is highly desired to fully understand all aspects regarding an ECC ozonesonde observation and should be provided with the raw data.

B-2.3.1 ECC Interface Board Model

The interface model used to digitize the ozonesonde measurements of cell current, pump temperature, pump motor current, and sonde battery voltage.

B-2.3.2 ECC Interface Board Serial Number

The interface serial number is essential to evaluate potential manufacturer induced production variability. The interface serial number, where available, is stored with all prefixes and suffixes provided.

B-2.3.3 Processing Software and Version Number

The name of and version of the radiosonde system software used to process the sounding.

B-2.3.4 Ground Check

Some ozonesonde stations perform checks of the ozonesonde performance by comparing their measurements to a reference value prior to launch. The reference may be generated by an ozone calibrator that provides air with a well-defined concentration of ozone or it may simply be the measurement of a high quality surface ozone sensor, where the ozonesonde shares the same air that is being analysed by the surface ozone instrument.

The ground check generates three different metadata entries:

- Ground check reference value – [ppbv]
- Ground check ozonesonde reading – [ppbv]
- Source of the ground check reference value

It is important that the ground check values from the reference instrument and the ozonesonde be read at the same time and while both instruments sample the same air. The source of the ground check reference value specifies which instrument is used as reference. Most likely this instrument is a NIST traceable reference instrument which are commercially available.

B-2.3.5 ECC Sonde Model

Currently two main companies supply nearly all ECC ozonesondes in use: Science Pump Corporation (SPC) and ENSCI. These companies use a slightly different naming scheme for the serial numbers of their sondes, which are already captured under **Section B-2.2.5** and **B-2.2.6** of this Annex. To clearly identify the manufacturer and the sonde model type, both may be captured explicitly as the sonde model, with possible entries of:

ENSCI: EnSci-Z, ENSCI-1Z, ENSCI-2Z

SPC: SPC-6A, SPC-5A, SPC-4A, SPC-3A.

The older SPC models are listed for completeness but are unlikely to be used in current soundings. However, reprocessing efforts of historical data may be using these types.

B-2.3.6 Date of First Solution

New sondes are being filled for the first time with cathode and anode solution at the ozone sonde station. The date when this occurs should be recorded in the metadata to indicate how many days prior to launch an ECC was first filled with solutions.

B-2.3.7 Date of Previous Launch

Recovered ECC ozonesondes may be reconditioned and launched again. The date of the previous launch indicates that a sonde has been recovered and reconditioned. For new sondes, this field should be blank.

B-2.3.8 Motor Current at Ground

The motor current in mA drawn by the pump during the initial sonde check at the 0–1 day prior to launch procedure. Depending on the interface and the ground check station, this initial pump current may include the current drawn by the interface board or it may be the current drawn exclusively by the pump motor.

B-2.3.9 Manufacturer Reported Flow Rate

The manufacturer may provide a flow rate as part of their sonde checkout. In practice, this value is rarely used, but it may be captured as manufacturer specification.

B-2.3.10 Battery Type

The battery type (e.g. dry lithium battery, water activated battery, or other) used to operate ECC ozonesondes contributes to the thermal balance of a sounding and is a factor in the duration during which an ECC ozonesonde pump may be operated.

B-2.3.11 Sonde Heater

Stations in cold regions and stations predominantly launching at night might use additional heating devices to maintain a pump temperature sufficiently warm to prevent sensing solutions from freezing. Common methods include placing passive or active heating elements into the sonde compartment. Passive heaters include water bags and other materials that rely on thermal mass while active heaters include chemical heaters, unregulated electrical heaters, or thermostat heaters. Tracking the heater used by a station provides information about the temperature management inside the ECC box.

B-2.3.12 Reference for Pump Efficiency Correction Factors

The metadata should contain the reference to the publication from which the efficiency correction factors were taken (see **B-2.1.9**). This is likely either the empirical efficiency correction factors published by Komhyr [1986, **K86-Efficiency**], the efficiency correction factors by Komhyr et al. [1995, **K95-Efficiency**], or the truly measured pump efficiency published by Johnson et al. (2002).

If another source of the efficiency correction is used, then the full reference should be provided.

B-2.4 Obsolete Metadata

Metadata fields listed here have been evaluated and found not to add value. These fields are declared obsolete and their collection is no longer recommended.

B-2.4.1 Background Prior to Launch: I_{B2}

This measurement suffers from many inconsistencies in procedure and from the undefined quality of filters used to generate ozone-free air at the launch site. This field has not added value to analyses since its introduction.

B-2.4.2 Head Pressure and Vacuum Pressure

The head gauge pressure in hPa generated by the pump during the initial checkout. This field has been found not to add value.

The vacuum gauge pressure in hPa generated by the pump during the initial checkout. This field has been found not to add value.

B-3 Suggested Naming Convention

Long name	Short name	Type	Unit	Missing value	Section in Annex B
Background current used in processing (I_B)	Background	float	μA	NaN	B-2.1.1
Type of background used in processing	Background_type	string	--		B-2.1.2
Background correction method	Background_method	string	--		B-2.1.3
Measured mean flowrate time (t_{100})	Flowrate_time	float	s/100ml	NaN	B-2.1.4
Flowrate humidity correction (C_{PH})	Flowrate_humid_corr	float	--	NaN	B-2.1.5
Flowrate humidity correction source	Flowrate_corr_source	string	--		B-2.1.5
Flowrate temperature correction (C_{PL})	Flowrate_temp_corr	Float	-	NaN	B-2.1.6
Corrected flowrate (Φ_{PO})	Flowrate	float	ml/s	NaN	B-2.1.7
Lab humidity during flow rate measurement (RH_{Lab})	Lab_RH	float	%	NaN	B-2.1.8
Lab temperature during flow rate measurement (T_{Lab})	Lab_T	float	$^{\circ}\text{C}$	NaN	B-2.1.8
Lab pressure during flow rate measurement (P_{Lab})	Lab_P	float	hPa	NaN	B-2.1.8
Pump Efficiency (η_P)	Efficiency_Pump	float array	--	NaN	B-2.1.9
Pressures corresponding to pump efficiency	Efficiency_Pump_P	float array	hPa	NaN	B-2.1.9
Sensing solution recipe (SST)	Solution	string	--		B-2.1.10
Cathode solution volume	Cathode_volume	float	ml	NaN	B-2.1.11
Absorption efficiency applied (η_A)	Absorption_eff_applied	string			B-2.1.12
Conversion efficiency (η_C)	Conversion_eff	float	--	NaN	B-2.1.13
Response time from 4 to 1.5 μA (τ_{fast})	Response_time	float	s	NaN	B-2.1.14

Long name	Short name	Type	Unit	Missing value	Section in Annex B
Slow reaction time constant (τ_{slow})	Slow_time	float	s	NaN	B-2.1.16
Background prior to 5 μ A (I_{B0})	IB0	float	μ A	NaN	B-2.2.1
Background 10 min after 5 μ A (I_{B1})	IB1	float	μ A	NaN	B-2.2.2
Time when I_{B1} was measured	Time_IB1	ISO 8601	-		B-2.2.3
Pump temperature during flow rate measurement ($T_{P,Lab}$)	Pump_T_Flow	float	$^{\circ}$ C	NaN	B-2.2.4
ECC sonde serial number	ECC_serial	string	--		B-2.2.5
ECC sonde manufacturer	ECC_manufacturer	string	--		B-2.2.6
Radiosonde manufacturer	Radiosonde_manufacturer	string	--		B-2.2.7
Radiosonde model	Radiosonde_model	string	--		B-2.2.8
Radiosonde serial number	Radiosonde_serial	string	--		B-2.2.9
Sensing solution identifier	Solution_ID	string	--		B-2.2.10
Source of zero air	Zero_air	string	--		B-2.2.11
Comments	Comments	string	--		B-2.2.12
ECC interface model	ECC_interface	string	--		B-2.3.1
ECC interface serial number	ECC_interface_serial	string	--		B-2.3.2
Processing software and version	Software_version	string	--		B-2.3.3
Ground check reference value	GC_Reference	float	ppbv	NaN	B-2.3.4
Ground check ozonesonde reading	GC_Reading	float	ppbv	NaN	B-2.3.4
Source of the ground check reference value	GC_Instrument	string	--		B-2.3.4
ECC sonde model	ECC_Model	string	--		B-2.3.5
Date of first solution	Date_1st_solution	ISO 8601	-		B-2.3.6
Date of previous launch	Prev_Launch_Date	ISO 8601	--		B-2.3.7
Motor current ground check	Motor_Current_GC	float	mA	NaN	B-2.3.8
Manufacturer flowrate	Manufacturer_Flow	float	s/100ml	NaN	B-2.3.9
Battery type	Battery_Type	string	-		B-2.3.10
Sonde heater	Heater_Type	string	-		B-2.3.11
Reference for efficiency correction factors	Efficiency_corr_ref	string	--		B-2.3.12

**Practical Guidelines to Determine
Ozone Partial Pressure by ECC Sonde, and its Associated Uncertainty**

Lead authors

Herman G.J. Smit (FZ-Jülich/IEK-8, Jülich, Germany),

Roeland Van Malderen (RMI, Uccle, Belgium)

Table of Contents

C-1	Introduction	133
C-2	Metrological terminology: Uncertainty, Precision, Bias and Accuracy	133
C-2.1	What is precision and accuracy?	133
C-2.2	Some remarks on precision, accuracy	133
C-2.3	WMO/GAW definitions for error, uncertainty, precision, bias and accuracy	134
C-3	Overview Data Processing Steps and Needed Measure Parameters	135
C-4	Flight (i.e. sounding) time as independent profile variable (t_F)	137
C-5	Radiosonde: air pressure (P_{air}), geopotential and geometric height (H & Z)	138
C-6	Ozone pressure (P_{O_3}) derived from measured ECC ozonesonde data	139
C-6.1	Pump flowrate at ground (Φ_{P0} ; Section 3.3.2)	139
C-6.1.1	Determination of volumetric flowrate of the gas sampling pump (Φ_{PM})	139
C-6.1.2	Determination of humidity- and temperature-corrected volumetric pump flowrate (Φ_{P0})	139
C-6.1.2.1	Correction factor for humidification (C_{PH}) and its uncertainty (ΔC_{PH})	139
C-6.1.2.2	Correction for difference of temperature between pump and laboratory (C_{PL}) and its uncertainty (ΔC_{PL})	139
C-6.2	Measured cell current (I_M) and its uncertainty (ΔI_M)	140
C-6.3	Background current (I_B) and its uncertainty (ΔI_B)	140
C-6.4	Pump temperature (T_P) and its uncertainty (ΔT_P)	140
C-6.5	Absorption efficiency (η_A) and its uncertainty ($\Delta \eta_A$)	140
C-6.6	Pump efficiency (η_P) and its uncertainty ($\Delta \eta_P$)	140
C-6.7	Conversion efficiency (η_C) and its uncertainty ($\Delta \eta_C$)	141
C-6.8	Ozone pressure P_{O_3} by ECC sonde and overall uncertainty ΔP_{O_3}	141
C-6.9	Ozone volume mixing ratio μ_{O_3} derived from ECC sonde measurements and uncertainty $\Delta \mu_{O_3}$	141
C-7	Total ozone column: Total ozone normalization	141
C-7.1	Ozone column by ozonesonde (Ω_S)	141
C-7.2	Residual ozone column above burst point of ozonesonde (Ω_R)	142
C-7.3	Total ozone column by Dobson or Brewer spectrophotometer (Ω_C)	142
C-7.4	Total ozone normalization factor (N_T)	142

C-1 Introduction

In this Annex, we want to give practical guidelines for the different ozonesonde data processing steps that are recommended to calculate the ozone partial pressure, and its overall uncertainty, from the ozonesonde and radiosonde measurements as described in [Chapter 3 \(Section 3.3\)](#) and summarized in [Table 4–1 \(Section 4.3.2\)](#). We will start with the list of all the relevant variables, determined prior to launch and in the course of the ozonesounding, that are required as input parameters in the data processing. We note here that all relevant formulas are all in [Chapter 3](#), while the relevant formulas for the radiosonde parameters are in [Chapter 2 \(Section 2.4.3\)](#).

We caution that some of the available radiosonde software packages have implemented several of the data processing steps discussed here, but not all (e.g. the uncertainty estimation is currently lacking). Therefore, we advise users of commercial software packages to check carefully for themselves which steps are in fact included. **We strongly recommend that the radiosonde and ozonesonde manufacturers will introduce all the recommended data processing steps in a future update of their sounding software.**

In [Section C-2](#) we give a short survey of some basic metrological definitions and the terminology of the WMO/GAW related definitions of error, uncertainty, precision, bias and accuracy. [Section C-3](#) gives an overview of the different processing step and list of measured parameters directly relevant to the ozonesonde data processing. [Section C-4](#) defines the timeline of an ozonesounding from the preparation of the sonde until the end of the balloon flight. [Section C-5](#) describes the further data processing of radiosonde air pressure (P_{Air}) and GPS altitude in relation to geopotential and geometric height (H & Z). In [Section C-6](#) the step-by-step data processing is described in detail in order to obtain the partial pressure of ozone and its overall uncertainty. In [Section C-7](#), we refer to the formulas for calculating the total ozone normalization factor, a first quality indicator of the measured ozonesonde profile, and its uncertainty.

C-2 Metrological terminology: Uncertainty, Precision, Bias and Accuracy

C-2.1 What is precision and accuracy?

So, if you are playing soccer and you always hit the left goal post instead of scoring, then you are not accurate, but you are precise. This is illustrated in [Figure C-1](#) showing the difference between precision and accuracy of hitting the bullseye of a dartboard.

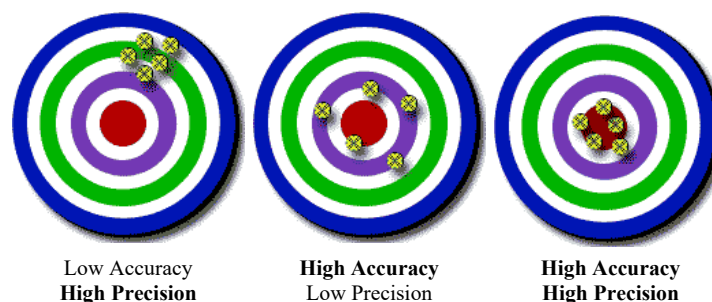


Figure C-1: The difference between precision and accuracy of hitting the bullseye of a dartboard

C-2.2 Some remarks on precision, accuracy

1. *Precision and accuracy are qualitative concepts and should be avoided in quantitative expressions;*
2. *Accuracy cannot be expressed as a numerical value;*

3. The term 'accuracy of measurement' should not be used for 'measurement precision';
4. Accuracy is inversely related to the combination of systematic error (bias) and random error (uncertainty) that occur in a single measurement result (**Figure C-2**);
5. Accuracy is concerned with the difference between a single measurement result and a true (or the best estimate) value.

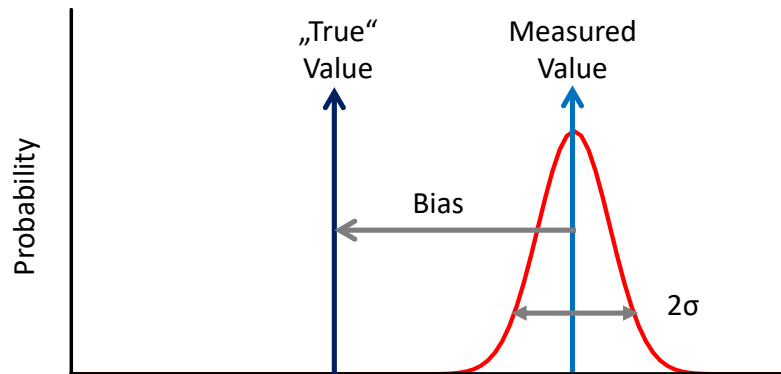


Figure C-2: If a distribution of measured values follows a symmetric (normal) probability distribution around an arithmetic average then a one- σ standard deviation is the standard uncertainty, or precision of the measurement, whereas accuracy is how close the measurement is to the "true" value

C-2.3 WMO/GAW definitions for error, uncertainty, precision, bias and accuracy

To ensure the comparability and compatibility of measurements the terminology on error, uncertainty, precision, bias and accuracy used here are based on recommendations made by WMO/GAW and documented in the WMO/GAW Glossary of QA/QC Related Terminology [2010–2020; (https://www.empa.ch/web/s503/gaw_glossary)]. Below are some QA/QC related definitions listed that are relevant for ozonesonde measurements and their uncertainties:

Measurand = particular quantity subject to measurement

Measurement = set of operations having the object of determining a value of a quantity.

True value (of a quantity)

- value consistent with the definition of a given particular quantity
- this is a value that would be obtained by a perfect measurement
- true values are by nature indeterminate

Conventional value (of a quantity) = Assigned value

- value attributed to a particular quantity, accepted as having an uncertainty appropriate for a given purpose

Precision

- degree of internal agreement among independent measurements made under specific conditions
- precision is expressed numerically by e.g. standard deviation or variation coefficient

- *it is a measure of the dispersion of measured values*

Random error

- *component of measurement error that in replicate measurements varies in an unpredictable manner random error is equal to measurement error minus systematic error*
- *because only a finite number of measurements can be made, it is possible to determine only an estimate of random error*

Repeatability (of results of measurements)

- *closeness of the agreement between the results of successive measurements of the same measurand carried out under the same conditions of measurement*
- *measurement precision under a set of repeatability conditions of measurement repeatability may be expressed quantitatively as a level of confidence, e.g. '±1 standard deviation'*

Uncertainty of a measurement

- *closeness of the agreement between the results of successive measurements of the same measurand carried out under the same conditions of measurement*
- *non-negative parameter characterizing the dispersion of the quantity values being attributed to a measurand*
- *includes components arising from systematic effects, such as components associated with corrections and the assigned quantity values of measurement standards, as well as the definitional uncertainty*

Standard uncertainty (of a measurement)

- *uncertainty of the result of a measurement expressed as a standard deviation*

C-3 Overview Data Processing Steps and Needed Measure Parameters

To derive the ozone partial pressure the basic equation **Eq. E-2-1** ([Chapter 2](#)) is used. This is schematically displayed in **Figure C-3** together with the different data processing steps to apply. The parameters in **Eq. E-2-1** are:

P_{O_3} ozone partial pressure [mPa]

T_P true temperature of the air sampling pump [K]

I_M measured electric current generated in the external circuit of the electrochemical cell [μA]

I_B background current [μA]

Φ_{P0} true gas volume flow rate of the air sampling pump at ground [ml s^{-1}]

η_P pump flow efficiency as a function of pressure,

η_A absorption efficiency for the transfer of the sampled gaseous ozone into the liquid phase,

η_C conversion efficiency of the absorbed ozone in the cathode sensing solution into iodine

where **0.043085** is a constant that is determined by the ratio of the gas constant to two times the Faraday constant.

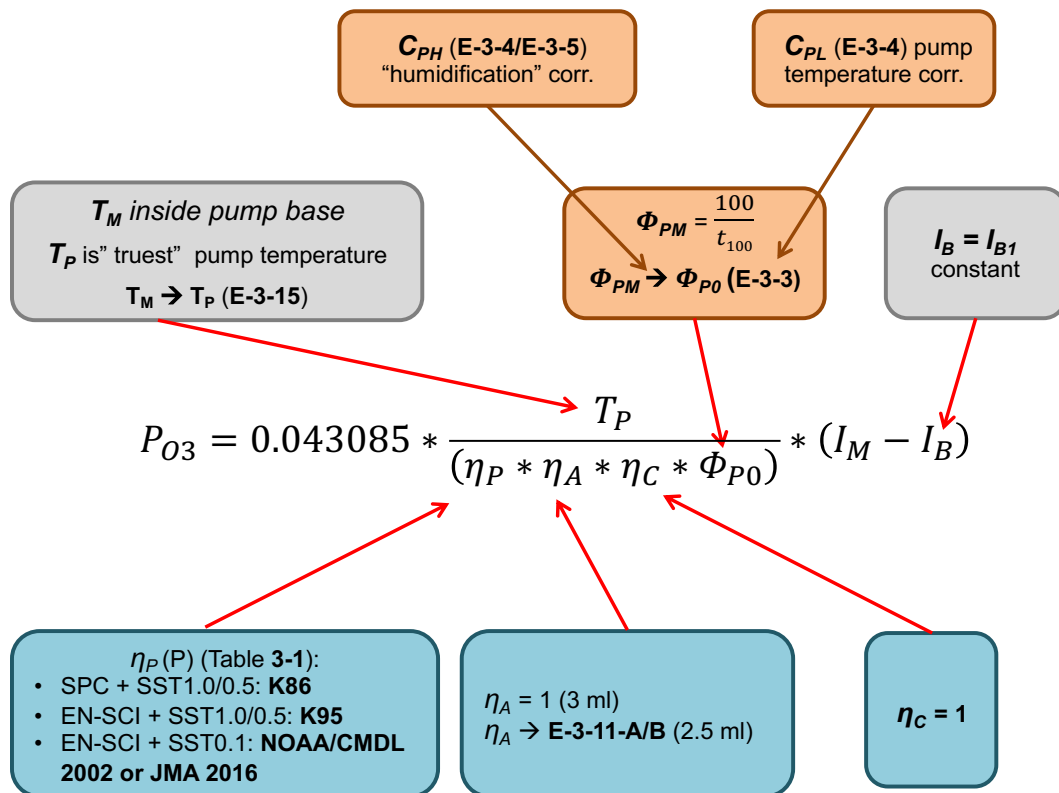


Figure C-3: Overview of the different data processing steps to derive ozone partial pressure with the ECC ozonesonde, applying Eq. E-2-1

To determine the measurement uncertainty of the ozone partial pressure determination with the ECC sonde, **Eq. E-3-1** (Chapter 3) is applied as shown in the schematic overview shown in **Figure C-4**. The term in ϵ_i represents additional random uncertainties due to e.g. uncertainties in the pressure coordinate or time registration of the ozone signal, which in practice are expressed as uncertainties in ozone partial pressure.

List of measured parameters necessary to do the data processing:

Preparation:

- Laboratory conditions: P_{Lab} [hPa], T_{Lab} , [K], RH_{Lab} [%]
- Type of ozone destruction filter (**simple or advanced**) used
- Background currents before and after ozone exposure: I_{B0} and I_{B1} [μA]
- **Time stamp of measured I_{B1} (UTC)**
- Pumpflow rate measured with bubble flow meter or calibrated flow meter: t_{100} (**seconds to pass 100 ml volume**) or Φ_{PM} [ml/sec]
- Response time from 4 to 1.5 μA (τ_{fast})

Launch platform:

- Latitude, Longitude: **Lat, Lon [decimal degrees]**
- Height: H_0 in **m** above sea level

- Ambient air conditions at surface: $P_{Surface}$ [hPa], $T_{Surface}$ [K], $RH_{Surface}$ [%]
- Time stamp (in UTC) of Launch [HH:MM:SS]

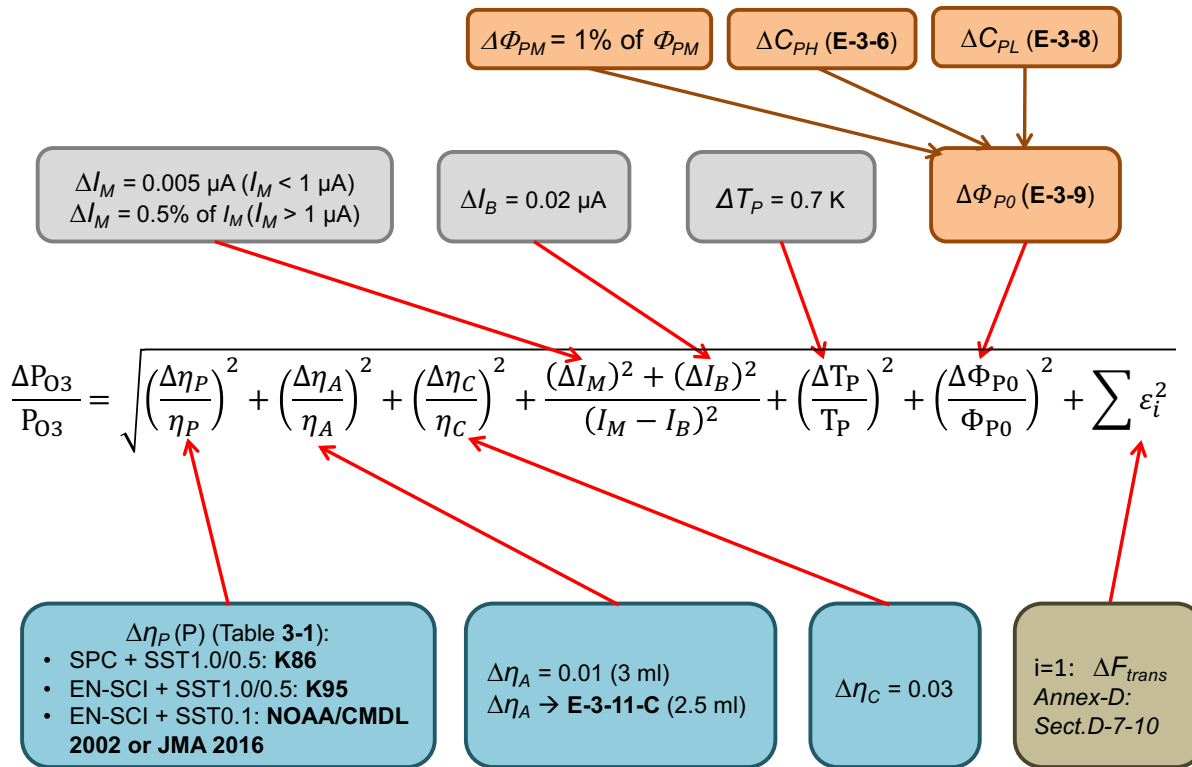


Figure C-4: Overview of the different data processing steps to derive the uncertainty of the ozone partial pressure measured by the ECC sonde, applying Eq. E-3-1

Measured sonde profiles as function of UTC-Time or Flight Time

- UTC-time : t_{UTC} [HH:MM:SS]
- Flight Time: t_F [seconds]
- Ambient Air Pressure: P_{Air} [hPa]
- Ambient Air Temperature: T_{Air} [K6]
- Ambient Air Relative Humidity: RH_{Air} [%6]
- GPS Height: Z [m, above sea level]
- Measured Cell Current: I_M [μA]
- Measured Internal Pump Temperature: T_M [K]

C-4 Flight (i.e. sounding) time as independent profile variable (t_F)

Since digital data recording began, in the 1990s, the actual time in UTC or the flight (i.e. sounding) time (t_F) is recorded and is therefore by definition the primary independent parameter of the measured ozonesonde and radiosonde profile data. This means at the launch the flight time t_F starts at zero and is increasing in the course of the sounding, while the flight time before launch will take accordingly by definition negative values. The flight time is expressed in seconds. The timeline of the different phases of an ozone sounding is illustrated schematically in **Figure C-5**.

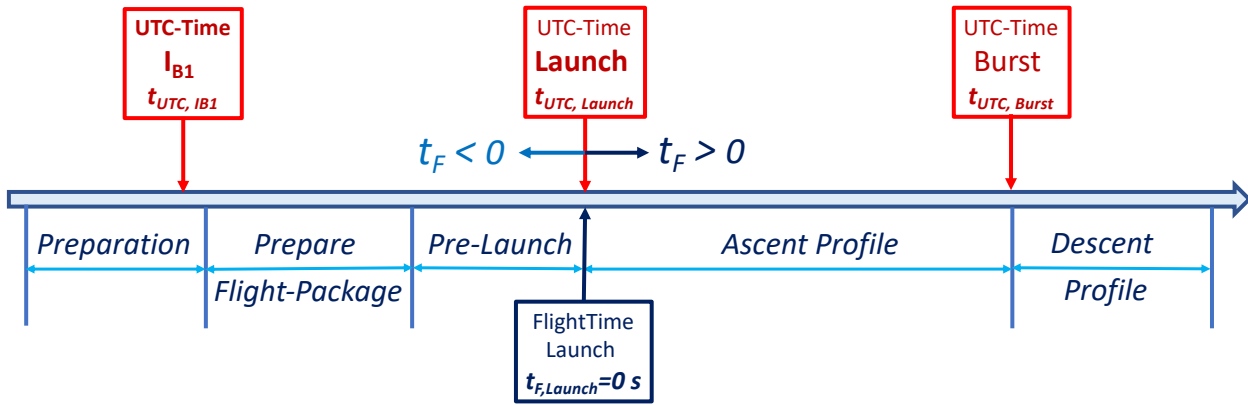


Figure C-5: Timeline showing the different phases of an ozone sounding with UTC-time markers (i) $t_{UTC, IB1}$ (measurement of **IB1, i.e. background current after exposure of ozone) during the preparation; (ii) $t_{UTC, Launch}$; (iii) $t_{UTC, Burst}$. Before launch the flight time $t_F < 0$, at launch $t_F = 0$ and after launch $t_F > 0$**

C-5 Radiosonde: air pressure (P_{Air}), geopotential and geometric height (H & Z)

From the ambient air pressure P , temperature T and relative humidity RH measured with the radiosonde, the in-situ geopotential height H is calculated step-by-step as the cumulative sum of the height difference between two successive pressure levels P_i and P_{i+1} with virtual temperatures $T_{v,i}$ and $T_{v,i+1}$ respectively using **Eq. E-2-6 (Section 2.4.3)**. The virtual temperatures T_v in K can be determined from T and RH using **Eqs. E-2-7 and E-2-8**.

The starting point of **Eq. E-2-6** is the (geometric) height H_0 (in m above sea level) of the launch platform and the surface pressure, temperature and relative humidity at the launch site. These P , T and RH values can be read from local surface sensors at the launch site. In the absence of surface sensors, the pressure, temperature and relative humidity of the radiosonde readings shortly before launch can be used.

When the radiosonde measures GPS geometric height Z (in m above sea level) then the corresponding geopotential height H can be derived applying **Eqs. E-2-9 and E-2-10 (Section 2.4.3)**.

Conversely, the geometric height Z can be derived from the geopotential height H by applying **Eqs. E-2-11 and E-2-12 (Section 2.4.3)**

In the case where the radiosonde only measures GPS altitude, and not pressure, the corresponding air pressure levels can be calculated as follows:

- (a) Determine from geometric height Z the corresponding geopotential height H **Eqs. E-2-9 and E-2-10 (Section 2.4.3)**
- (b) Applying **Eq. E-2-13** to determine the corresponding pressure level P_{i+1} step-by-step by starting with the surface pressure P_0 , virtual temperature T_{v0} and height H_0 at the launch platform.

The corresponding uncertainties of H or Z (radiosonde without GPS altitude) or P_{Air} (radiosonde with GPS altitude) as functions of pressure or altitude can be derived from **Tables 2-3 and 2-4 (Section 2.4.3)**, respectively.

C-6 Ozone pressure (P_{O_3}) derived from measured ECC ozonesonde data

C-6.1 Pump flowrate at ground (Φ_{p0} ; Section 3.3.2)

C-6.1.1 Determination of volumetric flowrate of the gas sampling pump (Φ_{PM})

Φ_{PM} is individually determined at the ground before flight with a bubble flow meter by measuring the time t_{100} needed for a bubble to traverse 100 ml of volume (Φ_{PM} is determined by Eq. E-3-2, Section 3.3.2) or with a commercial flow calibrator.

In both cases the relative uncertainty of Φ_{PM} is 1%:

$$\frac{\Delta\Phi_{PM}}{\Phi_{PM}} = 0.01$$

C-6.1.2 Determination of humidity- and temperature-corrected volumetric pump flowrate (Φ_{p0})

C-6.1.2.1 Correction factor for humidification (C_{PH}) and its uncertainty (ΔC_{PH})

C_{PH} is determined with Eq. E-3-4 (Section 3.3.2) where input parameters are:

P_{Lab} = Laboratory air pressure [hPa]

T_{Lab} = Laboratory air temperature [K]

$e_{sat}(T_{Lab})$ = Saturation vapor pressure [hPa] at T_{Lab} (Section 2.4.3: Eq. E-2-8)

RH_{in} = Relative Humidity of the airflow at the inlet of the cathode cell [%]

When the air intake is through a simple gas (ozone destruction) filter that does not dry the air, the RH_{in} equals RH_{Lab} . If more advanced gas filter techniques are used to obtain "zero ozone", or if purified air is used, then the air will typically be dry, i.e. $RH_{in}=0$.

Where P_{Lab} , T_{Lab} are recorded with uncertainties better than 2 hPa and 1 K, respectively, the uncertainty ΔC_{PH} is vanishingly small.

If RH_{Lab} and T_{Lab} have not been recorded, then an estimate of the range of RH_{Lab} (RH_{Low} to RH_{High}) and T_{Lab} (T_{Low} to T_{High}) is made to calculate C_{PH} (Eq. E-3-5, Section 3.3.2) and its uncertainty ΔC_{PH} (Eq. E-3-6, Section 3.3.2).

C-6.1.2.2 Correction for difference of temperature between pump and laboratory (C_{PL}) and its uncertainty (ΔC_{PL})

A typical temperature difference between the piston (= "truest") temperature of the pump and the ambient laboratory temperature is about 2 K (Section 3.3.2). From Eq. E-3-7 a correction factor C_{PL} for this temperature difference can be determined and the corresponding uncertainty ΔC_{PL} from Eq. E-3-8.

The corrected pump flow rate at ground Φ_{p0} can now be determined from Eq. E-3-3 and its relative uncertainty $\Delta\Phi_{p0} / \Phi_{p0}$ is determined after applying Eq. E-3-9.

C-6.2 Measured cell current (I_M) and its uncertainty (ΔI_M)

The uncertainty of the measured sensor current (I_M) is mainly determined by the uncertainty of the current measurement made by the electronics (current to voltage converter) of the sonde data interface board, which for current interfaces is (Section 3.3.6)

$$\begin{aligned} \Delta I_M &= \pm 0.005 \mu\text{A} && \text{at } I_M < 1.00 \mu\text{A} \\ \Delta I_M &= \pm 0.5\% \text{ of } I_M && \text{at } I_M > 1.00 \mu\text{A} \end{aligned}$$

C-6.3 Background current (I_B) and its uncertainty (ΔI_B)

Following the recommendations in Section 3.3.6, the following background current correction is to be applied:

- I. $I_B = I_{B1}$, i.e. the background current measured 10 min. after the ECC sonde has been exposed to a dose of ozone at a cell current of about 5 μA for 10 min.
- II. **Constant** through the entire sounding profile ((i.e. air pressure independent)
- III. $\Delta I_{B1} = \pm 0.02 \mu\text{A}$ in case of a proper background measurement ($I_{B1} < 0.07 \mu\text{A}$)

Note: To track the evolution of the background current I_{B1} and to estimate the contribution of previous ozone exposure via the slow response to the surface and boundary layer ozone measurements, it is important to know the time span between the measurement of I_{B1} and the launch of the sonde.

C-6.4 Pump temperature (T_P) and its uncertainty (ΔT_P)

The (internal) pump temperature T_M measured by a thermistor in a hole drilled into the Teflon block of the pump has to be corrected to approach the best representative pump temperature T_P (Section 3.3.8) by applying Eq. E-3-15.

The corresponding overall uncertainty $\Delta T_P = 0.7 \text{ K}$

C-6.5 Absorption efficiency (η_A) and its uncertainty ($\Delta \eta_A$)

Depending on the volume of sensing solution in the cathode cell the following recommendations for the absorption efficiency η_A and its uncertainty $\Delta \eta_A$ are made (Section 3.3.4):

- 1) Cathode cells charged with 3.0 cm^3 of cathode solution

$$\eta_A = 1.00 \quad \text{and} \quad \Delta \eta_A = 0.01 \quad (\text{Eq. E-3-10})$$

- 2) Cathode cells charged with 2.5 cm^3 of solution require a small correction as a function of ambient air pressure P_{Air}

$$\eta_A: \text{Eq. E-3-11-A/B} \quad \text{and} \quad \Delta \eta_A: \text{Eq. E-3-11-C}$$

C-6.6 Pump efficiency (η_P) and its uncertainty ($\Delta \eta_P$)

At ambient air pressures $< 100 \text{ hPa}$ the efficiency of the gas sampling pump degrades, as a function of the ambient pressure. For the two different ECC sonde types, the recommended efficiency tables should be used, depending on the sensing solution type (Section 3.3.3):

- a) **Komhyr 1986 (K86-Efficiency) for SPC-6A sondes with SST1.0 or SST0.5;**
- b) **Komhyr 1995 (K95-Efficiency) for ENSCI sondes with SST1.0 or SST0.5;**

c) NOAA/CMDL 2002 or JMA 2016 for ENSCI sondes with SST0.1.

The corresponding pressure dependent pump efficiencies η_p and their uncertainties $\Delta\eta_p$ as a function of ambient air pressure P_{Air} are listed in **Table 3-1 (Section 3.3.3)**.

C-6.7 Conversion efficiency (η_c) and its uncertainty ($\Delta\eta_c$)

In **Section 3.3.5**, for the conversion efficiency and its uncertainty, the following constant values are recommended:

$$\eta_c = 1.00 \quad \text{and} \quad \Delta\eta_c = 0.03$$

C-6.8 Ozone pressure P_{O3} by ECC sonde and overall uncertainty ΔP_{O3}

With the information given in the previous sections, the ozone partial pressure and its related uncertainty can be directly calculated with the equations given in the beginning of this appendix, **Eq. E-2-1** and **Eq. E-3-1**.

In case a station is deploying another combination of sonde type and SST than either SP6A-sonde with SST1.0 or ENSCI sonde with SST0.5, they need to apply a corresponding transfer function $F_T(P_{Air})$ to scale the P_{O3} sonde measurements to the common standard performance of SPC/SST1.0 and ENSCI/SST0.5. The methodology is described in detail in **Annex D: Section D-7.10**. The use of a transfer function F_T adds an extra uncertainty ΔF_T into **Eq. E-3-1 (Figure C-4)**, whereby

$$\epsilon_1 = \frac{\Delta F_T}{F_T} \quad [E-C-1]$$

C-6.9 Ozone volume mixing ratio μ_{O3} derived from ECC sonde measurements and uncertainty $\Delta\mu_{O3}$

The volume mixing ratio of ozone μ_{O3} is derived from

$$\mu_{O3} = \frac{P_{O3}}{P_{air}} \quad [E-C-2]$$

And the corresponding relative uncertainty is

$$\frac{\Delta\mu_{O3}}{\mu_{O3}} = \sqrt{\left(\frac{\Delta P_{O3}}{P_{O3}}\right)^2 + \left(\frac{\Delta P_{Air}}{P_{Air}}\right)^2} \quad [E-C-3]$$

C-7 Total ozone column: Total ozone normalization

Although normalization of ECC sonde profiles is not recommended, the normalization factor to a co-located Dobson or Brewer spectrophotometer total column ozone measurement provides a useful indicator for the quality of ozonesonde profile data (**Section 3.3.11**).

C-7.1 Ozone column by ozonesonde (Ω_s)

The ozone column from the sonde profile can be found by integrating the ozone partial pressure or concentration from the ground until the burst level, making use of **Eq. E-3-19**. The ozone concentrations in molecules cm^{-3} in this formula are obtained from the ozone partial pressure values through **Eq. E-3-21**. As at pressures smaller than 10 hPa, the solutions in the electrochemical cells often either freeze or evaporate/boil, rendering ozone measurements obtained by ozonesondes at these low pressures less accurate. Therefore, we recommend integration of the profile only to 10 hPa, for burst pressure levels inferior to this value.

The uncertainty of the integrated ozone column amount can be found by integrating the ozone concentration uncertainties (**Eqs. E-3-20** and **E-3-21**).

C-7.2 Residual ozone column above burst point of ozonesonde (Ω_R)

The residual ozone column above the burst point of the sounding balloon (or at 10 hPa) to the top of the atmosphere, **Eq. E-3-22**, should be derived from the satellite climatology of *McPeters and Labow* [2012], which also provide uncertainties for those residual ozone columns.

C-7.3 Total ozone column by Dobson or Brewer spectrophotometer (Ω_c)

The total column measurement of a co-located Dobson or Brewer spectrophotometer can be used as reference for the calculation of the total ozone normalization factor for the ozonesonde measurements. Ideally, a measurement close to the ozone sounding time should be chosen, and direct sun measurements are to be preferred above zenith sky observations. The relative uncertainty of those total ozone measurements is around 2% [*Fioletov et al.*, 2008]. Alternatively, if no co-located ground-based total column ozone measurements are available at the ozonesonde launch site, satellite total ozone column station overpass retrievals can be used, from e.g. OMI, OMPS, GOME-2, etc, with a similar uncertainty estimate of 2% [*Garane et al.*, 2018]

C-7.4 Total ozone normalization factor (N_T)

The total ozone normalization factor (N_T) is then defined as the ratio of the independent TCO measurement (Ω_c) and the TCO derived from the ozonesonde profile (Ω_T), see **Eq. E-3-17**, with uncertainty as defined in **Eq. E-3-2**

Practical Guidelines to Homogenize Historical Ozonesonde Records**Lead authors**

**Roeland Van Malderen (RMI, Uccle, Belgium),
Herman G.J. Smit (FZ-Jülich/IEK-8, Jülich, Germany)**

Table of Contents

D-1	Introduction	145
D-2	Principles of the Homogenization of Ozonesonde Data	145
D-3	Strategy of the O ₃ S-Homogenization Process	146
	D-3.1 In Time (O ₃ -trends at individual stations)	146
	D-3.2 Testing for Consistency	146
D-4	Preparatory Work on O ₃ S Data Homogenization	147
D-5	Reprocessing of O ₃ S Data	148
D-6	Validation of O ₃ S Data	148
D-7	General Guidelines for Homogenization of O ₃ S-Data	150
	D-7.1 Radiosonde: Correction Pressure Bias	150
	D-7.2 Flight (i.e. sounding) time as independent profile variable (t_F)	151
	D-7.3 Pump flowrate at ground (Φ_{PO})	151
	D-7.4 Measured cell current (I_M)	152
	D-7.5 Background current (I_B)	152
	D-7.6 Pump temperature (T_P)	154
	D-7.7 Absorption efficiency (η_A): Limitations for 2.5 cm ³ cathode sensing solution	160
	D-7.8 Pump efficiency (η_P)	161
	D-7.9 Conversion efficiency (η_C)	161
	D-7.10 Transfer Function F_T : Impact of Different Types of Sensing Solutions and Sondes	161
	D-7.11 Total Ozone Normalization	163
D-8	Storage of Data	164

D-1 Introduction

In 2010 within the SPARC-IGACO-IOC Initiative on "Past Changes in the Vertical Distribution of Ozone" (SI2N) (SPARC-News Article by Neil Harris, Johannes Staehelin and Richard Stolarski, Sept 2010: http://igaco-o3.fmi.fi/VDO/files/Harris_ozone_trends_initiative.pdf) the "Ozone Sonde Data Quality Assessment (O₃S-DQA)" activity was initiated with the following two major objectives:

1. Homogenization of ozone sonde data sets to be used for WMO/UNEP ozone assessment reports: Goal to reduce uncertainty from 10%–20% down to 5%–10% (focus on transfer functions)
2. Documentation of the homogenization process and the quality of ozonesonde measurements generally to allow the recent record to be linked to the older records.

In 2011–2012, the O₃S-DQA Panel of ozonesonde experts reviewed more than 40 years of ozonesounding practice in the global ozonesonde network. The Panel identified several instrumental and preparation changes of the ECC ozonesonde types that had been made which introduced significant inhomogeneities in the long-term ozonesonde records. The Panel, therefore, also formulated correction functions to resolve these artefacts. The corrections were compiled into a document giving guidelines for the homogenization of long-term ozonesonde data in the scope of the SI2N initiative ("SI2N/O₃S-DQA Activity: Guidelines for Homogenization of Ozone Sonde Data", <https://www.wccos-josie/o3s-dqa/>).

Two important aspects of the homogenization are to estimate the expected uncertainties of the measurements and to document in detail the reprocessing of the long-term ozonesonde records of the participating stations. At present, mid-2021, about half of the global ozonesonde stations have finished the homogenization of their time series: the Southern Hemispheric Additional Ozonesondes (SHADOZ) network [*Witte et al.*, 2017, 2018; *Thompson et al.*, 2017; *Sterling et al.*, 2018], the Canadian network [*Tarasick et al.*, 2016], the US network [*Sterling et al.*, 2018], and some individual sites [*Van Malderen et al.*, 2016; *Witte et al.*, 2019].

The purpose of these guidelines is to harmonize and update the "SI2N/O₃S-DQA Activity: Guidelines for Homogenization of Ozone Sonde Data" as formulated by the end of December 2012 now with the new guidelines for ozonesonde data processing as formulated in this GAW Report ([Annex C](#)).

D-2 Principles of the Homogenization of Ozonesonde Data

The homogenization of ozonesonde data serves three major needs:

1. removal of all known inhomogeneities or biases in an ozonesonde time series due to changes in equipment, operating procedures or processing.
2. Strengthen the consistency within the ozonesonde network by providing standard guidelines for data processing steps, now (see [Annex C](#)) and in the past (this Annex).
3. Provide an uncertainty estimate for each ozone partial pressure measurement in the profile.

The standard for the current data processing and uncertainty estimation calculation has been summarized in [Annex C](#) and relies on the basic **Eqs. E-2-1** and **Eq. E-3-1**. Implementing the data processing in [Annex C](#) ensures that the processed ozonesonde time series are traceable to the reference ozone photometer OPM in the simulation chamber of the World Calibration Centre for Ozonesondes in Jülich, with estimated systematic uncertainties of less than 5%. In this Annex, we provide only the additional steps that might be necessary to apply to historical ozonesonde data, in order to align them with the current processing, and so to the OPM as well.

Looking at **Eq. E-2-1**, these are the parameters that might need to be homogenized:

- Flight (i.e. sounding) time as independent profile variable (t_F)
- Radiosonde: air pressure (P_{Air}), geopotential and geometric height (H & Z):
- Pump flowrate at ground (Φ_{P0})
- Measured cell current (I_M)
- Background current (I_B)
- Pump temperature (T_P)
- Absorption efficiency (η_A)
- Pump efficiency (η_P)
- Conversion efficiency (η_C)
- Different sensing solutions and sonde type: Transfer functions (F_T)

D-3 Strategy of the O₃S-Homogenization Process

D-3.1 In Time (O₃-trends at individual stations)

Each station will homogenize its O₃S-record individually:

- Following guidelines prescribed by O₃S-DQA
- Using transfer functions based on dual soundings
- Collaborating with O₃S-DQA-experts

D-3.2 Testing for Consistency

- Total ozone normalization factors before and after homogenization
- Comparison with other O₃ profiling instrument at O₃S-site (e.g. NDACC)
- Troposphere-UTLS: MOZAIC/IAGOS-O₃
- Stratosphere: Vertical profiles from satellites (e.g. MLS)

Figure D-1 shows the scheme of the homogenization process. It is essential that during the entire homogenization process each station should collaborate with an O₃S-DQA expert, for consultation and for recommendations to the Station PI along the guidelines formulated by the O₃S-DQA Panel.

Storage of reprocessed O₃S-data:

1. Data format: In the most recent data format of the WOUDC (**Section 4.3.4**)
2. It is important that each station provides good documentation of the reprocessing (including decisions or compromises made) after reprocessing.

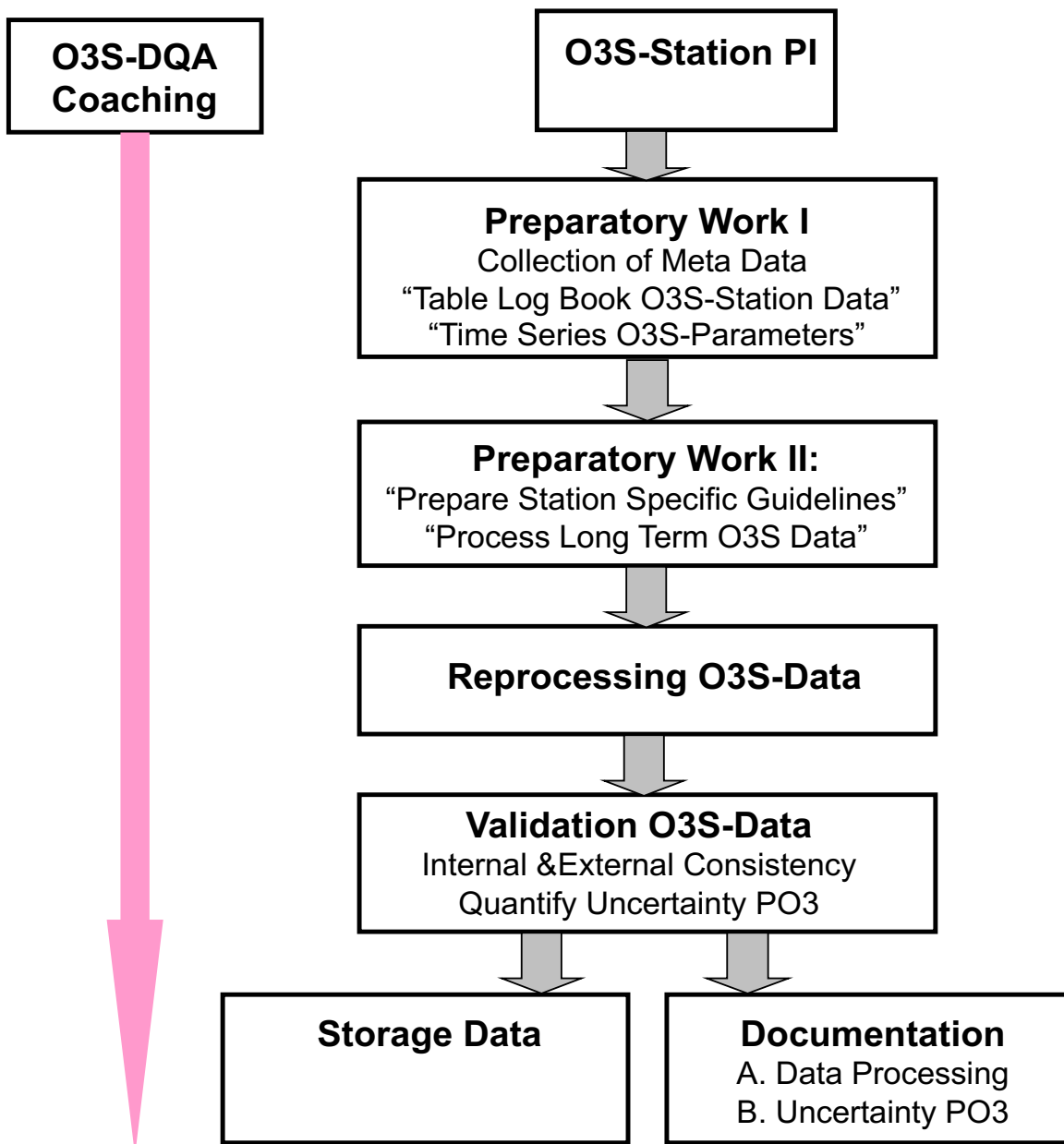


Figure D-1: Scheme of the Homogenization Process of Long-Term O₃S-Data Per Station

D-4 Preparatory Work on O₃S Data Homogenization

Preparatory Work Phase I:

As a first step, in advance of starting the reprocessing of the long-term O₃S-records each O₃S-Station should do "Preparatory Work I":

- (a) Create "**Table Logbook O₃S-Station Data**" (See **Table D-1** template below) with the major specifications of the O₃S-Station with time flags in order to track when changes have been made during long-term operation
- (b) Assemble "**Time Series O₃S-Parameters**" (in electronic form) of:
 1. Total ozone normalization factor ($N_T(t)$);
 2. Total ozone column by spectroscopic instrument (e.g. Dobson, Brewer or other instrument) ($\Omega_C(t)$);

3. Residual ozone column above burst altitude ($\Omega_R(t)$);
4. Background current ($I_{B0}(t)$, $I_{B1}(t)$, $I_{B2}(t)$) determined on the flight day;
5. Pump flow rate ($\Phi_P(t)$) obtained from flight preparation;
6. Pump temperature in-flight (T_P at launch and at $P_{Air} = 400, 200, 100, 50, 25$ hPa).

Preparatory Work Phase II:

Based on information collected, each station should consult an O₃S-DQA expert to compile the general guidelines for homogenization into guidelines specific for that individual station.

D-5 Reprocessing of O₃S Data

After completing these station-specific guidelines, the actual reprocessing of the data can be started. In the reprocessing and eventual revision of data, the data processing prescribed in [Chapter 3](#) and [Annex C](#) should be followed as closely as possible. In the case of a deviation from the prescribed SOPs, the additional uncertainty contribution to the overall uncertainty should be estimated to the extent possible.

Realistically, it is expected that for each station not all the recommended reprocessing tasks can be fulfilled. Even in these non-fulfilled cases, there should always be an estimate of the specific instrumental/procedural contribution to the overall uncertainty. The overall uncertainty will be included as an extra column in the reprocessed data. Further, a crucial aspect of the homogenization process is the documentation (i.e. logbook) of the procedures that have been followed.

D-6 Validation of O₃S Data

After the O₃S-Data have been reprocessed, quality checks must be done for internal consistency, but also for external consistency through comparison with other ozone profiling platforms, which should be achieved through collaborations with other investigators and O₃S-DQA experts. A final outcome of this validation process should be a detailed documentation of the reprocessing. It is essential that throughout the entire homogenization process individual error sources and their contributions to the uncertainty of the ozonesonde partial pressure profile data should be looked for, quantified and documented. An important challenge will be to quantify the total uncertainty of the measured ozone partial pressure as part of the long-term vertical ozonesonde profile data (entered as an additional column).

Table D-1: Template of "Table Logbook O₃S-Station Data" with major specifications of the O₃S-Station including time flags when changes have been done during long-term operation

Item	Remarks
Sensing Solution Type (SST)	For ECC sonde types: SST1.0%, SST0.5%, SST0.1% or any other SST (See Table 2-2)
Ozonesonde Type	Model Type and Manufacturer Do you have ozonesonde identification information: e.g. serial number-flight number?
Radiosonde Type	Model Type and Manufacturer Do you have radiosonde identification information e.g. serial number-flight number?

Item	Remarks
Data Interface Type	Electronic board interfacing ozone sonde and radiosondes Model Type and Manufacturer Do you have interface identification information e.g. serial number-flight number?
Background Current	<ul style="list-style-type: none"> • Which background current(s) have been recorded and are available and which was used? • Typical background currents (see Smit and ASOPUS Panel, 2011) <ul style="list-style-type: none"> ○ I_{BO}: Before exposure to ozone @ laboratory ○ I_{B1}: After exposure to ozone @ laboratory ○ I_{B2}: @ launch site • Or in case of any other background current please describe briefly how this was determined.
Total Ozone Normalization Factor	Factor available? How determined? Applied to measured vertical ozone sonde profile?
Total Ozone Measurement	Type of spectroscopic device measuring total ozone column during soundings
Residual Ozone Column (above balloon burst altitude)	Method of determining residual ozone CMR: Constant Mixing Ratio SRC: Residual from Satellite Climatology (e.g SBUV or other)
Temperature Pump Location	Pump temperature measured? 1. If Yes: location? <ul style="list-style-type: none"> a. Int = Internal: in Teflon block of pump b. Ext = Externally attached to pump or its tubings (taped or epoxied) c. Box = Location inside the Styrofoam box of O₃ 2. If No: What pump temperature has been assumed/estimated?
Pumpflow Measurement	Bubble flow meter or other type In case bubble flowmeter: Any corrections done for "wetting effect" (see Section 3.3.2)?
Source of Zero Ozone	<ul style="list-style-type: none"> • What kind of ozone removal techniques have been used to produce ozone-free air to record background current(s)? • If ozone destruction/absorption filter has been used: Can you describe the type of filter used?

Item	Remarks
Laboratory Air Conditions (PTU): Pressure (P) Temperature (T) Relative Humidity (U)	Ambient PTU conditions at location of preparation room when measuring pump flow rate. Have they been recorded? 1. If Yes: P, T & U data available? 2. If No: Can you give typical range of ambient air P, T and U in O ₃ S preparation room: approximate average plus/minus one standard deviation
Data Reduction Method	Using standard formula (Eq. E-2-1)? If not, describe deviations. What kind of corrections applied: 1. Pumpflow efficiency as function of pressure: Komhyr 1986, Komhyr 1995 or any other table? 2. Background correction: which background current I _B has been used (incl. pressure dependent or constant). 3. Total ozone normalization applied (Yes/No) 4. Any other correction(s)?
Software Data Reduction	Using commercial software package (e.g. Vaisala): Is there a record of version number?
Ozone cell current signal	Original (raw) ozone cell current available. Yes/No?
O ₃ S-Preparation Unit	Manufacturer and Type
Any other issues	

D-7 General Guidelines for Homogenization of O₃S-Data

Based on the information collected in Preparatory Phase I (**Table D-1**), the Station PI, possibly together with an O₃S-DQA expert, will compile the general guidelines for homogenization into guidelines specific for each station individually. The general guidelines addressing different instrumental/procedural aspects are described in this Chapter.

D-7.1 Radiosonde: Correction Pressure Bias

Rationale

Errors in radiosonde pressure or temperature will imply corresponding errors in calculated geopotential heights, causing measured ozone concentrations to be assigned to incorrect altitudes and pressures. This is potentially an important issue for the derivation of trends, as radiosonde changes may therefore introduce vertical shifts in the ozone profile, and apparent changes in ozone concentration at a given height. A number of different radiosonde designs, from several manufacturers, have been used in the global observing network over the last five decades. This history will in general vary by country, agency or even by station, and so will need to be documented for each station individually.

Temperature differences between the VIZ sonde, used widely in the 1980s and early 1990's, and the Vaisala RS-80 sonde, adopted subsequently by several agencies, including NOAA and Environment Canada, are well documented. The VIZ sonde showed a warm bias in the daytime by as much as 2 °C [Richner and Philips, 1981; Luers and Eskridge, 1995; Wang and Young, 2005]. From simultaneous measurements made during a WMO intercomparison in 1985, Schmidlin [1988] estimates that this bias contributed 17m at 50hPa and 71m at 10hPa to the

difference in geopotential height estimates from the two sondes. This corresponds to a shift of $\sim 1\%$ at 10hPa (31km), but less than 0.1% at 50hPa (21km). Nevertheless, statistical comparisons show that the switch from VIZ to Vaisala RS-80 at US stations introduced a shift of as much as 120m at 50hPa in the daytime [Elliot *et al.*, 2002].

Pressure errors appear to have a much larger effect. Comparisons with radar measurements of height showed the VIZ to be high, relative to the radar (and the Vaisala), in daytime by $\sim 150\text{m}$ at 20hPa and up to 500m at 10hPa [Schmidlin, 1988; Nash and Schmidlin, 1987], while at night both VIZ and Vaisala RS80 calculated geopotentials were low by $\sim 100\text{m}$ at 20hPa, and $\sim 150\text{m}$ at 10hPa. These daytime differences correspond to ozone differences of $\sim 2\%$ and $\sim 7\%$ at 20 hPa and 10hPa, respectively. The effect of pressure errors is most significant at higher altitudes: a 1hPa offset will introduce a geopotential height error of 63m at 100hPa, 120m at 50hPa, and over 300m at 20hPa; these correspond to ozone differences of 0.25%, 0.5% and $\sim 4\%$ respectively.

Pressure errors also seem more variable, Local noon flights during the same intercomparison show much smaller height differences between the VIZ and Vaisala; a separate investigation at Uccle [De Muer and De Backer, 1992] found that VIZ sondes launched between 1985 and 1989 calculate altitudes too *low* relative to a radar: up to 1410m at 30km and up to 870m at 15km. They estimate a corresponding ozone error of 14% at 30km. At 15km, 870m corresponds to an ozone error of $\sim 4\%$ but implies a rather surprising average pressure error of 17hPa.

The Vaisala RS-92 has replaced the RS-80. Comparison flights with GPS tracking show that the pressure sensor of the RS-92 sondes gives more accurate heights than the RS80; differences from the GPS are small except for sondes produced before July 2004 [Steinbrecht *et al.*, 2008; Nash *et al.*, 2006]. RS80 sondes, however, were found to be low by $\sim 20\text{m}$ in the troposphere, and high by 100m at 10hPa [Steinbrecht *et al.*, 2008; also da Silveira *et al.*, 2006].

Unfortunately, intercomparison experiments do not tell the whole story, as not all manufacturing changes are advertised by a change in model number. For example, Steinbrecht *et al.* [2008] note systematic differences between batches of RS-92 sondes produced before July 2004. It is therefore recommended that stations document, in as much detail as possible, changes in radiosonde type and the expected systematic differences in the ozone profile. These are probably small below 50hPa. At higher altitudes, it may be possible to correct offsets in the ozone record by statistical methods.

Recommendations:

No corrections but good documentation of radiosonde type(s) deployed (incl. time flags) is required to estimate/quantify the contribution of the radiosonde to the overall uncertainty of the ozonesonde performance. Also, a detailed documentation (incl. references) of eventual known bias effects in pressure and/or temperature readings of the radiosonde at different pressure levels is recommended.

D-7.2 Flight (i.e. sounding) time as independent profile variable (t_F)

In modern ozonesoundings, the flight time t_F is the primary (independent) sounding variable. However, when flight time is not part of the sounding data, a generic flight time could be calculated from the height of the sonde above the ground and assuming an average ascent velocity w_{Asc} of the sonde of 5 m s^{-1} .

$$t_F(H) = \frac{H-H_0}{w_{Asc}} \quad [\text{E-D-1}]$$

D-7.3 Pump flowrate at ground (Φ_{p0})

See [Annex C: Section C-6.1](#)

D-7.4 Measured cell current (I_M)

The uncertainty ΔI_M in the measured cell current I_M of the analog era (1970s-1980s) was taken as 3% of the measured cell current when $>1 \mu\text{A}$ and $0.03 \mu\text{A}$ for cell currents $<1 \mu\text{A}$ [Komhyr and Harris, 1971, Sterling et al., 2018]. In the more recent era, when using digital interfacing electronics, ΔI_M improved significantly to 1% when $I_M >1 \mu\text{A}$ and $0.01 \mu\text{A}$ for $I_M <1 \mu\text{A}$ for the period 1990–2010 [GAW Report No. 201, 2014], while currently, for the period after 2010, ΔI_M has further improved, to 0.5% when $I_M >1 \mu\text{A}$ and $0.005 \mu\text{A}$ for $I_M <1 \mu\text{A}$ (**Section 3.3.6, Eqs. E-14-A/B**).

D-7.5 Background current (I_B)

Rationale:

The origin of the background current of the ECC sonde has been long not well understood [Vömel and Diaz, 2010]. In literature, several sources have been mentioned. Komhyr [1969, 1986] assumed the background current was primarily caused by reaction with oxygen, and hence would decline with ambient air (i.e. oxygen) pressure and thus be pressure dependent; however, Thornton and Niazy [1982] and other investigators have shown that the background current is independent of oxygen. Since the mid-1970s the electrode in the cathode cell has been preconditioned by the manufacturer in such a way that oxygen interferences can be excluded. Thornton and Niazy [1982, 1983] suggested that the source of the background current is the reduction of triiodide normally present in the cathode solution. They explained time variations in the background current by the slow rates of solution mass transport and of heterogeneous electron transfer for triiodide. Thornton and Niazy [1983] found a pressure dependent factor in the background current below 30 hPa, but its impact on the O_3S measurements in the middle stratosphere is rather small.

Recent studies treat the background current as primarily due to previous exposure to ozone [**Section 3.3.6**; Tarasick et al., 2021; Vömel et al., 2020], caused by a slow reaction pathway of ozone with buffer components. This may be an improvement on the current recommendation.

At tropical sites (and perhaps other locations with high atmospheric moisture), background measurements using the standard ozone destruction filter to obtain ozone-free air may give very unrepresentative values (high backgrounds). It is postulated that moisture deactivates the ozone destroying sites in the “charcoal- or CuO/MnO_2 - based” filters. In the period ~ 1980 –1990, measured backgrounds at tropical sites fall in the range 0.1 – $0.7 \mu\text{A}$ at sites such as Hilo and Samoa. After 1990, backgrounds are systematically lower, but still may have been improperly measured when using the standard ozone destruction filter. In background current measurements made at Jülich with purified zero air, a definite change in the background current characteristics of the SPC-5A were noted beginning in 1990. Earlier results gave background currents after exposure to ozone generally in the range 0.15 – $0.25 \mu\text{A}$. Measurements made in 1990 and later gave values generally in the range 0.06 – $0.10 \mu\text{A}$. Properly measured background currents measured since the mid-1990s from both ENSCI and SPC are generally very low less than $0.05 \mu\text{A}$ (**Table D-3**).

The treatment of background current and its changes with time will have an impact particularly on tropospheric ozone amounts. This could be a particular problem in the tropics where tropospheric ozone levels are often lower, and problems with the standard ozone filter (also used in various test units) are largest.

Impacts on ozone in the stratosphere may arise from assuming an oxygen dependent background as done by some standard commercial processing routines. Up to now, many of the ozone processing routines used a “pressure declining background” formulation, in particular for SPC ozonesondes, that essentially reduce the background to zero in the stratosphere.

Table D-3: Survey of average background current ($\pm 1\sigma$) before and after exposure of ozone obtained during pre-flight preparations of ECC sondes “flown” during JOSIE 1996, 1998 and 2000 [Smit et al., 2007], BESOS 2004 [Deshler et al., 2008], JOSIE 2009 & 2010. The background currents were recorded before and after pumping for 10 minutes air with ozone (150–200 ppbv) through the sensor whereby each time before the background current was measured the sensor was flushed for 10 minutes with ozone-free air (purified air)

ECC Sonde Type		ENSCI-Z		SPC-6A	
JOSIE	Sensing Solution Type	Background Current Before O ₃ -Exposure [μ A]	Background Current After O ₃ -Exposure [μ A]	Background Current Before O ₃ -Exposure [μ A]	Background Current After O ₃ -Exposure [μ A]
1996	SST1.0	0.05 \pm 0.01	0.07 \pm 0.02	0.02 \pm 0.01	0.07 \pm 0.01
1998	SST1.0	0.05 \pm 0.02	0.11 \pm 0.03	0.03 \pm 0.02	0.11 \pm 0.01
2000	SST1.0	0.02 \pm 0.03	0.06 \pm 0.05	0.02 \pm 0.01	0.05 \pm 0.02
2000	SST0.5	0.02 \pm 0.02	0.05 \pm 0.02	0.00 \pm 0.01	0.03 \pm 0.02
2000	SST2.0	0.02 \pm 0.02	0.06 \pm 0.03	0.02 \pm 0.01	0.05 \pm 0.03
BESOS 2004	SST1.0	0.00–0.02	0.05–0.06	0.00–0.01	0.04–0.07
BESOS 2004	SST0.5	0.00–0.01	0.02–0.03	-0.02–0.02	0.01–0.02
2009	SST1.0	0.02 \pm 0.01	0.05 \pm 0.01	0.01 \pm 0.01	0.04 \pm 0.01
2009	SST0.5	0.02 \pm 0.01	0.04 \pm 0.01	0.01 \pm 0.01	0.03 \pm 0.01
2010	SST1.0	0.02 \pm 0.01	0.04 \pm 0.02	0.00 \pm 0.02	0.04 \pm 0.01
2010	SST0.5	0.01 \pm 0.01	0.02 \pm 0.01	0.00 \pm 0.03	0.03 \pm 0.01

Recommendations:

1. *With properly measured backgrounds, the current standard operating procedure of subtracting the full background current from the measured ozone current should be followed. For all ECC sondes flown, at least since 1975, there is no oxygen (i.e. pressure) dependence of the background current. A constant background current correction throughout the entire vertical O₃S-profile should be applied.*
2. *Unrealistic high background currents may be caused by a small leakage of anode cell solution through the ion bridge. However, from stations using purified air it has been clearly shown that this only happens very occasionally (less than 1 out of 100 launches). Impurities of chemicals or distilled water may also cause larger*

background currents, but then in most cases the sonde will also show a poor time response. Usually such sondes would also not pass the time response test of the pre-flight preparation.

3. Where "unrealistic" backgrounds were measured during a portion of the record, an average background value should be applied for reprocessing the data. This average value can be determined by inspecting measured backgrounds and determining a lower envelope of the measurements. Or alternatively, if more representative background measurements have been made during a portion of the record, the mean value from this period might be extrapolated to another period with poor measurements for the reprocessing. The background ranges suggested in the discussion above can be used as a guideline for determining the background current for correction.

General guidelines to obtain proper background current $I_B = I_{B1}$:

- A. Stations using purified air: I_B -climatology delivers a range of representative $I_{B,Mean} \pm \sigma_{IB}$
 - B. Stations using simple ozone destruction filters: If station I_B exceeds $I_{B,Mean} + 2\sigma_{IB}$, then I_B should be replaced by the more representative climatological value of $I_{B,Mean}$ with larger uncertainty $2\sigma_{IB}$
4. It is important that the contribution of the selected background correction to the overall uncertainty of the measured ozone concentration is estimated based on experimental evidence.

D-7.6 Pump temperature (T_P)

Rationale:

The measurement of pump temperature is required to properly account for the amount of air passing through the pump into the ECC sensor cell. The best representative pump temperature (applied in formula **Eq. E-2-1**) should be inside the volume of the cylindrical housing of the moving piston of the pump. Beginning with the introduction of the ENSCI-Z sonde in 1995 a thermistor was mounted in a hole drilled in the pump body. This was adopted by SPC in 1996 in the 6A model of the sonde. Currently all implementations of the ozonesonde measure the internal pump base temperature $T_{PM} = T_{P,Int.}$ However, before the mid-1990s the locations of pump temperature measurements have changed several times, introducing inhomogeneities in the ozone sounding record. Basically 5 different cases of pump temperature measurements have been identified and characterized here. The temperature corrections made for these cases are all referred to approximate the corresponding internal pump base temperature $T_{P,Int.}$

Case I: Box temperature measurements by thermal rod in analog sounding systems

In the 1960s to the end of the 1980s, in the initial configuration of the ECC ozonesonde, flown with analog radiosonde and paper chart recording system, the box temperature ($T_{P,Box}$) was measured in lieu of the pump base temperature ($T_{P,Base}$). This was a standardized system with the rod thermistor mounted at the bottom of the electronics circuit board near the base of the ozonesonde housing. This arrangement, which has been used for ECC-2A, ECC-3A and ECC-4A sonde types, appears to have produced a consistent relationship between the "box" temperature ($T_{P,Box}$) and the pump base (body) temperature ($T_{P,Base}$) [Komhyr and Harris, 1971] as shown in **Figure D-2**.

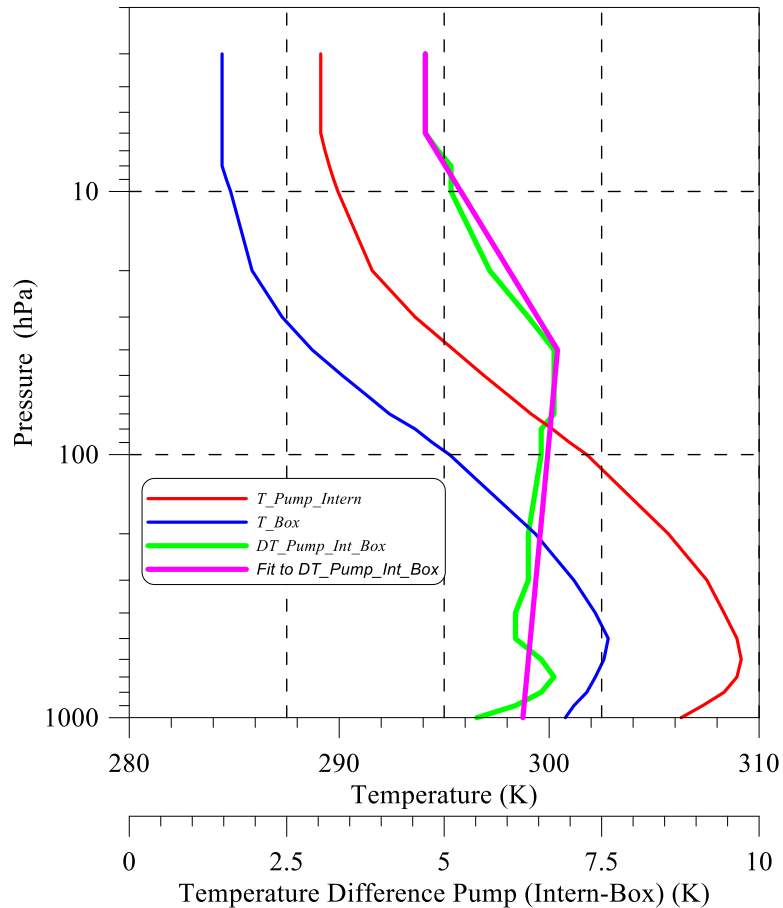


Figure D-2: Relation box temperature ($T_{P,Box}$) and internal pump temperature ($T_{P,Base}$) of ECC-2A, ECC-3A, and ECC-4A ozone sonde types manufactured in 1970's and 1980's.

Source: Komhyr and Harris, 1971

The difference DT_{PBB} between $T_{P,Box}$ and $T_{P,Base}$ can be approximated as a function of ambient air pressure by:

$$T_{P,Base} - T_{P,Box} = DT_{PBB}(P_{Air}) = 7.43 - 0.393 \text{Log}_{10}(P_{Air}) \quad \text{at } P_{Air} \geq 40 \text{ hPa} \quad [\text{E-D-2A}]$$

$$T_{P,Base} - T_{P,Box} = DT_{PBB}(P_{Air}) = 2.7 + 2.6 \text{Log}_{10}(P_{Air}) \quad \text{at } 6 < P_{Air} < 40 \text{ hPa} \quad [\text{E-D-2B}]$$

$$T_{P,Base} - T_{P,Box} = DT_{PBB}(P_{Air}) = 4.5 \quad \text{at } P_{Air} \leq 6 \text{ hPa} \quad [\text{E-D-2C}]$$

The uncertainty ΔDT_{PBB} of this approximation is assumed to be ± 1 K.

Case II: Box temperature measurements by thermistor in digital sounding systems

Beginning with the use of digital ozonesonde electronics in ~ 1990 , the capability of measuring the temperature of the pump directly, and thus the temperature of the air flowing through the pump, was possible. In some of the early implementations of digital ozonesondes, the measurement of "box" temperature was continued, based on adopting parts of the procedures in the instructions for analog ozonesondes. In this configuration the thermistor was suspended in the ozonesonde Styrofoam box in the vicinity of the pump (See Vaisala preparation guidelines recommended between 1988 and 1996). If Vaisala (or Science Pump Corporation) guidelines were strictly followed, then the relation of box temperature and internal pump

temperature is approximately very similar to Case III (see below) of a taped thermistor at the pump base. However, the thermistor was not always positioned consistently at the same location near the pump base, so the relationship between this "box" temperature and the internal pump temperature could be variable and here the O₃S-DQA experts and station PIs have to find the best compromise.

Case III: External pump (taped thermistors) temperature measurements in digital sounding systems

Experiments during JOSIE-2000 demonstrated that for a thermistor mounted on or within the pump base, good thermal contact is required. A thermistor taped at the surface of the pump body measuring the external pump temperature ($T_{P,Ext}$) deviates significantly from a thermistor mounted within the pump base that measures the internal pump temperature ($T_{P,Int}$). **Figure D-3** shows the typical evolution of the internal and external (taped) pump temperature as a function of pressure [Smit *et al.*, 2007]. Because of frictional heating of the moving piston of the pump the internal temperature within the pump base is higher than the external pump temperature. At the start of the simulations the differences were between 0.5 and 2 Kelvin, increasing to $\sim 7-10$ K at 50 hPa pressure and then slightly decreasing towards lower pressures. Similar observations of internal and external pump temperatures were made by O'Connor *et al.* [1998] during a series of ozone soundings in the field. In Sodankylä (Finland) a series of multi-thermistor flights were made. The flights showed that under Arctic wintertime conditions large differences can be observed depending on the placement of the thermistor [Kivi *et al.*, 2007]. The results (incl. pressure behaviour) are very similar to the JOSIE 2000 results [Smit *et al.*, 2007].

Based on the JOSIE 2000 results the relation of the difference between internal and external pump temperature has been fitted as a function of pressure P_{Air} :

$$T_{P,Int} - T_{P,Ext} = DT_{PIE}(P_{Air}) = 20.6 - 6.7 \text{Log}_{10}(P_{Air}) \quad \text{at } P_{Air} \geq 70 \text{ hPa} \quad [\text{E-D-3A}]$$

$$T_{P,Int} - T_{P,Ext} = DT_{PIE}(P_{Air}) = 8.25 \quad \text{at } 15 \leq P_{Air} \leq 70 \text{ hPa} \quad [\text{E-D-3B}]$$

$$T_{P,Int} - T_{P,Ext} = DT_{PIE}(P_{Air}) = 3.25 + 4.25 \text{Log}_{10}(P_{Air}) \quad \text{at } 5 \leq P_{Air} < 15 \text{ hPa} \quad [\text{E-D-3C}]$$

The corresponding uncertainty of $\square DT_{PIE}$ is expressed as:

$$\Delta DT_{PIE}(P_{Air}) = 3.9 - 1.13 \text{Log}_{10}(P_{Air}) \quad \text{at } P_{Air} > 70 \text{ hPa} \quad [\text{E-D-4A}]$$

$$\Delta DT_{PIE}(P_{Air}) = 0.3 + 1.13 \text{Log}_{10}(P_{Air}) \quad \text{at } P_{Air} \leq 70 \text{ hPa} \quad [\text{E-D-4B}]$$

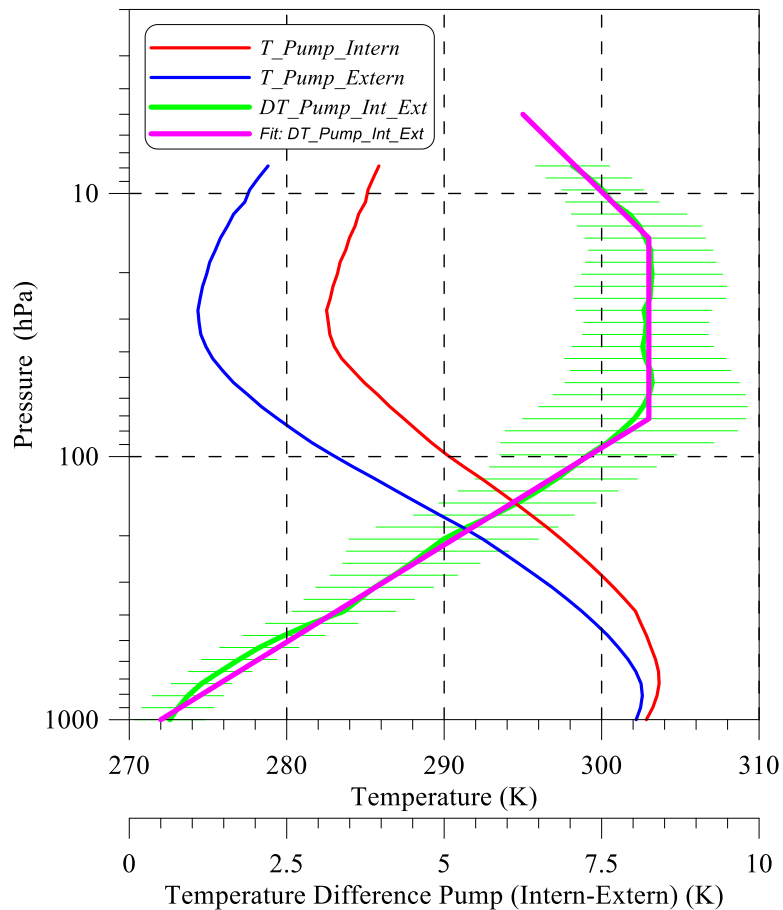


Figure D-3: Internal and external (taped) pump temperature and their relative differences as a function of pressure obtained from combined internal and external temperature measurements over an ensemble of 8 ECC sondes (3 ENSCI-Z and 5 SPC-6A) tested during JOSIE 2000 [Smit et al., 2007]

Case IV: External pump (epoxied/glued thermistors) temperature measurements in digital sounding systems

In the 1990s at several ozonesonde sites the thermistor was epoxied (glued) at the surface of the pump base. This configuration was used, for example, at NOAA for a limited period of time. Pump temperatures during the period when this configuration was used were compared to the current configuration as well as with the analog box temperature measurement. The epoxied thermistors appear to perform more like the box temperature in the analog ozonesondes. This configuration does not seem to be a direct measurement of the pump temperature as is the case when the thermistor is mounted within the block. Evidently the thermal contact with the block for the epoxied thermistor is not adequate and the thermistor is measuring a temperature closer to the box temperature, fortunately in a consistent way. The behaviour of the temperature difference between the internal pump base and the thermistor glued on the surface of the pump base has been investigated as a function of pressure in the ozone sonde simulation chamber at WCCOS (Jülich, Germany). Results are shown in **Figure D-4** for three ozonesonde simulation experiments (2x tropical and 1x midlatitude ambient air pressure and temperature profiles).

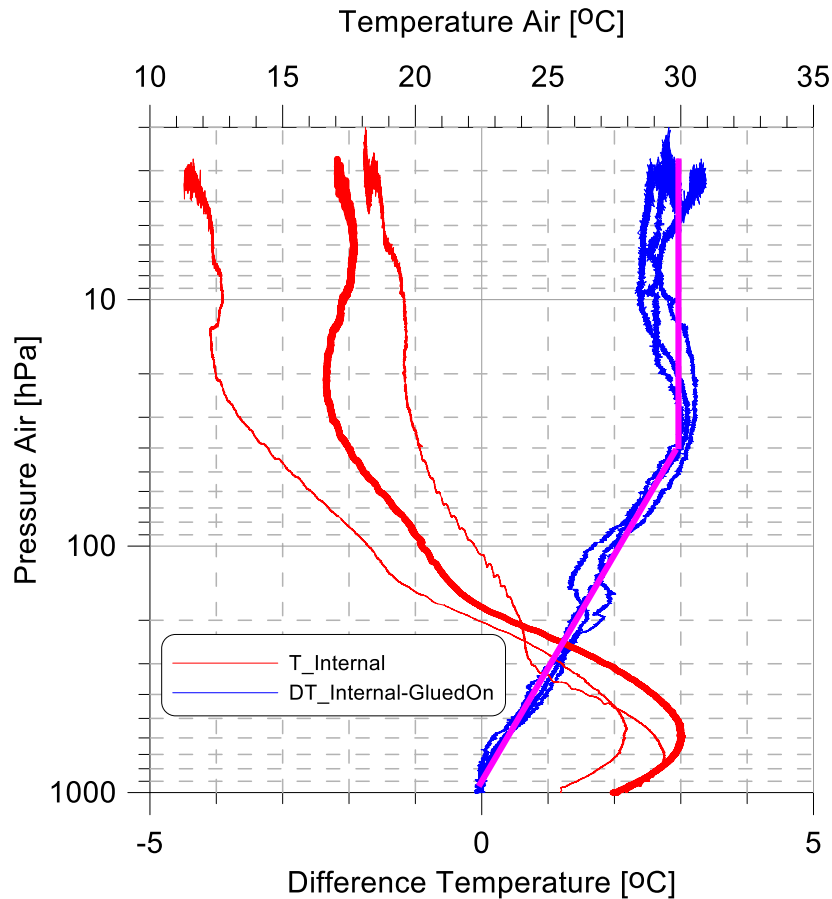


Figure D-4: Temperature measurements made at different locations of the ECC pump: Internal pump base temperature ($T_{P,Int}$), temperature difference between internal pump base ($T_{P,Int}$) and the thermistor epoxied (glued) on the surface of the pump base. Measurements were made in the simulation chamber at WCCOS during three ozone sonde simulation experiments (2x tropical and 1x midlatitude pressure and temperature profiles)

The pressure dependence of the temperature difference DT_{PIG} between the internal pump base and the epoxied thermistor can be approximated by:

$$T_{P,Int} - T_{P,Glued} = DT_{PIG}(P_{Air}) = 6.4 - 2.14 \log_{10}(P_{Air}) \quad \text{at } P_{Air} \geq 40 \text{ hPa} \quad [\text{E-D-5A}]$$

$$T_{P,Int} - T_{P,Glued} = DT_{PIG}(P_{Air}) = 3.0 \quad \text{at } 3 \leq P_{Air} \leq 40 \text{ hPa} \quad [\text{E-D-5B}]$$

The uncertainty ΔDT_{PIG} of this parameterization is estimated to be ± 0.5 K.

Case V: Internal pump (thermistors inside pump base) temperature measurements in digital sounding systems:

Beginning with the introduction of the ENSCI-Z sonde in 1995 a thermistor was mounted in a hole drilled in the pump body. This was a year later in 1996 adopted by SPC in the 6A model of the sonde. Currently all implementations of the ozonesonde measure the pump temperature.

Truest pump temperature

The pump temperature corrections described in the cases I-IV are all referred to the internal pump temperature (= pump base temperature). However, as noted before the best representative, "truest", pump temperature T_P that should be applied in formula **Eq. E-2-1** is the actual temperature inside the cylindrical housing of the moving piston of the pump. Laboratory measurements made in the simulation chamber at WCCOS have shown that the so-called piston temperature is about 1–3 K larger than the internal pump base temperature

depending on the pressure (**Figure D-5**). This means that to obtain the “best” pump temperature T_P the internal pump base temperature has to be corrected by this temperature difference DT_{PT} as a function of ambient air pressure by:

$$T_P - T_{P,Int} = DT_{PT}(P_{Air}) = 3.9 - 0.80 \text{Log}_{10}(P_{Air}) \quad \text{at } P_{Air} > 3 \text{ hPa} \quad [\text{E-D-6}]$$

the uncertainty ΔDT_{PT} of this correction is estimated to be about $\pm 0.5 \text{ K}$

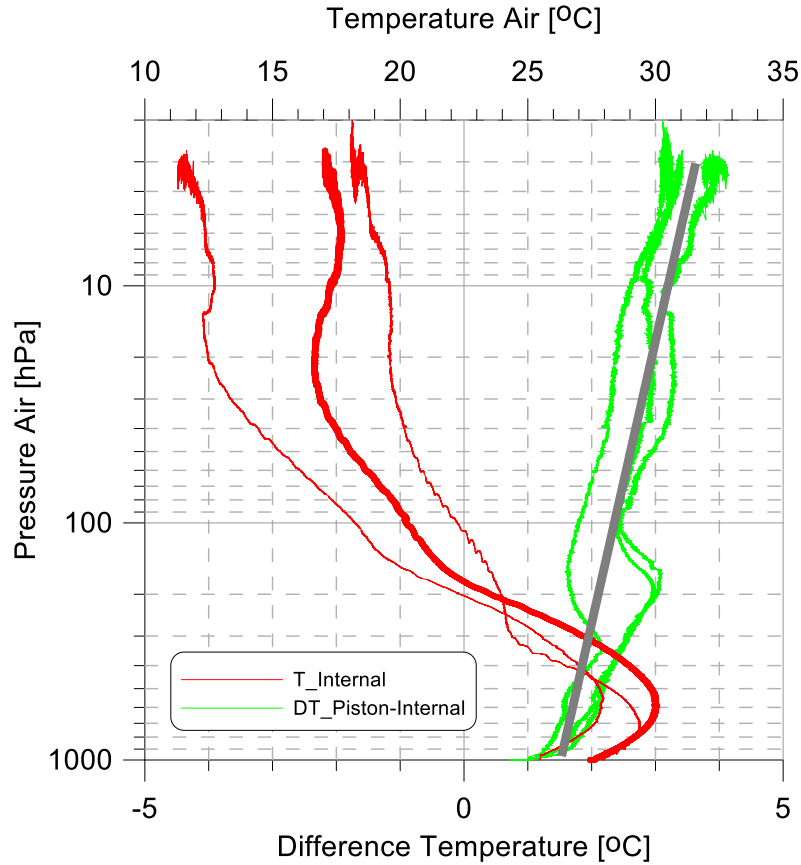


Figure D-5: Temperature measurements made at different locations of the ECC pump: Internal pump base temperature ($T_{P,Int}$), and difference of the temperature inside the cylindrical chamber of the moving piston (T_P) with the internal pump base temperature ($T_{P,Int}$). Measurements were made in the simulation chamber at WCCOS during three ozonesonde simulation experiments (2x tropical and 1x midlatitude pressure and temperature profiles)

Recommendations:

The “truest” pump temperature T_P to be applied in formula **Eq. E-2-1** is described as:

$$T_P = T_{PM} + DT_{PC}(P_{Air}) + DT_{PT}(P_{Air}) \quad [\text{E-D-7}]$$

Where $DT_{PC}(P_{Air})$ is the pump temperature correction for one of the cases I-IV described before.

The corresponding uncertainty of “truest” pump temperature T_P is:

$$\frac{\Delta T_P}{T_P} = \sqrt{\left(\frac{\Delta T_{PM}}{T_{PM}}\right)^2 + \left(\frac{\Delta DT_{PC}}{DT_{PC}}\right)^2 + \left(\frac{\Delta DT_{PT}}{DT_{PT}}\right)^2} \quad [\text{E-D-8}]$$

Where

- A. T_{PM} is the temperature as measured (recorded) by the sounding system. The uncertainty of this measurement depends on the type of temperature sensor and sounding system used. In general, it is assumed that for the “analog” sounding systems (Case I) the uncertainty is $\sim\pm 1.0$ K, while for the modern (digital) sounding systems (Cases II-V) the uncertainty is $\sim\pm 0.5$ K.
- B. $DT_{PC}(P_{Air})$ is the correction to obtain the internal pump base temperature from the measured temperature as characterized by the five cases I-V as described before.

Case I: Box temperature in analog sounding systems:

$$DT_{PC}(P_{Air}) = DT_{PBB}(P_{Air}). \text{ (Eq. E-D-2)}$$

$$\text{Uncertainty } \Delta DT_{PC} = \Delta DT_{PBB} = \pm 1.0 \text{ K}$$

Case II & III: Box or taped temperature measurements by thermistor in digital sounding systems

$$DT_{PC}(P_{Air}) = DT_{PIE}(P_{Air}). \text{ (Eq. E-D-3)}$$

$$\text{Uncertainty } \Delta DT_{PC} = \Delta DT_{PIE}(P_{Air}) \text{ (Eq. E-D-4)}$$

Case IV: External pump (epoxied/glued thermistors) temperature measurements in digital sounding systems:

$$DT_{PC}(P_{Air}) = DT_{PIG}(P_{Air}). \text{ (Eq. E-D-5)}$$

$$\text{Uncertainty } \Delta DT_{PC} = \Delta DT_{PIG} = 0.5 \text{ K}$$

Case V: Internal pump (thermistors inside pump base) temperature measurements in digital sounding systems

$$\text{No correction: } DT_{PC} = 0 \text{ K} \text{ \& Uncertainty } \Delta DT_{PC} = 0 \text{ K}$$

- C. $DT_{PT}(P_{Air})$ is the correction to obtain the “truest” pump piston housing temperature T_P from the internal pump base temperature as given by **Eq. E-D-6**, whereby the corresponding uncertainty contribution $\Delta DT_{PT} = 0.5 \text{ K}$.

Whether or not a correction is made, the contribution of temperature uncertainties to the overall uncertainty should be quantified by a realistic estimate.

D-7.7 Absorption efficiency (η_A): Limitations for 2.5 cm³ cathode sensing solution

Rationale:

Since laboratory and field investigations have shown that the absorption (i.e. capture) efficiency η_A is gas-phase diffusion limited in the lower troposphere [Davies *et al.*, 2003] and the sensing solution evaporates at a rate dependent on the temperature of the cell and the ambient pressure during the sounding, η_A may possibly change during a flight. However, this is not the case. Although evaporation lowers the amount of liquid for uptake of gaseous ozone, η_A is not significantly affected [e.g. Komhyr, 1971, Davies *et al.*, 2003]. At higher altitudes this uptake becomes very efficient due to much faster mass transfer (i.e. faster diffusion) at lower pressures. As a consequence, η_A stays at 1.00, with an uncertainty of less than 0.01 throughout the entire profile. This is true for sonde sensors which are charged with 3.0 cm³ of cathode sensing solution. For ECC sensors charged with 2.5 cm³, only $\sim 96\%$ of the ozone is captured by the sensing solution at 1000 hPa ground pressure [Davies *et al.*, 2003]. At lower pressures, the 4% deficit vanishes rapidly (faster gas-diffusion), such that at pressures below 100 hPa η_A equals 1.00. For determination of η_A and its uncertainty $\Delta \eta_A$ see **Section 3.3.4** and **Annex C: C-6.5**.

D-7.8 Pump efficiency (η_P)

Rationale:

At ambient air pressures below 100 hPa the efficiency of the gas sampling pump degrades due to pump leakage, dead volume in the piston of the pump, and the back pressure exerted on the pump by the cell solution [Komhyr, 1967, Torres et al., 1981, Steinbrecht et al., 1998]. This decrease in pump efficiency at reduced pressures is accounted for (**Section 3.3.3, Annex C: C-6.6**)

Recommendations:

1. Also, for the historical ozone soundings, the current recommendations for the pump efficiency correction tables should be used
 - a. Komhyr 1986 (**K86-Efficiency**) for SPC-2A & -3A & -4A & -5A & -6A sondes
 - b. Komhyr 1995 (**K95-Efficiency**) for ENSCI (later DMT=Droplet Measurement Technologies and now Ensci) sondes with SST1.0 or SST0.5
 - c. **NOAA/CMDL 2002** or **JMA 2016** for ENSCI sondes with SST0.1

The two Komhyr pump efficiency curves differ by about 1% at 10 hPa and 3% at 5 hPa;

2. A few stations (e.g. NOAA) in the network are using their own experimentally derived correction table (e.g. Johnson et al. 2002). For other stations using their own pump correction table, the impact on the homogenization has to be explored by the Station PI and the O₃S-DQA expert before starting the actual data processing for homogenization;
3. The **O₃S-DQA** process should estimate for each pump efficiency table used the contribution to the overall uncertainty as a function of pressure;
4. The pump efficiency η_P tables and their uncertainties $\Delta\eta_P$ as a function air pressure P_{Air} are listed in Table 3-1 (**Section 3.3.3**) η_P and $\Delta\eta_P$ values between specified air pressure levels can be estimated by linear interpolation in Log (P_{Air}).

Details on data processing for η_P and $\Delta\eta_P$ are in **Annex C: C-6-6**

D-7.9 Conversion efficiency (η_C)

See Annex C: Section C-6-7

D-7.10 Transfer Function F_T : Impact of Different Types of Sensing Solutions and Sondes

Rationale

Different compositions of sensing solutions (e.g. ECC sonde: SST1.0 or STT0.5) in cathode cell or different ozone sensor types (e.g. ECC sonde: SPC-6A or ENSCI-Z) can have conversion efficiency factors slightly different from one. These deviations from 1 may also increase through a sounding due to evaporation of water from the sensing solution causing an increase of solution strength. For this O₃S-DQA activity, these deviations of the conversion efficiency from one at different SSTs and/or ECC sonde types will be corrected by the use of **transfer functions F_T** .

One of the goals of earlier ozonesonde intercomparisons was to compare ozone sensitivity of the two types of ozonesondes, Science Pump Corporation (SPC) and ENSCI, and the two KI-solution strengths in wide use, 1.0% and 0.5%. This was done in the laboratory with the JOSIE experiments [Smit et al., 2007], field experiments using dual-sonde and multiple-ozonesonde

payloads [Kivi *et al.*, 2007] and in the BESOS multi-sonde photometer intercomparison flight [Deshler *et al.*, 2008]. To account for differences in solution strength and sonde type, Kivi *et al.* [2007] proposed altitude dependent transfer functions based on dual-sonde flights, while Deshler *et al.* [2008] proposed pressure dependent transfer functions from the BESOS multi-sonde flight.

A summary analysis of the dual-ozonesonde data [Deshler *et al.*, 2017] focused on the two primary WMO SOP recommendations of SPC 1.0% or ENSCI 0.5%. The comparison sonde profiles used in the analysis originated from the laboratory (JOSIE 2009), midlatitude multi-sonde (BESOS and NOAA), midlatitude dual-sonde (Payerne and Wallops Island) and polar dual-sonde (Sodankylä and McMurdo Station) flights. All data were compared using scatter plots, with a simple ratio fit to the measurements at pressures > 30 hPa and ozone partial pressures > 0.5 mPa. Including ozone partial pressures smaller than 0.5 mPa increased the uncertainty of the comparisons considerably, as is often the case when comparing small numbers, but did not change the average ratios substantially. At pressures <30 hPa the relationship has some pressure dependence but can be reasonably approximated by a linear equation in $\log_{10}(\text{pressure, in hPa})$. The results from all data sets are reasonably consistent across the different platforms, sensing solutions, and locations. The relationships are summarized in **Table D-3**. The standard deviation of these ratios is ± 0.05 , if the very low ozone values at low altitudes are removed.

The results in the table should be interpreted as follows: the ozone partial pressures for the chosen sonde type and SST combination (one of the primary WMO SOP standards, the "Y dependent" sonde measurements) can be obtained from the ozone partial pressure measurements from the used non-standard sonde type and SST used (the "X independent" sonde measurements) by a simple multiplication, using the ratio(p). Details of the analysis and the introduction of the transfer functions are described in Deshler *et al.* [2017].

Table D-3: Recommended relationships (i.e. transfer functions F_T) for conversion from SST1% to SST0.5% for both SPC6A and ENSCI and to convert from ENSCI to SPC6A for both SST1% and SST0.5%

Source: Deshler *et al.*, 2017

Equation	Y dependent	Ratio	X independent	Pressure	Ozone sonde or SST
Eq.7A	SST 0.5%	0.96	SST 1.0%	P ≥ 30 hPa	SPC & ENSCI
Eq.7B	SST 0.5%	$0.90+0.041*\log_{10}(p)$	SST 1.0%	P < 30 hPa	SPC & ENSCI
Eq.7C	SPC	0.96	ENSCI	P ≥ 30 hPa	SST0.5 & 1.0
Eq.7D	SPC	$0.764+0.133*\log_{10}(p)$	ENSCI	P < 30 hPa	SST0.5 & SST1.0
Eq.7E	SPC SST1.0	1.01	ENSCI-0.5%	P>0	

Recommendations:

- 1) Stations should reprocess their O_3S -data corresponding to the new WMO SOP guidelines on use of either SPC SST1.0 or ENSCI SST0.5 as described in this GAW report;

- 2) *If the only change in a data record is from one of the WMO SOP recommendation to the other, then no transfer function needs be applied. The ratio of SPC SST1.0 to ENSCI SST0.5 is 1.0 to within 1.0%;*
- 3) *If there were changes for a period of time using either ENSCI SST1.0 or SPC SST0.5 sondes, then the long-term record should be corrected to one of the two WMO standards, using the ratios provided in the table above. Typically, if a station switched from SPC to ENSCI they may have used ENSCI SST1.0 for a period of time before the switch to the recommended SST0.5 was made. Those stations should modify their data to ENSCI SST0.5 or SPC SST1.0 using the table above;*
- 4) *For the O₃S-DQA homogenization, the recommendation is to use the simplest approach to homogenize the data to one of the two standards. For example, if measurements are made using ENSCI SST1.0, then modify the measurements to ENSCI SST0.5 by multiplying the ozone partial pressure measurements by $m=0.96$ for $p > 30$ hPa, and by $m=0.90 + 0.041*\log_{10}(p)$, for $p < 30$ hPa; or to SPC SST1.0 using $m=0.96$ for $p > 30$ hPa, and by $m=0.764 + 0.1332*\log_{10}(p)$, for $p < 30$ hPa;*
- 5) *When the partial pressure measurements are modified using these transfer functions, an additional uncertainty of 0.05 (**Annex C: Section C-6-8, Eq. E-C-1**) must be added to the formula E-3-1 to account for the uncertainty of the transfer functions that were derived from dual-sonde comparisons (Deshler et al., 2016);*
- 6) *Stations which used SSTs outside of 0.5 and 1.0 should develop and document their own transfer functions to provide a sonde- and solution strength-independent record for the long-term stations.*

D-7.11 Total Ozone Normalization

Rationale:

The primary reason for the common practice of normalizing, or “correcting” ozone soundings by scaling linearly to a total ozone measurement is undoubtedly historical: the older Brewer-Mast sonde, when prepared according to the manufacturer’s instructions, had a typical response equivalent to about 80% of the actual ozone amount, and so needed to be scaled to give a more accurate result. Although the ECC sonde response is much closer to 100%, the practice has continued because it demonstrably reduces scatter in ozonesonde data [e.g. Kerr et al., 1994; Smit et al., 1996; Beekman et al., 1994, 1995]. Standard deviations are 7%-10% for non-corrected data and 5%-7% for corrected data [Fioletov et al., 2007, Liu et al., 2009]. This improvement is because of the greater accuracy of total ozone measurements: for well calibrated total ozone instruments the standard uncertainty of direct sun measurements is less than 3% [Basher, 1982].

However, the process introduces a degree of uncertainty because the amount of ozone above the balloon burst height can only be estimated. Several methods for doing this are in use, including the use of a climatological estimate [McPeters et al., 1997, McPeters et al., 2007, McPeters and Labow, 2012], or extrapolating the profile assuming a constant mixing ratio above the balloon burst altitude. Smit et al. [2007] and Deshler et al. [2008] showed that a scaling factor that is constant with altitude is not appropriate. This is of particular concern for the tropospheric part of the profile. If a normalization is used it will be necessarily weighted to the larger stratospheric part of the profile and the ozone profile record will no longer be independent of the total ozone record. This is an important issue for trend studies (although to some extent alleviated if there is no trend in correction factors) and will introduce errors if the total ozone calibration is in error.

The normalization or correction factor is unquestionably of value as a data quality control indicator. Since the scaling is linear in measured ozone, it can be applied (and as easily removed) in post-processing or by the data user.

Recommendations:

1. *ECC ozonesonde records should **NOT** be scaled to a total ozone measurement, but the total ozone normalization factor should be calculated as a useful quality indicator of the ozonesonde profile data, and reported according to the WOUDC and NDACC convention, as a negative value (i.e. not been applied);*
2. *If the total ozone normalization factor has been applied in parts of the ozonesonde data series, it should be removed (de-corrected);*
3. *For the calculation of the total ozone normalization factor (including the residual ozone above the balloon burst), we refer to **Section 3.3.11** and **Annex C: Section C-6**.*

D-8 Storage of Data

For storage of data we recommend following same guidelines expressed in **Section 4.3** and [Annex B](#).

List of Acronyms

ASOPOS	Assessment of Standard Operating Procedures for OzoneSondes
BESOS	Balloon Experiment on Standards for OzoneSondes
BM	Brewer-Mast (ozonesonde, not ECC type)
CAMS	Copernicus Atmosphere Monitoring Service
CARIBIC	Civil Aircraft for the Regular Investigation of the atmosphere Based on an Instrument Container
CFC	Chlorofluorocarbon
CMDL	Climate Monitoring and Diagnostics Lab (formerly called GMD, now GML)
CMR	Constant Mixing Ratio
CO	Carbon monoxide
DMT	Droplet Measurement Technologies (company that took over ENSCI for 2011–2015)
DOI	Digital Ozonesonde Interface
DQI	Data Quality Indicator
DQO	Data Quality Objective
DU	Dobson Unit, the unit to express vertical <i>ozone column abundances</i> , $1 \text{ DU} = 2.69 \times 10^{16} \text{ molecules per cm}^2 \text{ at STP } 1 \times 10^{-3} \text{ atm.cm at STP}$
ECC	Electrochemical Concentration Cell
EMF	Electro-Motive Force
ENVISAT	Environmental Satellite (satellite with SCIAMACHY instrument)
EN-SCI	Environmental Science Corporation; ECC ozonesonde manufacturer
ERA-5	European Centre for Medium-Range Weather Forecasts (ECMWF) Re-Analysis 5
ESA	European Space Agency
ESRL	Earth System Research Laboratories
EUMETSAT	European Organization for the Exploitation of Meteorological Satellites
FZJ	ForschungsZentrum Jülich
GAW	Global Atmospheric Watch
GCOS	Global Climate Observing System
GEMS	Geostationary Environment Monitoring Spectrometer
GMD	Global Monitoring Division (division of NOAA's ESRL; now GML)
GML	Global Monitoring Laboratory (division of NOAA's ESRL; formerly GMD)
GOME	Global Ozone Monitoring Experiment (onboard MetOp satellites)
gpm	geopotential meter
GPS	Global Positioning System
GRUAN	GCOS Reference Upper Air Network
H₂O₂	Hydrogen peroxide
IAGOS	In-service Aircraft for a Global Observing System
IAP	Institute of Atmospheric Physics, Beijing, China

IASI	Infrared Atmospheric Sounding Interferometer (onboard MetOp satellites)
IGACO	Integrated Global Atmospheric Chemistry Observations
IOC	International Ozone Commission
IPCC	Intergovernmental Panel on Climate Change
JMA	Japanese Meteorological Agency
JOSIE	Jülich OzoneSonde Intercomparison Experiment
KI	Potassium Iodide
LOTUS	Long-term Ozone Trends and Uncertainties in the Stratosphere
MERRA-2	Modern-Era Retrospective analysis for Research and Applications- version 2
MLS	Microwave Limb Sounder (on Aura satellite)
MOZAIC	Measurement of OZone and water vapor by AIRbus in-service airCRAFT (now IAGOS)
NASA	National Aeronautics and Space Administration
NBKI	Neutral-Buffered Potassium Iodide
NDACC	Network for the Detection of Atmospheric Composition Change
NOAA	National Oceanic and Atmospheric Administration
NO_x	Nitrogen Oxides
O3S-DQA	OzoneSonde-Data Quality Assessment
ODS	Ozone Depleting Substances
OMI	Ozone Monitoring Instrument (on Aura satellite)
OMPS	Ozone Mapping and Profiler Suite (onboard Suomi-NPP and JPSS satellites)
OPM	Ozone PhotoMeter Instrument (used as UV-reference)
PTU	Pressure-Temperature-Humidity (referring to vertical profiles)
RPM	Rotations Per Minute
RV	Research Vessel
SAG	Science Advisory Group
SAGE III	Stratospheric Aerosol and Gas Experiment (fourth generation on ISS)
SBUV	Solar Backscatter Ultraviolet (referring to instrument type on satellites measuring ozone)
Sentinel-4	Geostationary satellite measuring ozone in the future planned by ESA
SHADOZ	Southern Hemisphere ADditional OZonesonde
SI²N	Ozone trend assessment study supported by SPARC, IOC, IGACO, and NDACC
SMILES	Submillimeter-Wave Limb Emission Sounder onboard ISS
SO₂	Sulfur dioxide
SOP	Standard Operating Procedure
SOP-2014	GAW Report No. 201, 2014
SPARC	Stratosphere-troposphere Processes And their Role in Climate
SPC	Science Pump Corporation; ECC ozonesonde manufacturer
SST	Sensing Solution Type
SST0.1	1.0% KI & 1/10th buffer solution
SST0.5	0.5% KI & half pH-buffer solution

SST1.0	1.0% KI & full pH-buffer solution
SST2.0	2.0% KI & non-pH-buffered solution with no KBr
STP	Standard Temperature (=273.15 K) and Pressure (=1013.25 hPa) conditions
SWOOSH	Stratospheric Water and OzOne Satellite Homogenized data set
TCO	Total Column Ozone
TEI	Thermo Environmental Instruments
TEMPO	Tropospheric Emissions: Monitoring of Pollution
TOAR	Tropospheric Ozone Assessment Report
TOMS	Total Ozone Mapping Spectrometer
TROPOMI	TROPOspheric Monitoring Instrument
UNEP	United Nations Environment Programme
UTC	Universal Time Convention = Coordinated Universal Time
UV	Ultraviolet
UWYO	University of Wyoming
VOC	Volatile Organic Compound
WCCOS	World Calibration Centre for OzoneSonde
WDCRG	World Data Centre for Reactive Gases
WMO	World Meteorological Organization
WOUDC	World Ozonesonde and Ultraviolet Data Centre

ASOPOS 2.0 People Involved

Table F-1. List of ASOPOS 2.0 Panel Members and Manufacturer Associates

Name	Affiliation	Email Address
Allaart, Marc	KNMI, De Bilt, Netherlands	allaart@knmi.nl
Davies, Jonathan	EC, Toronto, Canada	jonathan.davies@ec.gc.ca
Johnson, Bryan	NOAA, Boulder, USA	bryan.johnson@noaa.gov
Kivi, Rigel	FMI, Helsinki, Finland	rigel.kivi@fmi.fi
Kollonige, Debra	NASA-GSFC, Greenbelt, USA	debra.e.kollonige@nasa.gov
Morris, Gary	St. Edward's University, Austin, USA	prof.gary.morris@gmail.com
Nakano, Tatsumi	JMA, Tokyo, Japan	tnakano@met.kishou.go.jp
Piters, Ankie	KNMI, De Bilt, Netherlands	piters@knmi.nl
Querel, Richard	NIWA, Lauder, New Zealand	richard.querel@niwa.co.nz
Smit, Herman G.J.	FZJ-IEK8, Jülich, Germany	h.smit@fz-juelich.de
Stauffer, Ryan	NASA-GSFC, Greenbelt, USA	ryan.m.stauffer@nasa.gov
Stübi, Rene	Meteo Suisse, Payerne, Switzerland	rene.stuebi@meteoswiss.ch
Tarasick, David	EC, Toronto, Canada	david.tarasick@ec.gc.ca
Thompson, Anne	NASA-GSFC, Greenbelt, USA	anne.m.thompson@nasa.gov
Van Malderen, Roeland	KMI, Uccle, Belgium	roeland.vanmalderen@meteo.be
Von der Gathen, Peter	AWI, Potsdam, Germany	peter.von.der.gathen@awi.de
Vömel, Holger	NCAR, Boulder, USA	voemel@ucar.edu

ASOPOS 2.0 Manufacturer Associates

Name	Affiliation	Email Address
Harnetiaux, Jonathan	Environmental Science Corporation	jonathan@en-sci.com
Hemming, Mika	Vaisala	mika.hemming@vaisala.com
Kok, Greg	Environmental Science Corporation	gkok@en-sci.com
Parker, Kathy	Science Pump Corporation	kathy@pcmco.com ; sales@pcmco.com

ASOPOS 2.0 Kick Off Meeting
19 September 2018, WMO, Geneva, Switzerland



Figure F-1. Participants from left to right: M. Nakano, R. Gonzague, R. Stübi, R. Van Malderen, A. Pipers, P. von der Gathen, H. Smit, R. Querel, A. Thompson, J. Witte, G. Braathen, H. Vömel, G. Morris, R. Stauffer, M. Allaart, B. Johnson, K. Parker, J. Harnetiaux, D. Tarasick, and P. Survo

ASOPOS 2.0 Second Meeting
17–18 September 2019, KMI, Uccle, Belgium



Figure F-2. Participants from left to right: H. De Backer, D. Tarasick, D. Kolonige, B. Johnson, A. Thompson, P. von der Gathen, H. Vömel, R. Stübi, M. Allaart, H. Smit, R. Stauffer, R. Van Malderen and G. Morris.

ASOPOS 2.0 Third Meeting
17–19 March 2020, NOAA, Silver Spring, USA

Due to the COVID-19 pandemic situation in 2020 this was a two-day virtual meeting, which was attended by the complete ASOPOS 2.0-Panel Members and -Manufacturer Associates, respectively (**Table F-1**). On 19 March the Authors met to review the first draft of this report.

LIST OF AUTHORS**Herman G.J. Smit**

Research Centre Jülich
Institute of Energy and Climate Research
IEK-8: Troposphere
52425 Jülich, Germany
h.smit@fz-juelich.de

Anne M. Thompson

NASA/Goddard Space Flight Centre
Mail Code 614
8800 Greenbelt Road
Greenbelt, Maryland 20771 USA
anne.m.thompson@nasa.gov

Bryan J. Johnson

NOAA ESRL/Global Monitoring Lab
325 S. Broadway
Boulder, CO 80305 USA
bryan.johnson@noaa.gov

Debra E. Kollonige

NASA/Goddard Space Flight Centre
Mail Code 614
8800 Greenbelt Road
Greenbelt, Maryland 20771 USA
debra.e.kollonige@nasa.gov

Gary A. Morris

Professor of Environmental Science and Physics
St. Edward's University
3001 South Congress Ave.
Austin, TX 78704-6489 USA
gmorris1@stedwards.edu

Ryan M. Stauffer

NASA/Goddard Space Flight Centre
Mail Code 614
8800 Greenbelt Road
Greenbelt, Maryland 20771 USA
ryan.m.stauffer@nasa.gov

David W. Tarasick

Air Quality Processes Research Section
Air Quality Research Division / Science and Technology Branch
Environment and Climate Change Canada / Government of Canada
4905 Dufferin Street
North York, ON M3H 5T4, Canada
david.tarasick@canada.ca

Peter von der Gathen

Alfred Wegener Institute
Telegrafenberg A45
14473 Potsdam Germany
peter.vondergathen@awi.de

Roeland Van Malderen

Koninklijk Meteorologisch Instituut/ Institut Royal Météorologique
Royal Meteorological Institute of. Belgium
Avenue Circulaire 3
180 Bruxelles, Belgium
roeland.vanmalderen@meteo.be

Holger Vömel

National Centre for Atmospheric Research (NCAR)
Earth Observing Laboratory
3090 Centre Green Drive
Boulder, CO 80301 USA
voemel@ucar.edu

Jacquelyn C. Witte

National Centre for Atmospheric Research (NCAR)
Earth Observing Laboratory
3090 Centre Green Drive
Boulder, CO 80301 USA
jwitte@ucar.edu

Richard Querel

National Institute of Water and Atmospheric Research (NIWA), Lauder
State Highway 85, Central Otago, Private Bag 50061
Omakau, New Zealand
richard.querel@niwa.co.nz

Jonathan Davies

Air Quality Processes Research Section
Air Quality Research Division / Science and Technology Branch
Environment and Climate Change Canada / Government of Canada
4905 Dufferin Street
North York, ON M3H 5T4, Canada
jonathan.davies@canada.ca

Patrick Cullis

NOAA ESRL/Global Monitoring Lab
325 S. Broadway
Boulder, CO 80305 USA
patrick.cullis@noaa.gov

List of Reviewers**María del Carmen Cazorla, PhD.**

Profesora de Ingeniería Ambiental
Colegio de Ciencias e Ingenierías, Politécnico
Universidad San Francisco de Quito
Diego de Robles y Vía Interoceánica, Quito, Ecuador
mcazorla@usfq.edu.ec

Gert J. R. Coetzee

South African Weather Service
Private Bag X097
Pretoria, 0001 South Africa
Gerrie.coetzee@weathersa.co.za

Masatomo Fujiwara, Associate Professor, Dr

Faculty of Environmental Earth Science
Hokkaido University
Sapporo 060-0810 Japan
Fuji@ees.hokudai.ac.jp

Samuel J. Oltmans

Cooperative Institute for Research in Environmental Sciences
University of Colorado
c/o NOAA ESRL/Global Monitoring Lab
325 S. Broadway
Boulder, CO 80305
Samuel.j.oltman@noaa.gov

Wolfgang Steinbrecht, PhD

Deutscher Wetterdienst – German Weather Service
Met. Obs. Hohenpeissenberg
Albin-Schwaiger-Weg 10
D-82383 Hohenpeissenberg Germany
Wolfgang.steinbrecht@dwd.de

Matthew Tully, PhD

Bureau of Meteorology
GPO Box 1289
Melbourne, Victoria 3001 Australia
Matthew.Tully@bom.gov.au

For more information, please contact:

World Meteorological Organization

Science and Innovation Department

7 bis, avenue de la Paix – P.O. Box 2300 – CH 1211 Geneva 2 – Switzerland

Tel.: +41 (0) 22 730 81 11 – Fax: +41 (0) 22 730 81 81

Email: GAW@wmo.int

Website: <https://public.wmo.int/en/programmes/global-atmosphere-watch-programme>